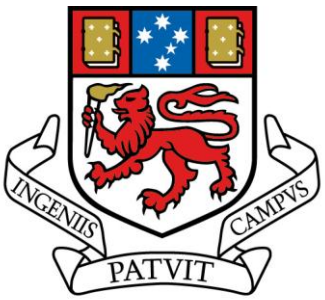


UNIVERSITY OF TASMANIA

# OPTIMISATION AND APPLICATION OF PNEUMATIC MODULATION TECHNIQUES FOR COMPREHENSIVE TWO-DIMENSIONAL GAS CHROMATOGRAPHY

by

Samuel Douglas Hewitt Poynter

BSc (Hons)

A thesis submitted in fulfilment of the

requirements for the degree of:

**Doctor of Philosophy**

August 2012

# Declaration of Originality

To the best of my knowledge, this thesis contains no material which has been accepted for the award of any other higher degree or graduate diploma in any other tertiary institution, and to the best of my knowledge, contains no material previously published or written by another author, except where due reference is made.

Samuel Douglas Hewitt Poynter

27th August 2012

# Acknowledgements

I am very thankful to my parents and close friends for their continued and unwavering support throughout my project. They have been a constant source of morale, patience, inspiration and reassurance and have helped me through every step of the process.

I am grateful of the encouragement shown by my uncle, Mr. Alan Poynter, who has offered continual interest in my studies.

The skills that I have learnt from my supervisors will prove valuable for my future career. They provided me with the space and freedom I needed to pursue my goals.

I would also like to acknowledge Dr. Simon Whittock and Dr. Christian Narkowicz for providing essential oil samples and hop cones respectively.

# List of publications arising from the research program

1. P.Q. Tranchida, L. Mondello, S.D.H. Poynter and R.A. Shellie. *Comprehensive two-dimensional gas chromatography combined with mass spectrometry*. Chapter in: L. Mondello (ed.) 2011. *Comprehensive Chromatography in Combination with Mass Spectrometry*. John Wiley and Sons, Inc., Hoboken NJ. p. 171-242.
2. S.D.H. Poynter and R.A. Shellie. High-speed, low-pressure gas chromatography–mass spectrometry for essential oil analysis. *J. Chromatogr. A* 1200 (2008) 28-33.
3. P.D. Morrison, P.J. Marriott, S.D.H. Poynter, R.A. Shellie. Selection of columns for GC×GC analysis of essential oils. *LC-GC Eur.* 23 (2010) 76-80.
4. R.A. Shellie, S.D.H. Poynter, J. Li, J.L. Gathercole, S.P. Whittock, A. Koutoulis. Varietal characterisation of hop (*Humulus lupulus* L.) by GC–MS analysis of hop cone extracts. *J. Sep. Sci.* 32 (2009) 3720-3725.
5. P. McA. Harvey, S.D.H. Poynter, R.A. Shellie. GC×GC with fluidic modulation for enantioselective essential oil analysis. *LC-GC Eur.* 24 (2011) 548-555.

# Statement of Co-Authorship

The following people and institutions contributed to the publication of the work undertaken as part of this thesis:

**P.Q. Tranchida, L. Mondello, S.D.H. Poynter and R.A. Shellie. Chapter in: L. Mondello (ed.) 2010. *Comprehensive Chromatography in Combination with Mass Spectrometry*. John Wiley and Sons, Inc., Hoboken NJ. p. 171-242.**

P.Q. Tranchida (40%), L. Mondello (10%), S.D.H. Poynter (25%), R.A. Shellie (25%)

Details of the Authors roles:

L. Mondello proposed the work and edited the manuscript. P.Q. Tranchida, S.D.H Poynter and R.A. Shellie reviewed literature and prepared the manuscript.

**S.D.H. Poynter and R.A. Shellie. *J. Chromatogr. A* 1200 (2008) 28-33.**

S.D.H. Poynter (50%), R.A. Shellie (50%)

Details of the Authors roles:

S.D.H. Poynter and R.A. Shellie prepared the manuscript and performed laboratory analysis.

**P.D. Morrison, P.J. Marriott, S.D.H. Poynter, R.A. Shellie. *LC-GC Eur.* 23 (2010) 76-80**

P.D. Morrison (33%), P.J. Marriott (1%), S.D.H. Poynter (33%), R.A. Shellie (33%)

Details of the Authors roles:

P.D. Morrison constructed the modulator and set up the analysis equipment. P.J. Marriott supported the research and provided feedback. S.D.H. Poynter and R.A. Shellie performed laboratory work and prepared the manuscript.

**R.A. Shellie, S.D.H. Poynter, J. Li, J.L. Gathercole, S.P. Whittock, A. Koutoulis. *J. Sep. Sci.* 32 (2009) 3720-3725.**

R.A. Shellie (50%), S.D.H. Poynter (20%), J. Li (3%), J.L. Gathercole (2%), S.P. Whittock (12.5%), A Koutoulis (12.5%)

Details of the Authors roles:

R.A. Shellie proposed the research, collected the samples, performed sample preparation and prepared the manuscript. S.D.H Poynter assisted with sample preparation, analysed and interpreted the samples and assisted with manuscript preparation. J. Li and J.L. Gathercole performed chemometric interpretation of collected data for publication[1]. S.P. Whittock contributed to research planning and sample collection. A. Koutoulis contributed to the research proposal and coordinated collaboration between all parties.

**P. McA. Harvey, S.D.H. Poynter, R.A. Shellie. *LC-GC Eur.* 24 (2011) 548-555.**

P. McA. Harvey (25%), S.D.H. Poynter (15%), R.A. Shellie (60%).

Details of the Authors roles:

P. Mc.A. Harvey performed modelling and laboratory work. S.D.H. Poynter performed laboratory work. R.A. Shellie proposed the research, performed laboratory work and prepared the manuscript.

1. S.D.H. Poynter recalculated all chemometric interpretations presented in this thesis.

We the undersigned agree with the above stated "proportion of work undertaken" for each of the above published (or submitted) peer-reviewed manuscripts contributing to this thesis.

Signed: _____ _____

| | |
|---|---|
| *Robert Shellie* | *Greg Dicinoski* |
| *Supervisor* | *Head of School* |
| *School Of Chemistry* | *School of Chemistry* |
| University of Tasmania | University of Tasmania |

Date:_____

# Authority of Access

# Abstract

Gas chromatography is the logical choice for the separation of volatile and semi-volatile mixtures and can provide exceptional peak capacity, particularly when used in a comprehensive two-dimensional configuration. Furthermore, coupling with a mass spectrometer provides a powerful tool for identification of components in complex mixtures. The key component in a comprehensive two-dimensional GC system is the modulation interface between the two separation dimensions, the primary purpose of which is to trap and release fractions of primary column effluent onto the secondary column whilst conserving the resolution of separated components from the first dimension throughout the two-dimensional separation.

This thesis explored the use of pneumatic modulation interfaces for comprehensive two-dimensional gas chromatography coupled to a quadrupole mass spectrometer. Little research had been conducted into the use of pneumatic modulation with mass spectrometric detection due to a conflict between the high carrier gas flow required for pneumatic modulation and the requirement for high vacuum in the mass analyser.

To commence, a series of one-dimensional separation approaches were investigated. A wide bore column was used under low pressure conditions for the analysis of moderately complex essential oils. Previous reports suggested that this technique was unsuitable for anything but simple mixtures, yet satisfactory separations of essential oils were possible. A high-temperature wax column was investigated subsequently, to determine if the claimed enhanced temperature stability would be beneficial for the second-dimension column in a comprehensive two-

dimensional separation approach. This stationary phase was only available in narrow-bore dimensions and was highly satisfactory for cryogenic modulation but the internal diameter was not appropriate for pneumatic modulation due to the high head pressure required for operation. Next, a long, narrow-bore column was used to evaluate the conditions at which optimum efficiency could be generated for a translatable method. Use of fundamental relationships revealed a simple technique for determining a suitable column length based on a desired head pressure which provides the best trade-off between speed and efficiency optimisation. To conclude these one-dimensional investigations, an application is presented. Metabolite extracts from hop (*Humulus lupulus* L.) were obtained and separated using a GC–MS approach. Simple statistical analysis techniques were performed to establish the suitability of the separation approach for generating sufficient information to allow varietal classification of the samples.

A range of modulation interfaces were explored to describe the suitability of such devices for GC×GC separation techniques. To commence, a commercial pneumatic modulation interface was used for the enantioseparation of a moderately complex essential oil. Results were critically evaluated in comparison to a thermally modulated approach, and suggested that the technique displayed significant potential as an alternative to traditional methods. Following this, a microfluidic Deans switch modulator was prepared. This utilised a switching system that only sampled a portion of the first-dimension column effluent for secondary separation. While exemplary separations of essential oil samples were achieved, it was clear that a total transfer method could provide superior results by improving sensitivity. To investigate this, a valve based pneumatic modulator was constructed and used in conjunction with the

optimum column dimensions for the final investigation presented herein. Dual secondary columns were utilised to facilitate both flame ionisation and quadrupole mass spectrometric detection. This approach provides a powerful analytical tool for both qualitative and quantitative separation of complex samples such as those investigated in this study and would satisfy the requirements of many potential applications.

# List of Abbreviations

| | |
|---|---|
| APC | Auxiliary Pressure Controller |
| DC | Direct Current |
| $d_f$ | Film Thickness |
| EO | Essential Oil |
| EOF | Efficiency Optimised Flow rate |
| EOV | Efficiency Optimised linear Velocity |
| FID | Flame Ionisation Detector |
| GC | Gas Chromatography |
| GC×GC | Comprehensive two-dimensional gas chromatography |
| GC×MS | Comprehensive gas chromatography mass spectrometry |
| GRAM | Generalised Rank Annihilation Method |
| I | Retention Index |
| i.d. | Internal Diameter |
| L | Length |
| $LN_2$ | Liquid Nitrogen |
| LOOCV | Leave-One-Out Cross Validation |
| LRI | Linear Retention Index |
| $M_R$ | Modulation Ratio |
| MS | Mass Spectrometry |
| N | Efficiency (Number of plates) |
| $N_{max,theor}$ | Nominal maximum theoretical efficiency |
| OFN | Octafluoronaphthalene |
| PARAFAC | Parallel Factor Analysis |
| PCB | Poly Chlorinated Biphenyl |

| | |
|---|---|
| PLS | Partial Least Squares |
| PFM | Pulsed Flow Modulation |
| $P_M$ | Modulation period |
| rf | Radio Frequency |
| $R_s$ | Resolution |
| RTL | Retention Time Locking |
| SOF | Speed Optimised Flow rate |
| SOV | Speed Optimised linear Velocity |
| SMB | Supersonic Molecular Beam |
| TOF | Time Of Flight |
| $t_M$ | Void time |
| $t_R$ | Retention time |
| $\bar{u}$ | Average linear velocity of carrier gas |
| $^1X$ | Parameter concerning the first dimension, eg. $^1d_f$ |
| $^2X$ | Parameter concerning the second dimension, eg. $^2d_f$ |
| ω | Peak width |

# Table of Contents

**DECLARATION OF ORIGINALITY ..... I**

**ACKNOWLEDGEMENTS ..... II**

**LIST OF PUBLICATIONS ARISING FROM THE RESEARCH PROGRAM ..... III**

**STATEMENT OF CO-AUTHORSHIP ..... IV**

**AUTHORITY OF ACCESS ..... VII**

**ABSTRACT ..... VIII**

**LIST OF ABBREVIATIONS ..... XI**

**TABLE OF CONTENTS ..... XIII**

**CHAPTER 1: INTRODUCTION ..... 1**

1.1 LITERATURE REVIEW ..... 1

1.1.1 GC×GC–MS ..... 1

1.1.2 INSTRUMENT REQUIREMENTS FOR GC×GC–MS ..... 5

1.1.3 QUADRUPOLE MS ..... 11

1.1.4 TIME-OF-FLIGHT MS ..... 12

1.1.5 DATA PROCESSING OF GC×GC–TOFMS RESULTS ..... 17

1.1.6 METHOD TRANSLATION IN GC×GC–MS ..... 18

1.1.7 GC×MS ..... 20

1.1.8 MODULATION TECHNIQUES FOR GC×GC ..... 24

1.2 APPLICATIONS OF GC×GC–MS ..... 33

1.2.1 THE EARLY YEARS ..... 33

1.2.2 GC×GC–MS LANDMARK YEAR: 2003 ..... 37

1.2.3 2004-2006 ..... 40

1.2.4 2007-2009 ..... 43

1.2.5 2010-2011 ..... 44

1.3 CONCLUDING REMARKS ..... 49

1.4 SCOPE OF THE THESIS ..... 50

**CHAPTER 2: EXPERIMENTAL ..... 53**

2.1 STANDARDS ..... 53

2.2 INSTRUMENTATION ..... 53

2.3 STATIONARY PHASES ..... 54

2.4 MODULATION ..... 54

2.5 DATA ANALYSIS ..... 56

2.5.1 GC–MS ..... 56

2.5.2 GC×GC ..... 56

**CHAPTER 3: SELECTION OF COLUMNS FOR GC–MS AND GC×GC APPROACHES ..... 58**

3.1 HIGH SPEED, LOW PRESSURE GAS CHROMATOGRAPHY-MASS SPECTROMETRY FOR ESSENTIAL OIL ANALYSIS ..... 58

3.1.1. INTRODUCTION ..... 58

3.1.2 EXPERIMENTAL ..... 61

3.1.3 RESULTS AND DISCUSSION ..... 69

3.1.4 Concluding remarks ..... 79

3.2 High temperature wax column for GC×GC analysis of essential oils ..... 81

3.2.1 Introduction ..... 81

3.2.2 Experimental ..... 83

3.2.3 Results and discussion ..... 85

3.2.4 Concluding remarks ..... 91

3.3 Investigation of high efficiency, high resolution columns for GC–MS approaches ..... 92

3.3.1 Introduction ..... 92

3.3.2 Experimental ..... 94

3.3.3 Results and discussion ..... 95

3.3.4 Concluding Remarks ..... 112

3.4. Varietal characterisation of hop from metabolite extracts ..... 113

3.4.1 Introduction ..... 113

3.4.3 Experimental ..... 115

3.4.4 Results and Discussion ..... 118

3.4.5 Concluding remarks ..... 134

3.5. Summary ..... 135

**CHAPTER 4: DEVELOPMENT, APPLICATION AND COMPARISON OF GC×GC–MS / FID APPROACHES FOR THE ANALYSIS OF PLANT ESSENTIAL OIL AND METABOLITE SAMPLES ..... 140**

4.1 GC×GC with pneumatic modulation for enantioselective essential oil analysis ..... 140

4.1.1 INTRODUCTION ..... 140

4.1.2 EXPERIMENTAL ..... 145

4.1.3 RESULTS AND DISCUSSION ..... 146

4.1.4 CONCLUDING REMARKS ..... 156

4.2. PREPARATION OF A PNEUMATIC-MODULATED GC×GC–QMS APPROACH ..... 157

4.2.1 INTRODUCTION ..... 157

4.2.2 EXPERIMENTAL PARAMETERS ..... 158

4.2.3. MS SENSITIVITY TESTING ..... 159

4.2.4. THEORETICAL CONSIDERATIONS AND GC×GC SYSTEM DEVELOPMENT ..... 165

4.2.5 RESULTS AND DISCUSSION ..... 171

4.3 ANALYSIS OF ESSENTIAL OIL SAMPLES WITH VALVE MODULATED GC×GC–MS/FID .. 172

4.3.1 INTRODUCTION ..... 174

4.3.2 EXPERIMENTAL ..... 177

4.3.3 RESULTS AND DISCUSSION ..... 177

4.3.4 CONCLUDING REMARKS ..... 189

4.4. SUMMARY ..... 189

**CHAPTER 5: CONCLUSIONS AND FURTHER RESEARCH ..... 193**

5.1 SUMMARY ..... 193

5.2 FURTHER RESEARCH ..... 201

**REFERENCES ..... R1**

**APPENDIX ..... A12**

# Chapter 1: Introduction

## 1.1 Literature Review

This literature review has been adapted from the following publication:

P.Q. Tranchida, L. Mondello, S.D.H. Poynter and R.A. Shellie. **Comprehensive two-dimensional gas chromatography combined with mass spectrometry.** Chapter in: L. Mondello (ed.) 2011. *Comprehensive Chromatography in Combination with Mass Spectrometry*. John Wiley and Sons, Inc., Hoboken NJ. p. 171-242.

### 1.1.1 GC×GC–MS

Ever since the inception of comprehensive two-dimensional gas chromatography (GC×GC), comparisons have been made between GC×GC analysis and gas chromatography-mass spectrometry (GC–MS) analysis. Initially these comparisons were drawn to illustrate the multidimensionality of the GC×GC approach [1]. For instance, Figure 1.1 shows the point of agreement between GC×GC and GC–MS. GC×GC uses a separation column rather than a mass analyser in the second analytical dimension, but this figure clearly illustrates that a device for chemical measurement is used to scrutinise the portions of the sample being eluted from the first-dimension GC column in both cases. The second-dimension column in the GC×GC instrument generates a series of chromatograms from first-dimension effluent 'packets', generally 2-3 s wide, while a series of mass spectra are generated by the GC–MS instrument at a frequency determined by the scan speed and mass range selected (in the case of a quadrupole instrument). Most GC–MS analyses utilise electron-impact ionisation (EI) so the spectra of co-eluted compounds exist as overlapping envelopes of fragment ions from each of the co-eluted compounds. For this reason GC–MS with EI is referred to as a **two-dimensional analysis**, not a two-

dimensional separation, although it is noteworthy that corresponding parts of the overlapping spectra can be very successfully apportioned to individual compounds by using MS deconvolution software, such as the freely available Automated Mass Spectral Deconvolution and Identification System (AMDIS) from NIST [2]. GC×GC very clearly produces a **two-dimensional separation** with the potential for compounds to be chromatographically resolved in each of the first- and second-dimensions respectively. It is also possible to perform a two-dimensional separation with a GC–MS instrument. This experiment, known as GC×MS, relies on soft ionisation to produce a single ion for each compound and when this criterion is met, compounds are separated according to their mass/charge ratio in the mass analyser. If the entire sample is subjected to these two separation dimensions, then these separation dimensions fit the definition of being comprehensively coupled [3] and GC×MS is denoted using the multiplex sign. This GC×MS concept is discussed in more detail later in the chapter.

The obvious congruity between GC–MS and GC×GC has also led several commentators to propose that GC×GC should be fit to perform analyses that are typically made by GC–MS without recourse to a mass analyser. However this promise is largely unfulfilled. GC×GC chromatograms often reveal thousands of peaks in highly complex samples. Under these circumstances, reliance upon pattern-formation or injection of reference materials for the purpose of qualitative peak assignment is inappropriate. Even though GC×GC is a powerful technique for the physical separation of volatile mixtures, it can realistically only give a broad indication of the nature or chemical class of many of the resolved components of individual components and their structural elucidation is the realm of selective and spectroscopic detectors. The complexity of many samples further dictates that mass

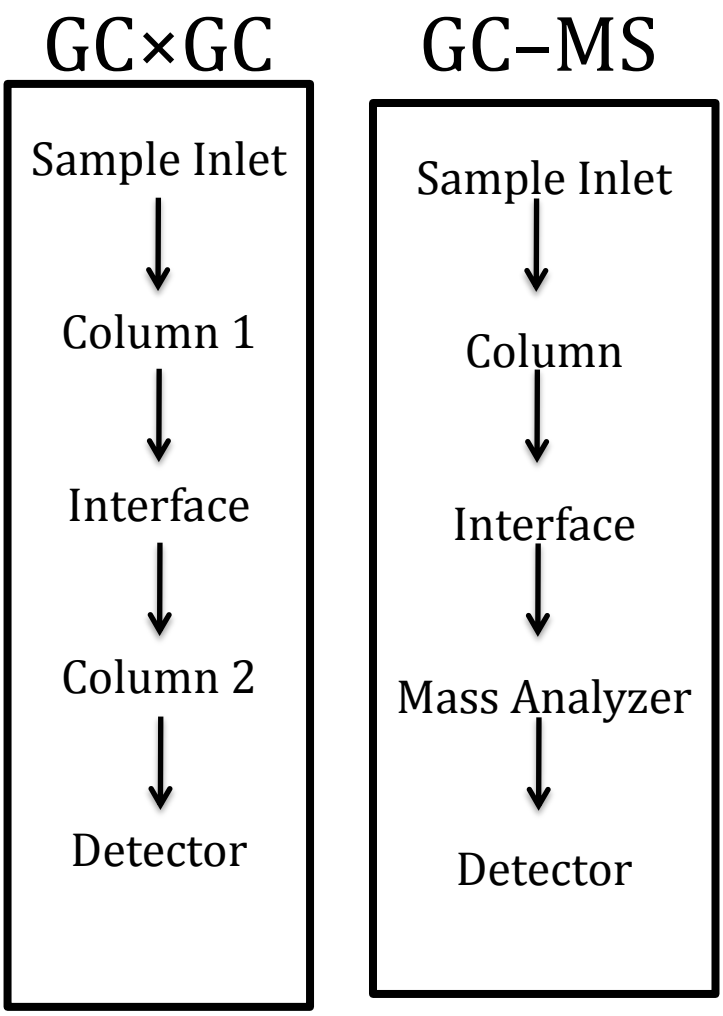


**Figure 1.1. Comparison of two multidimensional approaches: GC×GC vs GC–MS (adapted from Phillips and Beens [1]). The GC×GC approach demonstrates a two-dimensional separation, whereas the GC–MS approach represents a two-dimensional analysis.**

spectrometry be employed for confirmation of peak assignment and peak purity. The obvious extension of the technique involves coupling GC×GC **with** MS, giving rise to an undisputedly powerful analytical approach. Three independent dimensions of analysis in a GC×GC–MS experiment provide more qualitative information to the analyst compared to approaches offering lesser dimensionality. Harnessing this information in a meaningful way is a challenge, but users generally find that distilling the information down to smaller manageable bundles makes interpretation no more challenging than GC–MS data interpretation. Assuming that the aim of an experiment is to identify unknown components by way of GC×GC–MS with electron impact ionisation to give library searchable spectra then it is generally acceptable to zoom a single second-dimension modulation slice using GC–MS data analysis software and perform the library search routine according to standard practice for GC–MS. Specialised GC×GC–MS software is sparingly available, but regular automated functionality such as MS database searching is also able to be performed with minimal user input using dedicated commercial GC×GC–MS software packages. Compared to GC–MS the advantage of using GC×GC–MS is the ease with which positive assignment of peak identity can be made by way of database matching. There is unequivocal evidence that a carefully optimised GC×GC–MS separation makes peak assignment more facile than equivalent GC–MS data. The high quality spectra result from two of the general benefits of GC×GC [4]. The improved resolution offered by secondary chromatographic separation inherently allows the introduction of a higher-purity analyte flux to the MS. Furthermore, zone-compression of the first-dimension effluent often arises from the modulation process, depending on the type employed. This effect refocuses analyte bands and counteracts the band broadening from the first-dimension separation, which is often operated

outside optimum separation parameters. Combined, these enhancements greatly assist qualitative analysis of complex samples. By utilising selected ion monitoring or by careful use of extracted ion chromatograms it is possible to reveal the presence or absence of key target compounds or compound classes. Married to the highly praised "structured chromatogram" that is typical of a well-designed GC×GC separation, the combination of group patterns and MS information often provides undisputable confirmation of peak identity. Similarly, the technique is highly applicable to quantitative analysis via the enhancements available through the combination of three analytical dimensions. At the time of writing, implementation of this strategy has been limited in the literature [5-11], of which many approaches focus on a limited number of target components, generally less than twenty. The details of these applications are discussed in more detail toward the end of this chapter. This limited implementation may be due, in part, to slower development of data processing software in comparison to the analytical techniques, creating a perception of difficulty for analysts performing routine analyses. It is anticipated that simplified software solutions will become available in the near future.

### 1.1.2 Instrument requirements for GC×GC–MS

In order to provide effective sampling of the first-dimension effluent, the second-dimension separation speed in GC×GC has to be very fast. It is desirable to obtain 3-4 samples of each individual component for analysis on the second-dimension column to enable correct peak reconstruction in the two-dimensional chromatogram for accurate identification and/or quantification [12].

Frysinger and Gaines were first to demonstrate GC×GC–MS in 1999 [4]. Noting experimental challenges in their initial investigation, which were primarily

related to the slow acquisition rate of the MS used in the experiments, the first approach for implementing the GC×GC–MS system was realised by slowing the typical analysis speed of the first-dimension separation by a factor of approximately seven times, with concomitant reduction of second dimension throughput in the order of five times. The first reported GC×GC–MS chromatogram depicting the separation of a marine diesel sample is shown in Figure 1.2. The separation was achieved using a 13 m × 0.10 mm i.d. first-dimension column with a thick film (3.5 μm) 100% dimethylpolysiloxane stationary phase coupled to a 2 m × 0.10 mm 14% cyanopropyl methylpolysiloxane stationary phase column installed in a thermally modulated GC×GC system.

The experimental difficulties that Frysinger and Gaines described clearly portray the importance of high-speed detectors for GC×GC–MS. Notwithstanding the valuable illustration of GC×GC–MS, the detection rate of 2.43 full-scan spectra/s meant that the nearly 1 s wide second-dimension peaks were severely under-sampled. In the example given here an average of only one full-scan mass spectrum was recorded for each second-dimension peak. Although the reconstructed two-dimensional separation space provides a representation of the GC×GC separation there are insufficient data points recorded to faithfully portray the chromatographic result and permit measurement of important chromatographic metrics such as peak-area, height, width, asymmetry and resolution.

A list of accepted peak-widths associated with different GC separation speeds is presented in Table 1.1. The importance of data density being compatible with the chromatographic timescale is illustrated in Figure 1.3 where Gaussian peaks have been generated using the retention times and peak widths shown in Table 1.1. Three

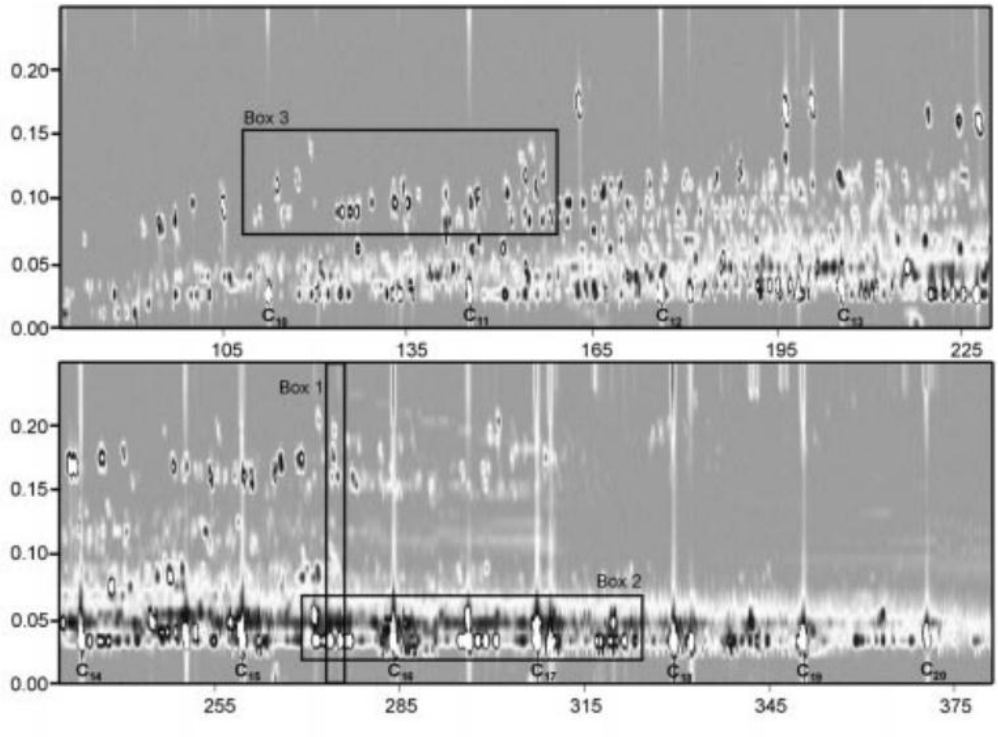


**Figure 1.2. GC×GC–MS total ion current chromatogram of a marine diesel fuel sample. Reprinted with permission from [4], copyright 1999, Wiley-VCH Verlag GmbH & Co. KGaA.**

**Table 1.1 Characteristic figures of merit for fast GC analysis. The second-dimension separation speed for GC×GC–MS typically fits the very-fast category [13].**

| Separation Speed | Column i.d. (mm) | Column Length (m) | Theoretical Plates | Retention Time (s) | Peak Width 2.354 σ (s) |
|---|---|---|---|---|---|
| *Standard* | *0.32* | *25* | *75,000* | *100* | *0.7* |
| *Fast* | *0.05* | *10* | *260,000* | *60* | *0.2* |
| *Very Fast* | *0.05* | *1* | *24,000* | *2* | *0.03* |
| *Ultra Fast* | *0.05* | *0.3* | *6,500* | *0.3* | *0.01* |

data acquisition rates are provided with the data points superimposed on each peak to illustrate the capabilities of a range of instrument types. First, 4 Hz represents the full-scan mass spectrum acquisition that is easily achieved by most quadrupole mass analysers. This data acquisition rate is suitable for conventional GC but it is hardly sufficient for fast-GC and very few full-scan spectra per peak will be collected using this instrument configuration with a fast-GC separation. The physical laws governing mass selection processes limit the ability of quadrupole mass spectrometers to achieve very fast data acquisition rates on par with those available with TOF instruments. A quadrupole MS passes ions of various *m/z* (one *m/z* at a time) to the detector by simultaneously ramping direct current (DC) and radio frequency (rf) voltages carried by the quadrupole rods. Contemporary quadrupole MS instruments are capable of mass scanning rates of up to 20,000 *m/z*/s. For a full scan mass range of 50-350 *m/z*, the maximum spectral acquisition rate would be expected to be less than 60 spectra/s (including an inter-scan period). Although these figures have improved considerably over the last decade, there is a limit to the scanning speed because transmission of the selected ions is affected if the rf and DC voltages change during the transit time of an ion through the quadrupole [14]. Very-fast GC is best mated with non-scanning time-of-flight mass spectrometry (TOFMS), which is capable of very fast full-spectrum data acquisition rates. Figure 1.3 shows that acquisition of 50 spectra/s will suffice for fast GC, but ultra-fast separations demand even faster data acquisition. Generally speaking, 50-100 spectra/s is applicable for GC×GC–MS analysis.

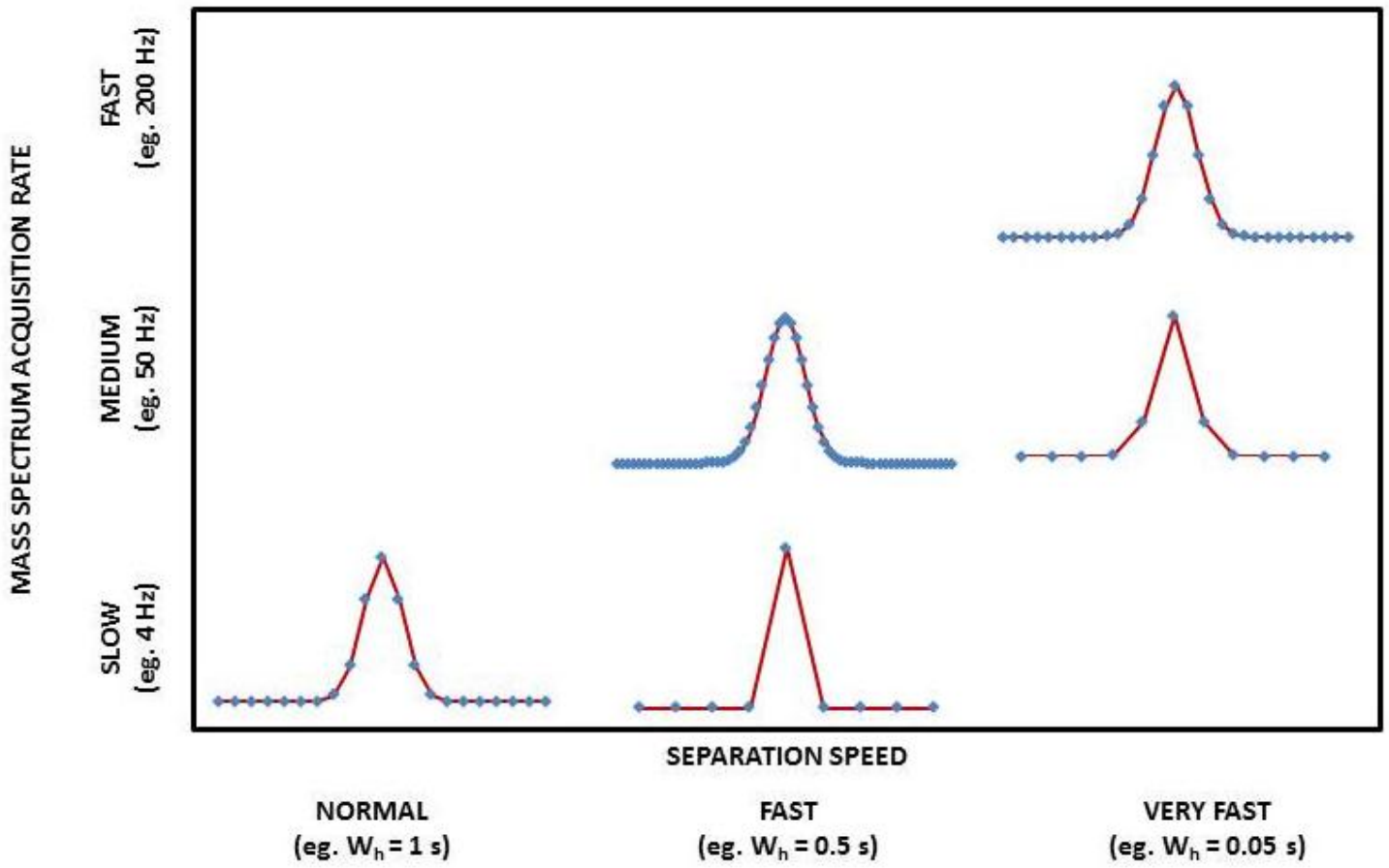


**Figure 1.3. Illustration of the detection requirements for GC×GC–MS. At normal separation speeds, the ideal peak shown above has sufficient data points. However, as separation speed increases, the mass spectral acquisition rate must increase similarly to avoid excessive interpolation of peak characteristics.**

### 1.1.3 Quadrupole MS

Following Frysinger and Gaines' introduction of GC×GC–MS there were no reports in the periodical literature regarding hyphenation of GC×GC with quadrupole instrumentation until 2002. This apparent lack of activity can be almost completely ascribed to the speed limitations of MS detection systems. However there is an alternative approach for coupling quadrupole MS instrumentation with GC×GC that does not depend on slowing the GC×GC analysis excessively but this is achieved at the expense of sacrificing some MS information to overcome the inherent spectral acquisition rate limitations. In 2002, Shellie and Marriott described an enantioselective-GC×GC experiment using a quadrupole mass analyser in single-ion selected ion monitoring mode with a nominal data acquisition rate of 20 spectra/s [15]. Although faster, this detection regime lacks information richness due to the loss of almost all mass spectral information. The experiments that Shellie and Marriott performed were designed to utilise the vacuum outlet condition of the MS detector to capitalise upon the theoretical efficiency benefits of low-pressure GC [16]. The dynamic diffusion coefficient of an analyte in the carrier gas and optimum carrier gas linear velocity are inversely proportional to the column pressure, so vacuum-outlet operation may offer speed and efficiency benefits over atmospheric-outlet operation under certain conditions [16]. In a later study, Shellie and co-workers attempted full-scan detection [17]. With the initial experiments aimed at characterisation of volatile plant extracts comprising terpenoid compounds, a reduced mass-scan range from 41-229 *m/z* was deemed appropriate since this permits detection of molecular ions of mono- and sesquiterpenes as well as the oxygenated monoterpenes [18]. The speed advantage attainable by reducing the mass range can be estimated by considering the

quadrupole duty cycle divided by the mass range. The absolute data acquisition rate will be less than this because the inter-scan delay must also be considered. By using a mass analyser with a maximum scan speed of 4,000 *m/z*/s and a mass scan range of 188 *m/z*, a data acquisition rate of approximately 20 scans/s is attainable [19]. Whilst the data acquisition rate was relatively slow compared to conventional GC×GC applications with fast detection, giving only ~ 4 data points for each narrow second-dimension peak, the quality of the spectra for the separated components was reportedly very high [17, 19].

Interestingly, by speeding up the detection rate as descried above, the total GC×GC–MS analysis times reported by Shellie and co-workers were only about 30% longer than the programmed solvent delay of the GC×GC–MS system reported by Frysinger and Gaines using rather similar equipment. The GC×GC–MS chromatogram of *Pelargonium graveolens* essential oil analyzed using a 30 m × 0.25 mm i.d. non-polar (5% diphenyl 95% polydimethylsiloxane) first-dimension column coupled to a 0.5 m × 0.32 mm i.d. polar (polyethylene glycol) second-dimension column is shown in Figure 1.4. The research performed in these early studies, combined with the continual speed improvements being made to contemporary quadrupole instruments themselves have provided impetus for further application of GC×GC–MS using quadrupole MS instrumentation [5, 20-23]. The key results from these investigations are further expanded later in this chapter.

### 1.1.4 Time-of-flight MS

The major advantage TOFMS has over other MS technologies is that a complete spectrum is produced at the detector for every pulse of ions from the ion source. In addition the spectral acquisition rate is essentially determined by the

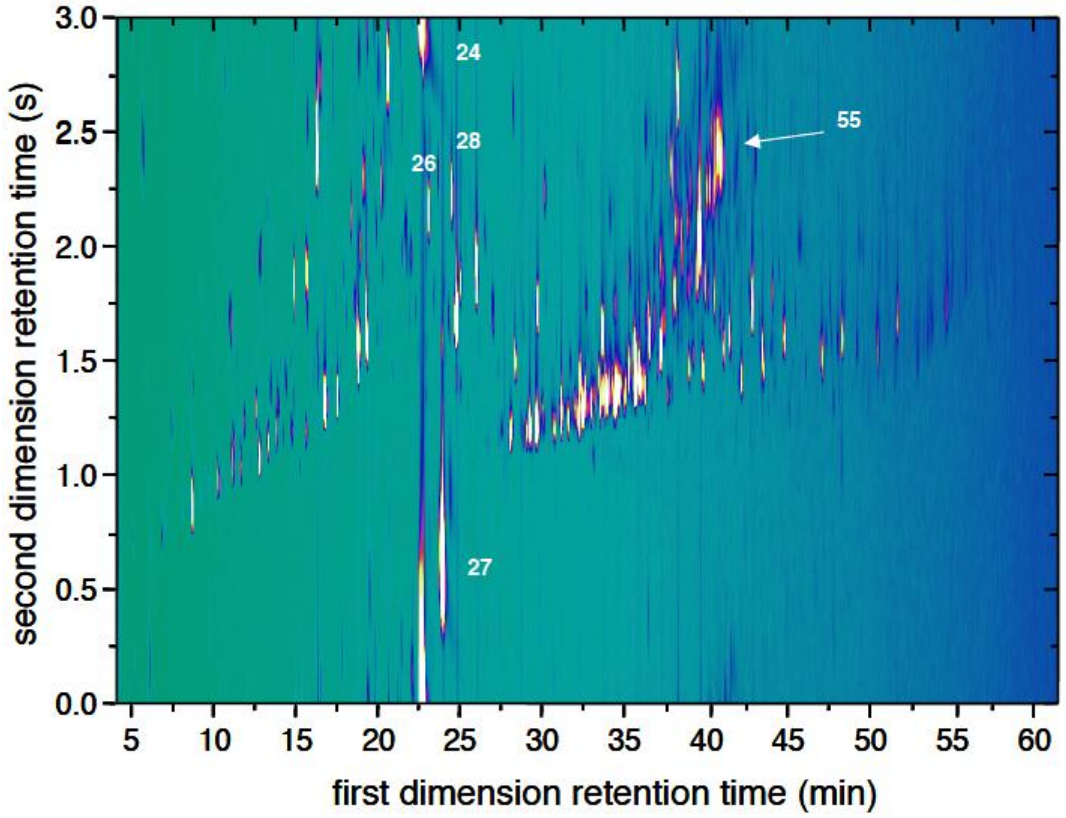


**Figure 1.4. GC×GC–MS analysis of *P. graveolens*. Reprinted with permission from [17], copyright 2003, The Royal Society of Chemistry.**

transit time of the heaviest ion in the mass spectrum, so very fast data acquisition is possible. Consider an ion of 800 *m/z* with an applied acceleration potential of 2,000 V; the ion will take approximately 90 μs to travel from the source to the detector in a 2 m flight tube [14]. In this example the instrument could acquire a full spectrum from 0 to 800 *m/z* every 90 μs, which equates to a spectral acquisition rate in excess of 11,000 spectra/s.

The first illustration of GC×GC–TOFMS confirmed the suitability of this detection system for GC×GC analysis [24]. In a preliminary investigation, van Deursen and co-workers performed a sub-1 s separation of a mixture of compounds spanning the volatility range $C_5$-$C_8$ in a one-dimensional approach to simulate a second-dimension separation. A cryogenic focussing system was employed in the injection system based on previous research [25] and peak widths as narrow as 12 ms were reported. Using a very high scan rate of 500 Hz, good agreement was observed between sample and library spectra, suggesting that the chromatographic speed and acquisition speed were in agreement. The same authors followed this research with the first illustration of GC×GC–TOFMS to perform group-type identification of petroleum samples [24]. The column set consisted of a 10 m × 0.25 mm i.d. DB-1 column in the first dimension and a 0.7 m × 0.10 mm i.d. BPX-50 column in the second dimension. A Zoex thermal sweeper modulator was employed in conjunction with a 0.7 m × 0.10 mm i.d. SE-30 modulation capillary. The TOFMS was obtained from Leco and was operated at 50 Hz. This frequency was reportedly sufficient and avoided generating file sizes too large to be handled properly.

A total ion current (TIC) chromatogram from the separation of a kerosene sample from this study is shown in Figure 1.5 [24]. As shown, the total run time was 73 min with a 7.5 s modulation period. This plot was produced using in-house

developed software. A second-dimension chromatogram from the GC×GC–TOFMS separation of kerosene is also shown in Figure 1.5 illustrating the class separation of alkanes (1), mono- (2) and di-naphthenes (3,4) from mono-aromatics (5-8). Of particular interest here is the residual peak-overlap in the second-dimension column, because the synergistic relationship between chromatographic and mathematical separation is highlighted. Even the best GC×GC separation will not separate the most complex sample; likewise the best de-convolution algorithm will fail if there is no chromatographic separation (with the caveat being that we are speaking of low-resolution MS). Fortunately in this example, the carrier gas velocity in the second-dimension column was close to optimum and the column efficiency was calculated to be approximately 4000 plates. This is significantly lower than the theoretical plate number of such a column, but it was thought that this resulted from insufficient zone focusing of the re-injected analyte plug on the second column delivered by the thermal sweeper modulator. Despite this deviation from the optimum efficiency, the response from eight partially resolved second-dimension peaks could still be successfully deconvolved from the separation, based on the highly reproducible spectra generated.

In 2001, Shellie and co-workers discussed the separation of an essential oil sample using GC×GC–TOFMS [26]. They utilised cryogenic modulation to generate the two-dimensional separation and reported excellent applicability of the approach to their sample.

Enhancements and developments of the technique have led to the almost routine application of GC×GC–TOFMS for a suite of analysis situations. The key results from investigations employing GC×GC–TOFMS are highlighted later in this chapter.

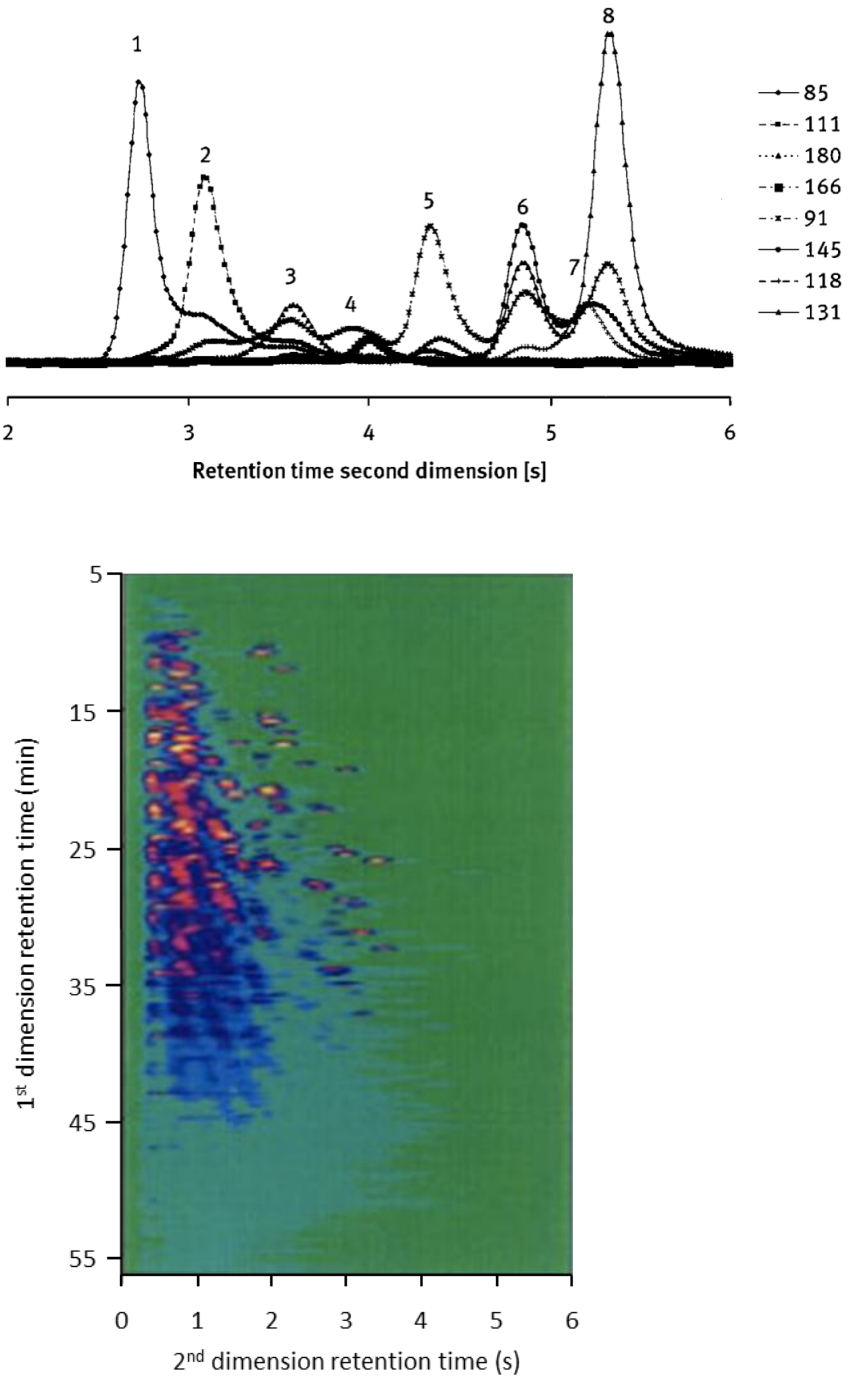


**Figure 1.5. An example of a second-dimension chromatogram from the analysis of kerosene using GC×GC–MS with the unique ion traces of each compound shown separately (top). Full GC×GC–TOFMS chromatogram of kerosene (below).**

**Reprinted with permission from [24], copyright 2000, Wiley-VCH Verlag GmbH & Co. KGaA.**

### 1.1.5 Data Processing of GC×GC–TOFMS Results

Following the first demonstration of a GC×GC–TOFMS analysis, Dalluge and co-workers optimised and characterised the technique [27]. Temperature programming, column selection, modulation temperature, time and frequency and reported analytical performance data were discussed in detail. A key part of their findings incorporated the difficulties imposed by the quantity of data generated from separations and how these are handled. Early GC×GC–TOFMS studies were plagued by troubles associated with large data files. A 73 min GC×GC–TOFMS analysis was reported to have collected $2.1 \times 10^5$ mass spectra (over 100 Mb of data), where a data acquisition rate of 50 spectra/s was used [24]. At the time of publication, no automated data handling was available and the screening of analysis results was laborious.

One of the setbacks encountered in peak assignment in GC×GC–TOFMS stems from the production of a two-dimensional chromatogram utilising a single detector collecting a one-dimensional signal array. As such, the time of primary elution and secondary injection are not recorded, making correct assignment of retention time significantly more difficult than in a one-dimensional separation. Should a component be strongly retained on the second-dimension column, its secondary retention time may be greater than the modulation period, causing the effect of wrap-around which may introduce ambiguity in the correct assignment of peaks. While prediction of retention times in two-dimensional separations have been successful [28, 29], Micyus and co-workers reported the noteworthy development of an algorithm to determine the absolute retention time of wrapped-around analytes in 2005 [30]. Despite not being specifically geared for GC×GC–TOFMS data, it could be described as an intermediate step towards fully automated data analysis for this

technique. The group based the research on a 30-year-old algorithm used for the automatic range estimation in multiple pulse radar [31]. The algorithm was examined both theoretically and experimentally through a series of one-dimensional and two-dimensional separations to verify the predicted retention time values. The group showed that the use of the algorithm in conjunction with a slight increase in the modulation period of a two-dimensional separation allowed accurate determination of the second-dimension retention time. In one extreme example, the retention time of a compound undergoing six wrap-around cycles could be accurately determined by repeating the injection with a 14% increase in modulation time.

Hoggard and co-workers have investigated an automated method for applying parallel factor analysis (PARAFAC) to complete GC×GC–TOFMS chromatograms for peak assignment and resolution [32]. The use of chemometrics techniques in comprehensive multidimensional GC is covered later in this chapter, but in brief, the group could correctly identify and assign both fully and partially resolved peaks without resorting to a labour-intensive manual approach. This greatly reduces the time required for comprehensive analysis and processing the large data files and is a step towards routine application of the technique.

### 1.1.6 Method translation in GC×GC–MS

Method translation is widely used by GC and GC–MS practitioners to permit transfer of a chromatographic method between different GC systems. The underlying concept involves varying instrument components or settings in such a way that the peak elution pattern for a sample can be retained [33]. Method translation permits reduction of analysis time, conversion of a method to an alternative carrier gas or transfer between ambient and vacuum outlet, ie. translation between FID and MS

detection. The key unit for method translation is the void time and effective translation can be achieved by scaling the temperature program to this value. Naturally, there are a number of essential criteria that must be fulfilled, the mathematical underpinnings of which are discussed at length in the literature [33-36]. To briefly summarise, translatable methods must have the same stationary phase coating and phase ratio, the column cannot be overloaded and the inlet and outlet pressure of the column cannot change during the run [33]. It is the final point of this summary which is of most interest in the current study. To generate a pressure gradient through the column that does not change with time (and therefore temperature, for temperature programmed separations), it is imperative that constant pressure mode be used for the separation. It is for this reason that constant pressure mode has been predominantly adopted for separations performed in this thesis.

An extension of method translation theory involves maintaining an equal retention time for components of a mixture across multiple chromatographic methods, usually involving different column dimensions. This technique is known as retention time locking (RTL) and can be desirable for GC×GC separations should the aim include profiling of a complex mixture or a similar outcome. Shellie and co-workers performed an in-depth examination into the RTL in GC×GC separations and reported that comparison of GC×GC–MS and GC×GC–FID chromatograms of ginseng extracts in a set of experiments which used the same nominal average linear velocity with the same column set moved between the MS and FID equipped instruments yielded marked differences in retention times [19]. The impediment to achieving matched retention times comes about *via* the dissimilar column outlet pressures of the two types of detectors. Different outlet pressure is easily accounted for in one-dimensional separations, but changes in outlet pressure affect the pressure

at the interface between the first and second-dimension columns and can make it more difficult to retention-time-lock GC×GC chromatograms. This challenge is exacerbated when dissimilar carrier gases are used to perform the GC×GC–FID and GC×GC–MS separations and retention time locking requires careful adjustment of the pressure drop across each section of a GC×GC coupled column set [37]. In practice this can be achieved by using a tee-union at the end of the second-dimension column and provide electronic pressure control of BOTH the inlet and outlet of the GC×GC column set. Under this arrangement it is possible to obtain near-matching retention in GC×GC–FID and GC×GC–MS [37].

### 1.1.7 GC×MS

The use of soft ionisation allows a two-dimensional GC×MS separation without recourse to specialised modulation instrumentation. Hard ionisation techniques frequently generate multiple ion fragments for each analyte. In the case of similar members of a compound class, the fragmentation pattern may be conserved between analytes, providing little, if any, separation information from the MS for such compounds. In contrast, soft ionisation techniques produce fewer fragments for each compound reaching the detector; in many cases only a molecular ion is generated. The potential for the fragmentation pattern to be retained between members of a compound class is greatly reduced. This is reflected as a comparable separation step to a non-polar second-dimension column in a comprehensive two-dimensional system, as the higher mass analytes in a complex mixture generally have lower boiling points [38].

Obviously, several critical parameters must be met to allow such a separation, most notably the amenability of the sample to soft ionisation. The most common soft

and selective ionisation methods for gaseous compounds are: i) Chemical Ionisation, where the analyte molecules are ionised by ion-molecule chemical reactions, ii) Field Ionisation, wherein very high electric fields in close proximity of an emitter needle ionises gas phase molecules, and iii) Photo-Ionisation, where ionisation is achieved by means of absorption of ultraviolet photons. Zimmermann and co-workers recently reviewed the use of photo-ionisation mass spectrometry as a detection method for one-dimensional and comprehensive two-dimensional gas chromatography [39].

Wang and co-workers presented the first example of this comprehensively-coupled approach in 2005 [40] based on the groundwork provided by coupling of GC and soft ionisation MS in 2002 [41]. Wang utilised a TOFMS equipped with field ionisation coupled to a GC for the separation of a diesel sample. A modulation device is not required in this technique as there is only a single chromatographic separation step.

In simplified terms, the use of a soft ionisation MS generates a separation of molecules based on their size. Should a non-polar column be used for the GC dimension, which possesses selectivity for analyte boiling point, a strong correlation would be witnessed between the two dimensions due to the relationship between boiling point and molecule size. Such an approach would not be orthogonal, and the resultant chromatogram would show negligible information in the second dimension separation space.

By using a polar GC column in the GC×MS experiment, additional selectivity, based on dipole moment, is introduced in the GC dimension. This reduces the correlation between the GC and the MS separations, generating a sufficiently orthogonal separation. ‘Linearisation’ is often required to make the chromatogram resemble a conventional GC×GC plot, as shown in the example in Figure 1.6.

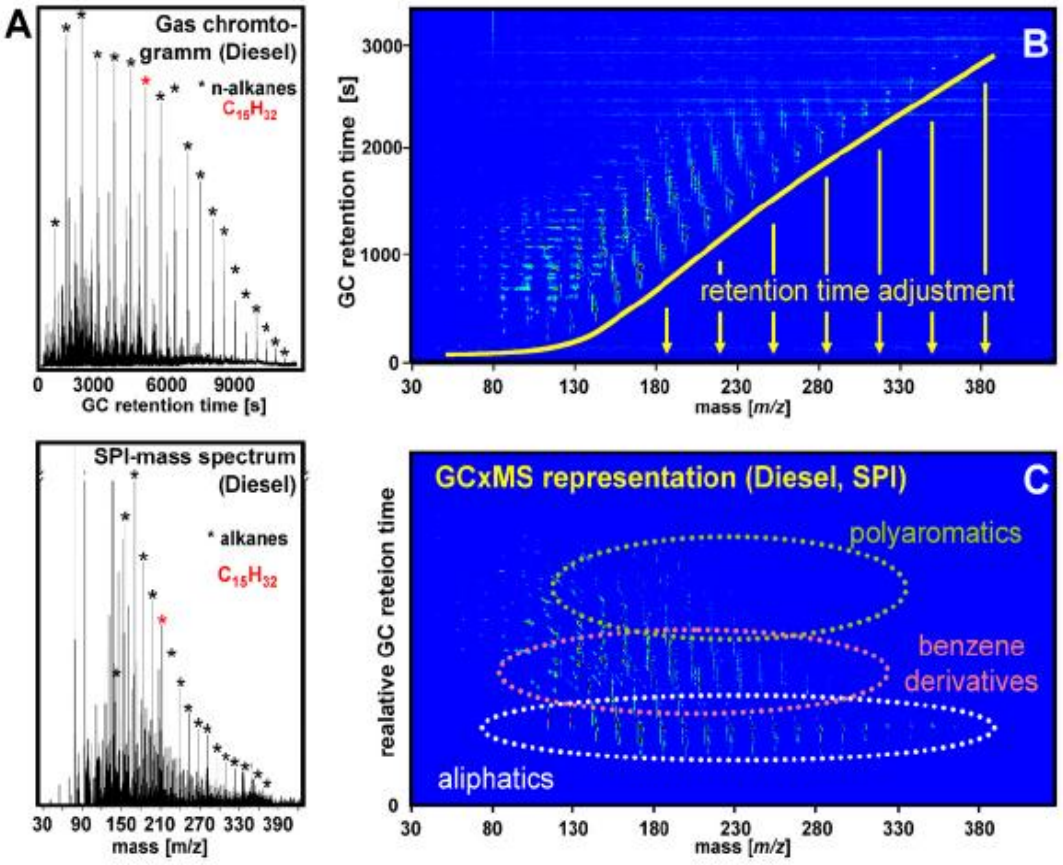


**Figure 1.6. Experimental results from a GC–laser SPI-TOFMS coupling. (A) Demonstration of the separation-similarity of a gas chromatogram using a non-polar column (TIC of Diesel GC–MS chromatogram with EI ionisation, top) and a soft ionisation mass spectrum (SPI mass spectrum of diesel obtained by summing up all mass spectra of a GC–SPI–MS run, bottom): the homologue row of the alkenes is indicated by asterisks, respectively. (B) Two-dimensional retention time/molecular mass-representation of a GC–SPI–TOF–MS run. The course of the *n*-alkanes is indicated by the continuous line. By transformation of the representation according to the indicated arrows one obtain the GC×GC–plot shown in (C). (C) Comprehensive two-dimensional GC×MS representation generated from (B) by "linearisation" of the *n*-alkane row, exhibiting similar "separation" properties as classical GC×GC.**

**Reprinted with permission from [39], copyright 2008, Elsevier.**

A transformation is required to plot the data in a manner which resembles a typical GC×GC separation obtained using an apolar-polar column set. The conversion of GC×MS data in this way allows the visualisation of the compound classes in a manner that is not possible with conventional GC–MS techniques, permitting a simpler fingerprinting method for class identification to essentially the same degree as a GC×GC separation. The procedure follows the illustration presented in Figure 1.6. In essence, the retention time axis is transformed in a way that the *n*-alkanes present in the sample are aligned parallel to the *x*-axis. By plotting the results according to time *vs*. mass, compound class separation information can be revealed.

Wang reported that the separation of individual compound groups within classes is easier using GC×MS than GC×GC due to the similarity in relative polarity provided by the latter technique. Furthermore, because only the molecular ions of many compounds are collected, individual chromatograms of sulfur or nitrogen containing compounds can be extracted in a similar manner to the single ion monitoring mode used in GC–MS. This feature would require the use of an element specific detector in conventional GC×GC–MS as established by Ochiai and colleagues in 2007 [23].

Other soft ionisation methods have been examined for GC×MS. Welthagen [42] used laser photo-ionisation coupled with TOFMS to perform a similar separation to Wang and followed up with the extension of the GC×MS approach by coupling the photo ionisation to a GC×GC system to give a true three-dimensional GC×GC×MS separation. Figure 1.7 provides a schematic of the instrument setup for GC×GC×MS with a typical result from the GC×GC×MS separation of a diesel sample. Three largely orthogonal separations can be achieved by combining a

carbowax column in the first dimension for separation according to “polarity”, a 50% phenyl 50% methyl polysiloxane second-dimension column for separation according to “polarisability” and soft-ionisation MS mimicking a “volatility” separation [42]. The primary limitation observed with the technique was the frequency of the ionisation laser, which limited spectral acquisition to 5 Hz and was not sufficient to generate five data points per peak for the early eluting compounds. As such, optimisation of the technique was hampered and the chromatographic steps were operated outside the most desirable parameters but the feasibility of such an application was critically examined. It was proposed that the use of a vacuum UV photo-ionisation method would enable continuous data acquisition and eliminate the problems encountered in the published study.

While the publication of further applications of this technique have been limited in comparison to the abundance of traditional two-dimensional GC techniques, research is continuing especially in the area of novel applications for the technology [43].

### 1.1.8 Modulation techniques for GC×GC

For a GC×GC separation to be differentiated from a coupled column separation, the information collected from the separation of the sample on the first-dimension column must be retained throughout the experiment [44]. This process is carried out by the modulation interface.

GC×GC is widely achieved by using thermal modulation devices. Thermal modulation interfaces can be broken down into either cryogenic or heating techniques. The former technique relies on the application of a cryogen to rapidly cool first-dimension column below that of the GC oven . This effectively traps

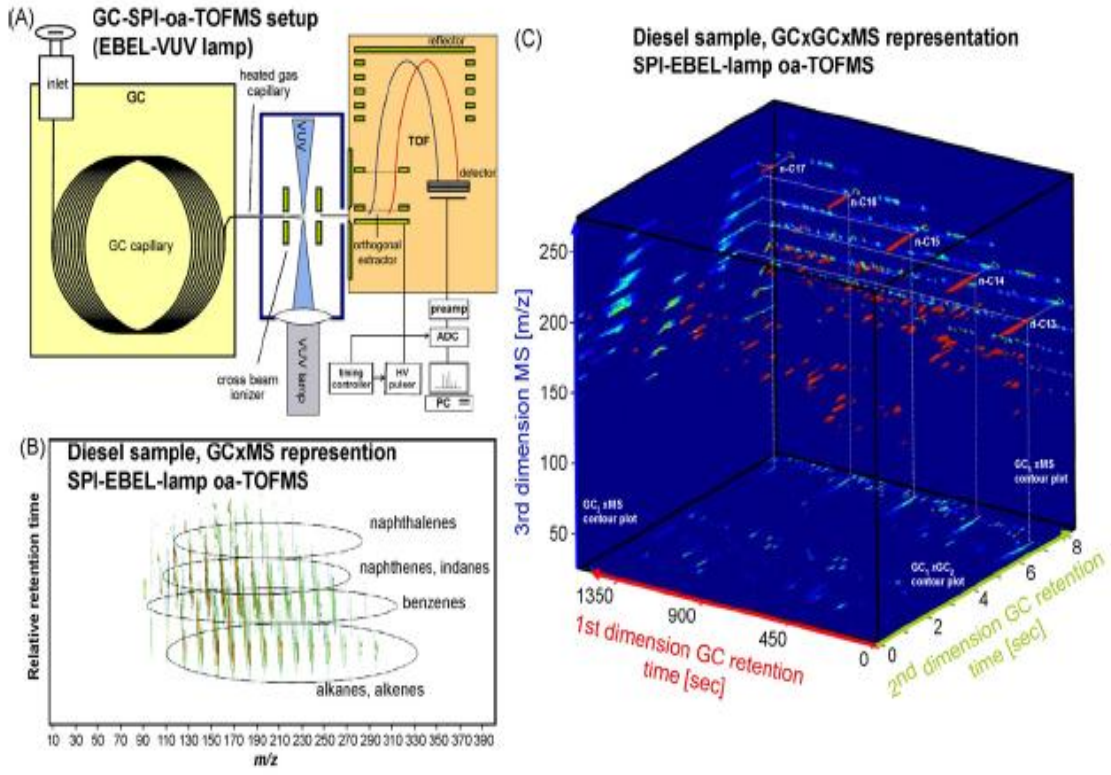


**Figure 1.7. (A) Experimental setup of the gas chromatography SPI-oaTOF-MS instrument. SPI is performed in a separated ionisation chamber with 126 nm photons from the Ar filled EBEL VUV lamp. (B) Comprehensive two-dimensional GC×MS representation obtained from a gas chromatographic analysis of a diesel sample with EBEL VUV-lamp for SPI. (C) If GC×GC is combined with soft SPI-TOF-MS, a three-dimensional comprehensive separation can be realised. The figure depicts a section of a GC×GC×SPI-MS separation of a diesel sample using the EBEL VUV lamp technology (Ar, 126 nm) for SPI. The position of the *n*-alkanes is indicated.**

**Reprinted with permission from [39], copyright 2008, Elsevier.**

'packets' of first-dimension effluent either in a transfer line between the first- and second-dimensions or on the head of the second-dimension column. Reheating the transfer line by cessation of cryogen flow or movement of the modulator causes rapid remobilisation of trapped analytes onto the second-dimension column. At the time of writing, cryogenic modulators are commercially available from companies including Thermo Scientific, Zoex, Leco and Chromatography Concepts. No doubt this list will grow as the uptake of the technology increases.

The strength of thermal modulation is the inherent focussing of trapped analyte plugs within the modulator. This involves the concentration the effluent fraction from the first-dimension column prior to reinjection and allows the injection band width to be very low (typically under 60 ms) and band broadening on the second column to be minimised. These factors are highly beneficial for analysis of complex samples as the reduction of band broadening increases the potential resolution between components. Sensitivity may also be increased by a factor of 10-30 fold [45].

The alternative thermal modulation approach relies on the trapping of analyte packets in a capillary stationary phase, often at room temperature, followed by their rapid remobilisation by the application of heat. This technique predates the use of cryogenic thermal modulators. In the seminal research conducted by Liu and Phillips in 1991 [45], an 'accumulator' transfer line was installed between the two dimensions, which was coated with a thick film stationary phase, promoting strong retention of the analyte packets. The outer surface of this capillary was coated with a conductive paint, allowing resistive heating to occur upon the application of a current. This allowed the trapped analytes to be remobilised onto the second-dimension column. Further iterations of this design followed, yielding satisfactory

results [46-48], although it was reported that the conductive paint coating was not very robust, nor the results reproducible. The thermal modulator evolved over time, resulting in the development of the thermal sweeper modulator [49, 50]. Similar to the resistively heated methods, a thick film accumulator was employed, but in this instance heating was performed by a rotating fork-like 'sweeper' which passed across the accumulator at intervals defined by the modulation frequency. A good comparison of the two techniques was presented by Marriott and co-workers in 2000 [51] and a summary presented in ref. [52]. The sweeper progressively remobilised trapped material onto the second-dimension column. It was noted that installation of the accumulator within the oven necessitated lower than desired temperatures (in the order of 100 °C) to allow a satisfactory temperature differential to be realised. This led to difficulties in rapidly desorbing trapped semi-volatile compounds and effective trapping of compounds with higher volatility. Furthermore, alignment of the moving sweeper proved difficult and the technique became maligned. This discrimination is somewhat unjustified, as demonstrated by the recent thermal modulator development published by Panic and co-workers [53]. This group employed a flattened Silcosteel® capillary, partially coated with a PDMS stationary phase, for the analysis of semi-volatile organic aerosol compounds. Low injection bandwidths and good separations were reported for compounds spanning the large volatility range between *n*-C5 to *n*-C40. Key to their success was the unique method for flattening the capillary, in addition to the selective removal of a section of stationary phase coating in the centre of the trap. This effectively created two independent sections, which could be heated independently. Furthermore, application of forced air cooling to the capillary enhanced the trapping of the more volatile components without compromising the effectiveness of the device for rapid mobilisation of semi-volatile components. Cold

spots generated by increased thermal mass around the electrical contacts were initially eliminated by the use of a hairdryer, and a subsequent modification to the way in which the contact was attached to the capillary generated even better results. Injection bands were in the order of 60 ms wide, with peak widths of 120 ms at half height. For reference, earlier methods [45, 54] reported peak widths of approximately 350 ms at half height. The robustness of the modulator was excellent, with an expected lifespan of up to 3 months if used for around 8 h per day.

With the current trend towards smaller, more economical instrumentation, traditional "total-loss" cryogenic modulators may not be appropriate for many applications in the modern laboratory. This has pushed the focus of hardware development towards consumable-free GC×GC systems, such as those presented by Panic [53]. Additionally, the use of pneumatic modulation devices has provided further avenues for research.

Bruckner and co-workers presented a paper in 1998 detailing the novel use of a 6-port nitrogen-actuated diaphragm valve to transfer 50 ms wide pulses of effluent from the first dimension to the second-dimension column [55]. The valve was operated twice per second and sampled approximately 10% of the column effluent. Seeley's group presented a seminal publication in 2000 which further developed the idea of a multi-port diaphragm valve as a modulation device [56] based on a previous application in two-dimensional liquid chromatography [44]. He utilised all six ports of the valve (unlike Bruckner's use of four ports) and incorporated a sample loop to collect column effluent prior to transferral to the second-dimension column. This allowed the first-dimension column sampling to increase to approximately 80%.

While the idea of flow modulation was not new [57], Seeley coined the term 'differential flow modulation' to describe the novel approach, based on the key

aspect of the technique. To effectively modulate the first-dimension effluent, the secondary column flow must be maintained at least 20 times higher than the primary flow. This requirement comes about because valve based modulation techniques are inherently lacking in the zone focussing effects witnessed with thermal modulation. Upon switching the valve from the 'collect' to the 'inject' position, the contents of the sample loop are transferred as a discrete package with a width of around 5% of the collection time. Seeley suggested that if moderate band broadening is assumed, the peak flux eluting from the second-dimension column is still greater than that of the first-dimension column as a result of the flow differential [56]. This high flow rate is not compatible with the vacuum systems of common mass spectrometers, suggesting the technique may be unsuitable for such an application.

A further limitation of this modulator is the temperature sensitivity of the valve which forces it to be located outside the oven and not be subjected to temperatures above 125 °C [56]. Sinha and co-workers presented the application of a valve-based modulator for GC×GC–MS in 2003, using careful valve placement allowing the working temperature range of the instrument to be increased to 250 °C [58]. It was necessary to utilise a mere 10% of the primary column effluent for second-dimension analysis, which naturally had an adverse effect on the available sensitivity. Detection limits were still acceptable however. Diehl and Di Sanzo [59] also used an open split arrangement in their valve-based modulator.

Seeley and co-workers presented an alternative differential flow modulation method in 2004 based on tee unions installed inside the GC oven [60]. A solenoid valve controlling the second-dimension carrier gas flow was located outside the oven and was not in the sample path, eliminating the temperature restrictions of previous valve-based systems. A GC×2GC arrangement was utilised (dual second-dimension

columns emanating from a tee union after the modulation device) and total transfer of primary column effluent to the secondary columns was observed. Further development of the device ensued [61], with the authors also introducing a less complex form of the device [62].

To circumvent the low carrier flux dictated by conventional mass spectrometers, Amirav and co-workers examined the performance capabilities of a unique kind of differential flow modulated GC×GC–MS based on direct coupling with a supersonic molecular beam (SMB) interface in 2007 [63]. Unlike most GC–MS interfaces, SMB-MS requires a high helium flow (typically 90 mL/min) for proper operation [64]. Under this general interface configuration the coupling of GC×GC with tandem mass spectrometry was later introduced with practical demonstration of the analysis of pesticides in vegetable matrices [65]. While the application of this technique was a resounding success, it was duly noted that it was primarily a target method, which is not suitable for all samples, and the technique was incompatible with library detection. In Figure 1.8, Amirav's GC×GC modulator is shown inside the oven of a Varian 3800 GC which is hyphenated with a Varian 1200-I triple quadrupole-based MS with SMB. Amirav called his technique 'pulsed flow modulation'.

In 2008, Shellie described GC×GC–MS results that were acquired by direct coupling of a pulsed flow modulation system with a quadrupole MS of high pumping capacity [66]. The instrument utilised was capable of handling up to 15 mL/min input which allowed the use of helium carrier gas at around 10 mL/min through the second dimension. Tea tree (*Melaleuca alternifolia*) and hop (*Humulus lupulus*) essential oils were examined using a (7.5 m × 0.10 mm i.d.) × (1 m × 0.32 mm i.d.) polar/non-polar column set. Shellie reported that despite the use of a high flow rate, the hold-up

time of the second dimension was at least double that of a comparable thermally modulated GC×GC system, causing broader peaks and increased analysis time. A detector acquisition rate of 33.33 Hz was utilised and this provided sufficient for peak detection and qualitative identification. While this research clearly showed the potential of pulsed flow modulated GC×GC–qMS, the separations obtained could be described as satisfactory at best and certainly not possessing comparable efficiency or resolution of similar thermally modulated separations. Additionally, Harvey and co-workers have recently published a dynamic flow model which is capable of predicting carrier gas flow rates and pressure requirements for pulse flow modulated GC×GC [67]. Their research suggests improvements to current modulator design, including the use equal internal diameter tubing for modulator construction, which improves baseline stability and improved robustness and modulation period flexibility through appropriate selection of restrictors at both ends of the first-dimension column. A separation of Special Antarctic Blend diesel was presented using the optimised system at two different modulation periods exhibiting the flexibility available with restrictors in place.

In brief, the coupling of comprehensive two-dimensional gas chromatography with mass spectrometry has provided means to enhance the separation space available for characterisation of samples considered too complex for one-dimensional analysis. This section has compared and contrasted one- and two-dimensional approaches and discussed the hardware choices utilised for comprehensive techniques, in addition to data processing and aspects of method translation. The literature referenced in this section has provided a solid basis for the research presented in later chapters of this thesis, which emphasises the use of pneumatic modulators in conjunction with quadrupole mass spectrometry. The

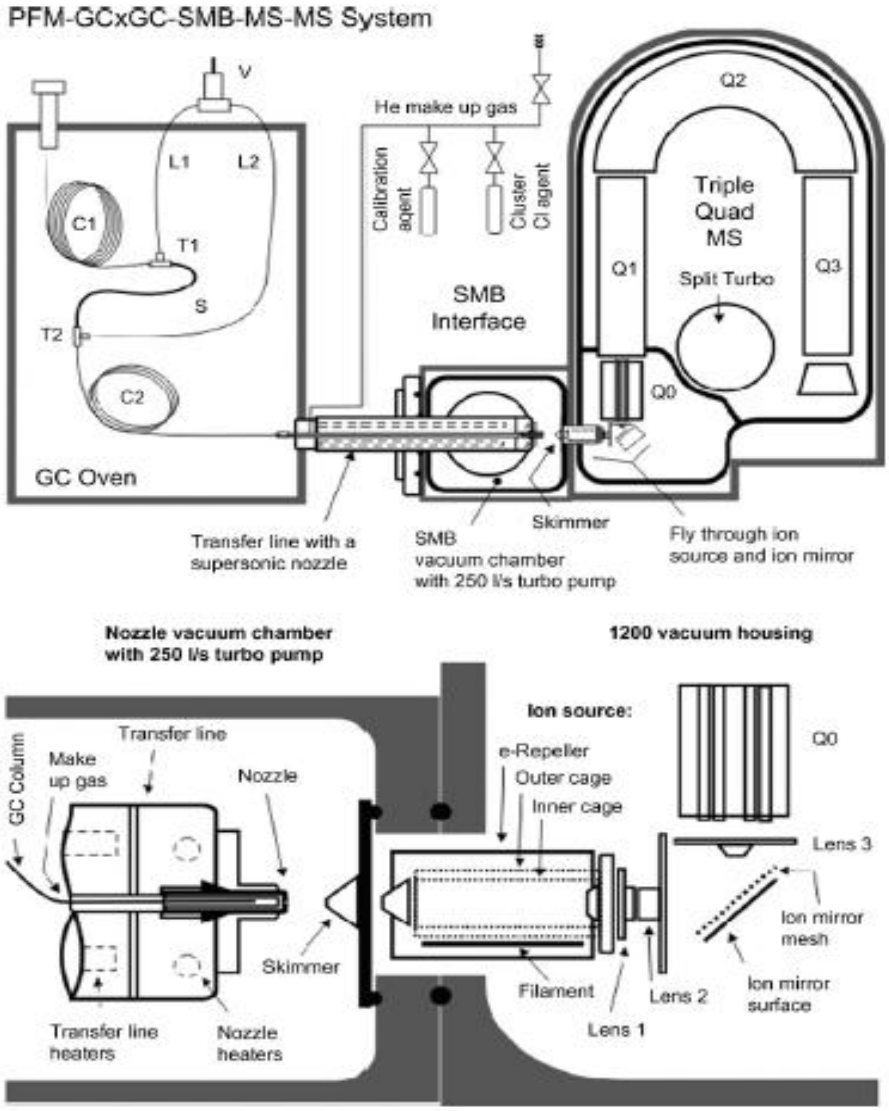


**Figure 1.8. Pulsed flow modulation set-up for GC×GC–MS (and GC×GC–MS–MS) with supersonic molecular beams inside a Varian 3800 GC. The bottom schematic diagram shows the SMB interface and its fly-through ion source at the entrance to the 1200 triple quadrupole MS system.**

**Reprinted with permission from [65], copyright 2008, Elsevier.**

remainder of this chapter covers applications of GC×GC–MS techniques in a chronological fashion.

## 1.2 Applications of GC×GC–MS

### 1.2.1 The early years

One of the first observations made about comprehensive two-dimensional chromatograms was the sheer quantity of resolved components. The nature of the separation space is naturally dictated by the column choices and operating parameters selected by the analytical chemist, hence relying solely upon an *x*,*y* coordinate to identify a peak is often inaccurate and imprecise. Mondello compiled a review in 2008 and remarked that the coupling of mass spectrometry is an almost obliged choice to allow identification and structural elucidation of components and is the most powerful tool available at the current time for the separation of complex volatiles and semi-volatiles [68].

For this reason, it is unsurprising that the technique of GC×GC–MS has been thoroughly, if not completely, explored since its inception in 1999. A total of nine publications were released in the early years of the technique (1999-2002), before a veritable explosion of interest in the topic. Over sixty studies were published between 2002 and 2005 and interest has only increased in the five years preceding the current day, with a considerable amount of progress.

As previously mentioned, the first foray into the technique involved the coupling of the already established GC×GC technique with a quadrupole mass spectrometer. Despite being a breakthrough, the results were somewhat disappointing from an application standpoint and it was noted that time-of-flight mass spectrometry appeared to be the way forward.

Dalluge *et al.* [69] described the GC×GC–TOFMS analysis of cigarette smoke, a very complex sample and described the difficulties of data processing; an affliction that continues to hamper the mainstream use of the technique. To perform the study, the constituents of the smoke were adsorbed in a sample tube, re-concentrated onto a cold trap then thermally desorbed and injected onto the first dimension. A six second modulation time was used for focussing onto the second-dimension column. It would appear that a less than optimal column selection was made, as the relatively thick film selected for the first-dimension stationary phase caused elution temperatures to be excessive, which limited the application range due to the relatively low temperature stability of the polar column used in the second dimension. This led to the observation that independent temperature control over the two dimensions would prove useful.

A two-dimensional chromatogram from this study is shown in Figure 1.9. It is evident that the resolving power was insufficient for the sample. Mass spectral deconvolution proved particularly useful for this application and when used in conjunction with automated library matching, 7500 components were resolved of which 152 were successfully library matched with adequate accuracy. It is noteworthy that while this process was automated, the data processing took seven hours of computing time.

To further investigate column selection and carrier gas optimisation, a follow up investigation was implemented [27]. A pesticide mix was examined several times and it was determined that using a higher than optimum carrier gas velocity in the first-dimension reduced the elution temperature of the analytes and improved the interaction of the analytes and the stationary phase in the second dimension. However when conditions were close to optimum, no substantial change in

resolution was observed for the sample. It was also observed that an optimal modulation period existed. Too long a period and the first-dimension separation is not conserved; too short and the sensitivity and separation space is compromised.

Towards the end of 2002, Shellie and Marriott performed an interesting study into the use of an enantioselective stationary phase in a GC×GC separation [15]. While the separation of volatile chiral flavour and fragrance compounds using multidimensional techniques was not new, the group sought to increase the optimum linear velocity of the carrier gas to allow a faster separation whilst maintaining efficiency. While the use of hydrogen as a carrier gas moves towards this goal, inducing sub-atmospheric pressure throughout the entirety of the second-dimension column may offer better results by increasing the diffusion coefficient and decreasing the retention time on the second column.

Research into vacuum outlet chromatography had been previously performed by van Deursen and co-workers [13] but had not been applied to a GC×GC environment before. In fact, while sub-1 min separations using packed columns and a near-critical fluid mobile phase had been performed [70], no information about similar separations on capillary columns had been collected [15]. In conjunction with an LMCS modulator and quadrupole mass spectrometer, Shellie reported the best results using a (10 m × 0.10 mm i.d.) × (1 m × 0.25 mm i.d.) column set. This length was sufficient to lower the pressure in the second-dimension column and increase the diffusion coefficient and separation speed as desired. A separation using these conditions is shown in Figure 1.10. Investigations with short 0.10 mm i.d. columns in the second dimension were also conducted but overloading was evident, particularly in the second dimension, in addition to poor resolution and peak shape. This research has provided impetus for further investigation in this thesis.

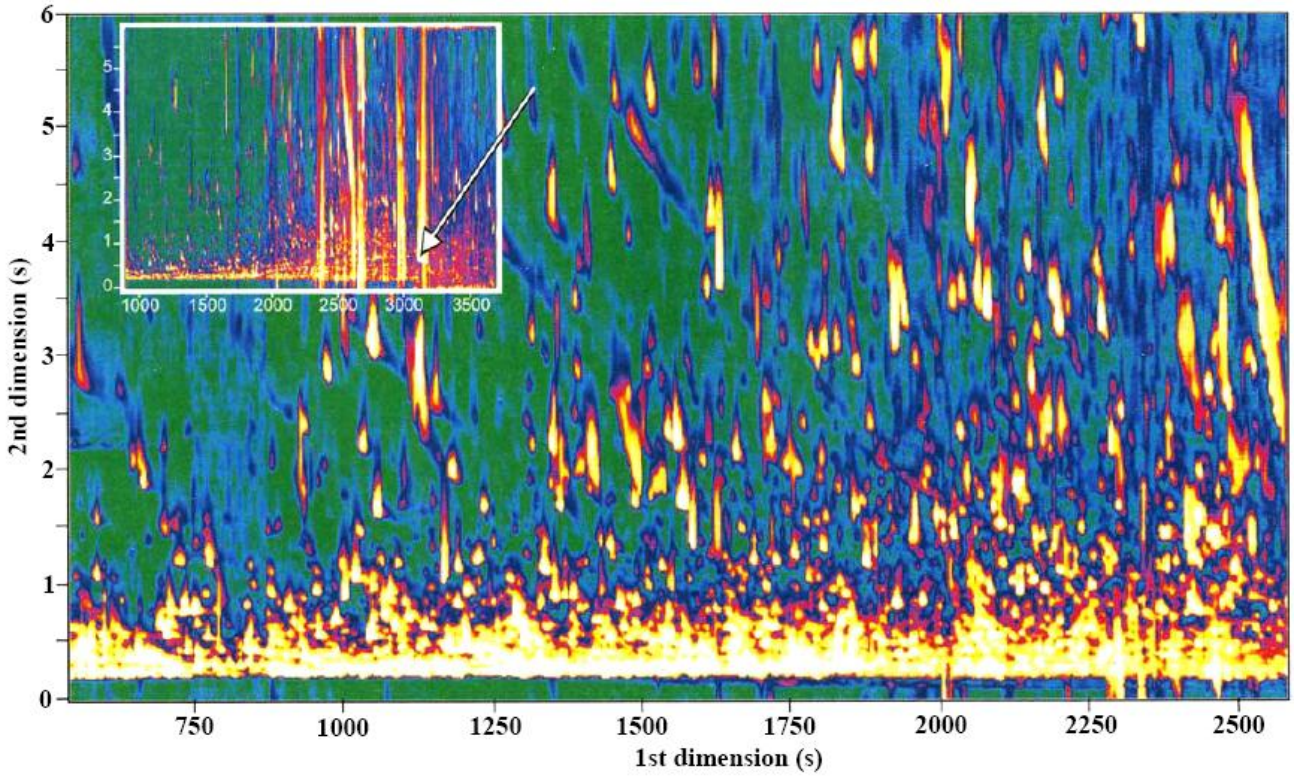


**Figure 1.9 Separation of cigarette smoke using GC×GC–TOFMS as performed by Dalluge.**

**Reprinted with permission from [69], copyright 2002, Elsevier.**

*Chapter 3* is dedicated to the investigation of appropriate column choices for GC×GC separations. The use of a column under low pressure conditions was investigated in detail in this chapter. Furthermore, Shellie's recommendation of a short length of 0.25 mm i.d. capillary column as a secondary column for a GC×GC–MS separation was followed in the research presented in *Chapter 4* where setup and optimisation of a GC×GC system with pneumatic modulation and qMS detection is presented.

### 1.2.2 GC×GC–MS landmark year: 2003

A significant advance in the facilitation of the widespread use of GC×GC–MS was achieved in 2003 with the introduction of the Pegasus 4D instrument from LECO. This incorporated a dual stage quad-jet cryogenic modulator, independent temperature control for first- and second-dimension columns and a time of flight mass spectrometer. The software package was capable of fully automated data processing and instrument control. Dimandja's group made use of this [71] and demonstrated the separation of a diesel sample. A concomitant decrease in sensitivity was also recorded and it was concluded that reducing the acquisition rate from 100 Hz to 50 Hz yielded a satisfactory separation.

As described previously, Synovec's group reported an example of a valve-based GC×GC system in 2003 [58]. A 60 m × 0.25 mm non-polar column was selected for the first dimension and interfaced to a six port diaphragm valve. Due to the temperature sensitivity of the internal components, the valve was located outside the oven. This continues to be a potential problem in the pneumatic modulation system to this day. A 5 µL sample loop was used in a manner similar to the techniques used in liquid chromatography and was used to transfer sample aliquots to

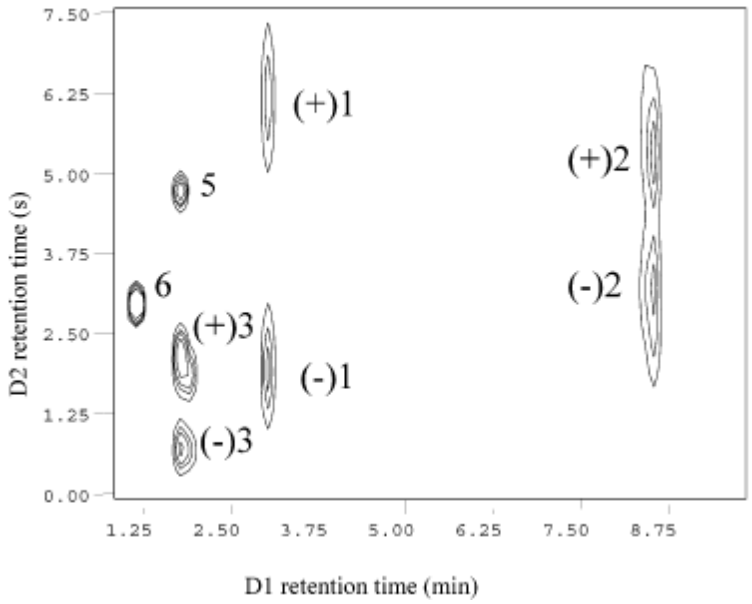


**Figure 1.10. A separation achieved by Shellie et. al on a test mixture, containing chiral compounds. While wrap-around is evident, the low data acquisition rate (8.33 Hz) was a good partnership for the large bandwidth. The achievement of rapid second-dimension enantiomer separations was successful.**

**Reprinted with permission from [15], copyright 2002, American Chemical Society.**

the TOFMS via a polar 3 m × 180 µm second-dimension column. For the system to function, an external gas supply was necessary to drive the second dimension. At constant pressure, the flow rate dropped from approximately 7 mL/min to 3 mL/min during the course of the temperature programmed run.

It was interesting to note that the primary column effluent was not continuously sampled. Instead, the sample loop was filled for 0.25 s then flushed for 2.25 s, during which time the first-dimension column effluent was not sampled. This corresponded to 90% of the sample running to waste. At the first International Symposium on Multidimensional Gas Chromatography (March 2003, Volendam, The Netherlands), there was some debate as to whether this type of separation may constitute a true two-dimensional comprehensive separation. It was concluded that as long as a faithful representation of the primary separation is realised, the technique can be considered to be comprehensive [72]. The present results show that no loss of first-dimension sample information is incurred due to the high sampling frequency (2.5 s) and the technique fulfils the requirements of GC×GC.

Whilst on the topic of novel hardware applications for GC×GC, it seems prudent to mention the use of alternative mass spectrometry technology. A good example of this is the use of an ion trap mass spectrometer coupled with GC×GC as studied by Wahl *et al.* in 2003 [73]. This instrument used valve-based modulation in a Deans switching arrangement to alternately inject on two second-dimension columns which were not recombined before the detector. Despite overcoming the shortcomings of the technique reported in the previous valve-based study by Synovec's group, the acquisition speed of the detector was excessively slow (less than 1Hz) and insufficient peak sampling was reported.

While the TOFMS is arguably the best suited to GC×GC separations, numerous authors produced some exceptional work during 2003 [17, 20, 74] highlighting the potential applications for quadrupole hardware driven at or close to the maximum duty cycle of the apparatus. The Agilent 5973 mass selective detector was selected for investigation as it allowed scanning at around 20 Hz with a narrow mass scan range. Quantitative analysis still proved difficult as under-sampling of components prevailed, although qualitative analysis was more than satisfactory.

### 1.2.3 2004-2006

The period between 2004 and 2006 saw the technique of GC×GC–MS take hold in both industrial and research laboratories. Twenty papers were published in 2004, covering both quadrupole and TOF detection. Ryan *et al.* [21] compared and contrasted the methodologies using solid phase microextracted coffee samples. An unorthodox polar-apolar column combination was used following successful results obtained by Mondello's group [75]. As with the preceding studies (and several subsequent ones), it was shown that while the quadrupole instrument was adequate for identification of components, quantification was unsatisfactory. Debonneville and Chaintreau [5] attempted quantification using a quadrupole MS operated in selected ion monitoring (SIM) mode at an acquisition rate of approximately 30 Hz. This was satisfactory for analysis of known analytes possessing large (> 200 ms) peak widths, but unsuitable for other components.

During 2005, 23 GC×GC–MS papers were published, 19 of which were focused on the use of TOF systems, while the remaining experiments were based on the use of quadrupole MS (qMS) instrumentation.

Adahchour *et al.* [22] reported an investigation on the principles, usefulness, and potential of rapid-scanning qMS instrumentation in GC×GC. The performance of a new generation qMS system (Shimadzu QP2010), which provided acquisition speed approaching GC×GC requirements, was studied for qualitative and quantitative purposes. The detector could reach the ultimate (GC×GC) goal of 50 spectra per second, albeit at a restricted mass range (95 amu). To avoid peak skewing, it was determined that the instrument should be operated such that acquisition rate approaches this maximum value. To determine the point where useful data may be collected, the peak area precision was examined at several acquisition rates between 20 and 50 Hz. The two highest acquisition rates were generated by restricting the MS scan ranges to 195 and 100 amu, respectively. Reliable quantification was obtained for scan rates above 33 Hz, where at least 7 data points per peak were recorded. Should the mass range required to reach this speed be insufficient, a smaller rate was necessary although this invoked difficulty in peak reconstruction. Should peak width drop below 200 ms, the use of the maximum acquisition rate of the instrument was necessitated but for general operation, 30 Hz was the most suitable.

From this study, it became clear that the use of a quadrupole MS for GC×GC provided acceptable results provided proper optimisation and selection of operating parameters is observed. Mondello's group [76] examined a perfume sample using GC×GC–qMS with an apolar 30 m × 0.25 mm i.d. column and a polar 1 m × 0.25 mm i.d. capillary employed in the first and second dimension, respectively. Peaks were assigned using one-dimensional linear retention index (LRI) filtered database matching and an acquisition rate of 20 Hz (40-400 amu) selected. The use of LRI filtering increases the chance of successfully identifying components within a

complex mixture by generating a normalised function of the retention time which can be cross referenced in the spectral library [77].

Shellie and co-workers [37] sought to match the output of GC×GC–FID and GC×GC–TOFMS experiments to allow direct comparison of retention times for identification and quantification purposes. This work followed on from the method translation theory of Blumberg and Klee [33] for adaption to the comprehensive two-dimensional separation. A first-dimension 30 m × 0.25 mm i.d. column and a second-dimension 0.5 m × 0.10 mm i.d. column with both atmospheric and vacuum outlet were used in this study. An equivalent 0.25 mm i.d. capillary can be derived for the second-dimension column for a nominal outlet pressure, allowing the correct column and injector split flow values to be determined. Through careful manipulation of outlet pressures and determination of average linear velocity and viscosity of carrier gas flows, a difference in absolute retention time for a mixture of 18 compounds of 3.7 s in the first dimension and 42 msec in the second dimension was calculated. The group made mention that to date, typical flow conditions for GC×GC experiments are almost always non-optimal [78]. This theme has continued throughout the research presented in this thesis and is discussed in more detail in Chapter 3 and 4.

A large body of work was completed in this period around the area of metabolite analysis using GC×GC–TOFMS, with fundamental papers completed by various authors [79-83]. Welthagen *et al.* [81] examined spleen extracts of obese (NZO strain) and lean (C57BL/6 strain) mice using both GC–TOFMS and GC×GC–TOFMS. GC–TOFMS enabled the detection of 538 peaks, whereas over 1,220 were reported for the comprehensive multidimensional experiment; a greater discrepancy would have been recorded if a larger injection was made on the GC×GC system.

### 1.2.4 2007-2009

Throughout this period the use of TOF detection for comprehensive analysis became more popular despite the occasional flirtation with current generation qMS technology. Research branched out into the investigation of TOF devices which traded resolution for high data acquisition rates, and those with high mass accuracy and concomitantly reduced collection frequency [27]. A veritable explosion of work was carried out in this period, with 24 papers published in 2007; 38 in 2008 and 27 in 2009. While discussion of all these publications would be of interest, two stood out as being an excellent representation of the direction in which GC×GC research is travelling.

Ochiai and co-workers [23] employed the GC×GC–TOFMS for the investigation of nanoparticulate atmospheric pollutants and were able to determine the presence of 9H-fluorene-9-one (-0.0007 Da mass error: 4 mg/L), 1H-phenalene-1-one (0.0046 Da mass error: 26 mg/L), 9(10H)-anthracenone (0.0005 Da mass error: 3 mg/L), naphto(1,2-c)furan-1,3-dione (0.0031 Da mass error: 16 mg/L), 7H-benz(de)anthracene-7-one (0.0016 Da mass error: 7 mg/L), and 11H-benzo(*a*)fluorine-11-one (0.0039 Da mass error: 17 mg/L) in a sample acquired from near a busy road.

Shunji *et al.* [84] performed a similar experiment on an incinerator ash extract with the aim of highly selective mass discrimination. This approach, using the ternary separation dimensions of boiling point × polarity × high resolution mass spectrometry proved highly advantageous for applications where an extremely high selectivity was required, but the financial outlay required for the technology outweighs the benefits for routine applications, especially when selected ion monitoring mode may produce similar results.

### 1.2.5 2010-2011

GC×GC continued to be an area of interest in 2010 and the current year. A variety of GC×GC–MS methods for the analysis of petrochemicals were reported [85-90] and investigation of environmental contaminants, including organohalogens [91-95] and pharmaceutical/personal care products (PPCPs) [96, 97] were also widely discussed. The use of comprehensive analysis techniques for metabolite analysis and biological 'fingerprinting' techniques proved popular, with many reports in the literature [98-106], some of which included quantitation.

Tranchida and co-workers performed an interesting investigation into the use of a high efficiency 0.05 mm i.d. column in the second dimension at optimum flow rate [107]. A quadrupole mass spectrometer was used as a follow-up to previous FID experiments [108]. The rationale behind this investigation considered the desirability for wide first-dimension peaks and a concomitant compensation of a fast, high resolution separation in the second dimension. Considering around 10,000 theoretical plates can be obtained from a 1 m × 0.10 mm i.d. second-dimension column, it stands to reason that greater efficiency can be afforded by a narrower column if operated close to optimum. The authors noted that using this column in a conventional instrument configuration, only a limited range of the available peak capacity could be exploited and very few peaks could be successfully identified, leading to the suggestion that this avenue was not suitable for separation of complex mixtures. However, when used in an optimised split flow arrangement with independent temperature control over the two separation dimensions, good performance was available.

To continue the trend of quadrupole experimentation, Purcaro *et al.* [109] evaluated the upgraded Shimadzu QP2010-Ultra qMS system which is capable of a

20,000 amu/s scan speed, corresponding to a frequency of 50 Hz over the range 40-330 *m/z* for comprehensive two-dimensional separations. The result was particularly pleasing with highly satisfactory repeatability, accuracy, linearity and sensitivity observed for the separation of a perfume sample. The authors reported that the instrument and method were suitable for routine analysis of perfume allergens. This observation overturned the previous paradigm that qMS is only suitable for identification purposes and cannot yield accurate peak reconstruction.

Vallejo and co-workers also investigated a comprehensive two-dimensional system with a valve-based modulator, splitting effluent via a tee union to FID and qMS detectors [110]. A similar method to this research was investigated in *Chapter 5* of this thesis. Vallejo's method involved the identification of components present in octyl- and nonylphenol isomer test mixtures using mass spectral data, and quantification of analytes of interest using the FID channel. A factorial experimental design was implemented to optimise the separation, based primarily on peak symmetry across the separation space. A HP5 MS column (30 m × 0.25 mm i.d.) was used in the first dimension, coupled to a DB-17 MS column (5 m × 0.25 mm i.d.) in the second dimension. The splitter was installed *after* the second dimension column, directing flow to the FID via a 0.7 m × 0.32 mm i.d. transfer line while the MS flow passed through a 0.45 m × 0.1 mm i.d. transfer line. Under these conditions, the group concluded that optimum separation was obtained using 1 mL/min in the first dimension and 17.75 mL/min in the second, with a 1.5 s modulation period and 0.12 s modulator flush time.

In contrast to this method, Tranchida *et. al* employed a partially-modulated GC×GC–qMS system with a Zoex loop-type modulator, directing a proportion of the flow to waste prior to analysis on the second dimension [111]. To counteract the

compromise in sensitivity inherent by not analysing the majority of the sample, the carrier gas linear velocities were operated under optimised conditions in both dimensions. This outcome is difficult to achieve, as under normal circumstances with a 'traditional' (long 0.25 mm first-dimension/short 0.10 mm second-dimension) column set, the second dimension flow rate is usually pushed above optimum. The group sought to acquire at least 10 spectra/peak, enabling the potential for quantitation based on the calculations of Adachour [112]. This outcome was successfully obtained using a 25 Hz data acquisition rate and a mass range of 40-360 *m/z*.

Whilst not strictly GC×GC–MS, Semard and co-workers [113] examined a new method of optimising the separation space available in a two-dimensional separation. Dorman and co-workers [114] had previously developed a method for predicting and optimising GC×GC separations by calculating the enthalpy and entropy of target compounds. This information was then used to generate simulated separations covering a wide variety of column and operational variables to generate a optimum parameters. Semard and co-workers based their method on convex hull triangulation algorithms and reported better accuracy and precision when compared to the earlier approach. In essence, their technique allows the prediction of the percentage of the separation space utilised for the separation of a particular sample. In conjunction with attentive column selection, the group was able to tailor the system to give acceptable resolution for their separation of a wastewater sample. The quest for ever-increasing peak capacity was continued by Wilson and co-workers [115]. The group reflected that the injection pulse width obtained using many GC instruments is a leading cause for extra-column band broadening and sought to modify the procedure to improve the use of the available separation space. By using

a resistively heated transfer line coupled to a high-speed diaphragm valve, the peak capacity production rose from 40 peaks/min to some 120 peaks/min.

Utilising hardware contemporaneous to that discussed in this thesis, Harvey and Shellie investigated peak shapes evolving from non-focussing modulation devices. Considering that diffusion of analyte packets occurs within the sample loop of a pulsed-flow modulator, in addition to the partial preservation of the first-dimension concentration profile of the analyte throughout the second-dimension separation, a model establishing these influences on the second-dimension peak shape could be created. Validation of the model was successful and appropriate parameters for flow ratio between the two dimensions were presented.

Of particular interest to the current study, van Geem and co-workers [116] presented a novel system setup allowing the online qualitative and quantitative analysis of complex hydrocarbon mixtures by incorporating a two-way valve to allow switching between FID and TOFMS detection without venting of the instrument. The group used a dual jet cryogenic modulator in conjunction with a 50 m × 0.25 mm i.d. non-polar first-dimension column and two 2 m × 0.15 mm i.d. polar second-dimension columns feeding each detector. While the aim of the project was based on an industrial application, the ‘online’ coupling of the two systems was a novel approach and certainly worthy of further investigation.

The use of ionic liquid stationary phases in GC×GC applications was also reported during this period. Following on from the high efficiency one-dimensional PCB analysis of Sandra *et. al* [117], Zapadlo and co-workers analysed a similar sample containing 209 PCB congeners and achieved resolution of 196 compounds [118]. A GC×GC–TOFMS system was used with a SPB-Octyl first-dimension column (poly(50%-*n*-octyl-50%-methyl)siloxane coating) and a SLB-IL 59 second-

dimension column (1,12-di(tripropylphosphonium)dodecane bis(trifluoromethansulfonyl)amide coating). Both of these columns are produced by Supelco. The group reported highly satisfactory separation of the toxic 'dioxin-like' congeners available from the particular selectivity available with the selected column set.

A subsequent publication evaluated the use of two other Supelco ionic liquid columns, namely SLB-IL 82 and SLB-IL 100 in GC–MS and GC×GC–FID applications for the analysis of fatty acid methyl esters (FAMEs) from algae [119]. In comparison to polyethylene glycol and cyanopropyl columns tested under the same conditions, the Supelco ionic liquid columns showed improved sensitivity arising from increased stability of the coating and less column bleed. A similar resolution was obtained, affirming the suitability of the selection for this application.

Despite the fact that MS detection was not used, arguably the most interesting application for this stationary phase arose from the research presented by Siegler and co-workers early in 2010 [120]. Using two diaphragm valves and three serially-connected columns, the group presented a comprehensive three-dimensional separation with a triflate ionic liquid column in the second dimension. Unsurprisingly, exceptional peak capacity production was observed with 180 peaks/min resolved which is in the order of four times greater than the previous report [121]. As before [121], the use of PARAFAC was also reported to aid in the deconvolution of the three-dimensional space for the construction of concentration profiles of analytes of interest contained in the diesel sample investigated. It was concluded that the use of the ionic liquid column provided complementary selectivity to the other two separation dimensions (DB-5 non-polar and DB-wax in the first and third dimensions, respectively) and went a long way towards addressing the

perceived deficiency in available separation space with ‘less orthogonal’ column choices.

The use of chemometric data analysis approaches in conjunction with GC×GC–MS techniques also featured highly during this period. Due to the ever-increasing amount of information accessible with this approach, evolution of appropriate results interpretation becomes important. Appropriate use of the diverse ‘toolbox’ of interpretation strategies available to the analyst ensures the presentation of meaningful conclusions. Almstetter and co-workers investigated the use of the Statistical Compare alignment algorithm developed by LECO for profiling bacterial metabolites separated with GC×GC–TOFMS and compared the results to those obtained using an in-house method [105]. Their results showed that the commercial approach improved quantitative precision and provided a satisfactory fingerprinting technique for the application. Whilst only investigating a one-dimensional approach, Jalali-Heravi *et al.* applied several chemometric techniques to deconvolute components of interest in mandarin and lemon essential oil samples [122]. The group reported that their preferred technique of mean field independent component analysis (MF-ICA) provided satisfactory results for the samples investigated. Synovec and collaborators published several manuscripts during this period detailing a series of in-depth approaches [123-126]. The use of Principal Component Analysis (PCA) as a data comparison tool featured heavily in these publications.

## 1.3 Concluding remarks

From reviewing the research published in the area of GC×GC–MS analysis, it is clear that the technique is almost the analytical chemists’ ‘silver bullet’; yielding exemplary selectivity across three (or more) separation dimensions, high sensitivity

through zone focussing and enhanced separation power as a result of the large peak capacity afforded. As the first decade of the 21st century draws to a close, an interesting analogy may be drawn between the technique of GC×GC–MS and the increase in popularity of 'lifestyle' technology reaching the consumer market. It would not be unreasonable to expect the initial scepticism surrounding this analytical methodology to be swept away with the tide of reduced initial and on-going expenditure, open source software packages and the thirst for information as witnessed in so many areas throughout recent years, yielding a constant expansion and uptake of the technique in the very near future.

## 1.4 Scope of the thesis

The continued development of gas chromatographic techniques and technology has generated multiple approaches for the separation of complex samples. Generally speaking, there is always a degree of compromise when pairing a particular sample with a separation technique. This is witnessed in areas such as separation time, efficiency and peak capacity, and to a lesser degree in secondary separation aspects including the size and complexity of the collected data.

The present investigation seeks to develop a GC×GC–qMS approach for the analysis of plant extracts of varying complexity that did not rely upon the use of a liquid cryogen for modulation. This process commences in Chapter 3, where the selection of suitable stationary phase dimensions for this application is investigated. While it is often performed in cryogenically-modulated GC×GC–MS approaches, the use of narrow-bore (eg. 0.10 mm i.d.) columns in the second dimension of a GC×GC–MS approach relying on pneumatic modulation is not desirable. This section critically examines the use of a wide bore column under low outlet pressure conditions. Such a combination aims to marry high capacity with moderate

efficiency for potential use as a second-dimension column. A high temperature stable wax column was investigated as another potential second-dimension stationary phase, although the available column dimensions did not suit this application. To contrast this study, very long narrow-bore columns were also investigated for potential use in the first dimension, leading to discussion on selection of column length based on desired pressure parameters and required efficiency.

The development of a pneumatic modulator for GC×GC–qMS and GC×GC–FID is discussed in Chapter 4. The study began with the determination of the limitations of the quadrupole mass spectrometer under different flow conditions. Development and optimisation of a modulator ensued, and a partial modulation interface was deemed to be the most appropriate to operate the instrument and stationary phases at close to optimum values. To conclude the chapter, a study was conducted using the information collected in Chapter 3 to select an appropriate column set for the system. This involved data collection across a broad combination of conditions to determine the optimum trade-off between available sensitivity, efficiency and analysis time.

Chapter 5 commences with an investigation of a high-efficiency one-dimensional GC–MS separation of metabolite extracts from hop cones for group-type classification of the varieties from which the samples originated. This research was conducted as a proof-of-concept approach, as varietal classification techniques reported in the literature focus on the use of essential oil samples. Based on the highly satisfactory results obtained in this pilot study, it is envisaged that further research will be conducted in this area to evaluate more advanced chemometric techniques in conjunction with a GC×GC–MS approach in subsequent flowering seasons.

Finally, the use of a total-transfer valve-based modulator utilising a stop-flow approach for the first-dimension column was performed once again examining an essential oil sample. This allowed a subjective comparison to be performed with the partial sampling Deans switch approach previously described. To conclude this chapter, a commercially available Agilent CFT modulator was evaluated in a GC×GC–FID approach and compared with a GC×GC–MS method using a dual stage, loop type modulator. Spearmint essential oil was examined using an enantioselective column in the first dimension to offer an illustrative example of the benefit of a comprehensive multidimensional separation and evaluate the robustness of the technique.

# Chapter 2: Experimental

This chapter describes an overview of the experimental parameters utilised throughout this thesis. Full experimental details are provided in the relevant discussion chapters.

## 2.1 Standards

A $C_8$-$C_{20}$ *n*-alkane standard mix and individual $C_{21}$-$C_{30}$ standards were purchased from Sigma-Aldrich (Castle Hill, Australia). The concentration of each alkane was 40 mg/L in hexane. For the calculation of retention indices, a 20 mg/L mix of $C_8$-$C_{20}$ *n*-alkanes was prepared by dilution of the stock solution with dichloromethane.

## 2.2 Instrumentation

Unless otherwise stated, all analyses were performed on a Shimadzu QP-2010 Plus gas chromatograph–quadrupole mass spectrometer (Shimadzu Scientific Instruments Oceania, Mt. Waverly, Australia). The instrument was equipped with two split/splitless injectors, dual heating ovens (primary and satellite), flame ionisation detector and an AOC20i auto-injector. A heated transfer line was incorporated as the interface between the two heating ovens and was maintained at the maximum ramp temperature selected for each analysis. These options were utilised for different aspects of the research, and individual configurations are detailed subsequently. For all experiments, the quadrupole ion source temperature was set to 200 °C and the MS transfer line held at 250 °C. Injection volume for all analyses was 1 µL, and the injector(s) were held at 250 °C. The mass spectrometer was auto-tuned at approximately weekly intervals. The mass spectrometer was used in mass scanning mode at a data acquisition frequency of 14.29 Hz over the mass

range 40-455 *m/z* (70 ms scan period) for one-dimensional separations and at a data acquisition frequency of 25 Hz over the mass range 35-350 *m/z* for two-dimensional separations, unless otherwise stated.

For GC×GC–FID separations, the FID was held at a temperature of 260 °C and was operated at an acquisition rate of 250 Hz. Nitrogen was used as the make-up gas and was supplied either from a cylinder (BOC, Tasmania) or via the reticulated $N_2$ gas system within the laboratory.

Either hydrogen or helium was used as the carrier gas for all experiments. Hydrogen was supplied by a Parker Balston Hydrogen Generator (Restek Distributor, Baulkham Hills, Australia) and ultra-high purity helium delivered from a cylinder (BOC, Hobart, Tasmania).

Some confirmatory GC×GC analyses were carried out using an Agilent 6890 GC (Agilent Technologies, Forest Hills, Australia) equipped with a custom dual-jet cryogenic ($CO_2$) modulation system based on the design of Beens et al. [127] and a flame ionisation detector.

## 2.3 Stationary phases

The stationary phases selected for this study are shown in Table 2.1.

## 2.4 Modulation

A 5-port Deans switch microfluidic flow wafer was obtained from SGE (SGE Analytical Science, Ringwood, Australia) for evaluation and the preparation of a pneumatic modulation system. More details on this device are reported in Chapter 4.

**Table 2.1. Stationary phases selected for this study**

| **Column Coating** | **Stationary Phase Composition** | **Manufacturer** |
|---|---|---|
| BPX-5 | 5% phenyl polysilphenylene-siloxane | SGE Analytical Science, Ringwood, Australia |
| RTx-wax | Polyethylene Glycol | Restek Corporation, Bellefonte, PA, USA |
| BPX 35 | 35% Phenyl Polysilphenylene-siloxane | SGE Analytical Science, Ringwood, Australia |
| BP 20 | Polyethylene Glycol | SGE Analytical Science, Ringwood, Australia |
| IL-111 | Ionic Liquid | Supelco, Castle Hill, Australia |
| Rxi-5 | 5% phenyl polysilphenylene-siloxane | Restek Corporation, Bellefonte, PA, USA |
| MEGA-WAX HT | Polyethylene Glycol | Mega, Legnano, Italy |
| PS-086 | Diethyl-t-butylsilyl β cyclodextrin | Mega, Legnano, Italy |

Modulation times were controlled by an Omron H5BR timer (Lawrence and Hanson, Hobart, Tasmania) acting upon a Parker 91-0094-900 valve (Parker Hannifin, Castle Hill, Australia). For all experiments, the timer commenced at the beginning of the analysis period and was triggered from a relay incorporated in the GC instrument. Connections to the Parker valve were made with Swagelok fittings (Swagelok, Broadmeadows, Australia), and connections to microfluidic wafers were made with SGE SilFlow™ fittings (SGE Analytical Science, Ringwood, Australia). Stainless steel tubing with a 1.07 mm o.d. and 0.38 mm i.d. (SGE Analytical Science, Ringwood, Australia ) was used between the APC, valve and microfluidic flow wafer.

## 2.5 Data analysis

### 2.5.1 GC–MS

Peak tables were populated using the Shimadzu GC–MS Solution software and simple statistics and preliminary data normalisation performed using Microsoft Excel 2007 or 2010. Chemometric analyses (principal component analysis and discriminant analysis, refer *Chapter 5*) were performed using XLSTAT 2006/2011 (Addinsoft, New York, USA). To identify components in all instances, the spectral scan at the peak apex was used.

### 2.5.2 GC×GC

For GC×GC–MS separations, data files (.qgd format) were imported directly into Chromsquare (Chromeleont, Messina, Italy) and integrated in a converted two-dimensional format.

GC×GC–FID data files (.gcd format) were converted into a tab separated ASCII format for importation and integration in Chromsquare and preparation of figures using Transform (Fortner Inc., Savoy, IL, USA).

The Flavour and Fragrance Natural and Synthetic Compounds library (FFNSC) was selected for qualitative analysis of essential oils and the NIST (National Institute of Standards and Technology) library used for qualitative analysis of hop metabolites in conjunction with Shimadzu GCMSolution post-run analysis software and coupled Shimadzu spectral library (SHIM). Details on the operation of this analysis software and library search algorithms are reported in Section 3.1.2.

# Chapter 3: Selection of columns for GC–MS and GC×GC approaches

## 3.1 High speed, low pressure gas chromatography-mass spectrometry for essential oil analysis

This section has been adapted from the following publication:

S.D.H. Poynter and R.A. Shellie. **High-speed, low-pressure gas chromatography–mass spectrometry for essential oil analysis.** *J. Chromatogr. A* 1200 (2008) 28-33.

### 3.1.1. Introduction

There are a variety of practical routes for achieving high-speed separations of complex samples [128] and many of them have been employed for essential oil analysis. Most commonly 10 m × 0.10 mm i.d. columns (with appropriately reduced stationary phase film thickness) have been employed in place of 25 m × 0.25 mm i.d. columns [129] and it has been shown many times this approach leads to a significant speed gain while preserving resolution [130]. In a similar way Mondello *et al.* [75] demonstrated fast analysis of lime essential oil using a 5 m length of 0.05 mm i.d. capillary with a 0.05 µm stationary phase coating. Lime oil analysis was achieved in around 90 s by employing the fastest possible temperature program rate of the GC oven (50-150 °C in 75 s, 150-200 °C in 43 s, 200-250 °C in 55 s) as well as an average linear carrier gas velocity of 120 cm/s which was significantly higher than the optimum value of 38.5 cm/s. An additional approach for achieving faster analysis includes direct resistively heated column GC [131] which, by marrying rapid temperature programming (up to 20 °C/s) with fast data acquisition (using flame ionisation detection) and high split ratio [132] can lead to essential oil analysis times between 40 and 100 s [131, 132]. Fast analysis approaches often try to maintain

efficiency, however having highlighted that the efficiency of a capillary column often exceeds analytical requirements, Bicchi and co-workers investigated the use of short 0.25-0.32 mm i.d. columns with appropriate selectivity for the analysis of rosemary (*Rosmarinus officinalis* L.) and chamomile (*Matricaria recutita* L.) essential oils [133]. Both of these essential oils are considered as moderate complexity samples, and effective analysis was performed by substituting the standard (*ca*. 25 m) capillary column comprising around 150,000 theoretical plates with 5 m columns comprising 20,000-50,000 theoretical plates. A 5% phenyl- 5% vinyl-polydimethylsiloxane stationary phase was used for the separation of chamomile oil but lacked the selectivity to adequately resolve the key components of rosemary oil so a polyethylene glycol stationary phase was used in its place. Analyses were performed 5 to 10 times faster than the corresponding analysis with conventional columns. The primary interest in fast GC in the current study relates to its application in comprehensive multidimensional gas chromatography (GC×GC) where fast operation of the second-dimension columns is particularly important [134]. Short (≤ 1.5 m) narrow-bore (0.10 mm i.d.) columns have been utilised in more than 80% of published GC×GC applications [78] in order to produce chromatograms over the required retention window, which is typically 2-8 s. However, by considering the events taking place inside GC×GC columns, Ong and co-workers suggested that peak resolution may be lost through the onset of 'non-linear' conditions evidenced by sample overloading in low capacity narrow bore columns [135]. This theory was supported by further investigations which concluded that 0.10 mm i.d. second-dimension columns may not be the best choice for GC×GC [78, 136]. The use of a narrow second-dimension column leads to very high average linear velocity in the second-dimension column; high resistance to flow in these

narrow columns leads to a high pressure at the junction of the first and second columns, which in turn reduces the optimum average linear carrier gas velocity in the first-dimension column [78]. The combined result of these events is slow total analysis time coupled with reduced second column efficiency. Thus, a fast GC approach that utilises columns with low flow resistance is of interest. In practical terms, this means the use of wide bore and/or shorter columns. This topic is supported by outstanding theoretical and experimental works [13, 137, 138].

A straightforward means of operating 0.53 mm i.d. columns at reduced pressure was realised by de Zeeuw et al. [138]. This method directly couples the outlet of the column to a mass spectrometer and the entire length of the column is operated at very low pressure. A restrictor has to be applied at the inlet side of the system to ensure that the column head pressure can be precisely maintained by electronic pressure control. Later van Deursen et al. [139] explored three options for producing the restriction at the inlet of the wide-bore column, including (1) the use of a micro-injection valve (2) the use of a supercritical fluid chromatography restrictor and (3) the use of a narrow capillary, as employed by de Zeeuw and co-workers. Comparable performance was reported for the latter two options, both being slightly better than the micro-injection valve, which was thought to contribute to band broadening by additional dead-volume effects. Optimum average carrier gas velocity ($\bar{u}$) is proportional to the average binary gas-phase diffusion coefficient and both of these vary inversely with pressure, so the low-pressure GC arrangement opens opportunity for fast separations. Low-pressure GC–MS has been used for analysis of lanolin steryl esters [140], pesticide analysis [141-144] and for environmental contaminants [145-148]. A review of the literature revealed a single study of low-pressure GC–MS with 0.53 mm i.d. columns for essential oil analysis [149] in which

the analysis of *Turnera diffusa* essential oil was performed in 3 min and compared to conventional analysis using a 30 min temperature program with a 0.20 mm i.d. column.

It is noteworthy that van Deursen and co-workers specifically stated *"A distinct disadvantage of wide-bore columns is that the plate-number is not very high. This system therefore is not very suitable for complex separations"* [13]. While this point may have discouraged the application of low-pressure GC for essential oil separations, the current study sought to investigate the validity of this comment with respect to the analysis of moderately complex essential oils, in terms of peak capacity, separation speed, and sample capacity. The work described here is important because it compares wide-bore columns with the more accepted narrow-bore columns in fast GC–MS analysis, and most notably, provides an indication of the suitability of this technique as the second dimension in a comprehensive two-dimensional approach. Only by directly comparing the performance of these two separation systems side-by-side, can these benefits be truly appreciated.

### 3.1.2 Experimental

*Samples*

Fennel and parsley essential oil samples were provided by Essential Oils of Tasmania (Kingston, Australia). These samples were obtained by hydrodistillation and were diluted to 1% v/v in dichloromethane (Sigma-Aldrich, Castle Hill, Australia). Standards of terpinen-4-ol, dodecane and decan-1-ol were obtained from Sigma-Aldrich (Castle Hill, Australia) and prepared in a similar manner.

*Instrumentation*

A 12 m × 0.53 mm i.d. BPX-5 capillary column coated with a thin layer (0.25 µm film thickness) of 5% phenyl polysilphenylene-siloxane stationary phase (SGE Analytical Science, Ringwood, Australia) was employed throughout for the low-pressure GC separations. A 0.60 m × 0.10 mm i.d. length of deactivated fused silica tubing (SGE Analytical Science, Ringwood, Australia) was connected to the inlet of the analytical column using a stainless steel union and appropriately sized SilTite metal ferrules (SGE Analytical Science, Ringwood, Australia). The narrow-bore restrictor column was inserted a few millimetres into the wide bore analytical column to ensure that there were no dead-volume effects caused by the union. Narrow-bore GC–MS separations were performed using a 10 m × 0.10 mm i.d. (0.10 µm film thickness) BPX-5 capillary column (SGE Analytical Science, Ringwood, Australia). The chromatograms presented here were acquired using a split ratio of 250:1. The carrier gas was helium and the average linear carrier gas velocity used was 89 cm/s for the 0.53 mm i.d. column and 33 cm/s for the 0.10 mm i.d. column. Full-scan mass spectra were acquired using a 70 ms scan period (14.29 Hz data acquisition) over the mass range of 40-455 *m/z* using a quadrupole scan rate of 10,000 *m/z*/s.

The temperature programs employed for each column were 40 °C (hold 0.21 min); 40-240 °C in 4.28 min; 240 °C (hold 0.21 min), giving a total time of 4.7 min for the 0.53 mm i.d. column and 40 °C (hold 0.5 min); 40-240 °C in 10 min; 240 °C (hold 0.5 min), giving a total time of 11 min for the 0.10 mm i.d. column.

*Limit of detection (LOD)*

To perform quantification and estimate LOD, the response factor of an analyte peak can be compared to an internal standard of *n*-nonane [150]. Because the

comparison with an internal standard was not performed for this separation, some inaccuracies may arise, but the approach used herein provides a relative approximation, especially when it is considered that the terpenes examined for this section provide a stable response factor across the chemical class. To calculate the LOD for the standards of terpinen-4-ol, dodecane and decan-1-ol, samples of concentration 5000, 1000, 500, 100 and 10 mg/L were prepared by serial dilution of a stock solution with dichloromethane. The standards were injected using identical conditions to the essential oil separations. Baseline noise signal intensity (from EIC) was averaged for a period of 30 s either side of the peak. A calibration curve was constructed based on the peak height from an extracted ion chromatogram for each standard. The LOD was calculated by extrapolation from the curve when the peak height was equal to three times the intensity of the baseline noise.

*Mass Spectral Skewing Evaluation*

Mass spectral skewing is an undesirable phenomenon that was problematic in early generation quadrupole instruments and GC–MS approaches involving a fast chromatographic step hyphenated with a relatively slow-scanning mass spectrometer. It arises as a result of variation in the concentration of an analyte within the ion source of the mass spectrometer, generating variability in the intensities of ion fragments between consecutive spectrometer scans during peak elution [151]. Misidentification of components can occur if a number of spectra for a peak are averaged but show excessive variability. If an insufficient number of scans per peak are obtained (for example, in the case where an early-generation slow-scanning quadrupole instrument is used in conjunction with a fast GC separation, as depicted in Figure 1.3), the average spectrum used for component identification is not necessarily representative of the actual spectrum of the analyte. This causes more

difficulties in cases where analytes coelute, as the probability of collecting a 'clean' spectrum for the coeluting compounds diminishes [151].

To determine the extent of mass spectral skewing with the instrument used for this research, 1μL of 1% v/v tea tree oil in dichloromethane was injected onto a 20 m × 0.1 mm i.d. Rtx-5 column (Restek Corporation, Bellefonte, PA, USA). Hydrogen was used as the carrier gas at a flow rate of 0.6 mL/min (constant linear velocity mode) and a split ratio of 200:1 was employed. The MS was set to a scan range of 40-455 *m/z* at an acquisition frequency of 5 Hz. While this scan rate is below commonly accepted minimum values for GC×GC–MS applications, undersampling was not observed.

Three well-resolved peaks were selected for evaluation, eluting at 4.80, 7.72 and 10.93 min. Using the FFNSC library and *a priori* knowledge of the elution pattern of tea tree oil using this hardware combination, the peaks were tentatively identified as α-pinene, γ-terpinene and α-terpineol respectively. A total of 25 scans were collected for the α-pinene peak, with 11 scans collected for γ-terpinene and 9 scans collected for α-terpineol. The base peak for α-pinene and γ-terpinene was 93 *m/z*, with 100 % repeatability between scans. A repeatability of 100 % was also observed for the 40 *m/z* base peak collected for α-terpineol.

Figure 3.1 shows a chart depicting the normalised intensity of the next 10 most abundant ions for each of the 25 scans collected for α-pinene. Minor variation was observed between these abundances, with slightly higher intensities recorded at the start of the peak compared to the tail. The ratios of 5 ions (namely 94, 92, 91, 79 and 77 *m/z*) against the 93 *m/z* value are shown graphically in Figure 3.2. The average ratio of the 93 *m/z* ion to the 94 *m/z* ion was 11.2, with a variance of 0.48. A similar value was recorded for γ-terpinene, with the 93:94 *m/z* ratio being 10.7 with a

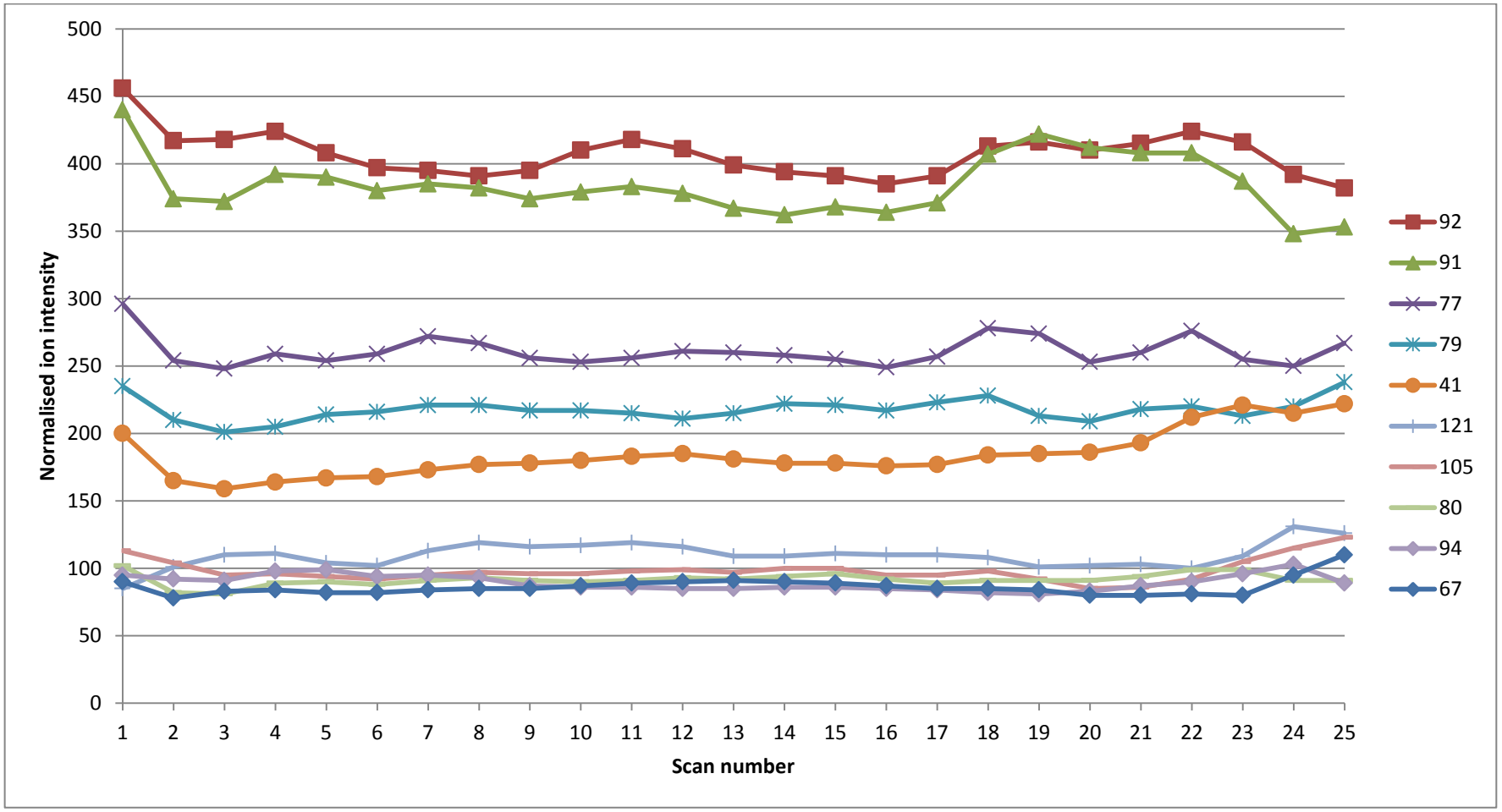


**Figure 3.1. Intensity of high abundance ions collected for a peak tentatively identified as α-pinene. Instrumental conditions are described on Page 64. Values are normalised against the most abundant ion, 93 *m/z* (1000 counts).**

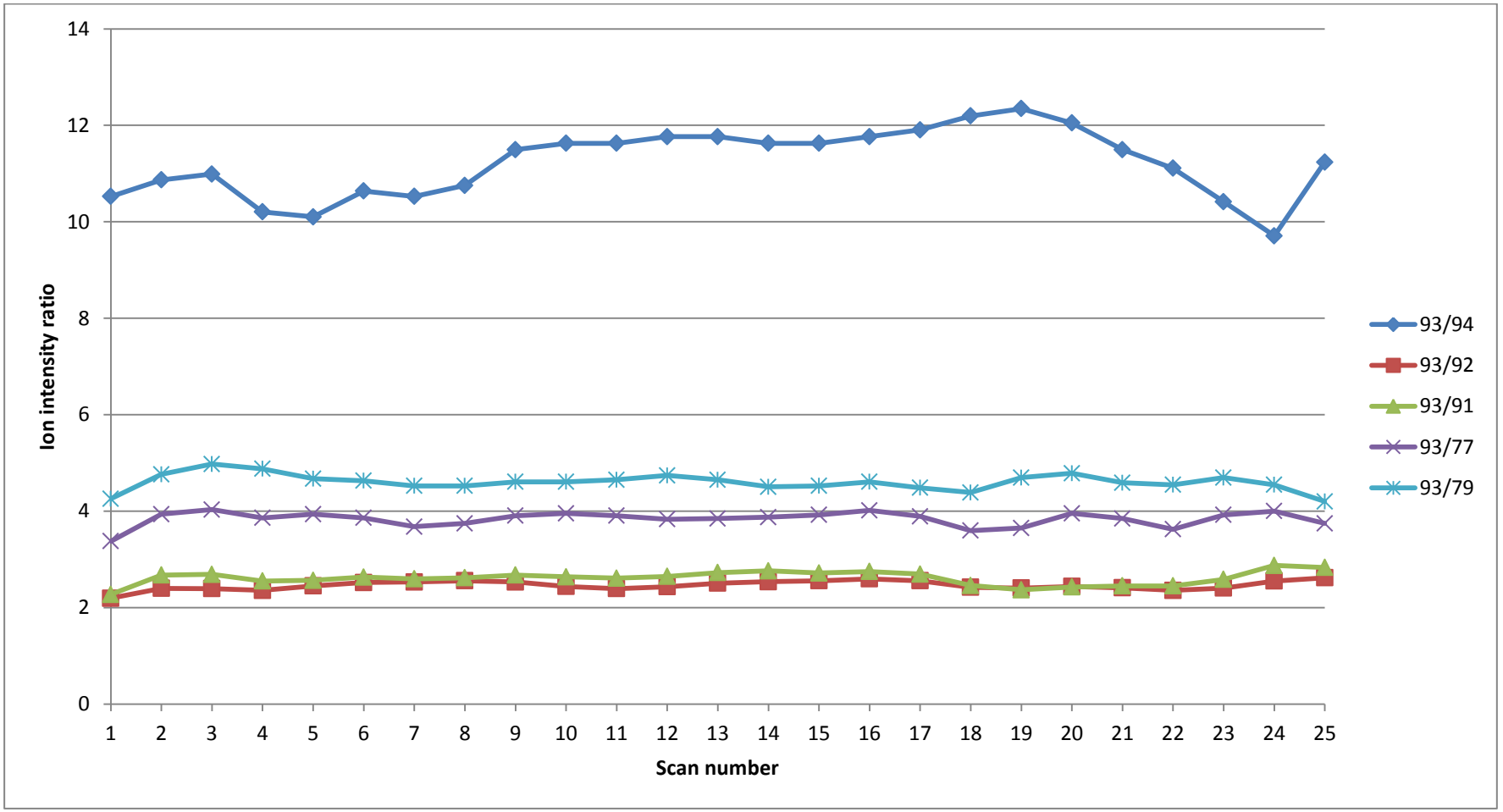


**Figure 3.2. Ratio of normalised intensities of selected ions against the most abundant ion (93 *m/z*, 1000 counts). Instrumental conditions are described on Page 64.**

variance of 0.28. Considering that each of these compounds contains 10 carbon atoms and the natural abundance of the $C^{13}$ isotope is 1.1%, the expected 93:94 *m/z* ratio would be 11:1 based on the probability of the heavier isotope occurring in the compound. The values of 11.2 and 10.7 are consistent with this expected value.

Shellie and co-workers discussed the extent of mass spectral skewing using an Agilent instrument in 2003 [19] and suggested that despite only sampling 3-4 spectra for each fast eluting peak in their GC×GC system, consistent ion abundances and only small differences in spectra were witnessed. Using the same instrumentation as was utilised in the present study, Mondello and co-workers provided a similar evaluation in 2007 [152]. Reconstruction of a several pesticide 2D peaks was performed, including that of fonofos, for which 14 spectra were acquired. The group similarly concluded that only limited spectral differences were present.

Although these prior studies did not report ratios of ion abundances as presented here, the degree of spectral skewing was concluded to be minimal in both cases as corroborated by 'minimal spectral differences' across a sample peak. Based on this conclusion, the similarity in ion abundances witnessed here suggested that spectral skewing was essentially negligible for the purposes of approach development and application reported in this thesis.

*Spectral library matching*

Tentative peak assignments were generated from a single scan at the peak apex from which the Shimadzu GCMSolution software compared to the FFNSC library. This software uses probability based matching (PBM) with forward and reverse search procedures to compare 'target' spectra (generated by the instrument)

with ‘reference’ spectra in an electronic database (or ‘library’) [153]. In addition, a tertiary filter was applied based on linear retention index (LRI).

A mixture of *n*-alkanes ($C_8$-$C_{20}$) was injected under identical instrumental conditions to sample separations was used to create a LRI scale using the Shimadzu software. A window of ± 10 LRI units was applied to the results of the library search results, and any potential matches falling outside this range were discarded. Any matches reflecting less than 80% similarity between target and reference spectra (using both the forward and reverse search procedures) were also discarded.

PBM was developed in the 1970’s by McLafferty and co-workers [154, 155]. Unlike earlier search algorithms, PBM added a weighting function to the *m/z* values and peak intensities. This weighting was used to determine the uniqueness of the spectrum and to calculate a probability for encountering this particular combination randomly (ie. obtaining a false positive) [156]. The ‘similarity’ of the target and reference spectra was returned as the reciprocal of this probability (log-base-2 confidence factor *K*) [156].

The forward search method involves comparing the target spectrum with every reference spectrum contained in the library. These retrieval systems act as a secondary filter for potential matches. Potential agreements from a forward search method (which will always be achieved) are ranked by an ‘agreement index’, which may allow elucidation of the chemical class to which the target spectrum refers [156]. In contrast, the reverse search function compares reference spectra against the target spectrum to establish the presence of similar *m/z* peaks from the reference spectrum in the target spectrum [156]. The presence of peaks in the target spectrum which are absent in the reference spectrum is not relevant to this search function, meaning that the target spectrum need not be ‘pure’ to generate a match [153, 156].

The performance of the PBM algorithm has been evaluated by several authors [157-159]. In their 1994 investigation, Stein and Scott compared 5 search algorithms, including a version of PBM, by matching test spectra against reference spectra in the NIST spectral database [158]. The PBM method ranked fourth, with 65% accuracy reported. The top ranking search algorithm, a dot-product function-based INCOS data system [160], improved on this value by some 10%. McLafferty and co-workers followed up on this report, by comparing versions the PMB and INCOS methods [159]. For high purity spectra referenced against the NIST database, both methods gave correct first ranked assignments to three out of four (75%) compounds. The PBM method generated better accuracy for 85% pure spectra, although only 48% were correctly assigned (cf. 27% with INCOS).

With this level of accuracy in mind, it is prudent to report that peak assignments reported in this section (and throughout this thesis) are tentative, unless otherwise stated and supported by analysis of reference standards. Despite the further inclusion of an LRI filter, the reporting of compound names does not indicate that a comprehensive characterisation of the sample has been performed.

### 3.1.3 Results and discussion

Characterisation of many essential oils requires very high resolution techniques and may not be amenable to high-speed analysis. However, essential oils with fewer components are more amenable to analysis using fast GC using columns with lower peak capacity. Fennel and parsley essential oils are produced for the international flavour market and exhibit moderate complexity. The present investigation examines the feasibility of applying lower peak capacity separations to the analysis of fennel and parsley essential oils using a wide-bore column (0.53 mm

i.d.) that was operated at sub-ambient column pressure. First, a 10 m × 0.10 mm i.d. column was used to generate a set of benchmark results upon which the quality of the separations achieved using the 12 m × 0.53 mm i.d. column could be measured. An initial carrier gas flow rate of 0.4 mL/min (helium) was used for all analyses using the 0.10 mm i.d. column. This carrier gas flow rate was selected according to recognised criteria for optimising flow rates in GC [35].

The temperature program rate for essential oil analysis was empirically optimised by performing analysis of a $C_8$-$C_{20}$ *n*-alkane mix using temperature program rates of 5, 10, 15, 20 and 28 °C/$t_M$. Predictably, the results of these analyses showed that a faster temperature program rate leads to shorter analysis timen with the potential for a loss in peak capacity. A temperature program rate of 20 °C/min (10 °C/$t_M$) was selected as a good compromise between speed and efficiency by using the weighting function described by Blumberg and Klee [34, 35]. There was no observable difference in retention time repeatability between the separations performed using the 0.10 mm or 0.53 mm i.d. columns; neither approach exceeded 0.15% RSD for retention time repeatability of selected reference compounds (terpinen-4-ol, dodecane and decan-1-ol). Peak response precision did not exceed 10% RSD for non-overloaded peaks in either approach. A typical chromatogram illustrating the separation of parsley essential oil using a 0.10 mm i.d. capillary and employing the optimised conditions described above is shown in Figure 3.3. The separation is performed in around 600 s and provides satisfactory peak capacity to separate the moderately complex sample. For comparative purposes, a chromatogram that illustrates the separation of parsley essential oil using a 0.53 mm i.d. column operated at sub-ambient pressure is also shown in Figure 3.3.

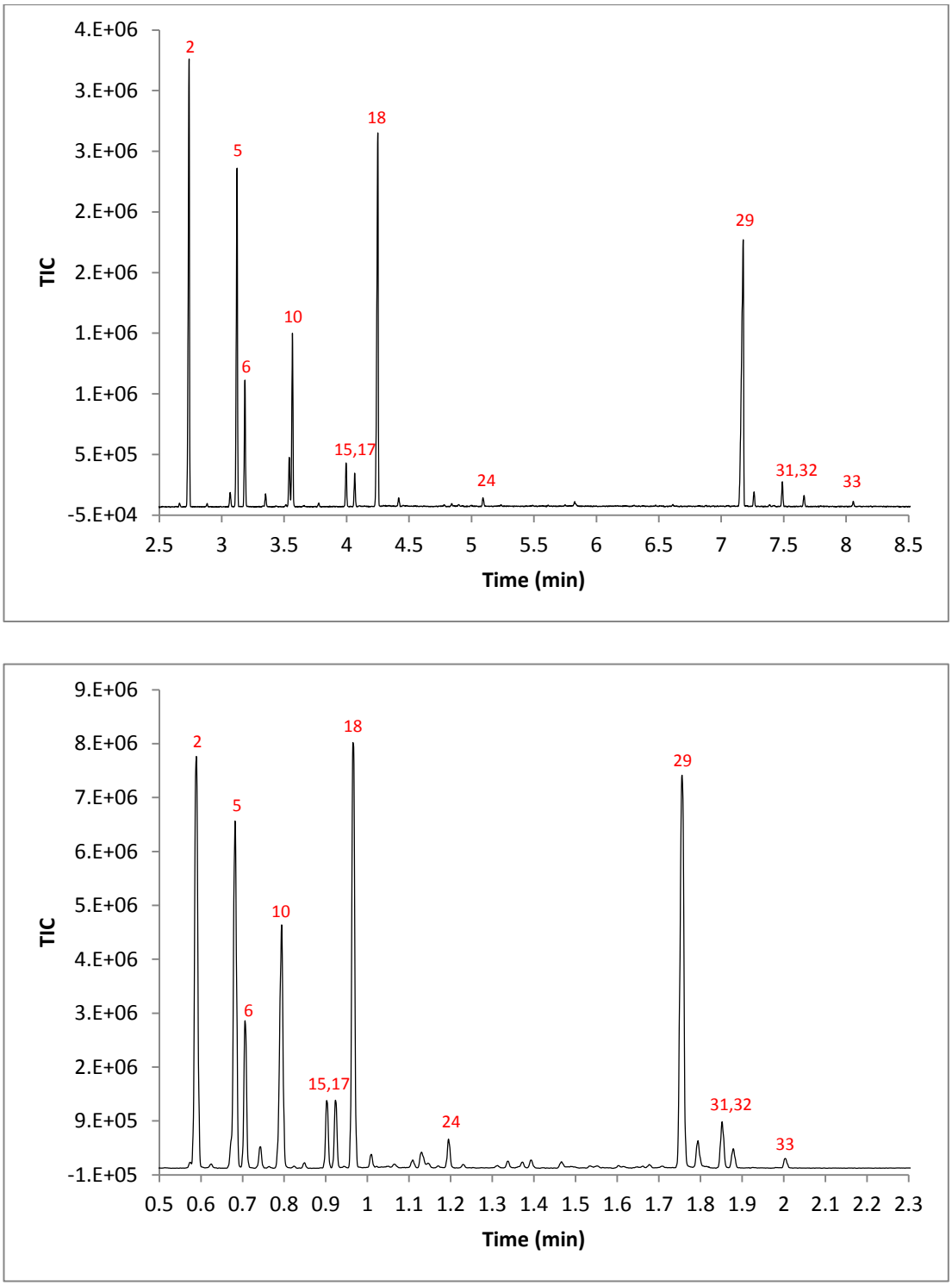


**Figure. 3.3. GC–MS (TIC) chromatogram of parsley essential oil acquired using a 10 m × 0.10 mm i.d. BPX-5 capillary column (top) and using a 12 m × 0.53 mm i.d. BPX-5 capillary column (bottom). Peak numbers refer to tentative identities listed in Table 3.1.**

Each separation was achieved using optimal flow rate and both use the same normalised heating rate of 10 °C/$t_M$. An approximate 2.5-fold speed gain is apparent for the 0.53 mm i.d. column separation, but this is accompanied by a concurrent loss in efficiency. The loss of efficiency is highlighted in Figure 3.4 by expanding the limonene/α-phellandrene peak pair, which are baseline resolved using the narrow-bore column, but these two components are almost completely overlapped in the chromatogram acquired using the wide-bore column. While a reduction in rate of the temperature program might partially alleviate the peak overlap observed on the wide-bore column, and it is expected that the use of a faster temperature program would speed up the analysis using the narrow-bore column, these steps were not followed to maintain a valid comparison of the two approaches.

A comparison of performance (using separation number, SN) of the two separation systems was made with one of the fastest separations reported in the literature that employed a conventionally heated GC oven [75]. In this fast separation using a 0.05 mm i.d. column, SN = 28 for the $C_8$ / $C_9$ homologue pair was reported. In the present investigation, the measured performance figures are SN = 27 and SN = 10 for the narrow-bore and wide-bore columns, respectively. For the $C_{19}$ / $C_{20}$ homologue pair, SN = 20 was achieved with a 0.05 mm i.d. column and under the analysis conditions used in the present investigation, the measured values were SN = 13 and SN = 6 for the 0.10 mm i.d. and 0.53 mm i.d. columns, respectively. To calculate the separation number of the peak pairs, the following equation was used:

$$SN = \left[\frac{t_{R,2} - t_{R,1}}{\overline{W_{h,1}} + \overline{W_{h,2}}}\right] - 1$$

As expected, the separation performance of the wide-bore column falls short of its narrower counterpart. However, sample capacity is also an important consideration

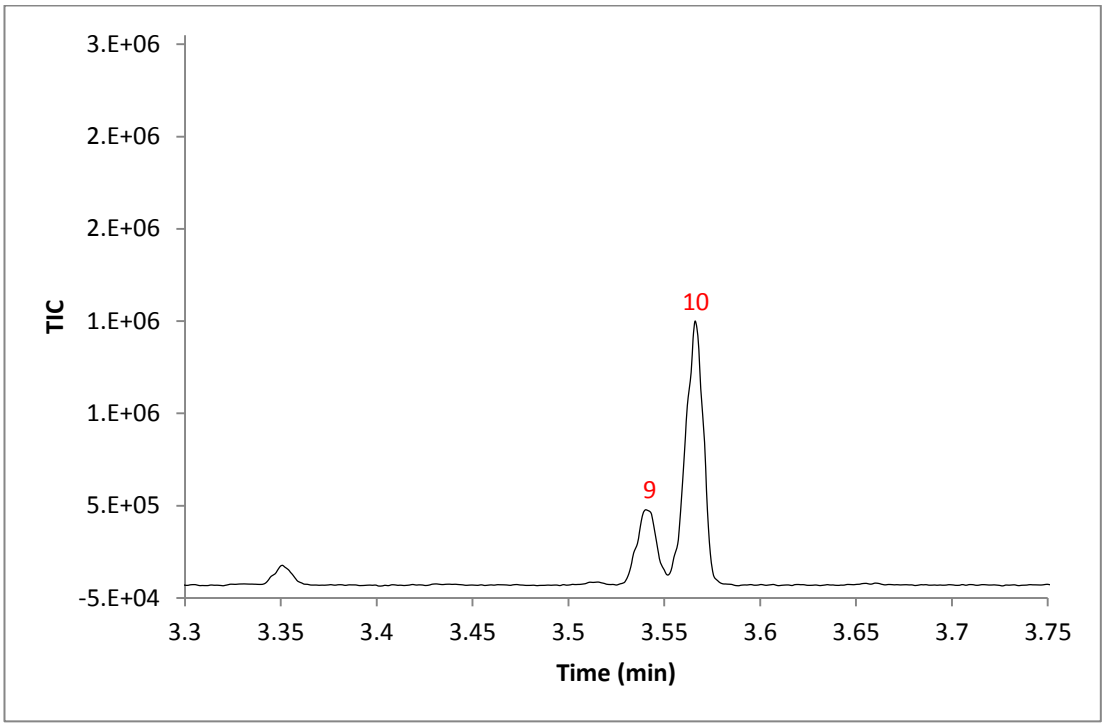


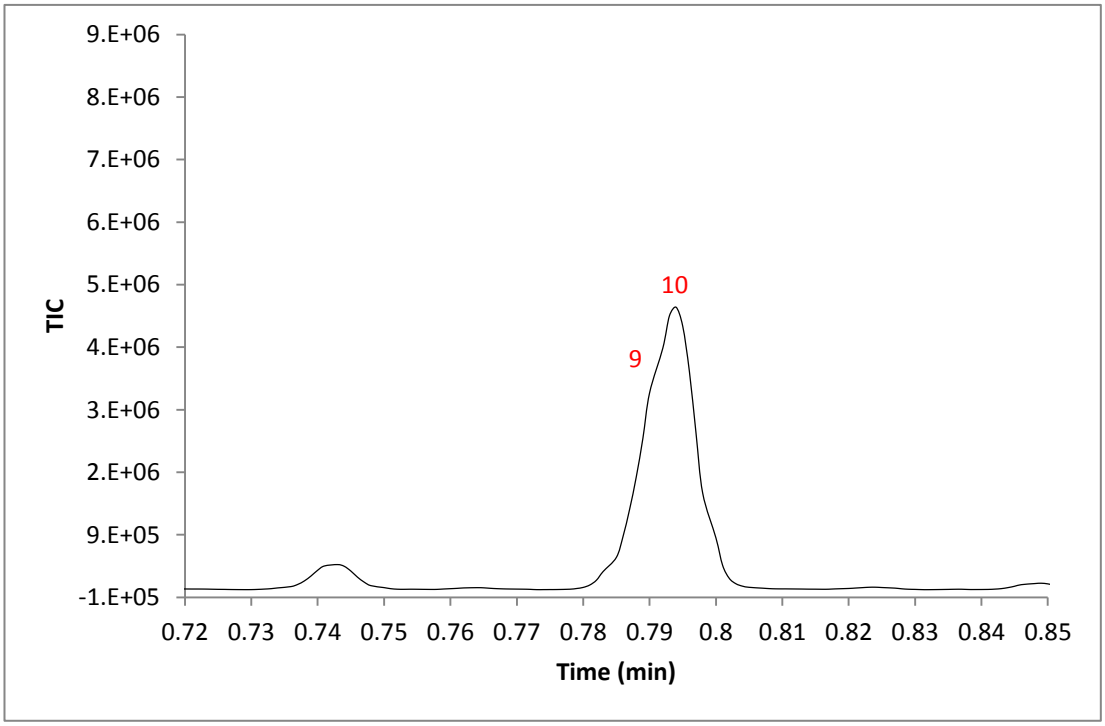


**Figure. 3.4. Comparison of resolution achieved between the limonene (9) and α-phellandrene (10) peak pair using a 10 m × 0.10 mm i.d. capillary column (top) and a 12 m × 0.53 mm i.d. capillary column (bottom).**

for GC–MS analysis of essential oils, particularly if the goal of the analysis is to completely characterise the sample in a single injection.

Although it represents a subjective measure, lower total ion current (TIC) signal intensity often creates ambiguity in providing tentative peak assignments. Decrease in the signal intensity of an analyte peak is not indicative of a concurrent decrease in background intensity, suggesting that the composition of background spectra becomes more significant. This may result in interference and a loss of spectral purity for the analyte peak. McLafferty *et al.* reported a significant decline in correct identification of peaks between those exhibiting high purity spectra and those of moderate purity using the same fundamental library search algorithm as the present study [159]. This suggests that a high TIC intensity and signal-to-noise ratio is important for correct peak assignments.

In the current investigation, identical MS settings (most notably data acquisition rate and scan range [112]) were used to eliminate the variable of detector sensitivity. The potential effects of mass spectral skewing were also reported, and are discussed in Section 3.1.2, wherein it is concluded that the effects are minimal. In general, separations performed using the 0.53 mm i.d. column generated larger TIC signal intensity than similar separations performed 0.10 mm i.d. column. Some of this effect may be attributed to the increased amount of sample introduced to the 0.53 mm i.d. column. This trend was observed quantitatively by comparison of LOD values for selected standards; terpinen-4-ol, dodecane and decan-1-ol. Using the method described in Section 3.1.2, the LOD was determined to be 2.9 mg/L versus 2.0 mg/L (terpinen-4-ol *m*/*z* 71 extracted ion chromatogram, EIC), 1.5 mg/L versus 0.5 mg/L (dodecane *m*/*z* 57 EIC) and 1.7 mg/L versus 1.0 mg/L (decan-1-ol *m*/*z* 55 EIC) for the wide-bore versus narrow-bore columns, respectively. These values

should be used for comparative purposes only because lower levels could be reached by modifying the injection, but this effort is beyond the scope of the present investigation. For instance, the approximate percent abundance (measured as percentage of GC–MS total ion current) of α-phellandrene in parsley essential oil is <1% so it is considered to be a minor component. The peak shape of α-phellandrene in each of these chromatograms is satisfactory, with measured asymmetry being 1.2 and 1.1 for the 0.10 mm i.d. and 0.53 mm i.d. columns, respectively. However, by visual comparison of a major component, myristicin (*ca*. 20% abundance) within these chromatograms (Figure 3.5), the reduced sample capacity of the 0.10 mm i.d. column is clearly evident for peaks of quite similar peak area ($2.6 \times 10^6$ in each chromatogram). Here the major component is quite severely overloaded in the narrow bore column ($A_s = 0.34$); in contrast the greater capacity of the 0.53 mm i.d. column offers excellent peak shape ($A_s = 1.0$). While the quantitative comparison of efficiency indicated that the narrow-bore column is superior, the increased propensity for band broadening in the narrow-bore column indicates that maximum utilisation of the available peak capacity would be difficult to achieve while keeping the TIC signal intensity at a sufficiently high level to afford high quality spectra.

Table 3.1 shows the library match quality (expressed as a percentage) for several tentative peak identifications in the fennel and parsley essential oil samples for the two columns. It must be noted that while confirmation of peak identities via injection of reference standards was not performed, a general trend is apparent in the library match qualities. On average, the percentages obtained using the method described in Section 3.1.2 were 5% greater in the separation performed with the wide-bore than those obtained using the narrow-bore column. For many components, tentative peak assignment could not be made without a degree of ambiguity in the

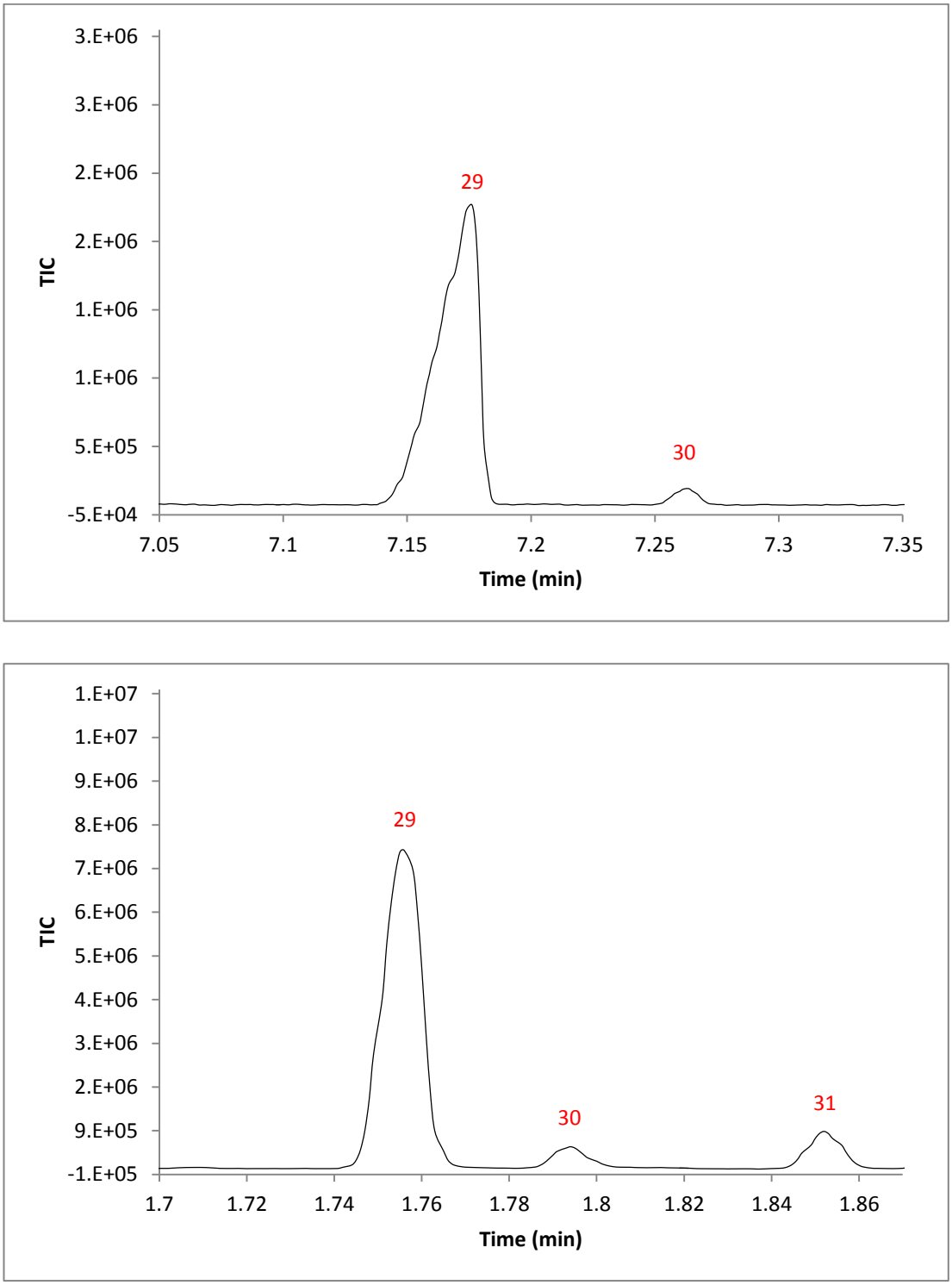


**Figure 3.5. Comparison of sample capacity available by using a major component myristicin using a 10 m × 0.10 mm i.d. capillary column (top) and a 12 m × 0.53 mm i.d. capillary column (bottom).**

**Table 3.1. Tentative peak assignments listed with library match value (per cent) for parsley and fennel essential oil illustrating library match quality for identified components. Peaks were identified using Shimadzu GCMSolution and the FFNSC library with a LRI filter as described in Section 3.1.2. Hyphens indicate that a match could not be generated using the filters employed.**

| Peak | Name | Match % of parsley essential oil | | Match % of fennel essential oil | |
|---|---|---|---|---|---|
| | | 0.10 mm i.d. | 0.53 mm i.d. | 0.10 mm i.d. | 0.53 mm i.d. |
| 1 | α-thujene | 90 | 97 | - | - |
| 2 | α-pinene | 94 | 98 | 91 | 98 |
| 3 | camphene | 86 | 95 | 85 | 98 |
| 4 | sabinene | 85 | 97 | 84 | 97 |
| 5 | β-pinene | 92 | 98 | 88 | 98 |
| 6 | myrcene | 93 | 98 | 91 | 98 |
| 7 | α-phellandrene | 92 | 97 | 91 | 98 |
| 8 | α-terpinene | - | 92 | - | 92 |
| 9 | limonene | 90 | - | 91 | 97 |
| 10 | β-phellandrene | 89 | 98 | - | - |
| 11 | 1,8-cineole | - | - | - | 93 |
| 12 | E-β-ocimene | - | 93 | 88 | - |
| 13 | γ-terpinene | 84 | 93 | 88 | 97 |
| 14 | linalool | - | - | - | 87 |
| 15 | terpinolene | 90 | 97 | 88 | 95 |
| 16 | fenchone | - | - | - | 98 |
| 17 | α-p- dimethylstyrene | 91 | 96 | - | - |

| Peak | Name | Parsley essential oil | | Fennel essential oil | |
|---|---|---|---|---|---|
| | | 0.10 mm i.d. | 0.53 mm i.d. | 0.10 mm i.d. | 0.53 mm i.d. |
| 18 | 1,3,8-*p*-menthatriene | 93 | 97 | - | - |
| 19 | cis-pinene hydrate | - | - | - | 91 |
| 20 | camphor | - | - | - | 98 |
| 21 | pentylbenzene | 76 | 82 | - | - |
| 22 | terpinen-4-ol | - | - | - | 95 |
| 23 | estragole | - | - | - | 97 |
| 24 | cis-ocimenone | - | 83 | - | - |
| 25 | Z-anethole | - | - | - | 95 |
| 26 | E-anethole | - | - | - | 96 |
| 27 | triacetin | - | 85 | - | - |
| 28 | germacrene D | - | - | - | 93 |
| 29 | myristicin | 92 | 97 | - | - |
| 30 | elemicin | - | 94 | - | - |
| 31 | 6-methoxyelemicin | - | 97 | - | - |
| 32 | carotol | - | 97 | - | - |
| 33 | apiole | - | 96 | - | - |

separation obtained using the narrow-bore column. The peak assigned as E-β-ocimine is an example of this effect. While this observation is not conclusive in itself, the trend observed supports the previous observations regarding sample loadability and capacity contrasts between the two columns, and may be attributed to the greater TIC signal intensity witnessed in separations performed using the 0.53 mm i.d. column.

### 3.1.4 Concluding remarks

High throughput GC–MS analysis is highly desirable in many situations. Depending on the complexity of the sample, chromatographic efficiency may be sacrificed in search of faster analysis times. This reasoning was employed in the current investigation, in which the performance of a wide-bore column operated under sub-ambient outlet conditions was evaluated by direct comparison with a narrow-bore column. Parsley and fennel essential oil are among those produced in Tasmania for the international flavour market. The Tasmanian essential oil industry has a reputation as a reliable supplier of consistent quality essential oil products and maintaining this reputation depends upon regular quality monitoring. These two oils were selected for evaluation in the current study, as they are of moderate complexity and typify samples for which this technique may be employed.

Highly satisfactory separations of the essential oil samples were generated using both columns, suggesting that these fast GC–MS methods are amenable to separation of moderately complex essential oil samples. Considering the narrow-bore column was of higher efficiency by design, the separation number calculated for two pairs of *n*-alkanes was commensurately higher. In contrast, the increased sample

capacity afforded by the wide-bore column permitted better peak shapes of major constituents, decreased LOD and increased TIC signal intensity.

Despite the applicability of this technique for GC–MS applications, the efficiency afforded by this column is unlikely to be sufficient for use as the second dimension of a GC×GC approach. In general, comprehensive two-dimensional approaches are ideally suited, and generally reserved for, complex samples requiring high peak capacity and resolution. For this reason, columns possessing higher theoretical efficiency were used in subsequent sections of this thesis.

## 3.2 High temperature wax column for GC×GC analysis of essential oils

This section has been adapted from the following publication:

P.D. Morrison, P.J. Marriott, S.D.H. Poynter, R.A. Shellie. **Selection of columns for GC×GC analysis of essential oils.** *LC-GC Eur.* 23 (2010) 76-80.

### 3.2.1 Introduction

A substantial majority of GC×GC publications for essential oil analysis in the periodical literature have utilised a 'non-polar' column in the first dimension and a 'polar' column in the second dimension [161]. In practice this almost always translates to use of a 100% polydimethyl siloxane or 5% diphenyl 95% dimethyl polysiloxane stationary phase in the first-dimension combined with a 50% diphenyl 50% dimethyl polysiloxane or a polyethylene glycol (wax) second-dimension column, although there are notable departures from this convention, including applications reversing the order of 'polarity' [162], providing class-type separation of citrus oil components, and those using cyclodextrin derivative stationary phases for enantioselective analysis [15, 163-165]. Even in the case where a conventional non-polar / polar column ensemble is used, the mechanism of retention for solutes in the second dimension depends on volatility and polarity, but using an appropriate temperature program cancels out the influence of volatility on retention in the second-dimension column [1]. For this reason, GC×GC separations are temperature-programmed to maximise differences in separation mechanisms in the two dimensions. However, since both columns are commonly installed in the same oven, the temperature stability of one of the separation columns typically imparts an upper temperature limit on the separation system. Applications that utilise 50% diphenyl

50% dimethyl polysiloxane second-dimension columns are benefited in terms of high-temperature stability compared to those applications employing wax columns, but more suitable selectivity of wax columns for polar essential oil components was shown many years ago [166] and wax stationary phases are almost universally preferred.

For a GC×GC separation to be effective there should be a degree of independence between the retention factors of the sample components on the two dimensions. Should there be no relationship between the two retention factor values, the system is described as being orthogonal. In a non-polar/polar column set, it is conventional to select a temperature program which aims to have sufficiently low ramp rate such that each second-dimension separation is carried out under approximately isothermal conditions. This decreases volatility effects in the second-dimension (polar) column, with the aim of maximising the available orthogonality available separation space. While the orthogonality is indeed decreased in the case of a polar/non-polar column set, this combination may prove appropriate for samples containing a large proportion of polar compounds within a narrow volatility range. In such a separation, the increased resolution afforded by performing the primary analysis on a longer polar column may outweigh the loss in peak capacity observed by reducing the window of separation space in the two-dimensional chromatogram.

A 5 m × 0.10 mm i.d. MEGA-WAX HT high-temperature wax column with a stationary phase film thickness of 0.10 μm (Mega, Legnano, Italy) was obtained with the intention of incorporating it in GC×GC work involving essential oil analysis. The wax second-dimension column used in the current investigation has more than 9000 N/m tested in isothermal mode and an upper column oven limit of 300 $^{o}$C (as claimed by the manufacturer). Results from the GC×GC analysis of

kunzea essential oil obtained by steam distillation of aerial parts of *Kunzea ambigua* are reported here.

### 3.2.2 Experimental

Kunzea (*Kunzea ambigua*) essential oil was provided by Dr. Christian Narkowicz (School of Pharmacy, UTAS) and was obtained through in-house hydrodistillation and was diluted to 1% v/v in dichloromethane (Sigma-Aldrich, Castle Hill, Australia).

A series of fast GC–MS analyses were performed using the 5 m column as received. A fast temperature programmed gradient from 40 $^{o}$C to 300 $^{o}$C in 6.5 min (40 $^{o}$C/min) was employed for these analyses and the oven was held at the maximum temperature for 1 min at the end of the temperature programme. The carrier gas (He) was delivered at a constant pressure of 36 psi (248 kPa). Figure 3.6 shows an overlay of five replicate blank analyses that were overlaid to assess the level of stationary phase bleed. Even using a reasonably aggressive rapid temperature program rate up to 300 $^{o}$C, these results are highly satisfactory and demonstrate acceptable repeatability for the purposes of this study, and support the manufacturer's claim regarding the stability of the coating at high temperature. The level of stationary phase bleed is compared in Figure 3.7 with that of two other columns, possessing similar selectivity and identical film thickness and dimensions. A total of ten replicate blank analyses were performed for each column and the results for each column were averaged to generate this plot. The temperature ramp was reduced to a 250 °C maximum to avoid excessive bleed on the less stable columns. It is clearly evident that the bleed from the HT-WAX column is significantly less than that witnessed from the other two columns.

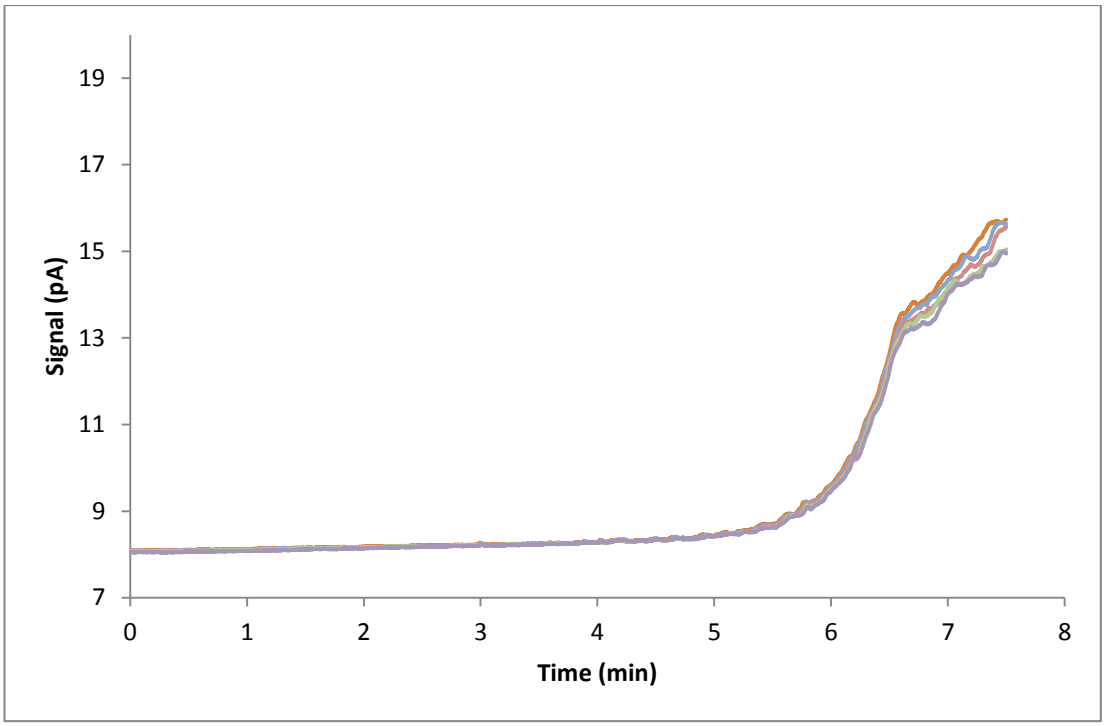


**Figure 3.6. Overlay of five replicate blank analyses with a 5 m × 0.1 mm i.d. MEGA-WAX HT column collected with flame ionisation detection. Conditions: He carrier gas at 36 psi (248 kPa) constant pressure, temperature program 40-300 °C at 40 °C/min.**

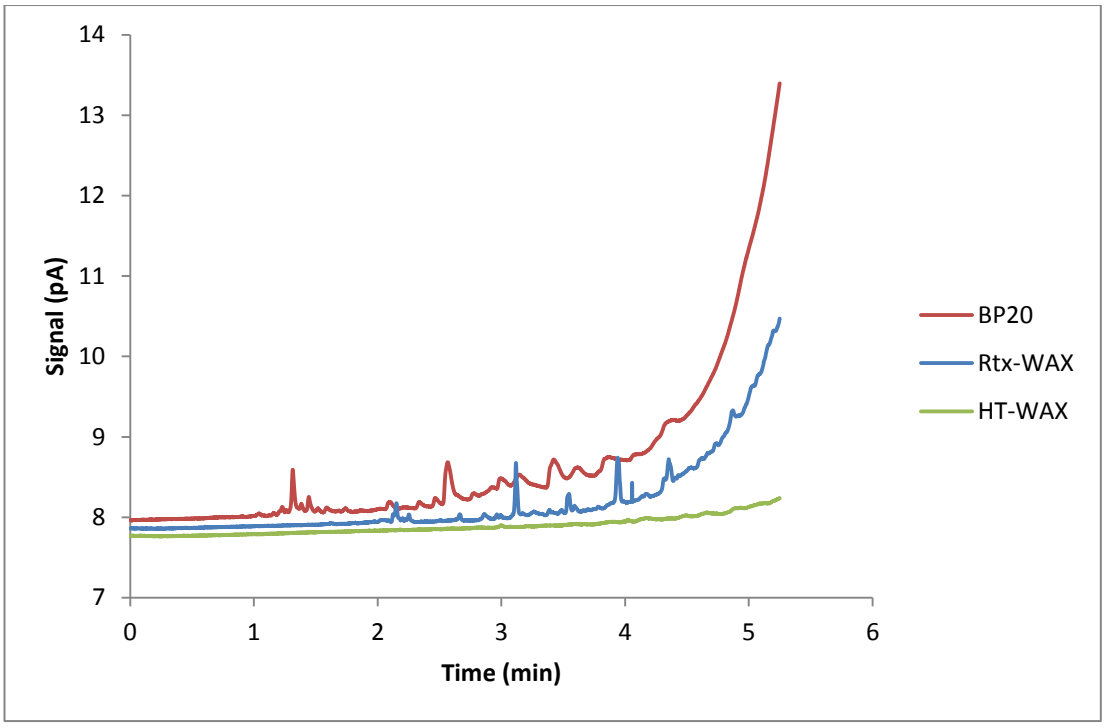


**Figure 3.7. Comparison between HT-WAX column and alternative wax columns. Each plot represents the average of ten replicate blank analyses. Conditions: He carrier gas at 36 psi (248 kPa) constant pressure, temperature program 40-250 °C at 40 °C/min.**

GC×GC analyses were performed using an Agilent 6890 GC (Agilent Technologies, Forest Hills, Australia) equipped with a custom dual-jet cryogenic ($CO_2$) modulation system based on the design of Beens *et al.* [127] and flame ionisation detector. A temperature program of 60 $^{o}$C to 300 $^{o}$C in 48 min (5 $^{o}$C/min) was employed for all analyses. A 1.0 m length from the MEGA-WAX HT column was used as the second-dimension column in this system in conjunction with a 30 m × 0.25 mm i.d. Rxi-5 Sil MS column with a stationary phase film thickness of 0.25 μm (Restek Corporation, Bellefonte, PA, USA) in the first dimension.

### 3.2.3 Results and discussion

*Kunzea ambigua* is a shrub native to the Eastern parts of Australia. As an effective killer of bacteria, kunzea essential oil has numerous traditional folk medicine uses and researchers have recently developed a kunzea oil formulation for veterinary use [167]. Kunzea oil is rich in sesquiterpene alcohols, and as a consequence, one-dimensional GC lacks the resolving power to provide adequate separation of the complex sample. The primary goal of this investigation was to determine the suitability of a short MEGA-WAX HT column as a second-dimension column for essential oil analysis using a pneumatically-modulated GC×GC–MS approach. Fast GC–MS analysis of the kunzea essential oil was also performed using this configuration and a typical chromatogram is shown in Figure 3.8. To compare the general selectivity of the MEGA-WAX HT column, a fast GC–MS chromatogram of kunzea essential oil using a 20 m × 0.10 mm i.d. Rtx-WAX column is shown in Figure 3.9. Temperature effects as well as differences in the stationary phase chemistry each influence the absolute retention order so an attempt to overlay these chromatograms would be pointless. The MEGA-WAX HT column

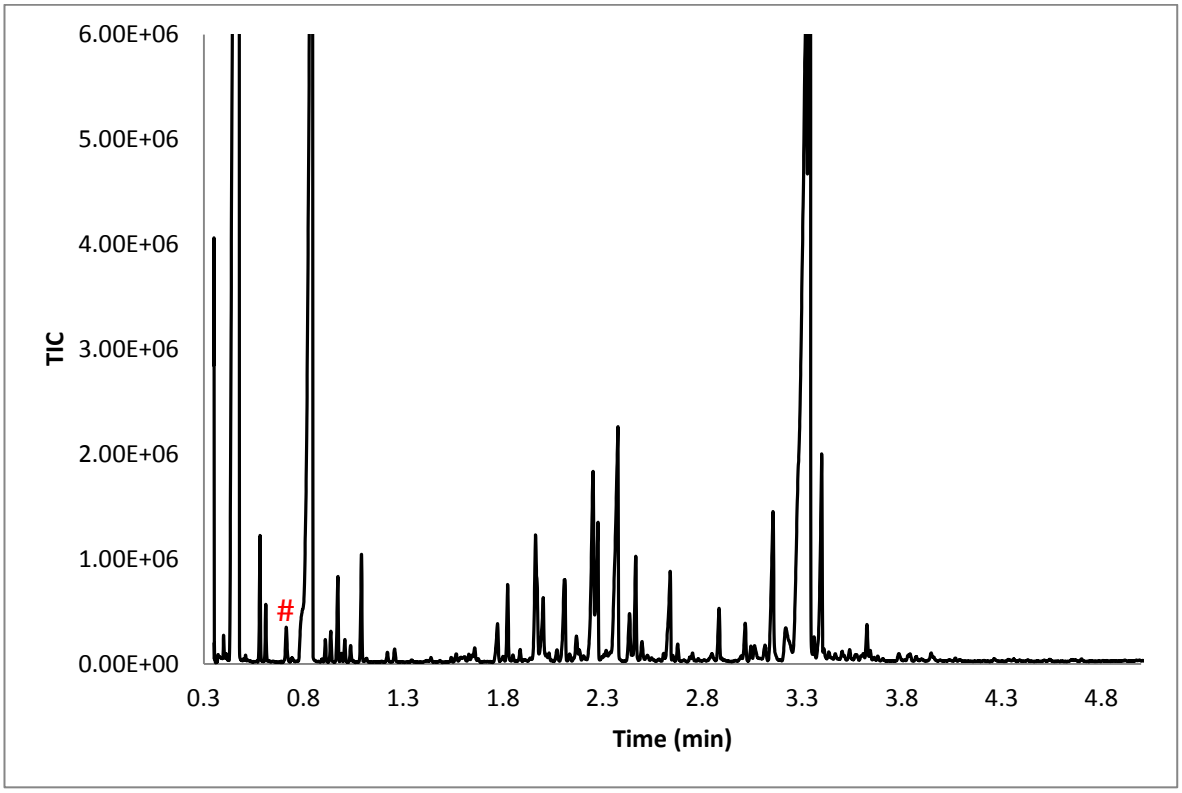


**Figure 3.8. Fast GC–MS analysis [GC–MS total ion current chromatograms (full-scan 35-350 *m/z*; 20 spectra/s)] of kunzea essential oil (2.5% v/v) using a 5 m × 0.10 mm i.d. MEGA-WAX HT column. He carrier gas was supplied at a constant pressure of 36 psi (248 kPa) and a temperature program of 40-300 °C at 40 °C/min. The injection volume was 1 μL using a split ratio of 1:50. Note the intensity of the small peak marked #, which has a low relative peak intensity of 1.09% which is more than 19× the average baseline response between 2 and 5 min.**

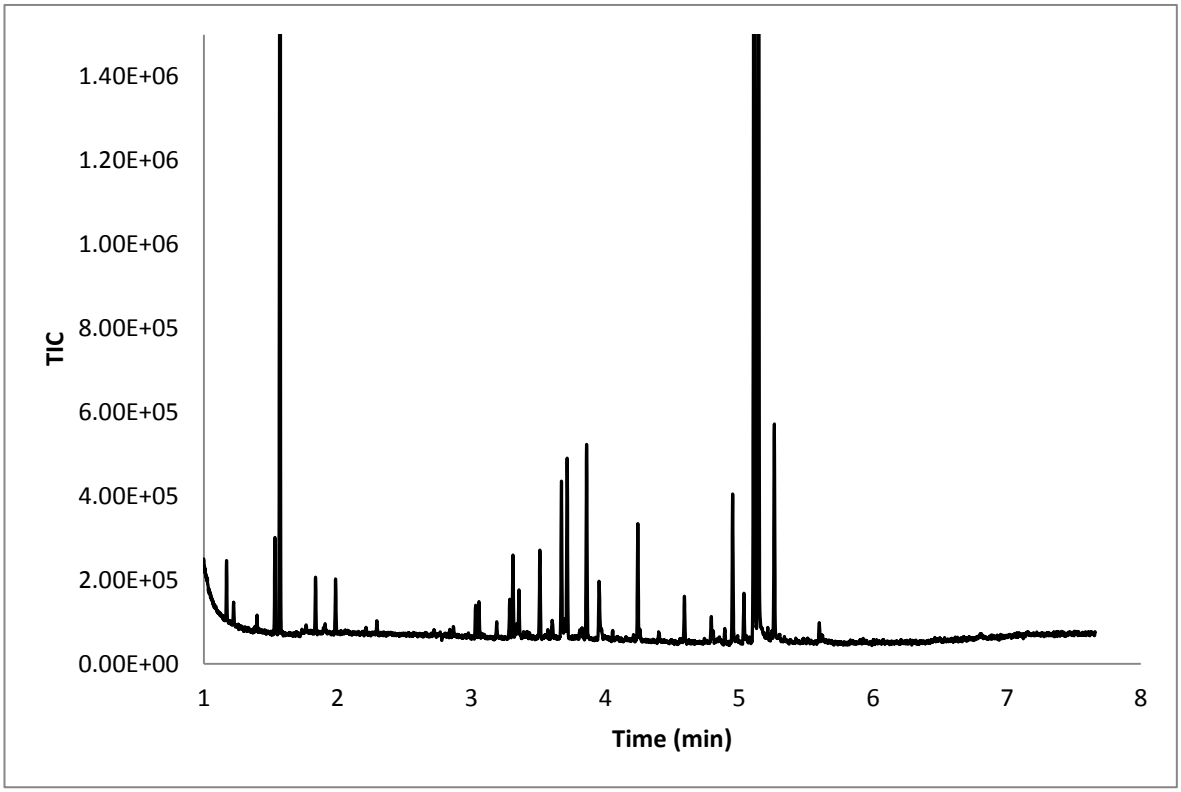


**Figure 3.9. Fast GC–MS analysis [GC–MS total ion current chromatograms (full-scan 35-350 *m/z*; 20 spectra/s)] of kunzea essential oil (5% v/v) using a 20 m × 0.10 mm i.d. Rtx-WAX column. $H_2$ carrier gas was supplied at a constant pressure of 100 psi (689 kPa) and a temperature program of 40-240 °C in 6.67 min (30 °C/min) was utilised. The injection volume was 1 μL using a split ratio of 1:50.**

is also 75% shorter than the Rtx-WAX column, so the resolution using the latter column is understandably better. Nonetheless, elution of the monoterpene and sesquiterpene hydrocarbons, followed by the monoterpene and sesquiterpene alcohols is in general congruence between the two columns.

A typical GC×GC chromatogram of kunzea essential oil is shown in Figure 3.10. Following application of a 3 s modulation period, there is excellent utilisation of the two-dimensional separation space albeit with a substantial amount of wrap-around of the more polar solutes. Such degree of wrap-around is not uncommon for essential oils analysis by GC×GC and this is generally acceptable provided that the wrapped-around components do not interfere with those belonging to the next modulation. It would be possible to re-optimise the separation using a four or five second modulation period to reduce the observed wrap-around, but this option was avoided in the current study primarily because the wrap-around was not too extreme and the three to four slice-per-peak modulation criterion for maintaining first-dimension separation integrity was obeyed [3].

The separation performance of the MEGA-WAX HT second-dimension column is further highlighted in Figure 3.11, where an extracted peak slice is presented. The peak capacity of the second-dimension column is estimated to be approximately ten using the conditions described above.

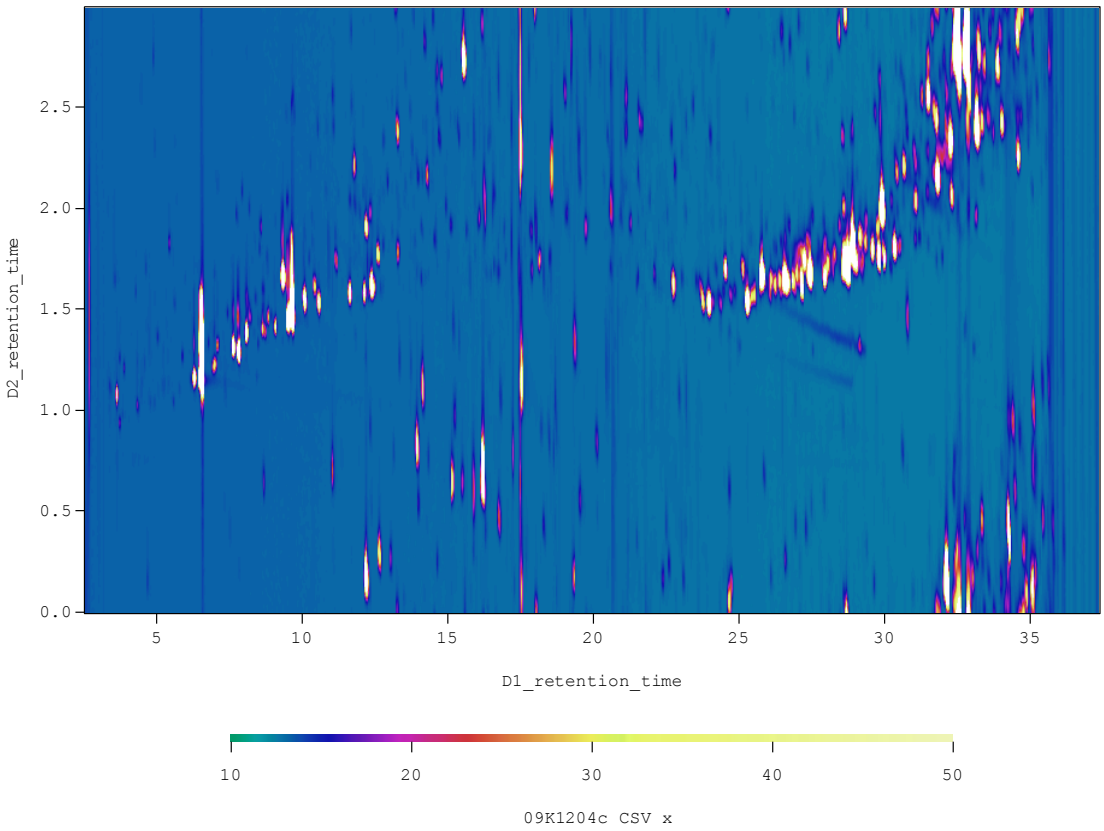


**Figure 3.10. GC×GC chromatogram of kunzea essential oil. $H_2$ carrier gas was supplied at a constant pressure of 27 psi (186 kPa). The injection volume was 1 µL using a split ratio of 1:50. A temperature program 60-300 °C at 5 °C/min was used with flame ionisation detection.**

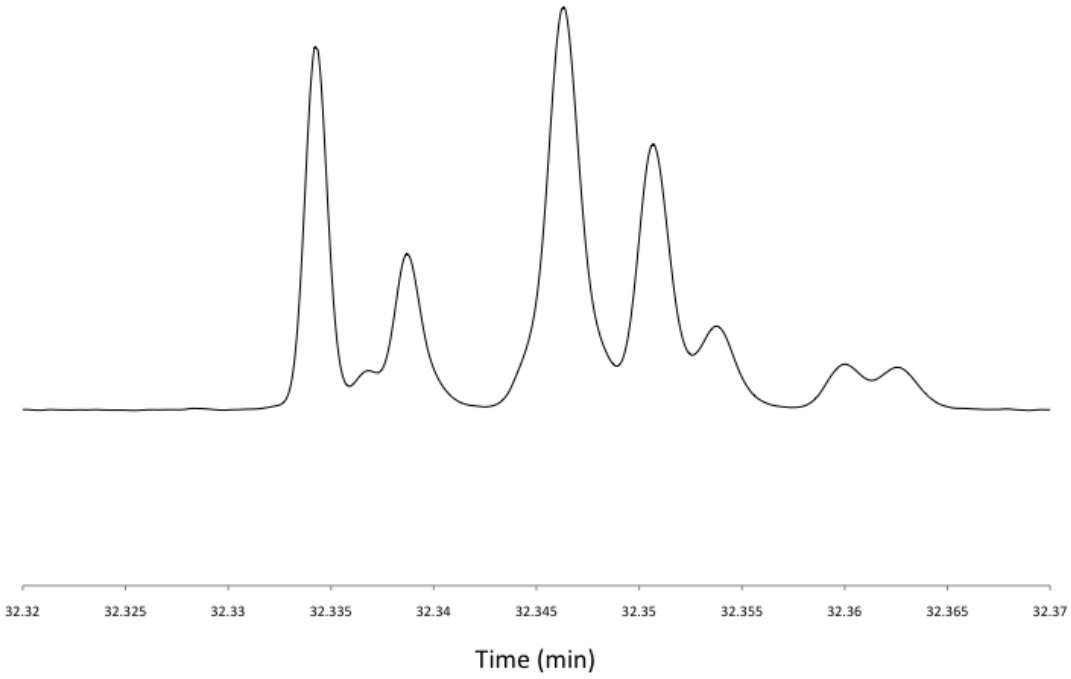


**Figure 3.11 Individual second-dimension slice from the GC×GC chromatogram of kunzea essential oil shown in Figure 3.10.**

### 3.2.4 Concluding remarks

The evaluation of a MEGA-WAX HT column for both high speed GC–MS separations and as the second dimension of a comprehensive two-dimensional GC set-up has been performed. The separation of an essential oil sample by GC–MS using a 5 m × 0.10 mm i.d. column was comparable to that obtained by a 20 m × 0.10 mm i.d. Rtx-WAX column, albeit with a decrease in resolution. However, the column held its own when used in a 1 m length in the GC×GC application. Separation of the complex sesquiterpene alcohol components in the kunzea oil examined yielded a good utilisation of the available separation space.

At the time of writing, this stationary phase coating was only available in a 0.10 mm i.d. column. The use of a narrow-bore column in the second dimension of a pneumatically-modulated GC×GC–MS approach presents numerous limitations, especially concerning the effect of applying flow ratios required to sustain modulation on the pumping capacity of the MS and the deviation from EOV in the first-dimension flow. While there is no doubt that the selectivity afforded by this stationary phase is well suited to GC×GC applications where a 0.10 mm i.d. column may be used, use of a column of these dimensions in a pneumatically-modulated GC×GC–MS approach would not be appropriate.

## 3.3 Investigation of high efficiency, high resolution columns for GC–MS approaches

### 3.3.1 Introduction

The evolving application field for gas chromatography has led to the desire to separate samples with ever increasing complexity, requiring high efficiency and concomitantly high peak capacity separation columns. While this may be achieved by simply increasing the length of the column, this would increase the holdup time which may prove undesirable for applications where high sample throughput is a priority. In this study, thoughts on the intelligent selection of column length using predetermined inlet and outlet pressures to generate a time and efficiency optimised separation are presented. Results indicate that commonly-used methods for selecting column flow may not provide the best trade-off between efficiency and separation time.

Samples of hop and vetiver essential oil were examined using a 60 m polar coupled column in a one-dimensional approach, with a view to utilising a similar length column in the first-dimension of a pneumatically modulated GC×GC–MS system. A separation of hop essential oil was performed on a 40 m non-polar coupled column to demonstrate a separation performed using conditions optimised for the available maximum carrier gas inlet pressure.

When utilising narrow bore columns for separations where high efficiency is desired, common practice relies upon the use of available column lengths as provided by the manufacturer. Some users will shorten columns to suit their efficiency requirements. A thin-film column with an internal diameter of 0.10 mm provides the highest efficiency per unit length of commonly available capillary columns. Whilst high speed gas chromatography has been an expanding field of research in recent

years due to the desire to reduce separation times, the need for separation methods for complex samples has not diminished.

In general terms, the analyst usually forgoes separation speed in search of efficiency. Considering that there is a square root relationship between the efficiency and separation speed, a large separation time penalty may be accrued from trying to reach higher plate numbers by increasing the length of the column. The hunt for high efficiency columns started as early as 1962 with Desty's examination of a 272 m × 0.153 mm i.d. capillary column [168]. Despite the extended analysis time (the retention time of nonane was 21 hours), 800,000 effective plates were witnessed and exceptionally high resolution separations were generated. Further work continued throughout the 1960s and 1970s [169, 170] and culminated in the investigation by Berger in 1996 [171], who utilised a 450 m × 0.20 mm i.d. column for the separation of a gasoline sample. Separation of 970 compounds was possible in a 650 min temperature program, and 1.3 million effective theoretical plates were observed. Unfortunately, the long separation time is not conducive to the majority of applications.

Sandra and co-workers recently reported the resolution of 195 out of 209 PCB congeners using a high efficiency column in a GC–MS approach [117]. This peak count is comparable with the best results available to-date by GC×GC–MS techniques. An 80 m × 0.10 mm i.d. capillary column was utilised, which required hydrogen carrier gas at 140 psi (965 kPa) in constant pressure mode. Previous reviews [172, 173] suggested that resolution of all 209 PCBs was not possible with a simple one-dimensional approach, so the group aimed to provide the most thorough one-dimensional analysis of the congener series.

Essential oils are another example of complex mixtures requiring high peak capacity for satisfactory separation. A vital element in imparting flavour and bitterness to beer, hop (*Humulus lupulus* L.) varieties can be characterised by analysis of hop cone metabolite extracts [174] or, more commonly, by GC–MS or GC×GC–MS analysis of essential oil fractions [175, 176]. The essential oil of hop is of complex composition and may contain up to 1000 compounds from a variety of chemical classes, with terpene hydrocarbons making up a considerable percentage [177, 178]. The peak capacity required to separate and identify every component is currently beyond the means of a one-dimensional separation, however a high resolution separation may still yield useful data.

### 3.3.2 Experimental

A sample of hop (*Humulus lupulus* L.) essential oil was provided by Hop Products Australia (Bellerive, Australia) and diluted to 0.5% v/v (unless stated) in dichloromethane (Sigma-Aldrich, Castle Hill, Australia). The sample was obtained by hydrodistillation. A commercial vetiver (*Vetiveria zizanioides*) essential oil sample was obtained from Australian Botanical Products (Hallam, Australia) and was prepared in a similar manner.

Three 20 m × 0.10 mm i.d. capillary columns coated with a thin layer (0.1 µm) of polyethylene glycol stationary phase (RTx-WAX, Restek Corporation, Bellefonte, PA, USA) were connected in series using appropriately-sized alumoseal™ connectors (Restek Corporation, Bellefonte, PA, USA) to create the 60 m × 0.10 mm i.d. coupled analytical column used in this investigation. Tentative peak analysis was performed on a separation of hop essential oil using a 40 m x 0.10

mm i.d. Rtx-5 coupled column (Restek Corporation, Bellefonte, PA, USA) which was constructed in a similar manner.

Hydrogen carrier gas was supplied by a Parker Balston Hydrogen Generator (model H2PEM-100, Haverhill, MA, USA) at its maximum outlet pressure of 100 psi (689 kPa), providing an initial flow rate of approximately 0.75 mL/min. A 1 µL split injection at 230 °C was employed for all separations with a split ratio of 200:1. The GC was temperature programmed from 40 °C to 240 °C at 1.5 °C/min and 3 °C/min ramps and held at 240 °C for 15 min. Data were collected in full-scan mode operating between 35-350 *m/z* at an acquisition rate of 5.3 Hz.

### 3.3.3 Results and discussion

*Investigating optimum conditions*

In a series of papers on the theory of fast capillary GC [179-181], Blumberg discussed aspects of column efficiency, analysis speed and the relationship between column performance and gas flow rate. Of primary concern was the optimisation of pneumatic parameters to either extract the maximum available efficiency of a column, or find the minimum separation time required to realise a given efficiency [179]. For columns displaying high pressure drop (which can be generalised to incorporate long, narrow-bore columns), an approach for optimising available efficiency had not been established in the literature. Blumberg drew upon the relationships described in the van Deemter [182] and Giddings [183] equations to propose that the plate height, H, is related to the average linear velocity of the carrier gas, $\bar{u}$, as shown below :

$$H = \frac{B}{\bar{u}^2} + C_1\bar{u}^2 + C_2\bar{u}$$

The expressions *B* and *C* incorporate fixed values describing the film thickness, solute diffusivity, outlet pressure, column length, carrier gas viscosity and retention factor. Using this equation, an average carrier gas velocity for which the plate height approaches a minimum value can be established. Blumberg referred to this value as $\bar{u}\mathrm{min}_H$, or the Efficiency Optimised Velocity (EOV) [179].

While maximisation of available efficiency can be a key objective, some circumstances dictate that the time required to complete a separation is more important. The van Deemter equation states that increasing the average linear velocity to 2× the EOV value results in a separation taking half the time of one performed under EOV conditions, yet efficiency is only sacrificed by one quarter [180]. This led Blumberg to propose an alternative optimisation parameter, namely the Speed Optimised Velocity (SOV), or $\bar{u}\mathrm{min}_Q$. For long, narrow bore columns with a thin film coating, the increase in speed can be in the order of 10% [180]. As a corollary to EOV and SOV, which provide an average value based on the varying carrier gas velocity through the column, Speed- and Efficiency Optimised Flow (SOF and EOF) rates were also proposed [181]. These values are consistent throughout the column during the course of a temperature program, assuming that the instrument is operated in a *constant flow* mode.

In the case where a temperature gradient and *constant pressure* mode are employed, the flow rate and average linear velocity decrease throughout the temperature program. This means that an optimised flow or velocity (be it speed- or efficiency-) can only be realised at one point in the temperature program. This is shown in a graphical format in Figure 3.12. Three plots have been constructed, representing columns of 20, 40 and 60 m in length, each with a thin film coating and an internal diameter of 0.10 mm. A temperature program of 40-240 °C is described

on the *x* axis for each column. In each chart, a plot of average linear velocity throughout the temperature program, *should constant pressure mode be enforced*, is shown in blue. To calculate this value, the linear velocity at the column outlet ($u_o$) was calculated using the following equation:

$$u_o = \left(\frac{r^4(p_i^2 - p_o^2)}{16\eta L p_o}\right)$$

Where $r$ is the column radius, $p_i$ is the column inlet pressure, $p_o$ is the column outlet pressure (0 psi for MS use), $\eta$ is the dynamic viscosity of the carrier gas and $L$ is the column length [37]. A fixed value of 100 psi (689 kPa) was used for $p_i$ in all instances. To generate an average velocity, this value was multiplied by a compressibility factor ($j$), to account for the compressibility of the mobile phase:

$$j = \frac{3(p^2 - 1)}{2(p^3 - 1)}$$

where $$p = \frac{p_i}{p_o}$$

This function clearly demonstrates the decrease in average linear velocity throughout the temperature program should constant pressure mode be utilised.

The second function on each plot (shown in brown) similarly displays average linear velocity throughout the temperature program, but in this instance, *constant flow* mode is enforced at the EOF value of 0.5 mL/min. Outlet velocity was calculated using the formula:

$$\bar{u}_o = \frac{F_o}{\pi d_c^2 / 4}$$

Where $F_o$ is the flow rate at column outlet and $d_c$ is the column diameter. The outlet velocity was then converted to average velocity as before. These formula are derived

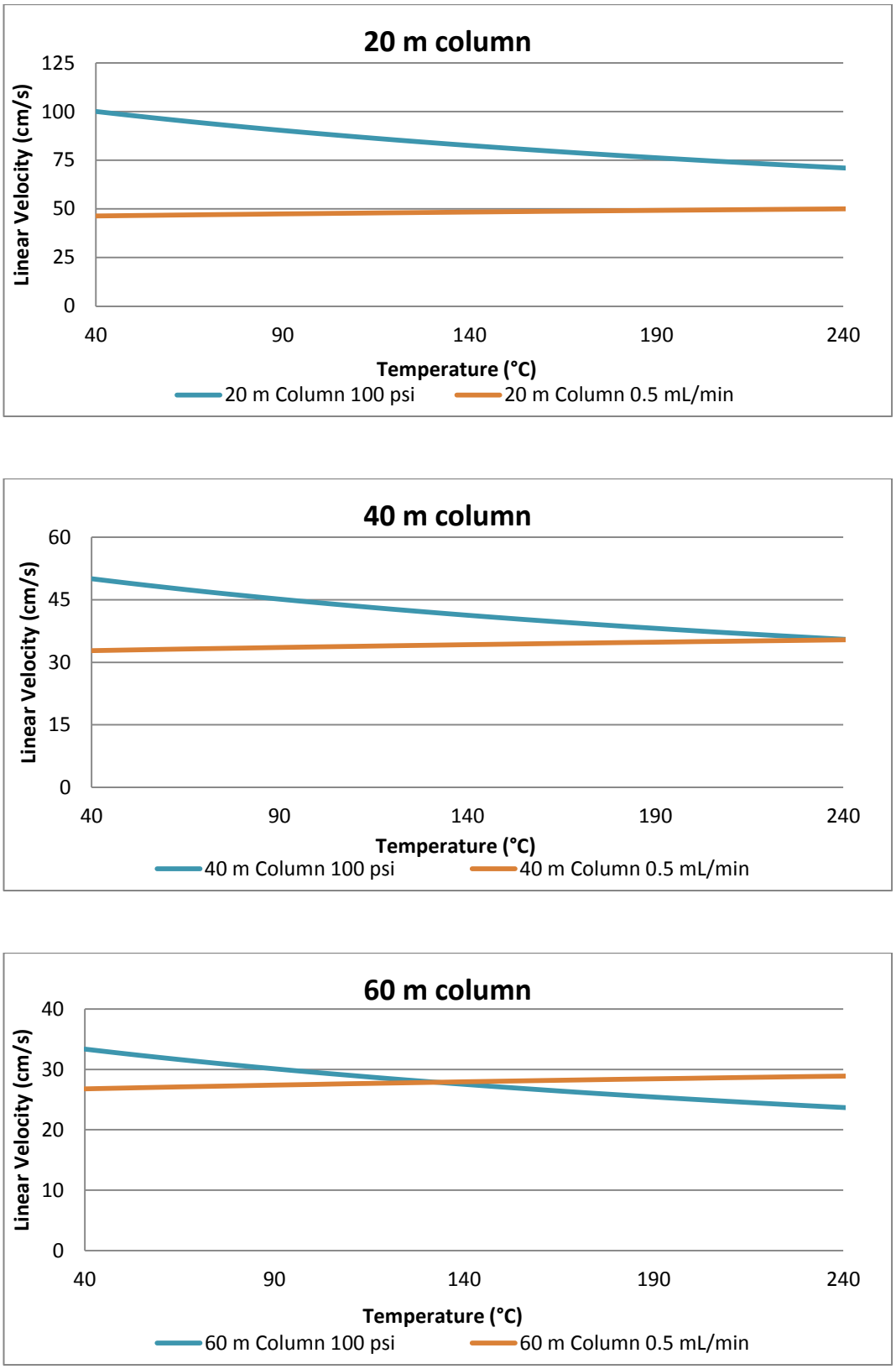


**Figure 3.12. Relationship between flow rate and temperature program for 20, 40 and 60 m columns (top, centre and bottom, respectively). The blue line represents the linear velocity in constant pressure mode, while the brown line shows the linear velocity in constant flow mode at EOF.**

from basic gas flow principles [184]. The point where the EOF plot and the constant pressure plot intersect represents the temperature at which EOF is realised should a constant pressure mode be employed. In the case of the 60 m column at 100 psi (689 kPa), this value is achieved at approximately 130 °C. While maintaining this pressure, as the length of the column is decreased, the temperature at which EOF occurs increases. In the case of the 20 m example, the intersect is above the maximum recommended temperature for the wax stationary phase examined.

Returning to the 60 m example, it is immediately evident that the optimum linear velocity occurs around the middle of the temperature program. In the separation of essential oils, this region of the temperature program often corresponds with the elution of sesquiterpenes. Complex essential oils are often rich in these compounds, many of which possess similar retention characteristics, so the coincidence of maximum available efficiency at this point in the temperature program would appear to be a desirable trait of the separation system.

However, these conditions do not make the best use of the efficiency offered by this long column. Figure 3.13 represents a typical Golay curve, depicting the effect of increasing linear velocity on the efficiency (in terms of HETP) of a chromatographic separation. The EOV is represented by the broken line, which coincides with the minimum point on the curve. Three arrows are overlaid on the curve, representing the constant pressure programs used for the three column lengths investigated. In the case of the 60 m column, a significant penalty in efficiency is paid by allowing the linear velocity to drop below optimum in the second half of the temperature program. In contrast, the shorter columns remain above optimum, where the gradient of the Golay curve is much shallower. This suggests that to provide the best use of the available efficiency of a column using *constant pressure*

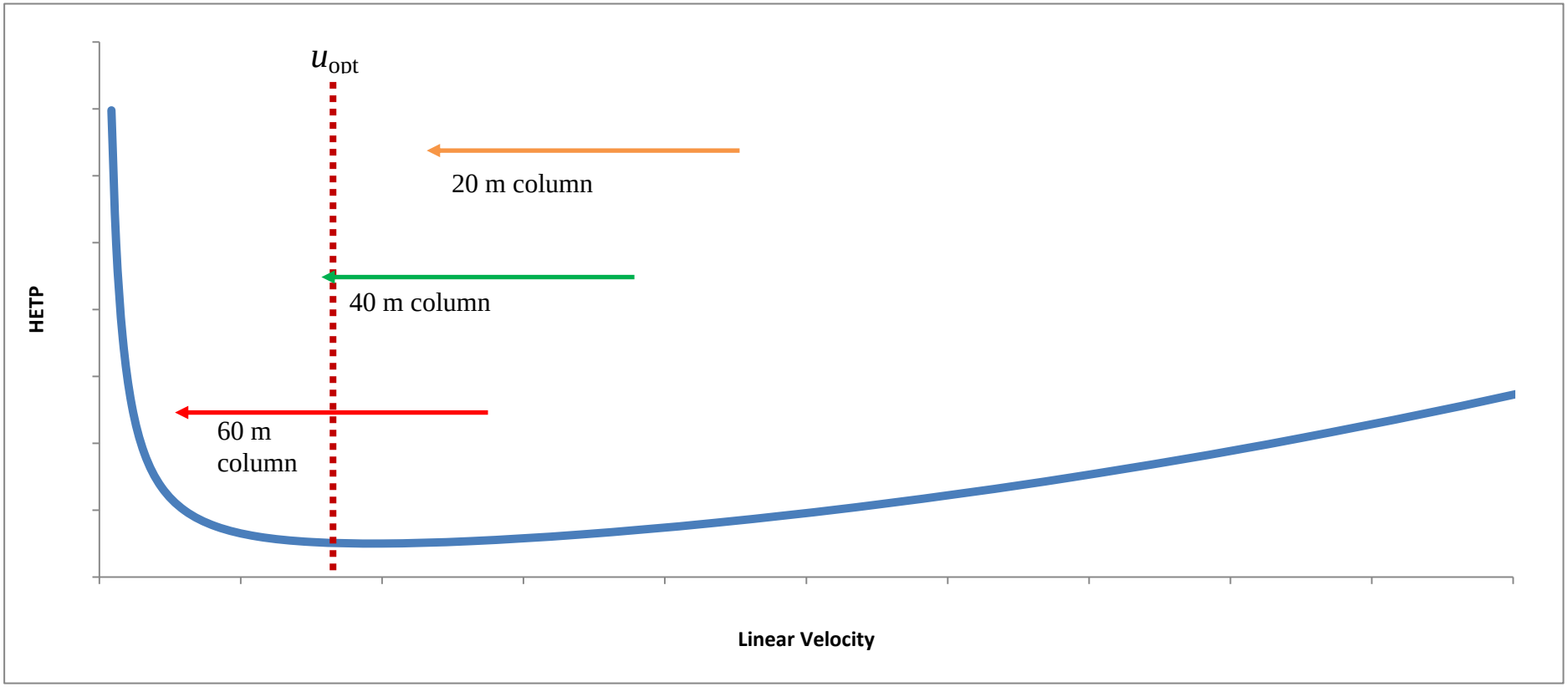


**Figure 3.13. Representative Golay curve showing two constant pressure modes – the first (green arrow) commences at optimum linear velocity and concludes below optimum as the temperature program proceeds. The second (purple arrow) commences above optimum linear velocity and concludes at optimum. Data collected using a 10 m × 0.25 mm column at 140°C, $H_2$ carrier gas.**

*mode*, the column length *or* the inlet pressure should be tailored such that the optimum linear velocity is approached at the *highest* point in the temperature ramp.

In their recent study, Sandra and co-workers employed an 80 m × 0.10 mm i.d. column at a constant 140 psi (965 kPa) [117], with a temperature program of 80-300 °C. They stated:

*"The 80 m × 0.10 mm i.d. column, operated at 140 psi hydrogen inlet pressure and vacuum outlet pressure, represents the longest narrow bore column that can be operated near optimum gas velocity at 80 °C (31 cm/s, 0.86 mL/min) using standard GC equipment"*.

In other words, the *lowest* point in the temperature ramp was selected for velocity optimisation. Based on this, the column would have been operated below EOV for a proportion of the temperature program, suggesting that the maximum efficiency of the column was not realised.

In the current investigation, a scaled-down version of Sandra's approach was performed at the maximum delivery pressure of the available carrier gas generator. A second approach, using a column length optimised for this pressure based on the rationale presented herein, was also performed for comparison. To allow effective comparison between these approaches, the method translation theory first described by Klee and Blumberg [33, 35, 181] was used, which permits the conservation of peak elution characteristics between different length columns.

Klee and Blumberg reported a series of practical conditions which must be met to achieve this outcome, which were described in detail (with mathematical reasoning) in Reference [33]. Of primary importance, the generation of a time-independent pressure gradient along the column is required. To describe this

condition in simpler terms, the pressure of the inlet and the outlet must not change during the run, ie. a constant pressure mode must be employed [33]. Blumberg and Klee suggest that this constraint should not be relaxed, and conclude that *"practically speaking, any constant-pressure method is translatable"* [33]. While there are some advantages in using constant flow mode [185], it has been shown experimentally that there is no significant difference between the maximum peak capacity and analysis time at the same peak capacity between the two operation modes [186]. This forms the primary reason for selection of a constant pressure mode for the separations described in this section.

*Separation performance and observations*

By connecting three columns in series, a 60 m × 0.10 mm i.d. coupled column was constructed. Such a column would possess in the order of $6 \times 10^5$ theoretical plates and exceptionally high peak capacity. By operating this column at the maximum pressure limit of the hydrogen generator (100 psi, or 689 kPa), the initial column flow at 40 °C was 0.75 mL/min, with the average linear velocity being 32.7 cm/s. Throughout this investigation, the 60 m coupled column was progressively shortened to 40 m and 20 m lengths. A separation of hop essential oil obtained using the 60 m coupled column is shown in Figure 3.14.

Two temperature program rates were selected for hop essential oil analysis, namely 1.5 °C/min (~4.5 °C/$t_m$) and 3 °C/min (~9 °C/$t_m$), yielding analysis times of 133 min and 65 min respectively. The former temperature ramp was selected to maximise the available peak capacity on offer using the high efficiency 60 m column, while the latter rate was selected as an approximation of the optimal heating rate as proposed by Blumberg and Klee [34] and to provide a comparison with Sandra and co-workers' approach [117].

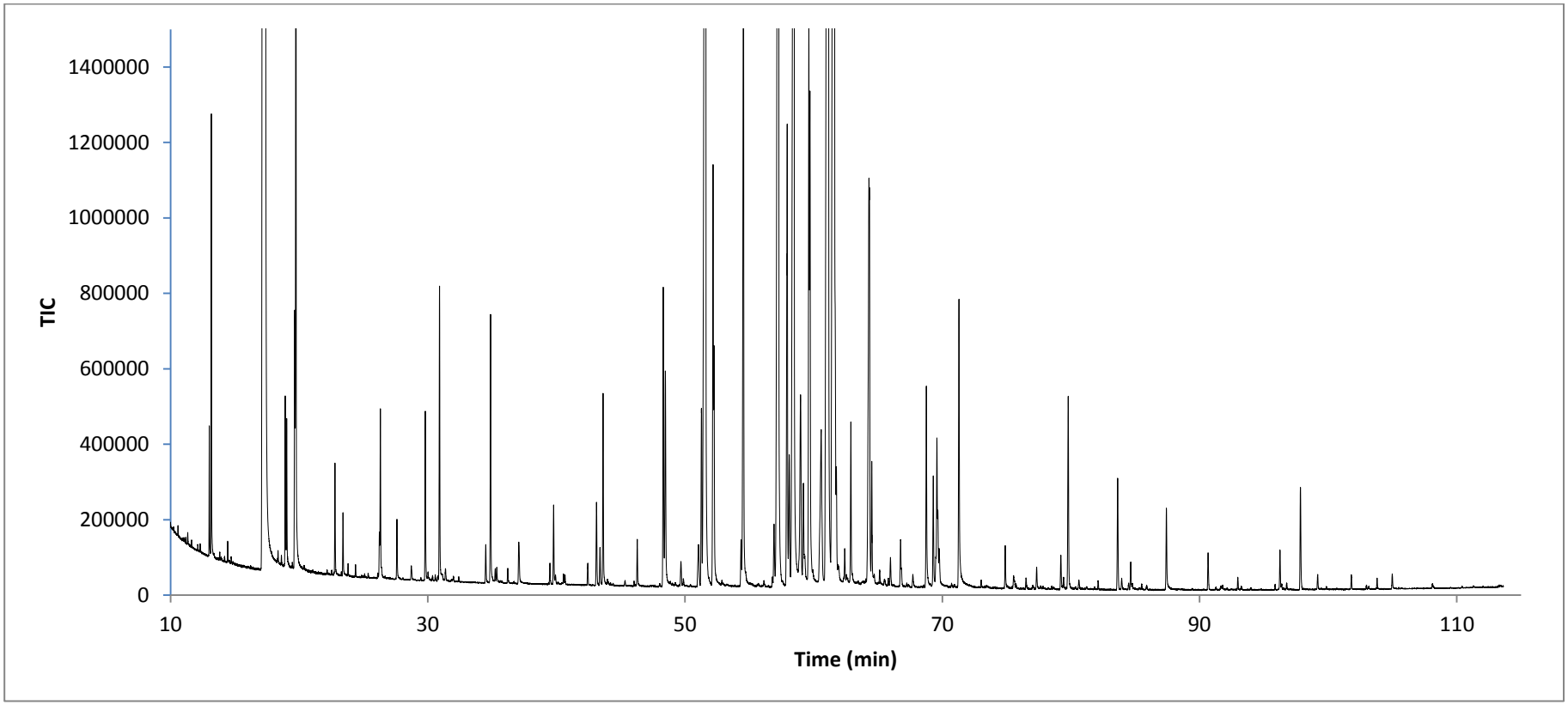


**Figure 3.14. GC–MS chromatogram of Hop (*Humulus lupulus L.*) essential oil obtained on a 60 m × 0.10 mm coupled column with Rtx-WAX stationary phase using $H_2$ carrier gas at 100 psi (689 kPa), constant pressure mode. Temperature program 40-240 °C at 1.5 °C/min, MS operated in full-scan mode at 5.3 Hz over mass range 35-350 *m/z*.**

Bicchi and co-workers examined the performance of a conventional polar GC column in comparison to fast and ultra-fast methods in 2004 [131]. The available peak capacity of a polar PEG 20M column was 267 with a separation number, defined as the average number of well-separated peaks able to be resolved between *n*-alkane homologue pairs [187, 188] of 31.7. The 60 m coupled column used in this study showed significantly more performance based on these metrics, with an available peak capacity of 890 and an average separation number of 77.5. The separation number was maximal between the $C_{17}$ and $C_{18}$ peaks, giving a value of 88.2. Mondello and co-workers examined the use of a 0.05 mm i.d. column for GC analysis in 2004 [189]. Despite its extremely low plate height, the column yielded a separation number of 32 for the $C_{17}$-$C_{18}$ pair, as the length of the column was minimised to increase speed and decrease optimum carrier gas pressure. Performing a similar separation on the 60 m × 0.10 mm i.d. coupled column at the higher temperature program of 3 °C/min yielded a peak capacity of 662 and average separation number of 51.0, notably greater than that achieved using the narrower-bore column.

The approach presented herein also compares favourably with that reported by Sandra and co-workers [117]. Using an 80 m column, an effective peak capacity of 724 was reported, which is only 1.09× greater than that observed with the current method. In contrast however, is the relative speed of the two separations. The void time for the 80 m column using the stated experimental conditions was approximately 4.29 min, while a void of 3.00 min was recorded for the 60 m coupled column. Using the quotient of $N/t_m$, some $1.86 \times 10^5$ plates/min were generated on the 80 m column, compared to $2.00 \times 10^5$ plates/min using the 60 m coupled column under appropriately scaled conditions. A further comparison can be drawn to the

seminal research of Berger [171], who generated some 1.3 million effective plates on a 450 m × 0.20 mm i.d. column. As a head pressure of 116 psi (814 kPa) hydrogen was available, the void time was some 36.3 min. Consequently, only $3.59 \times 10^4$ plates/min could be generated based on this effective efficiency. Using the theoretical efficiency of the column (in the order of 5 million plates), this value increased to $1.38 \times 10^5$ plates/min. A summary of these comparisons and performance characteristics is shown in Table 3.2.

As described in the first part of this discussion, operation of the column below the EOV using the pneumatic parameters desired for this study represents a significant deterioration in available efficiency. The suggested conditions for a constant pressure program involve selecting a pressure and temperature program rate whereby the average velocity is above the EOV at the start of the temperature ramp. As the ramp progresses, EOV is approached at the highest temperature. Should the temperature program of 40-240 °C and pressure of 100 psi (689 kPa) be fixed, systematic calculations using the formulae described above (facilitated by freely available software [190]) suggest that shortening the column to 39 m would fulfil this objective. While this represents a sacrifice in overall efficiency, the speed of the separation was increased significantly.

To validate this proposal, a 40 m × 0.10 mm i.d. column was constructed and used for the separation of a hop essential oil sample, maintaining the separation parameters listed above. The void time of the column was experimentally determined to be 1.4 min and the peak capacity was approximately 408. Using the $N/t_m$ quotient, this equates to some $2.92 \times 10^5$ plates/min, which is in the order of 1.5× greater than that observed using the 60 m column. While it must be noted that this metric will understandably increase as the column length decreases, shortening the

**Table 3.2. Summary of separation characteristics of the two columns investigated in the present study (40 m and 60 m), in comparison to two literature examples. While the two literature examples generate higher efficiencies, the 40 m column yields the best balance between efficiency and speed based on the discussion presented above.**

| Column Dimensions | Theoretical efficiency (plates) | $t_m$ (min) | Peak Capacity (effective) | $N/t_m$ (theoretical) | Nominal separation time (min) |
|---|---|---|---|---|---|
| **80 m × 0.10 mm** [117] | **800,000** | **4.29** | **724** | **$1.86 \times 10^5$** | **110** |
| **60 m × 0.10 mm** | **600,000** | **3.00** | **662 (9 °C/$t_m$ temperature program)** | **$2.00 \times 10^5$** | **65** |
| **40 m × 0.10 mm** | **400,000** | **1.4** | **408** | **$2.92 \times 10^5$** | **35** |
| **450 m × 0.20 mm** [171] | **5,000,000** | **36.25** | **> 1000** | **$1.38 \times 10^5$** | **650** |

column beyond 39 m *whilst maintaining the desired pneumatic and temperature conditions* represents undue sacrifice of efficiency in search of speed. As the average velocity increases far above EOV, the effective efficiency of the column deviates significantly from the theoretical efficiency. Only by approaching the EOV at the highest point in the temperature program can the approach be optimised for both speed *and* efficiency. This observation represents an important and often overlooked aspect of method development.

*Essential oil separations*

A typical chromatogram illustrating the separation of hop essential oil using a 60 m × 0.10 mm i.d. coupled column with the aforementioned separation conditions and a 1.5 °C/min temperature program was shown in Figure 3.14. As mentioned previously, while the peak capacity for this separation was exceptional, the conditions used did not represent the best trade-off between speed and efficiency.

Sandra and co-workers reported that despite the exceptional efficiency of their 80 m column, a one-dimensional GC–MS analysis is not sufficient to resolve every one of the 209 PCB congeners [117]. While exceptional peak capacity has been obtained using the 60 m coupled column investigated here, a similar outcome may be expected for the analysis of an essential oil sample displaying high complexity should complete characterisation be required.

The separation of hop essential oil was also performed using a 40 m × 0.10 mm i.d. Rtx-5 non-polar coupled column. This is an approximation of aforementioned optimised length for 100 psi (689 kPa) inlet pressure and a 40-240 °C temperature program. A chromatogram of this separation presented in Figure 3.15 and a summary of tentative peak identifications is reported in Table 3.3.

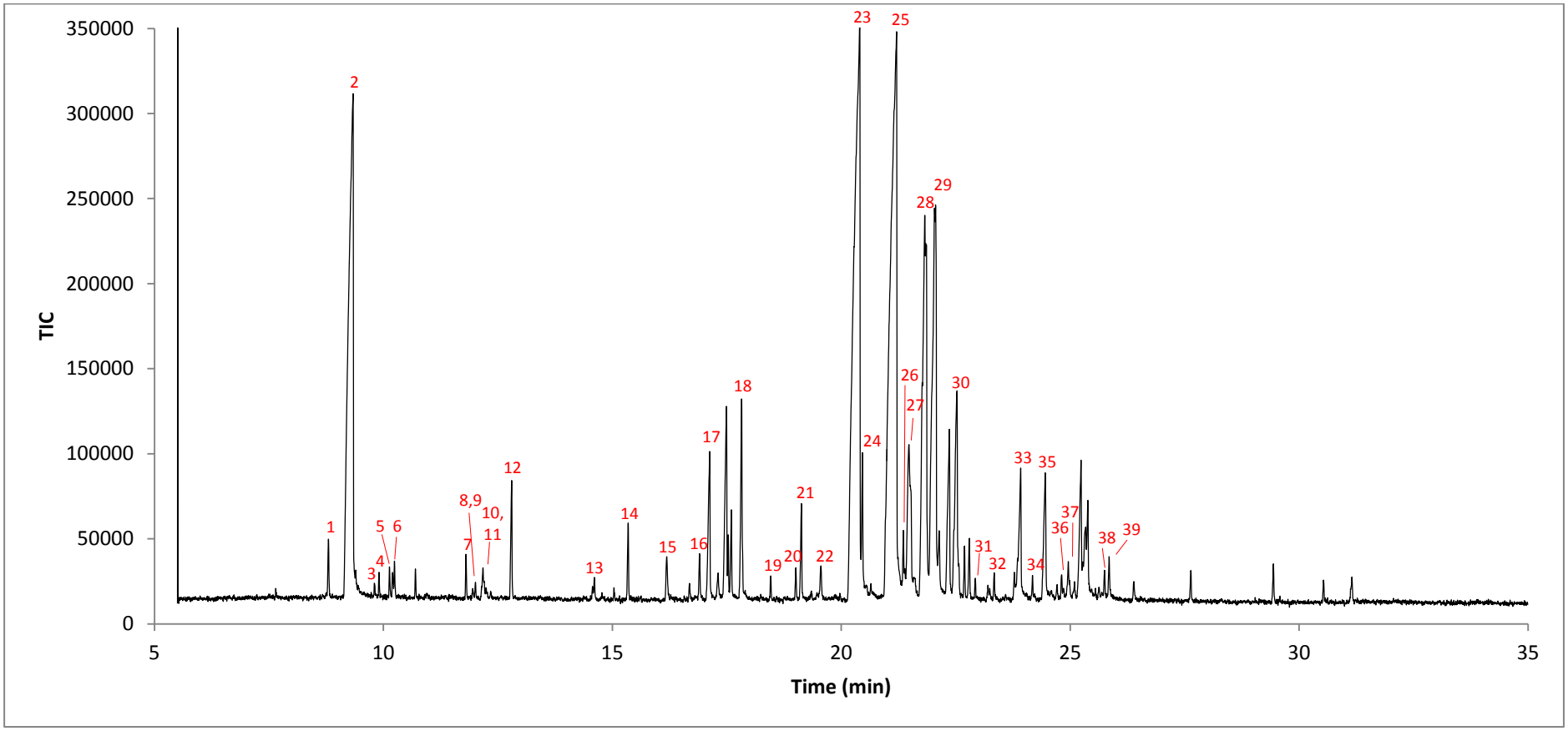


**Figure 3.15 GC–MS chromatogram of Hop (*Humulus lupulus L.)* essential oil obtained on a 40 m × 0.10 mm Rtx-5 stationary phase using $H_2$ carrier gas at 100 psi (689 kPa), constant pressure mode. Temperature program 40-240 °C at 6 °C/min, MS operated in full-scan mode at 5.3 Hz over mass range 35-350 *m/z*.**

**Table 3.3. Tentative peak assignments for hop essential oil analysed on a 40 m × 0.10 mm i.d. Rtx-5 column using the FFNSC library and separation conditions as shown in Figure 3.15. Library match quality refers to similarity ranking as discussed in Section 3.1.2. Peak numbers refer to those shown in Figure 3.15.**

| Peak number | $t_R$ (min) | Experimental LRI | Library LRI | Library match percent | Tentative identity |
|---|---|---|---|---|---|
| **1** | 8.800 | 976 | 978 | 97 | β-pinene |
| **2** | 9.334 | 997 | 991 | 98 | myrcene |
| **3** | 9.806 | 1014 | 1014 | 96 | isopentyl isobutyrate |
| **4** | 10.136 | 1026 | 1025 | 97 | methyl heptanoate |
| **5** | 10.203 | 1029 | 1030 | 95 | limonene |
| **6** | 10.702 | 1047 | 1046 | 98 | e-β-ocimene |
| **7** | 11.953 | 1094 | 1089 | 92 | methyl lavender ketone |
| **8** | 12.010 | 1096 | 1100 | 97 | *n*-undecane |
| **9** | 12.176 | 1102 | 1101 | 91 | linalool |
| **10** | 12.243 | 1105 | 1107 | 86 | *n*-nonanal |
| **11** | 12.344 | 1109 | 1109 | 89 | 2-methylbutyl isovalerate |
| **12** | 12.802 | 1126 | 1125 | 97 | methyl octanoate |
| **13** | 14.610 | 1195 | 1200 | 96 | *n*-dodecane |
| **14** | 15.348 | 1225 | 1224 | 96 | methyl nonanoate |
| **15** | 16.190 | 1258 | 1255 | 83 | geraniol |
| **16** | 16.687 | 1278 | 1272 | 83 | dec-9-en-1-ol |
| **17** | 17.127 | 1296 | 1294 | 98 | undecan-2-one |
| **18** | 17.824 | 1325 | 1327 | 95 | methyl decanoate |
| **19** | 18.461 | 1352 | 1349 | 96 | α-cubene |
| **20** | 19.010 | 1376 | 1371 | 95 | ylangene |
| **21** | 19.131 | 1381 | 1375 | 97 | α-copaene |
| **22** | 19.557 | 1399 | 1400 | 93 | *n*-tetradecane |
| **23** | 20.405 | 1437 | 1438 | 90 | aromadendrene |
| **24** | 20.467 | 1440 | 1434 | 90 | calarene |
| **25** | 21.199 | 1473 | 1464 | 85 | linalyl isovalerate |
| **26** | 21.362 | 1480 | 1473 | 92 | drima-7,9(11)-diene |
| **27** | 21.481 | 1485 | 1478 | 93 | γ-muurolene |
| **28** | 21.831 | 1501 | 1495 | 84 | tridecan-2-one |
| **29** | 22.048 | 1511 | 1501 | 96 | α-selinene |
| **30** | 22.524 | 1534 | 1526 | 91 | zonarene |
| **31** | 22.937 | 1554 | 1544 | 95 | α-calacorene |
| **32** | 23.209 | 1567 | 1561 | 88 | E-nerolidol |
| **33** | 23.919 | 1601 | 1594 | 89 | viridiflorol |
| **34** | 24.181 | 1614 | 1610 | 81 | cedrol |
| **35** | 24.456 | 1628 | 1624 | 80 | epi-γ-eudesmol |
| **36** | 24.723 | 1641 | 1631 | 89 | epicubenol |
| **37** | 24.963 | 1653 | 1651 | 92 | α-muurolol |
| **38** | 25.754 | 1692 | 1697 | 97 | tridecyl methyl ketone |
| **39** | 25.855 | 1697 | 1700 | 97 | *n*-heptadecane |

It is noteworthy that tentative identities could not be assigned to many of the peaks in the sesquiterpene-rich section of the chromatogram, possibly due to a lack of peak capacity in this area and subsequent peak coelutions. This observation suggests that the increased peak capacity inherent with a comprehensive two-dimensional separation may be more appropriate should characterisation of the sample be desired, supporting the observations noted from the vetiver oil separation.

A drawback associated with the use of a narrow bore column for the separation of complex samples is the low sample capacity that is often afforded. In the case of an essential oil, the major components may be present in concentrations that are orders of magnitude greater than minor components. An example of this effect can be seen in Figure 3.16 which shows the expanded section (60-70 min) of a hop oil chromatogram acquired using the 60 m coupled column at a 1.5 °C/min temperature program. While the peak shapes of the minor components are acceptable, the major components have asymmetrical peaks indicating overloading. A similar occurrence can be witnessed in separations performed on the 40 m Rtx-5 coupled column. To obtain appropriate peak symmetry using the conditions presented here, analysis of both dilute and concentrated samples will most likely become a requirement.

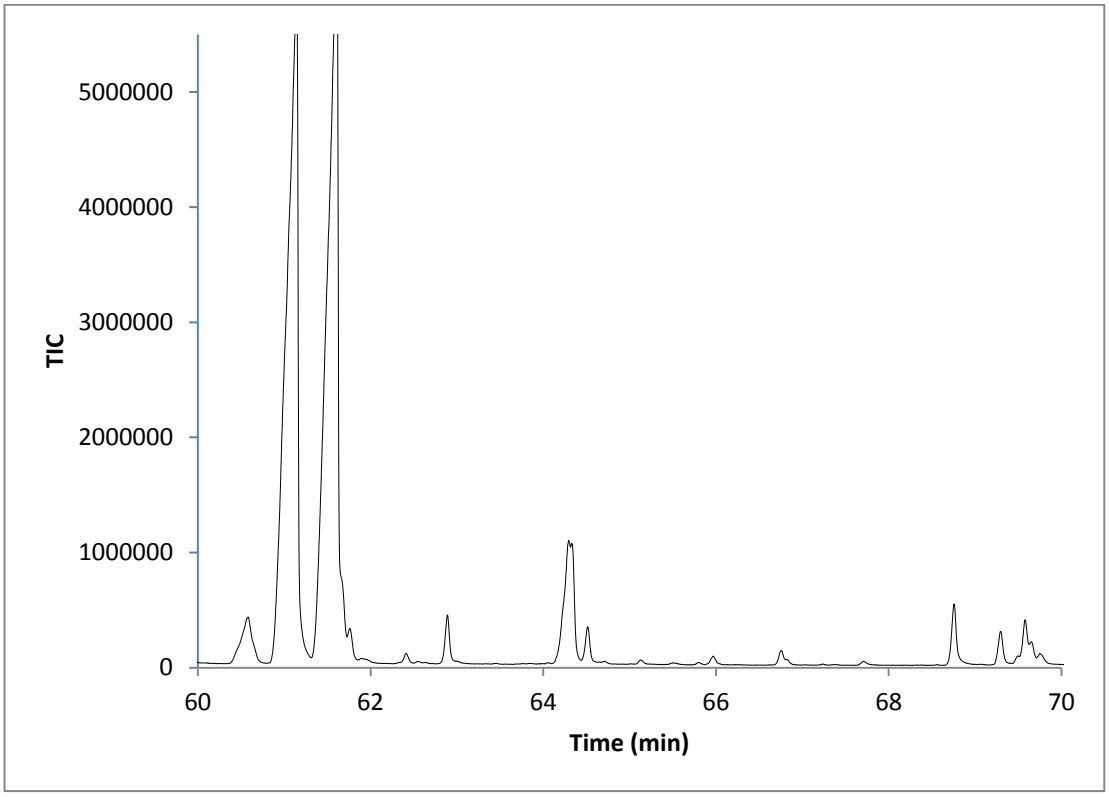


**Figure 3.16. Expanded section of a hop oil chromatogram showing TIC values from 60-70 min acquired using the 1.5 °C/min temperature program. Minor components display peaks approximating Gaussian distribution, but major components are overloaded. This demonstrates the conflict between available sample capacity on a narrow-bore column and the large variation between concentration of major and minor components.**
**Experimental conditions as per Figure 3.15.**

### 3.3.4 Concluding Remarks

A 60 m × 0.10 mm i.d. coupled column with a polar stationary phase was constructed and operated with hydrogen carrier gas in constant pressure mode at the maximum available pressure to permit the separation of two essential oil samples of moderate and high complexity. A theoretical peak capacity of 662 was observed based on the separation of a $C_8$-$C_{20}$ *n*-alkane series and appropriate temperature ramp, which compared well with a recent high-efficiency study [117]. A sample of vetiver essential oil was also examined, although the increased complexity of the sample required a greater peak capacity than was offered by this one-dimensional separation.

To perform a separation in constant pressure mode and generate the best trade-off between speed and efficiency, the column should be operated such that the EOV is reached at the maximum programmed temperature. Whilst operating above the EOV for almost the entire temperature program sacrifices efficiency, the deviation from optimum is much less than is observed through the operation of the column below the EOV value for the majority of the temperature program.

A non-polar coupled column column of approximately kinetically-optimal length was used for the separation of hop essential oil. The available peak capacity was reduced to 408, yet the increase in separation speed was clearly witnessed.

The observations presented in this section have been applied to the selection of an appropriate first-dimension column for the comprehensive two-dimensional separation of essential oils described in Chapter 4. While it was initially thought that the 60 m coupled column presented here would be suitable for this purpose, it does not represent an optimised option.

## 3.4. Varietal characterisation of hop from metabolite extracts

This section has been adapted from the following publication:

R.A. Shellie, S.D.H. Poynter, J. Li, J.L. Gathercole, S.P. Whittock, A. Koutoulis. **Varietal characterisation of hop (*Humulus lupulus* L.) by GC–MS analysis of hop cone extracts.** *J. Sep. Sci.* 32 (2009) 3720-3725.

### 3.4.1 Introduction

Hop extracts are vital to the brewing industry and some of their unique chemicals have the potential to be used in the nutraceutical industry. There are already many commercial hop varieties but the search for newer types with improved characteristics is continuous [191]. Traditional classification of hop cultivars divides them into three groups, i) high-α acid, ii) intermediate-α acid, and iii) aroma (noble) varieties [192]. In the past, the varietal characterisation of hop was performed by gas chromatographic analysis of terpenoid compounds in hop essential oils [193], with modern studies almost exclusively utilising two analytical dimensions brought about by hyphenation with mass spectrometry [194]. While this approach is very robust, there are potential disadvantages, mainly associated with the extraction of the oil. Steam distillation is a common approach for obtaining essential oils from plant material, but this typically requires large amounts of sample (typically > 50 g) and is time consuming (~ 4 h per sample). It is also recognised that the distillation process can impart changes in the oil composition [195, 196] so extra care is required for consistency. Eri and co-workers described an approach employing direct thermal desorption (DTD) GC–MS analysis [196]. The DTD-GC–MS approach required only approximately 1 g of plant material with a sample preparation time of approximately 20 min. The authors reported higher recovery of oxygenated compounds in the DTD

experiment compared to traditional distillation approach, the reasons for which were not fully established. Later Kovačevič and Kač utilised solid-phase microextraction with a 30 min extraction time at 70 $^{o}$C from Aurora hop cones showing that repeatable routine analysis could be performed using as little as 2 g of sample [197]. Other investigators have differentiated hop varieties by using analysis of hop acids or flavonoids using reversed phase HPLC [192]. In 2001, Roessner *et al.* showed that profiling metabolites in plant extracts allows comprehensive phenotyping of genetically or environmentally modified plant systems [198]. Such studies draw on simple extraction procedures that have been shown to be very robust [199] and have permitted wide-ranging high-throughput applications, including phenotyping and diagnostic analyses in plants.

A simple approach is described to allow characterisation of hop (*Humulus lupulus* L.) varieties based on extracted metabolite profiles. This study focuses on commercial hop varieties and was timed to coincide with the 2008 commercial hop harvest in Tasmania, Australia. Analysis of hop extracts was performed using GC–MS. A 60 m capillary column was employed with helium carrier gas under constant pressure conditions. These conditions were chosen to evaluate the available resolution from the one-dimensional approach employed, whilst allowing the possibility for method translation at a later stage (according to recognised methods [33]). Separated analytes were subjected to basic pre-processing (normalisation to sum of peak areas and conversion to the log scale) and a Student's t-test and F-test approaches employed to determine variables representative of the aroma and α-acid subgroups. A matrix of appropriate metabolites was compiled for both feature selection methods, and a principal component analysis (PCA) approach was employed to summarise the variance observed between the aroma and α-acid hop

varieties. To further characterise the sample population, a simple linear discriminant analysis (LDA) technique was performed using the t-test matrix to determine if the selected variables could be used to assign a varietal classification to individual samples. It is acknowledged that more powerful chemometric techniques could have been selected for this investigation, the emphasis for the current study centred on simplicity.

### 3.4.3 Experimental

*Samples*

Samples of hop (*Humulus lupulus* L.) were collected from the Bushy Park Estates (Tasmania, Australia) in March 2008 to coincide with the commercial harvest. The experiment drew on analysis of four hop varieties nominally classified as high α-acid, and four varieties nominally classified as aroma (low α-acid). The study was designed to focus on the commercial varieties listed in Table 3.4. Duplication of one high α-acid and one aroma variety was performed as part of the experimental design.

The sampling strategy took three cones at a consistent ripeness within each variety from each of ten plants in a line plot in commercial paddocks of each variety. Cones were picked and placed immediately into 50 mL plastic centrifuge tubes prior to freezing with liquid nitrogen in the field. Samples were stored at -70 °C until required for analysis.

To extract the metabolites from the hop cones, a single bract with lupulin glands attached (~ 30 mg fresh weight) was removed from each hop cone and placed into a pre-chilled round-bottom Eppendorf tube containing a grinding ball. Samples were homogenised for 30 s at 25 Hz shaking using a Grinding Mill (Retsch GmbH,

**Table 3.4. Details of the samples collected in this investigation.**

| **Hop variety** | **Number of plants sampled** | **Number of samples collected** |
|---|---|---|
| AROMA (NOBLE) | | |
| Cascade | 10 | 30 |
| Southern Hallertau | 10 | 30 |
| Willamette | 10 | 30 |
| Southern Saaz | 20 | 60 |
| ALPHA ACID | | |
| Super Pride | 10 | 30 |
| Pride of Ringwood | 20 | 60 |
| Victoria | 10 | 30 |
| Millennium | 10 | 30 |

Haan, Germany) and then placed immediately into liquid nitrogen. Pre-chilled (~ 1 °C) extraction solvent mixture (1 mL; 1 : 2.5 : 1 $H_2O$ : MeOH : $CHCl_3$) was added to each tube and was vortexed for 10 s before being centrifuged at 14,000 RPM for 2 min. MilliQ water (200 µL, ~ 1 °C) was added to a 500 µL aliquot of the supernatant. This mixture was vortexed for 10 s and centrifuged at 14,000 RPM for 2 min. The polar phase of the sample was collected and concentrated to complete dryness.

Derivatisation of hop cone extracts was performed according to recognised protocols [200]. The dried samples were removed from the freezer and allowed to thaw for approximately 20 min. Extracts were reconstituted in 10 µL of a 40 mg/mL solution of methoxyamine hydrochloride in pyridine, then heated for 90 min at 30 $^{o}$C. N-methyl-N-trimethylsilyltrifluoroacetamide (90 µL) was later added and the solution heated for a further 30 min at 37 $^{o}$C. Samples were then transferred to 200 µL glass crimp top vials in preparation for analysis.

*GC Analysis*

A 60 m × 0.25 mm i.d. BPX-35 capillary column (SGE Analytical Science, Ringwood, Australia) with 0.25 µm film thickness was used for GC–MS analysis throughout. Helium carrier gas was supplied at a head pressure of 35 psi (241 kPa) to provide an initial flow rate of 2 mL/min. A 1 µL splitless injection (230 $^{o}$C, 1.5 min) was employed and the GC was temperature programmed from 85-330 $^{o}$C at 4 $^{o}$C/min and held at 330 $^{o}$C for 10 min. Full-scan mass spectra were collected from 85-550 *m/z* at a data acquisition rate of 10 spectra/s. The MS transfer line was held at 250 $^{o}$C and the ion source temperature was 200 $^{o}$C.

### 3.4.4 Results and Discussion

This investigation sought to investigate the potential for utilising simple data visualisation tools to differentiate between a series of hop varieties based on components observed in a high efficiency, one-dimensional GC–MS analysis of hop cone extracts. The study was designed to be a preliminary, proof-of-concept approach to evaluate whether the method for metabolite extraction and analysis provided sufficient and relevant data to reveal the identity of the plant variety.

GC–TOFMS is a benchmark approach for metabolomics data acquisition [201] which provides excellent sensitivity and sufficiently high data density to permit deconvolution of overlapping metabolite peaks. While quadrupole instrumentation generally provides less data density, it involves a significantly lower initial expenditure and still provides satisfactory spectral information, as described in the references presented in Chapter 1. In the present investigation, a quadrupole mass spectrometer was used in conjunction with a 60 m column in an attempt to address the potential for shortfalls in the choice of detector by aiming to generate high resolution chromatographic separations.

The column selected for this investigation possesses a nominal maximum theoretical efficiency ($N_{max,theor}$) of 240,000 plates and is longer than those typically used in GC–TOFMS metabolomics analysis [202]. The separation was performed at the speed optimised flow rate (SOF) [181] to facilitate sample throughput by reducing analysis time with minimum negative impact on efficiency. Whilst a 6% greater efficiency could be realised by operating under efficiency optimised (EOF) conditions [181], the SOF method reduces the analysis time by 41%.

The initial and final temperatures in the temperature program used in the present study were based on the conditions described in reference [202], but an

alternative temperature ramp was selected to achieve optimal peak capacity. A normalised temperature ramp of ~10 $^{o}C/t_M$ = 4 $^{o}C$/min was utilised. A typical GC–MS total ion current (TIC) chromatogram of a hop extract (Willamette) is shown in Figure 3.17. An expansion of a 10 min region of the chromatogram (27.5 min - 37.5 min) is inlaid to show the occupation of the available peak capacity and generally good peak shape of the derivatised metabolites.

*Variable selection*

To identify metabolite peaks present in samples and construct peak tables and subsequently data matrices, a retention index window of ± 10 units was employed based on the injection of a $C_8$-$C_{20}$ *n*-alkane mixture under identical instrumental conditions. The Golm GC–MS spectral library was used to assign tentative identities to metabolite peaks in the samples and the minimum library match was set to 80%. More than 150 peaks were detected in the TIC chromatograms and from these, 57 tentatively identified components were selected from the chromatograms to construct peak tables for qualitative/quantitative analysis. Selection of these components was based on a minimum area of 5000 units and library search procedures as detailed in Section 3.1. An extracted ion was used as the quantitative mass for each metabolite. Not all of the 57 metabolites could be positively identified using mass spectrometry library matching and confirmation using linear retention index. Table 3.5 reports the identity of those that could be positively identified, and includes several examples where the metabolite class could be established based on MS fragmentation patterns.

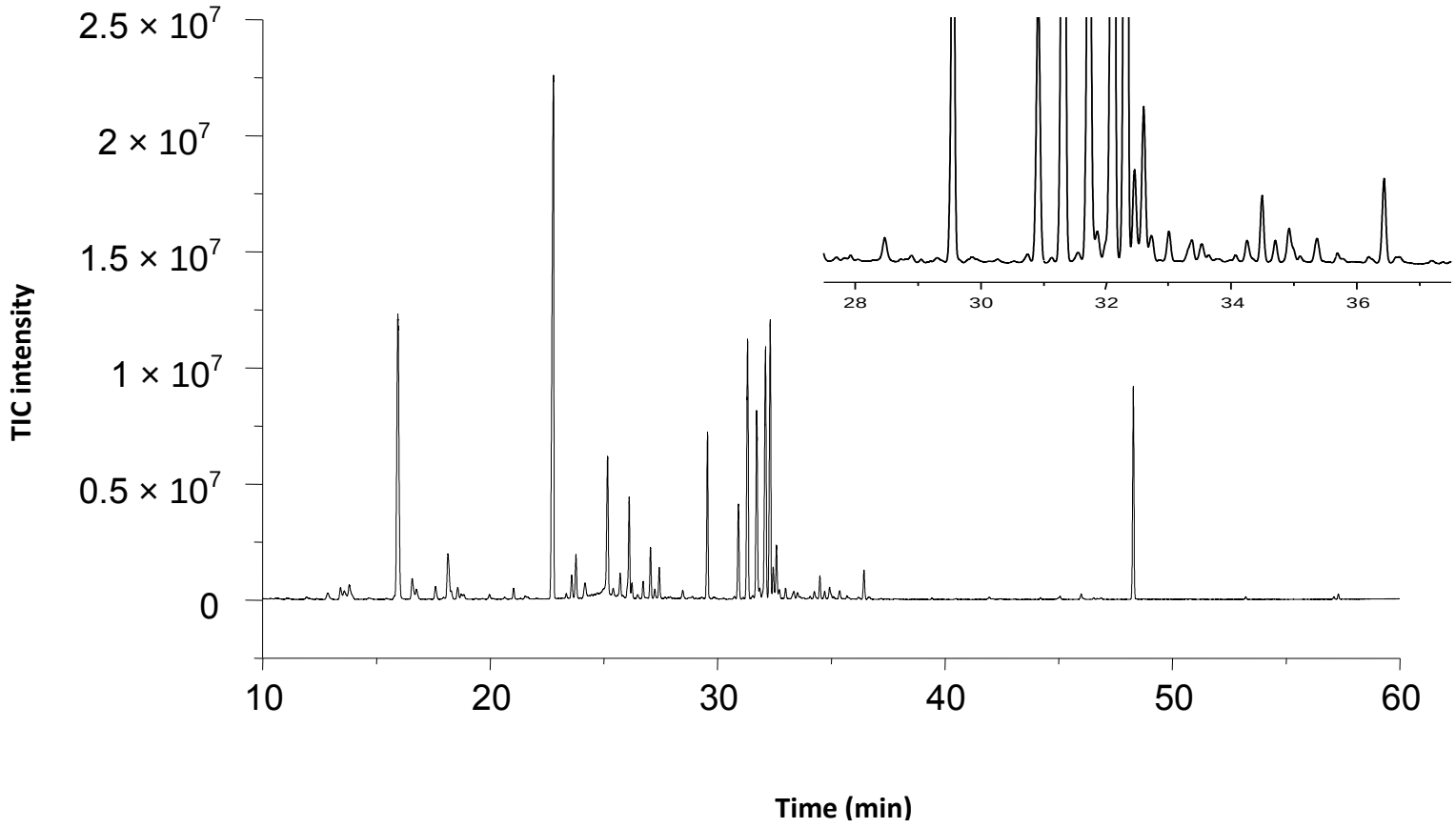


**Figure 3.17. TIC chromatogram of a Willamette hop extract. Experiemental conditions: 60 m × 0.25 mm i.d. BPX-35 column, He carrier gas at 35 psi (241 kPa) head pressure, temperature program 85-330 oC at 4 oC/min and held at 330 oC for 10 min. 85-550 m/z at 10 Hz acquisition frequency.**

The metabolite data were normalised relative to the sum of peak area of the 57 metabolites in each sample and transformed to the log scale, keeping the missing values in the data set. The peak tables for the samples were then aligned based on retention time and separated into two groups (high α-acid and aroma varieties). Any components which were present in less than 80% of each sample group were rejected from the array. A paired Student's t-test was then performed to determine which components showed a significantly different response between the two sample groups. Of the 57 original metabolite peaks, 34 were determined to be significantly different ($p < 0.05$) between the high α-acid and aroma varieties. This follows the protocol employed by other groups [83, 123] and ensured that the variables selected for inclusion in this study were relevant and exhibited significant variance across the range of hop varieties examined. In addition, a second variable matrix was constructed using the Fisher ratio method [203]. Similar approaches have been adopted by other researchers [204, 205]. As the Fisher ratio compares the mean squares between and within sample groups, it should display robustness against biological diversity in the sample population [204]. Using this approach, 12 variables were significantly different ($p < 0.05$) between the two subgroups. The variables selected using these two approaches are indicated by asterisks in Table 3.5.

*Principal Components Analysis*

Both PCA and DA were performed using XLSTAT (Addinsoft, New York, USA) software. PCA is a simple and useful unsupervised pattern recognition method which condenses the number of parameters that describe a group of observations. A series of new variables are constructed based on the original variables, via the generation of a covariance matrix, created by subtracting the variable mean and

**Table 3.5. Metabolites identified in the present investigation by MS library search (Golm GC–MS library) and confirmation with Retention Index (denoted LRI in the 'Identified via' column). Those in red text were not positively identified, however compound class assignment was made using their characteristic fragmentation patterns (denoted MS in the 'Identified via' column). Compounds marked with an asterisk were selected variables using the t-test approach; a double asterisk indicates variables selected using Fisher ratio approach.**

| | Compound / class of compound | Identified via | | Compound / class of compound | Identified via |
|---|---|---|---|---|---|
| **1** | Aromatic | MS, LRI | **30** | Fructose ** | MS, LRI |
| **2** | Phosphoric acid * | MS, LRI | **31** | Aldohexose * | MS |
| **3** | Proline | MS, LRI | **32** | Altrose ** | MS, LRI |
| **4** | Serine * | MS, LRI | **33** | Fructose ** | MS, LRI |
| **5** | Threonine | MS, LRI | **34** | Idose ** | MS, LRI |
| **6** | Cycloleucine ** | MS, LRI | **35** | Citric acid ** | MS, LRI |
| **7** | Fumaric acid * | MS, LRI | **36** | Idose * | MS, LRI |
| **8** | Itaconic acid * | MS, LRI | **37** | Aldohexose * | MS |
| **9** | *Unknown* | | **38** | Carbohydrate | MS |
| **10** | Glutaric acid | MS, LRI | **39** | *Unknown* | |
| **11** | Carboxylic acid ** | MS | **40** | Carbohydrate * | MS |
| **12** | Malic acid * | MS, LRI | **41** | Carbohydrate * | MS |
| **13** | γ-amino-butyric acid * | MS, LRI | **42** | Myo-inositol * | MS, LRI |
| **14** | Aspartic acid * | MS, LRI | **43** | *Unknown* | |
| **15** | Adipic acid | MS, LRI | **44** | Palmitic acid * | MS, LRI |
| **16** | *Unknown* | | **45** | Carbohydrate * | MS |
| **17** | Xylitol ** | MS, LRI | **46** | Stearic acid | MS, LRI |
| **18** | 2-amino adipic acid | MS, LRI | **47** | Tryptophan | MS, LRI |
| **19** | *Unknown* | | **48** | Carbohydrate * | MS |
| **20** | *Unknown* | | **49** | Cellobiose ** | MS, LRI |
| **21** | Arabitol * | MS, LRI | **50** | Sucrose * | MS, LRI |
| **22** | Oxoproline | MS, LRI | **51** | *Unknown* * | |
| **23** | Glutamic acid ** | MS, LRI | **52** | Carbohydrate * | MS |
| **24** | Phenylalanine ** | MS, LRI | **53** | Carbohydrate | MS |
| **25** | Di-carboxylic acid * | MS | **54** | Carbohydrate | MS |
| **26** | Mannopyranosid α methyl ** | MS, LRI | **55** | *Unknown* * | |
| **27** | Amine | MS | **56** | Epicatechin | MS, LRI |
| **28** | *Unknown* * | | 57 | Catechin | MS, LRI |
| **29** | Carbohydrate | MS | | | |

calculating the quotient of the standard deviation. The two eigenvectors that best describe the variance in the sample population are selected as new axes for data visualisation, and the original observations are converted to eigenvalues to transform their characteristics into the new visualisation space.

As with other examples in the literature [206, 207] Catchpole and co-workers adopted a similar strategy when comparing similarities between genetically modified (GM) and conventional (non-GM) potato samples [208]. The group sought to determine "substantial equivalence" between two sample groups (GM and non-GM). Having considerable previous experience with the use of advanced chemometric techniques in conjunction with metabolite profiling [209-211], the group chose to employ PCA over techniques which could potentially extract more information from the data available. The authors stated "*for substantive equivalence we are interested in data similarity rather than the ability to discriminate classes. We reason that if an unsupervised algorithm* [ie. PCA] *clusters metabolome samples close together, then they can be objectively considered to be similar, and if classes cannot easily be discriminated by supervised methods then they are objectively similar"* [208]. The rationale for the use of PCA in the current study to group samples based on α-acid content follows the same lines.

In the current study, it was anticipated that differentiation in the visualisation space would occur between varieties possessing the high α-acid phenotype and those displaying low α-acid (ie. aroma varieties). The first (PC1) and second (PC2) principal components generated from the two feature selection approaches supported this theory, generating a satisfactory differentiation between the high α-acid hop varieties from the aroma hop varieties. A plot showing the separation of the two subgroups utilising the two matrices is shown in Figure 3.18. It is worth noting that

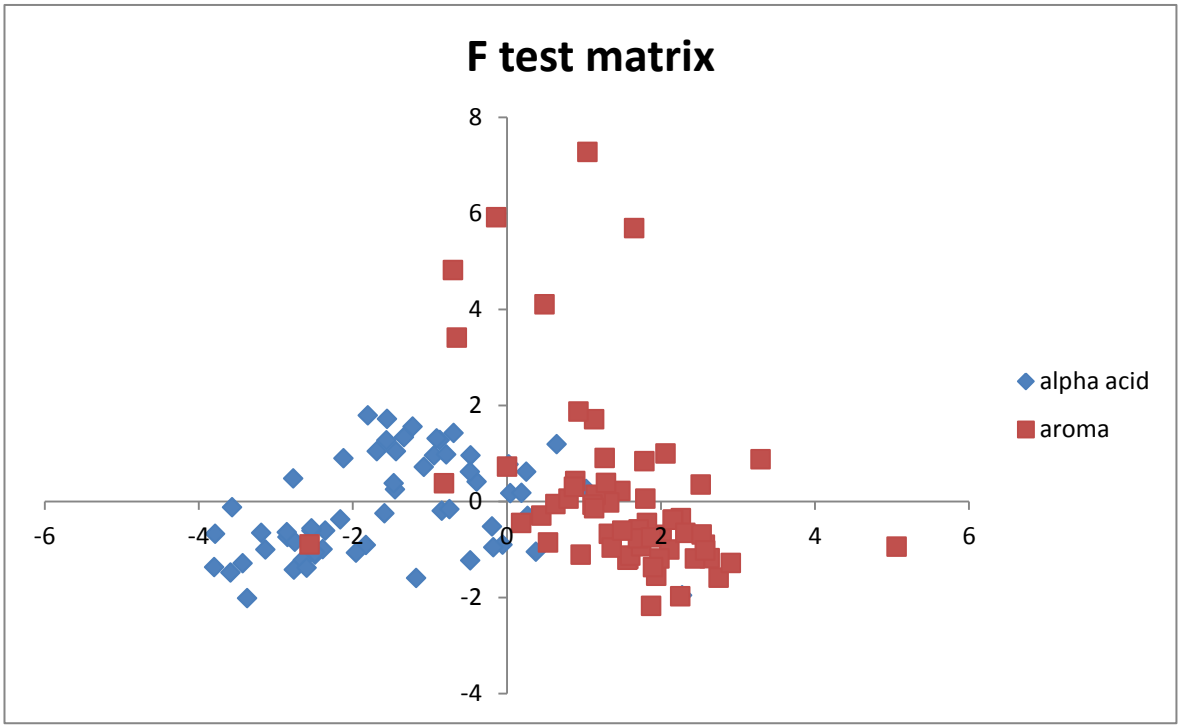


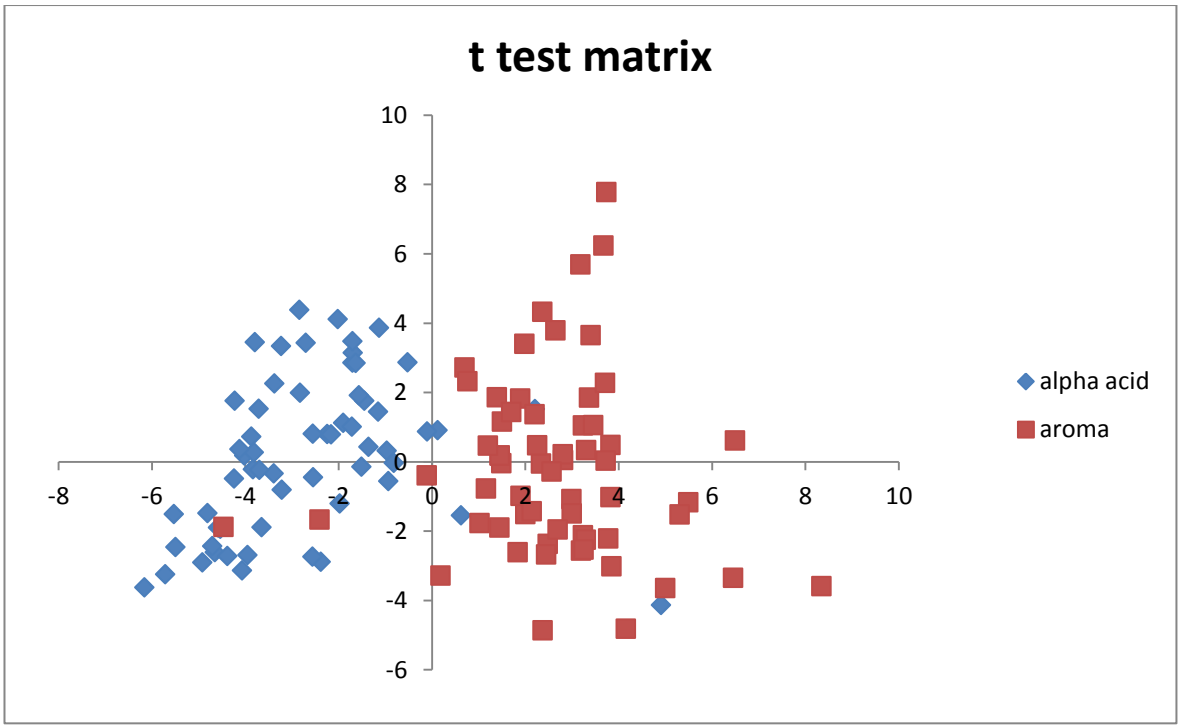


**Figure 3.18. PCA plot for the hop samples described by Table 3.5 using the two feature selection approaches.**

variability was observed in the PC1 and PC2 between the two feature selection approaches (47.5% using t-test *versus* 51% using F test). This difference was mainly witnessed in PC2, which represented 19.8% of the population variability for the F-test matrix and 16.7% of the population variability for the t-test matrix. Loadings plots describing the contribution of each metabolite on the principal components are shown in Figure 3.19. The F-test method should provide a greater degree of robustness towards biological diversity than the t-test approach. With this in mind, the factors selected using the former method should show increased dissimilarity in loading values. Figure 3.19 supports this suggestion, as several metabolites selected using the t-test method are similarly up- or down-regulated for both principal components. Metabolites 3, 8, 18, 22 and 25 are good examples of this observation.

While some overlap is observed in both plots, the differentiation between the two subgroups is clearly apparent. Figures 3.20 and 3.21 show the differentiation between varieties observed using the two variable selection methods. This study also provides some assessment of the plasticity of the individual varieties' metabolite profiles and these plots reflect that the variability within varieties is rather high.

Focusing first on the aroma varieties (Figure 3.20) it is apparent that the variability within each variety does not allow for suitably robust discrimination between the different varieties within the class. While there is clearly some grouping of like samples within this class, the extent of overlap between varieties is also substantial. Similarly for the high $\alpha$-acid varieties (Figure 3.21), the within-class intermingling of results is high and it is not possible to use this analysis to adequately discriminate varieties within the class.

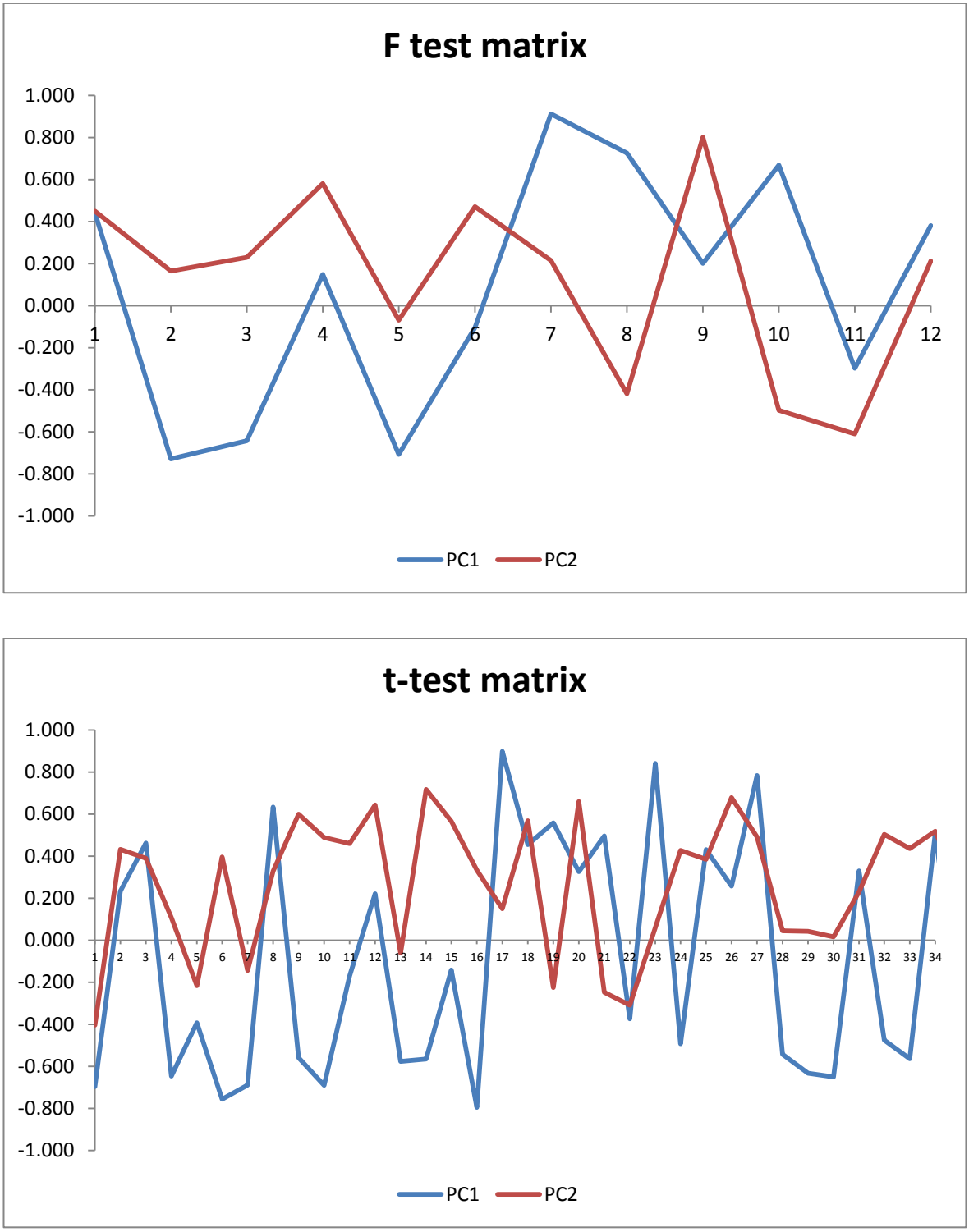


**Figure 3.19. Loadings plots depicting the two principal components used for group-type classification of α-acid and aroma varieties obtained using the two alternate variable selection methods.**

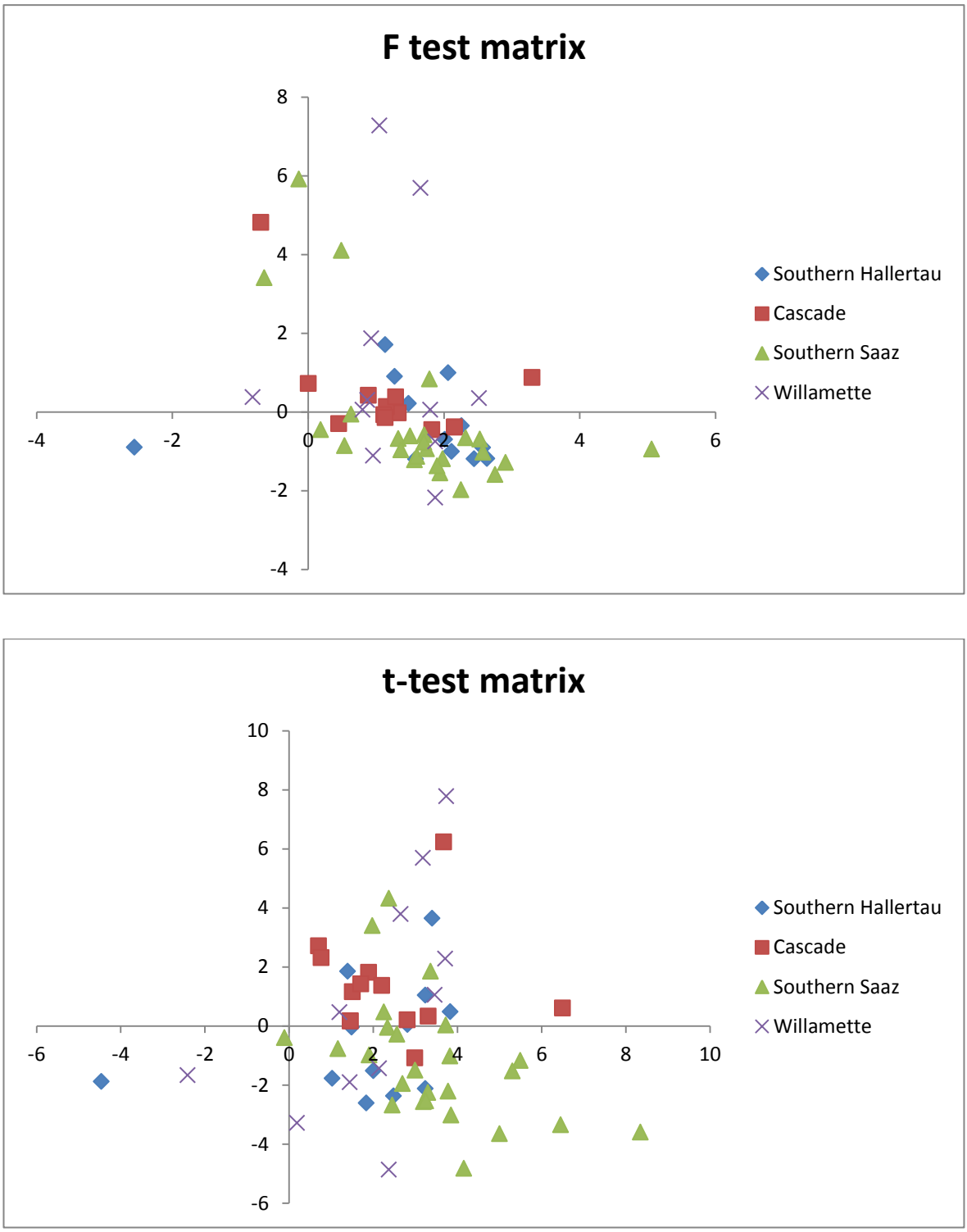


**Figure 3.20. PCA plots showing only the aroma varieties using the two feature selection approaches.**

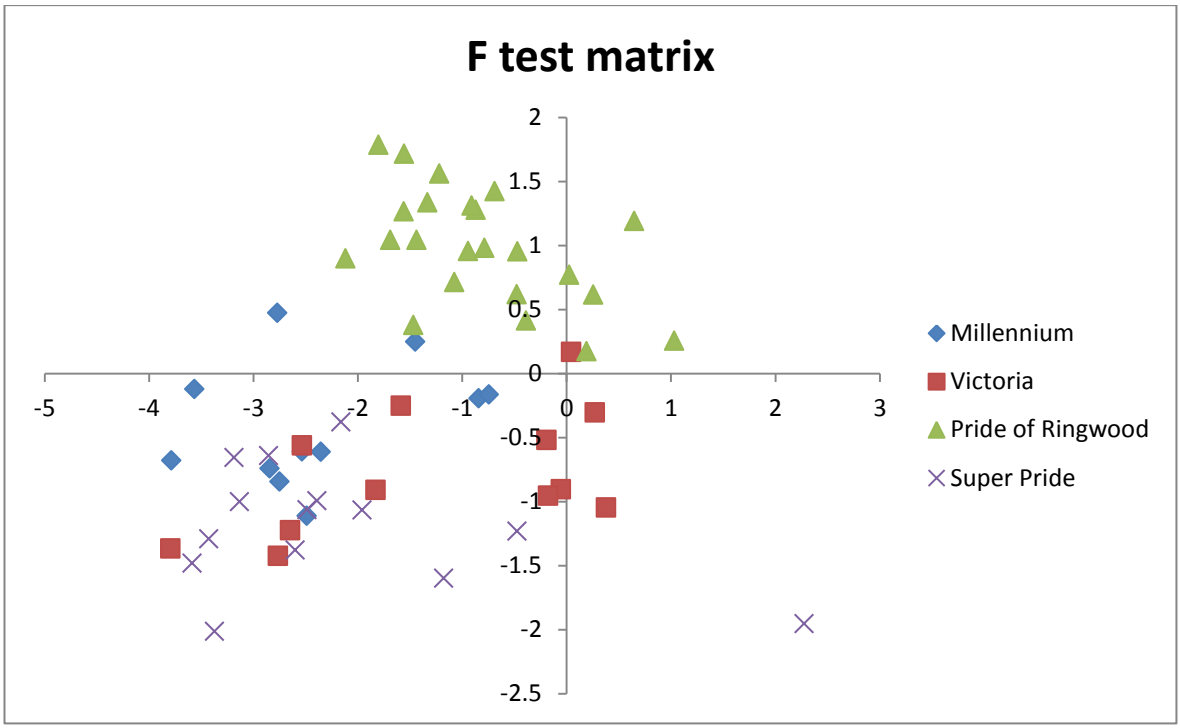


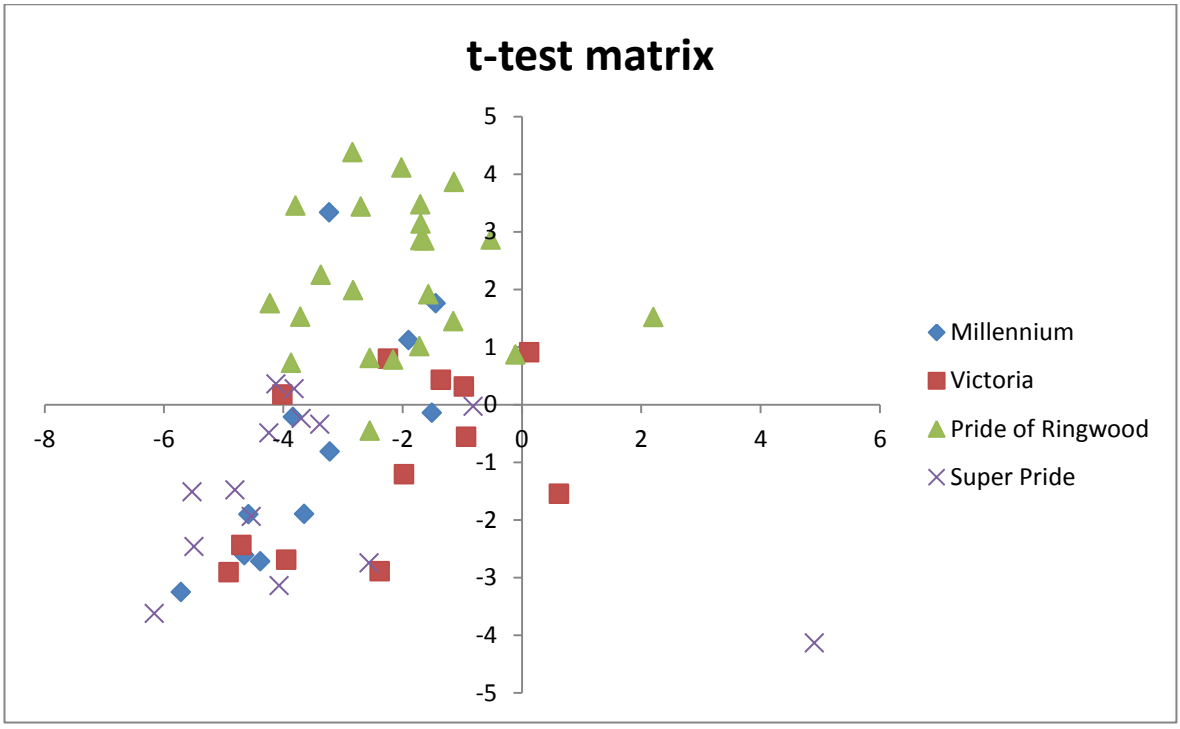


**Figure 3.21. PCA plots showing only the high α-acids varieties using the two feature selection approaches.**

*Discriminant Analysis*

Linear discriminant analysis (LDA) gives the potential for providing reliable characterisation and was hoped to enhance and support the differentiation based on the α-acid phenotype generated using the PCA approach. The technique was employed to create a classification model to determine the feasibility of assigning varietal classification to the samples based on the relative abundances of metabolites extracted and separated from the hop cones. This supervised pattern recognition approach builds a model to differentiate samples according to a number of predetermined subdivisions, in this case, the variety to which the plant sample belongs.

To select the number of factors to include in the LDA model, the Cattell Scree Test [212] was employed. This test involves graphical interpretation of the variance expressed by the eigenvalues through the construction of a simple line plot. As the variance described approaches 100%, the gradient of the line approaches zero, suggesting that factors beyond this point are 'scree'. Using this method, seven factors were selected for inclusion in the LDA model. While other methods, such as the Kaiser Criterion [213] exist to determine the number of factors to include, the Scree Test was considered to provide an acceptable method for this investigation.

Cross validation is particularly important in predictive modelling techniques such as linear discriminant analysis to determine how well the model will perform on real samples. Picard and Cook examined cross validation in 1984 [214] and framed its basis around the Optimism Principle. Their example of this principle was sourced from the earlier work of Mosteller and Tukey [215], who stated on p. 37: *Testing the procedure on the data that gave it birth is almost certain to overestimate performance, for the optimizing process that chose it from among many possible*

*procedures will have made the greatest use possible of any and all idiosyncrasies of these particular data…As a result, the procedure will likely work better for these data than for almost any other data that will arise in practice".* This suggests that to avoid overfitting of the model to the dataset, the model needs to be carefully optimised for accuracy on normally distributed samples. For the current LDA model, cross validation was performed using the leave-one-out approach (LOOCV).

The training set for the LDA model consisted of 100 samples, as listed in Table 5.2. Each of the 100 samples contained in the dataset were temporarily removed from the array, then the LDA model was applied to the remaining $n - 1$ data points. The error was reported for each row and used to calculate the mean error for the model. The model was iteratively optimised to minimise this error value. To finalise the cross validation, the model was applied to an additional 21 samples which were not part of the original training set. These 21 samples were sourced from Southern Saaz and Pride of Ringwood varieties and a mean error consistent with that obtained for the optimised model was recorded.

Figure 3.22 illustrates the assignment of the hop samples based on the two variable selection approaches employed. Utilising the matrix generated from the Fisher ratio approach, samples belonging to the Pride of Ringwood variety could be accurately assigned in 100% of cases. A degree of overlap was witnessed between the other varieties, which were split into two clusters. Southern Hallertau, Willamette and Cascade were densely populated in one cluster, while Millennium, Victoria, Super Pride and Southern Saaz compiled the second cluster, albeit with a greater degree of differentiation between the varieties.

By repeating the LDA method on the t-test matrix, a significant improvement was witnessed. Super Pride and Willamette were very well resolved from other

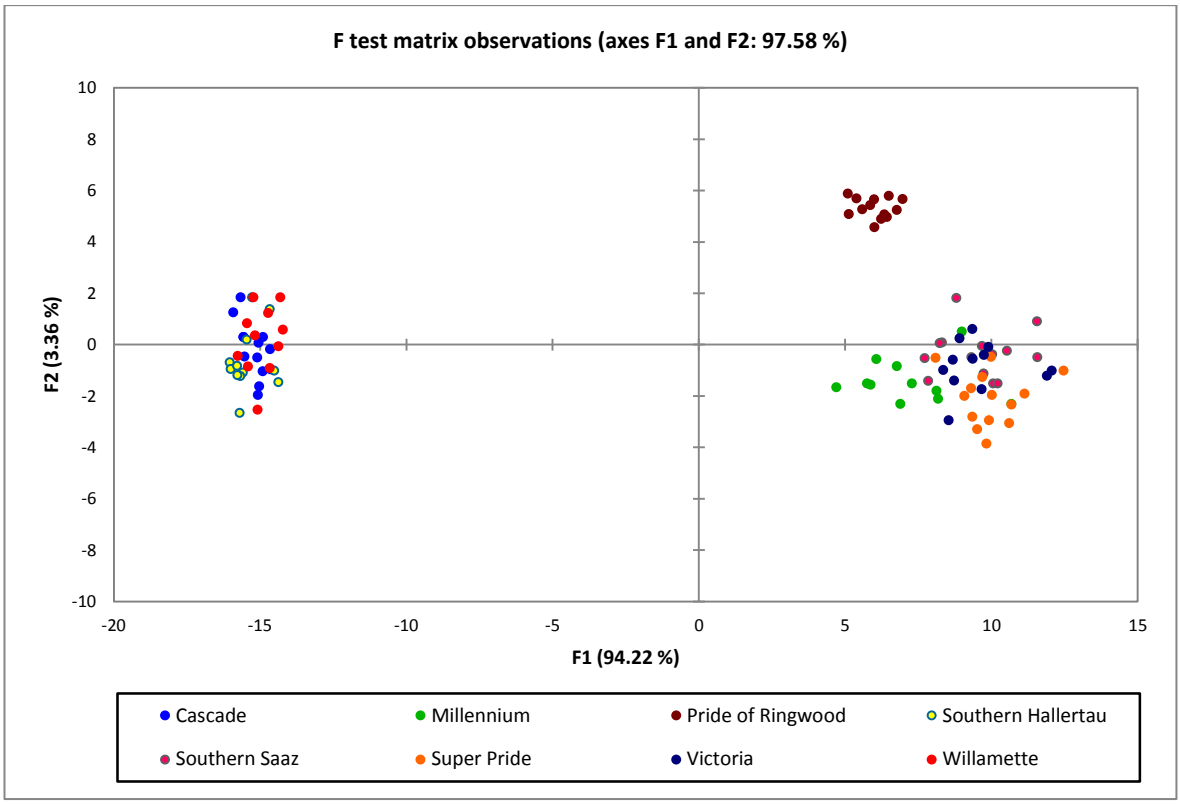


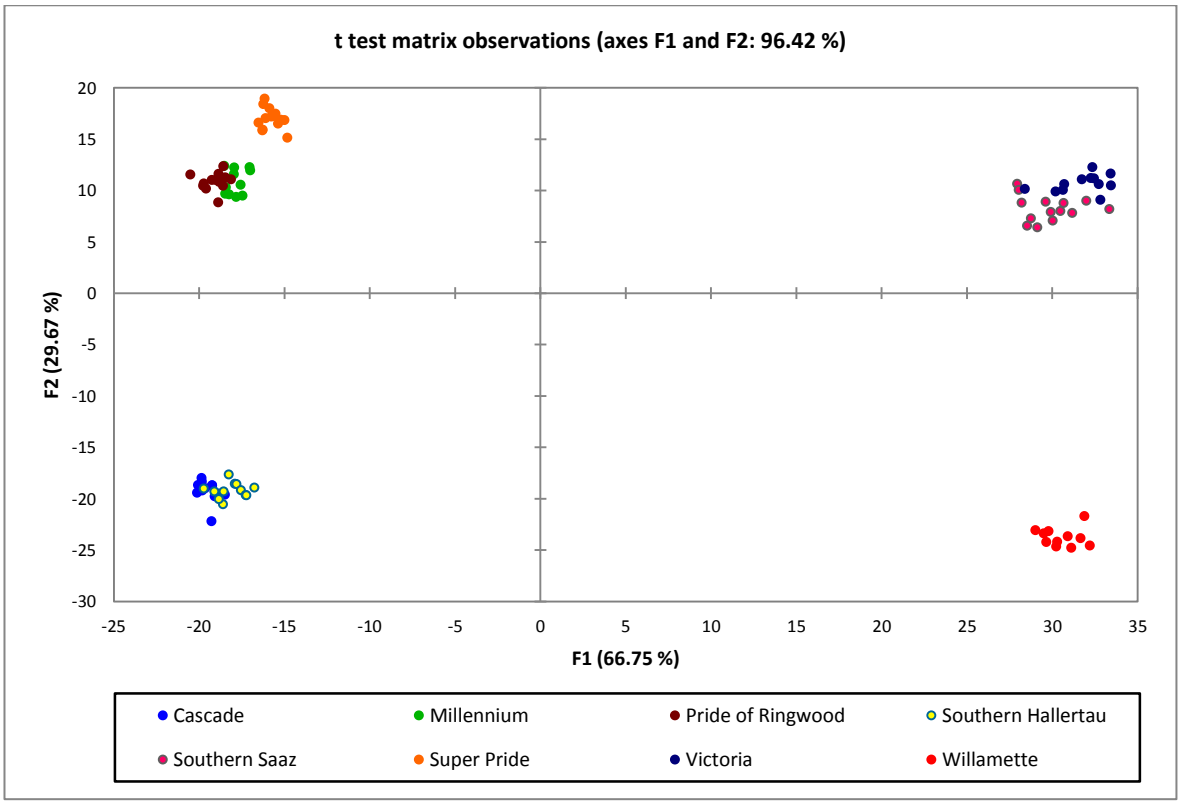


**Figure 3.22. LDA plots generated from variables selected using F test and t-test methods.**

varieties. Some overlap was witnessed between Pride of Ringwood and Millennium, but classification was not hampered. Some overlap was witnessed between Cascade and Southern Hallertau; and between Victoria and Southern Saaz.

A third LDA model was constructed using all 57 metabolites to determine if the resolution could be improved between these overlapping varieties. Samples belonging to Millennium, Super Pride, Pride of Ringwood and Willamette were well resolved. The resolution between the Cascade and Southern Hallertau, and Southern Saaz and Victoria clusters was not increased. An observations plot for this model is shown in Figure 3.23. Undoubtedly, some of the variables included in this model did not adequately represent the variance between the varieties and may have been omitted, but it is unlikely that an improved classification function could have been realised by pursuing this.

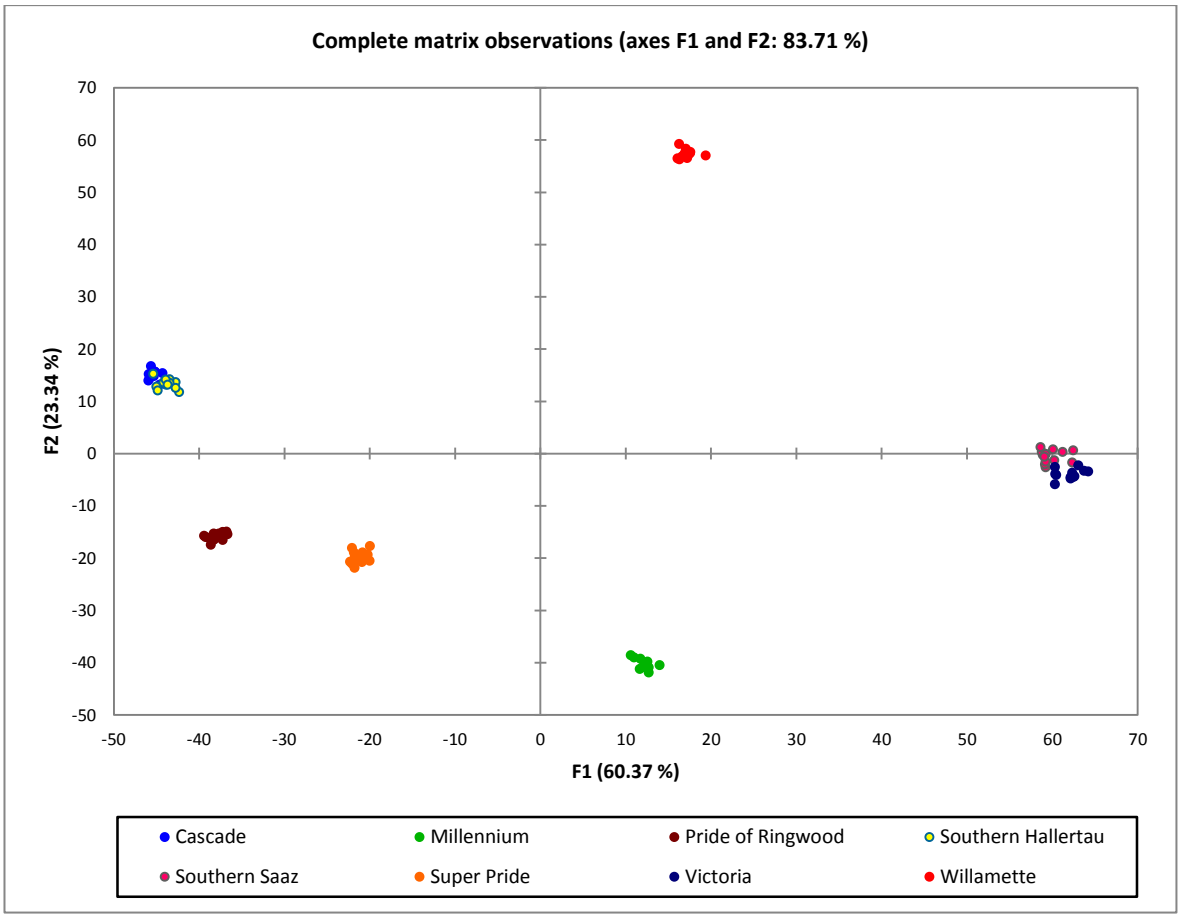


**Figure 3.23. LDA plot generated from all 57 variables presented in Table 3.5.**

### 3.4.5 Concluding remarks

The extraction and fractionation of metabolites from hop cones is a straightforward procedure. Following derivatisation and GC–MS analysis, good differentiation was observed between high α-acid and aroma varieties using PCA in which the variables were selected using both a Student's t-test and the Fisher ratio (F-test) method. While the DA model could classify some varieties based on the metabolite matrix generated, the differentiation between other varieties was problematic. Increasing the number of variables included in the model assisted in resolving these samples somewhat, although this may have incorporated unnecessary information in the model which was not representative of the variance in the sample populations.

This study was designed as a pilot project for the utilisation of metabolite profiling to support the Australian Hop Breeding Program and the investigators are encouraged by the potential ability to discriminate different varieties, which exhibit different characteristics, from a beer making point-of-view. There is demonstrable and growing interest in the use of metabolite profiling in agriculture and the results of this study have provided impetus for future work in this direction. While the approach employed did not incorporate the most powerful analysis techniques available, it demonstrated the suitability of the sampling method and extraction procedure for collecting an interpretable array of information about the plant's metabolome. It is anticipated that follow-up research will be conducted and may provide a novel use of high-quality data analysis techniques for the Tasmanian hop industry. This may highlight the significance of various metabolites identified and of the differences in metabolite composition between varieties, in addition to supporting decision-making in the breeding program.

## 3.5. Summary

The merits of three column choices for potential inclusion in a GC×GC system have been evaluated. First, a wide-bore column operated under low pressure conditions was examined to establish the suitability of this approach for separation of moderately complex samples.

The rationale for this investigation stems from the ideal situation of a hypothetical pneumatically modulated GC×GC–MS approach in which both separation dimensions are operated at (or approximately at) their optimum efficiency. To achieve effective modulation using a typical pneumatic modulator [56], a flow ratio in the order of 1:20 must be employed between the two separation dimensions. Operation of a narrow-bore first-dimension column at optimum efficiency would push the required flow rate in the second dimension above the pump capacity of the average MS detector. As the EOF for a wide-bore column operated under low pressure conditions is much less than a conventional column, it was hypothesised that optimum efficiency could be achieved in both separation dimensions despite the limitations imposed by the detector.

It had previously been reported that a low-pressure GC–MS approach was unsuitable for complex separations [13], and only one other essential oil analysis had been reported using a comparable method [149]. This investigation presented a novel application for a low-pressure GC–qMS approach for the separation of parsley and fennel essential oils to establish the suitability of this column for the analysis of moderately complex essential oils.

Separations performed using this approach were compared to those obtained using a narrow-bore column. The results using both methods were highly satisfactory, with sufficient peak capacity observed for tentative characterisation of

the samples. The increased sample capacity inherent in the use of a wide-bore column was witnessed, although this was countered by the anticipated higher overall efficiency offered by the narrow-bore approach.

It was concluded that despite the suitability of this approach for the presented application, the benefits of using a wide-bore column under low pressure in a GC×GC–MS column set did not outweigh the reduction in theoretical maximum efficiency possible with this column. Considering that many GC×GC–MS approaches aim to exceed the efficiency available with even the most efficient GC–MS methods, it was decided that insufficient efficiency was afforded by this column set-up to warrant further investigation.

The second study presented in this chapter described the use of a commercially available high temperature wax column in a cryogenically modulated GC×GC system for the separation of a complex essential oil. This column posesses a theoretical plate count in excess of 9000 N/m and can withstand temperatures up to 300 °C as claimed by the manufacturer. This claim was investigated by performing a series of blank injections at a rapid temperature ramp to observe column bleed. The results of this test were highly satisfactory. Using hydrogen as a carrier gas, an exemplary separation of kunzea essential oil was obtained using a (30 m × 0.25 mm Rxi-5 Sil MS) × (1 m × 0.1 mm MEGA-WAX HT) two-dimensional column set. The use of a 3 s modulation period induced a degree of wrap-around of the sample but provided a sensible use of the available separation space.

It must be remembered that employment of a cryogenic modulator does not necessitate the flow ratio as required for operation of pneumatic modulator. For this reason, the use of a ‘traditional’ short length of 0.10 mm i.d. (or smaller) second-dimension column may not be appropriate for pneumatic modulation as the column

will most likely be operated well above the optimal carrier gas flow rate. Although the optimal carrier gas flow rate may be exceeded in a cryogenically-modulated system, the high second-dimension flow rate (typically greater than 10 mL/min) as required for operation of a pneumatic modulator provide an even less amenable environment for optimal operation. Unfortunately, the stationary phase coating on this column is only currently available in 0.10 mm i.d. capillary, so further application of this column was not investigated.

The observations from the first two investigations presented in this chapter suggest that to operate a column close to the EOV in a pneumatically modulated GC×GC–MS system, the options investigated are not appropriate. While the use of a wide bore column at high flow and low pressure generates a separation close to the EOV of the column, the available efficiency is not sufficient to generate a large enough separation space for analysis of the complex mixtures typically examined in GC×GC. Conversely, while the theoretical efficiency of a narrow bore column operated at EOV does meet this criteria, the instrumental parameters necessary for operation of a pneumatic modulator do not allow this theoretical efficiency to be realised. It was therefore concluded that the use of a moderate length of 0.25 mm i.d. capillary would provide the optimum compromise for use as the second dimension of a pneumatically modulated GC×GC–MS system. Such a column would generate more theoretical plates at EOV than a wide-bore, low pressure arrangement, yet possess an EOV compatible with the limitations imposed by the modulation method.

Following this study, a high-efficiency column was investigated and some observations regarding intelligent selection of columns when operated using constant pressure were reported.

This column was chosen for investigation for several reasons. Most notably, the exceptionally high theoretical efficiency is ideally suited to generating a large separation space in a comprehensive two-dimensional analysis. Furthermore, operating the column in constant pressure mode at the maximum available pressure could generate a separation in a reasonable amount of time (~1-2.5 h).

As expected, this separation produced unprecedented efficiency and excellent resolution between components when used for GC–MS. Using constant pressure mode, which may prove useful should this method be translated in the future, the average linear velocity at the start of the run was set at an approximation of the EOV value. As the temperature program proceeded, the average linear velocity decreased below this value. This operational parameter was selected to minimise the deviation between theoretical maximum efficiency and observed efficiency.

Intelligent use of theory and method translation software allows the calculation of the length of column required for EOV to be reached at the *end* of the temperature program, given a fixed head pressure. This reduces the deviation from theoretical maximum efficiency and provides an approach for determining column length providing the best trade-off between effective efficiency and hold-up time. These observations hinge on the fundamental work of Fuller [216] and Beens [78] and would be appropriate for the selection of a first-dimension column in a pneumatically-modulated GC×GC approach.

To conclude this chapter, the use of GC–MS for the separation and characterisation of a series of hop varieties was explored. The simple chemometric approaches of PCA and DA were used to determine whether a matrix of relevant variables could be generated from the one-dimensional separation of metabolite extracts extracted from the lupulin glands of the hop cones. The PCA approach

showed that high α-acid and aroma varieties could be differentiated, but the individual varieties were not resolved using this method. Application of DA on the two metabolite matrices prepared showed that some samples could be correctly classified, but again resolution was less than anticipated. While more advanced data visualisation techniques could have been utilised to extract more information from the available metabolite data, the intention of this study was to determine the feasibility of utilising lupulin gland extracts for identification. This goal was achieved, and a follow-up study is planned whereby a comprehensive two-dimensional separation approach is included. Discussion on further research is provided in Section 5.2.

# Chapter 4: Development, application and comparison of GC×GC–MS / FID approaches for the analysis of plant essential oil and metabolite samples

## 4.1 GC×GC with pneumatic modulation for enantioselective essential oil analysis

This section has been adapted from the following publication:

P. McA. Harvey, S.D.H. Poynter, R.A. Shellie. **GC×GC with fluidic modulation for enantioselective essential oil analysis.** *LC-GC Eur*. (2011) **24**(10) 548–555.

### 4.1.1 Introduction

The suitability of GC×GC for performing enantioselective analysis of essential oil samples is described here. For this application, the use of an Agilent CFT Modulator (Agilent Technologies, Forest Hills, Australia) has been evaluated [217]. It is worth noting that the specific dimensions of the channels in the CFT device are not necessarily identical to those described by Seeley *et. al* but the fundamental approach is consistent. The monolithic structure of the CFT modulator and its use of SilTite™ ferrules offer several advantages over homemade pneumatic modulators. Notwithstanding, many investigators have found fluidic modulation using this device to be less than satisfactory and the limited number of publications using the technology may be partially ascribed to the difficulty in determining rugged modulation conditions.

There are a few key considerations to optimising GC×GC instrument settings for pneumatic modulation. Some of these considerations are unique to pneumatic modulation while others are more generally applicable. Starting with the general

considerations, a wide body of literature indicates that it is highly desirable to maintain a suitable modulation ratio [218]. There is a rule of thumb (which has sound theoretical and practical underpinnings [12]) that suggests there should be four modulation slices across each first dimension peak. This ensures that peak capacity of the first dimension separation is not too greatly diminished by the modulation process. Secondly, it is also highly desirable to minimise the extent of wrap-around [219]. In other words, the elution window in the second dimension should not significantly exceed the modulation period. As mentioned previously, if the modulation period is exceeded there can be detrimental effects on resolution in the second separation dimension. There is often a practical compromise of each of these criteria but the best GC×GC results typically come from carefully optimised systems that adhere strictly to both considerations. Furthermore, stationary phase selection is a key consideration for all GC×GC approaches; a recurring theme throughout this thesis.

Among the important specific considerations for pneumatic modulation, the critical consideration is that proper pneumatic conditions are applied i) to ensure stop-flow modulation (at point X in Figure 4.1), ii) to provide sufficient time to flush the modulator sample loop (Figure 4.1), and iii) to prevent breakthrough from the sample loop during the modulation cycle. In addition, a large volumetric flow ratio (column 2:column 1) has to be applied to facilitate peak-compression-in-time, which minimises the injection bandwidth into the second dimension column. Typically this flow ratio needs to be 10:1 or higher [67].

Maintaining appropriate pneumatic conditions, whilst satisfying the general considerations described above can be troublesome. An example drawn from the literature describing fatty acid methyl esters analysis using pneumatic modulation is

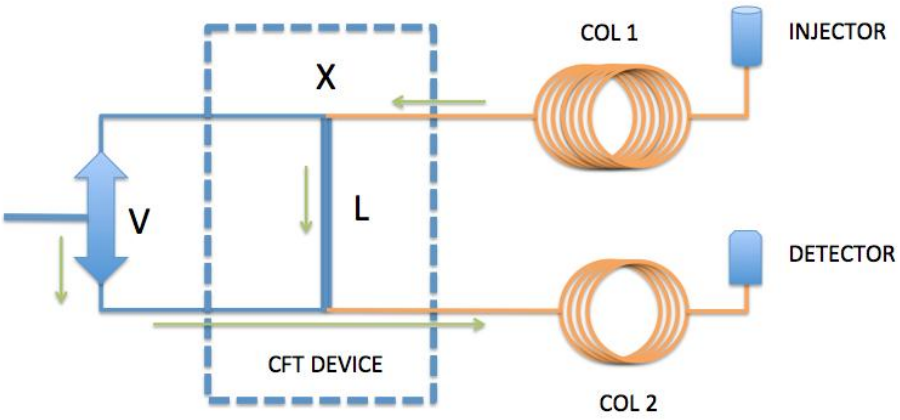


**Figure 4.1. Plan of the fluidic modulator employed, showing the sample loop (L), 3-way switching valve (V), connecting tubing and the connecting points of the first (COL 1) and second (COL 2) dimension columns.**

shown in Figure 4.2 [220]. In this example, the column set dimensions were (30 m × 0.25 mm) × (2 m × 0.25 mm), each column having a 0.25 μm film thickness. The first-dimension column was coated with a 70% cyanopropyl polysilphenylene-siloxane stationary phase and the second-dimension column was coated with a 5% polysilarylene-95% polydimethylsiloxane copolymer stationary phase. The most striking feature of this chromatogram is how the broad second dimension peaks sometimes fill the entire y-axis. This indicates the peak capacity of the second dimension is <1 in these locations. The observed low performance may be a result of modulator breakthrough, incomplete flushing or a combination of both. These undesirable effects can be eliminated by informed column choice, along with appropriate instrument settings.

A primary argument of the research presented in this thesis is that *properly informed column choice greatly simplifies the process of method development* and gives greater flexibility in instrument settings for pneumatic modulation. Previously, Harvey *et al.* showed that it was possible to increase the modulation period to at least 9 s without adverse chromatographic affects [67] using a homemade pneumatic modulation device. In the present investigation, the principles reported in earlier studies [67, 221] have been applied with a CFT pneumatic modulator. Enantioselective analysis of essential oils offers a good illustrative example of the benefit of multidimensional separations. There are two options for performing enantioselective GC×GC separations. First, it is possible to follow the path laid by the myriad of heart-cut *enantio*-MDGC applications for essential oils analysis [222] and employ an achiral first-dimension column coupled to an enantioselective column in the second dimension. However, practical implementation of this approach may be obstructed by the need for rapid second-dimension separations [15]. The preferred

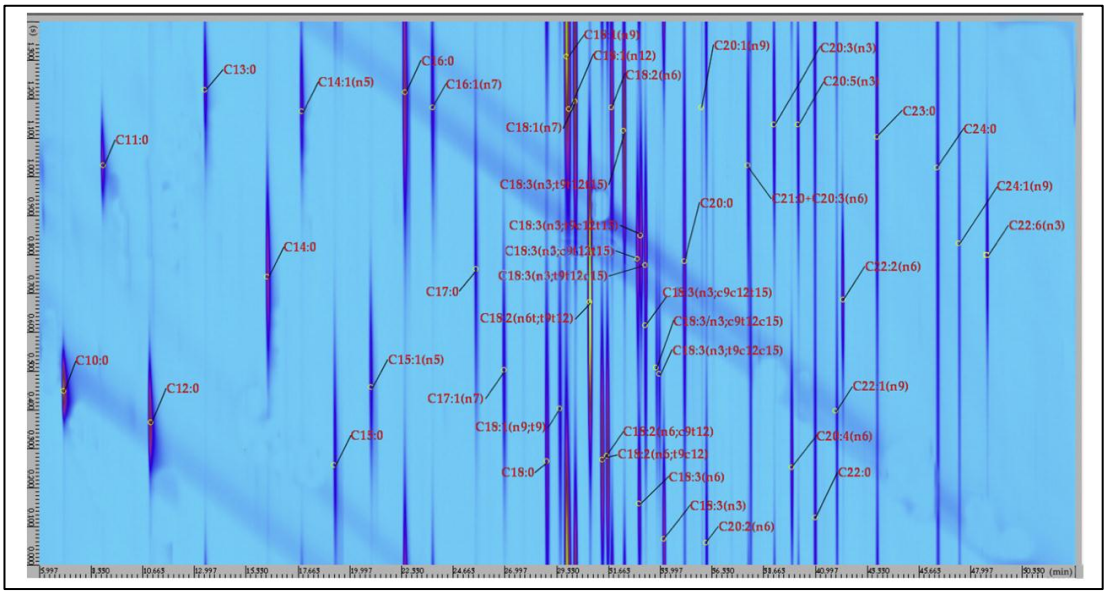


**Figure 4.2. GC×GC–FID chromatogram of the standard mixture of 45 FAMEs (Reprinted with permission from [220], copyright 2011, Elsevier)**

approach is to employ an enantioselective stationary phase column in the first dimension and follow this separation with one performed using an achiral stationary phase in the second dimension [163]. The results from enantioselective GC×GC analysis of spearmint essential oil are presented here to highlight suitability of a fluidic modulation system for this dedicated application.

### 4.1.2 Experimental

Enantioselective GC×GC analysis of spearmint essential oil was performed using an Agilent 7890A GC×GC instrument with CFT modulator and flame ionization detector (Agilent Technologies, Forest Hills, Australia). The first dimension column was a 20 m × 0.10 mm i.d. capillary coated with a thin film (0.1 μm) of diethyl-t-butylsilyl β cyclodextrin in PS-086 stationary phase (Mega, Legnano, Italy). The first dimension column was connected to the CFT device using a SilTite ferrule (SGE Analytical Science, Ringwood, Australia). The second dimension column was a 5 m × 0.25 mm i.d. capillary coated with a thin film (0.15 μm) of polyethylene glycol stationary phase (Agilent Technologies, Forest Hills, Australia). The second column was connected to the CFT device using a SilTite ferrule. Carrier gas ($H_2$) was supplied at a flow rate of 0.4 mL/min (constant flow) in the first dimension from the split/splitless injector and 20 mL/min (constant flow) in the second dimension using the auxiliary pressure controller. The detector temperature was 280 $^{o}$C and the injector was 230 $^{o}$C. The injection volume was 1.0 μL throughout and a split ratio of 20:1 was employed for all analyses.

For qualitative comparison purposes, GC×GC analyses were also performed using a Shimadzu GC×GC system, consisting of two independent GC–2010 gas chromatographs and a QP-2010 Plus quadrupole mass spectrometer as described in

Chapter 2. The transfer line temperature was held at 280 °C and the injector at 250 °C. The first dimension column was a 25 m × 0.25 mm i.d. capillary coated with a thin film (0.25 μm) of diethyl-t-butylsilyl β cyclodextrin in PS-086 stationary phase (Mega, Legano, Italy). The second dimension column was a 1 m x 0.05 mm i.d. capillary coated with a thin film (0.25 μm) of polyethylene glycol stationary phase (Supelco Sigma-Aldrich, Castle Hill, Australia). A modulator loop was formed using a 2 m x 0.25 mm i.d. uncoated column that was first passed through the heated transfer line between the two GC instruments. A dual-stage loop-type modulator (under license from Zoex Corporation) was used to couple the two dimensions. The modulation period was 4 s and the duration of the hot pulse (325 °C) was 375 ms. Helium carrier gas was used at a constant flow rate of 0.5 mL/min.

### 4.1.3 Results and Discussion

Harvey and co-workers showed by modelling the flow of carrier gas in a pneumatic modulator, a distinct advantage can be obtained by using a restrictor immediately before the sample loop [67]. It is a critical performance criterion that the flow from the first dimension column is ‘stopped’, otherwise modulation will be ineffective and the two separation columns will not be properly decoupled to permit GC×GC separation. However, it is widely recognised that ‘stop-flow’ is not a realistic expectation when the modulator valve is actuated. Instead, the direction of flow is reversed briefly upon valve actuation and the subsequent raising of the first dimension column outlet pressure. If the first dimension column has a low resistance to flow, then the direction of flow is affected along a significant length of the column. By using a restrictor column, with high resistance to flow, flow modelling

showed that perturbation of flow is limited to the restrictor column. Practical implementation agreed with predicted enhanced modulator effectiveness [67].

In the present investigation, the restrictor column (along with the corresponding connection in the GC×GC column ensemble) was eliminated and a long (15-20 m) narrow-bore (0.10 mm i.d.) column was used in the first separation dimension. In this way, the separation column itself provides sufficient pressure-drop to minimise flow disturbance and restricted the perturbation to a short section of the column near its terminus. Employing narrow-bore columns in the first dimension provides further benefit since their optimal performance is achieved at lower volumetric flow rates (compared to wider-bore capillaries) and therefore permit use of a longer modulation period without causing sample loop breakthrough. To this end, it is interesting to determine how low the volumetric flow rate can be without causing significant longitudinal diffusion and subsequent increase in plate height. The optimal carrier gas flow rate is easily determined using the teachings of Blumberg and Klee [35]. In the present investigation, a flow rate was selected that was slightly below the EOF value for the first dimension column. Although the downfalls of operating at a sub-optimal flow rate have been discussed at length in this thesis, for this specific application the compromise was deemed worthwhile because it improved the ruggedness of the instrument settings. It is a common belief that even a small departure from the default instrument settings for the CFT device can lead to sub-optimal modulation. To evaluate the effectiveness of this decision, a series of injections were performed using an Agilent 6850 GC instrument (Agilent Technologies, Forest Hills, Australia) to determine plate height at different volumetric flow rates for a 20 m x 0.10 mm i.d. Rtx-5 (0.10 μm $d_f$) column (Restek Corporation, Bellefonte, PA, USA). Carrier gas ($H_2$) was provided via the

split/splitless injector. The detector temperature was 280 $^{o}$C and the injector was 230 $^{o}$C. Plate height was measured for *n*-dodecane at 140 $^{o}$C (k~3) using calculated volumetric flow rates between 0.07 mL/min and 0.5 mL/min corresponding to a linear velocity range spanning *ca*. 10 cm/s to *ca*. 32 cm/s. The mean results (n=3) are summarised in Figure 4.3. The H/u curve is remarkably flat between 0.2-0.5 mL/min so using flow rates as low as 0.2 mL/min in a GC×GC setup is justifiable. Low first-dimension flow rates are further justified, since the injection bandwidth (*w*) into the second dimension column is a function of the modulation period ($P_M$) and the flow ratio according to Equation 4.1. Using a low first-dimension flow rate may lead to improved observed performance in the second separation dimension by minimising extra-column broadening in this dimension [221].

$$w = \frac{^{1}F \cdot P_M}{^{2}F}$$

Equation 4.1

($^{1}$F and $^{2}$F are the first and second-dimension volumetric flow rates respectively)

The dimensions of the internal sample loop in the CFT modulator are unknown, so optimisation of instrument settings was performed by an iterative approach.

Essential oil analysis is made difficult by the wide dynamic range of the components in most samples. Spearmint essential oil is predominantly comprised of mono- and sesquiterpene hydrocarbons as well as mono- and sesquiterpene alcohols. These components span a relatively wide volatility range and exhibit substantially different retention characteristics; consequently a relatively long modulation period is generally required to obtain sufficient second-dimension peak capacity. In the present investigation, meaningful separation is achieved by setting the second

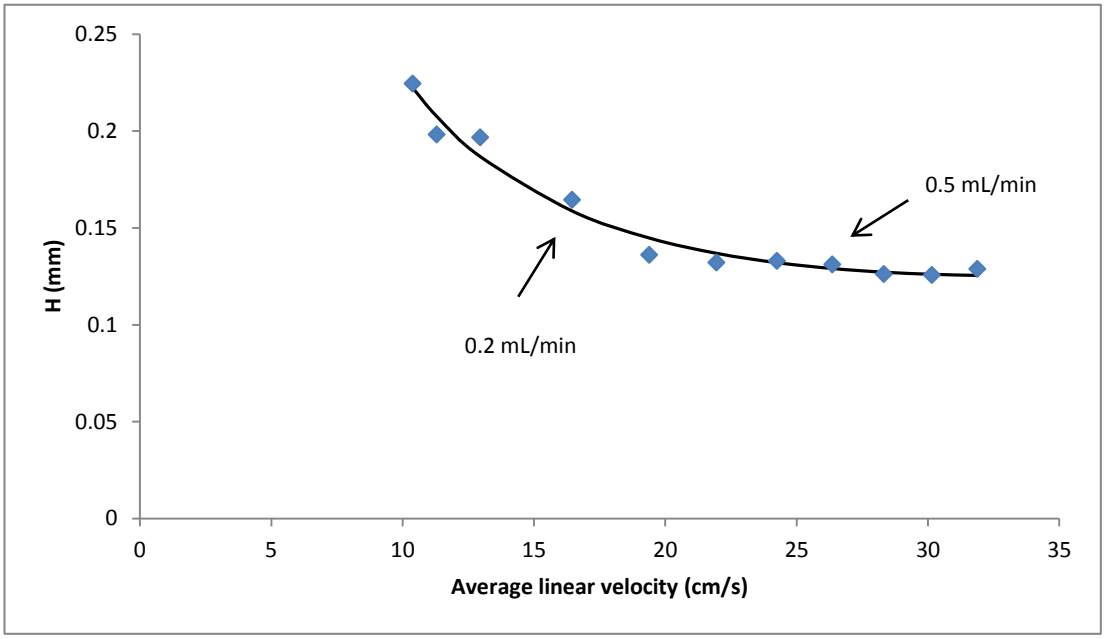


**Figure 4.3. Experimental H/u curve justifies use of low first dimension flow rate. Plate height (H) was measured for *n*-dodecane at 140 °C using calculated volumetric $H_2$ flow rates between 0.07 mL/min and 0.5 mL/min and a 20 m × 0.10 mm Rtx-5 column.**

dimension separation window to 3 s. While it could be argued that increasing the oven temperature would compress the second-dimension elution window, this leads to a substantial loss of resolution in the second-dimension column and should be avoided if possible. Figure 4.4 illustrates the GC×GC separation space from the pneumatic modulation GC×GC system investigated in this study and the corresponding chromatogram from a thermal modulation GC×GC experiment is shown in Figure 4.5. Although the two-dimensional peak capacity from the thermal modulation experiment is notably greater than that achieved by pneumatic modulation, the results from the latter are satisfactory. While no attempt has been made to match closely the retention times in each system, this comparison does permit one to draw an important conclusion that appropriate column selection brings pneumatic modulation into genuine contention as an alternative to thermal modulation GC×GC. A 3 s separation window provides adequate space with minimal wrap-around for separation of the terpenoid compounds present in the spearmint essential oil sample and the present column ensemble and flow arrangement easily permits a 3 s modulation period.

Tentative identification of the sample components was performed by GC×GC–MS and confirmed by injection of authentic reference standards; the identities of the separated components are reported in Table 4.1. Thirty-five terpenoid compounds were positively identified in the two-dimensional separation space. Extensive characterisation was not attempted, although several other sample components were well resolved. Among the separated components, the individual optical isomers, including β-pinene, limonene, sabinene and terpinen-4-ol were well resolved. Authentic reference standards of sufficient purity to perform quantitative analysis were available for three of these chiral compounds. Triplicate analyses were

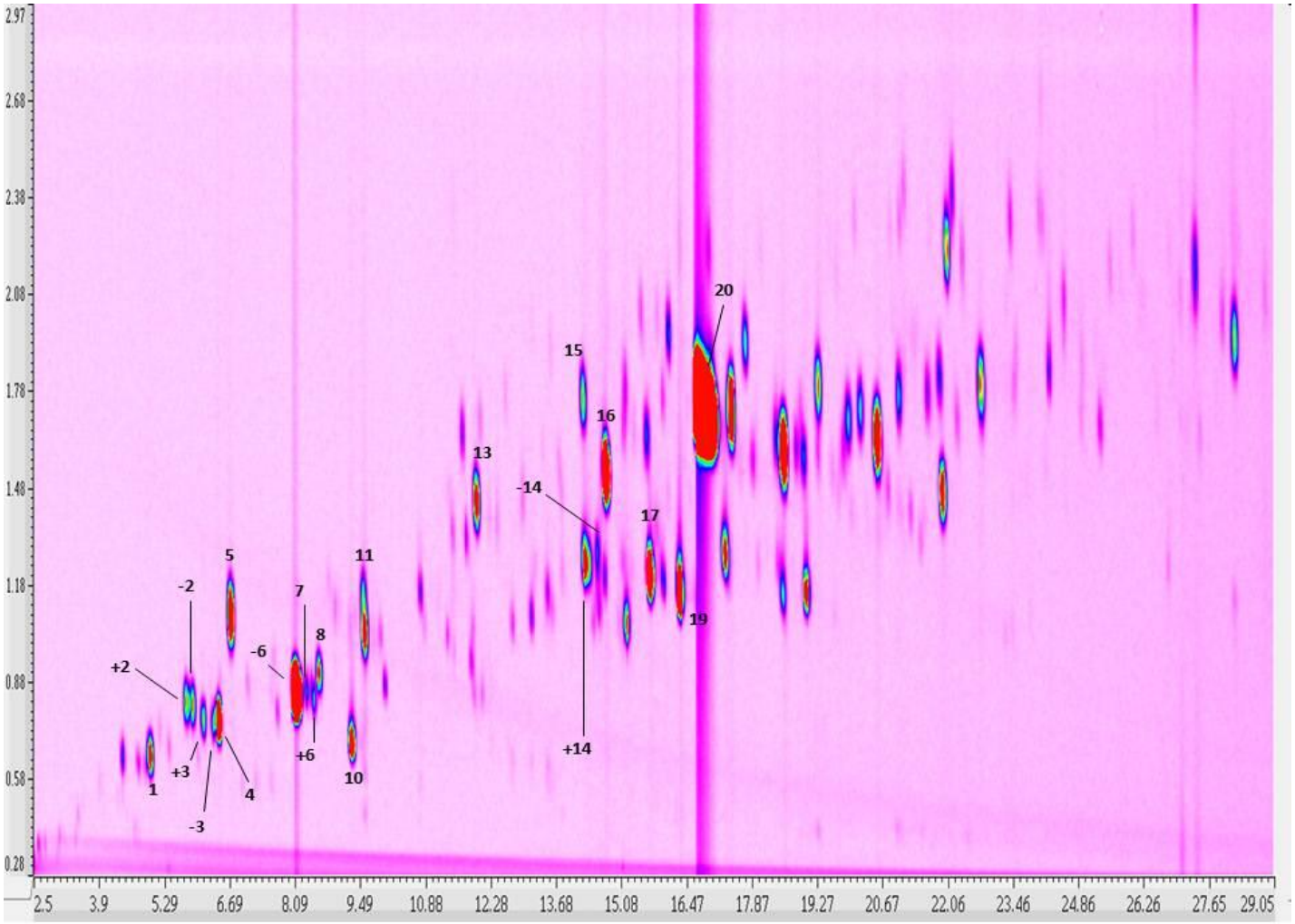


**Figure 4.4. Two-dimensional separation space for the GC×GC–FID separation of spearmint essential oil using fluidic modulation. Refer to Table 4.1 for tentative peak identification. Column set was (20 m × 0.10 mm) × (5 m × 0.25 mm ). $H_2$ carrier gas at 0.4 mL/min in the first dimension and 20 mL/min in the second dimension.**

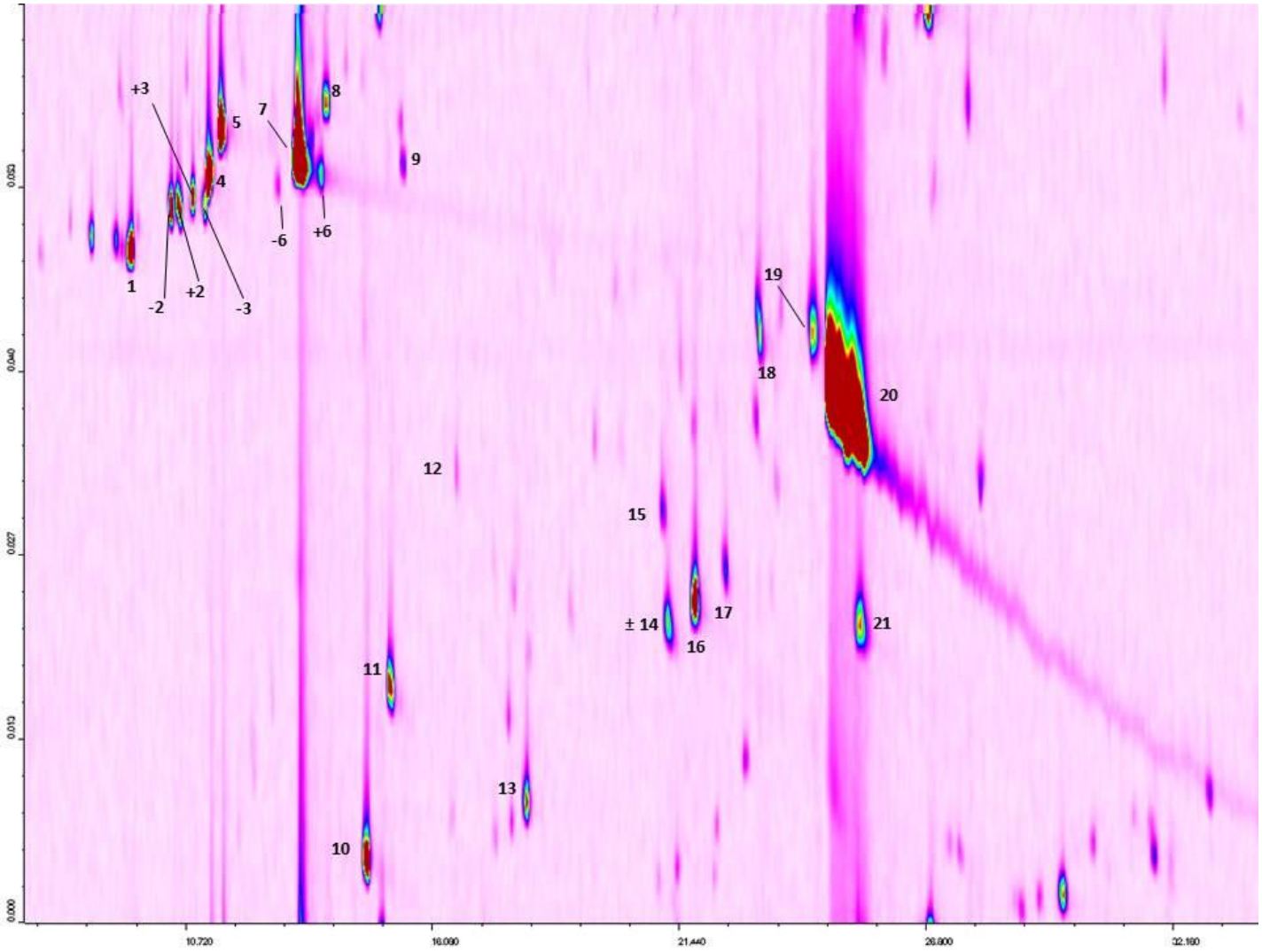


**Figure 4.5. Two-dimensional separation space for the GC×GC–MS separation of spearmint essential oil using cryogenic modulation. Column set (25 m × 0.25 mm) × (1 m × 0.05 mm) with a 2 m × 0.25 mm i.d. modulator loop. He carrier gas was used at 0.5 mL/min.**

**Table 4.1. Tentative peak identities of those labelled in Figure 4.4. Identification was made by comparison with authentic reference standards.**

| Peak number | Tentative identity |
|---|---|
| 1 | α-pinene |
| +2 | (+)-β-pinene |
| -2 | (-)-β-pinene |
| +3 | (+)-sabinene |
| -3 | (-)-sabinene |
| 4 | β-myrcene |
| 5 | 1,8-cineol |
| -6 | (-)-limonene |
| +6 | (+)-limonene |
| 7 | cis-ocimene |
| 8 | p-cymene |
| 9 | γ-terpinene |
| 10 | 3-octanol |
| 11 | trans-sabinene hydrate |
| 12 | cis-sabinene hydrate |
| 13 | menthone |
| +14 | (+)-terpinen-4-ol |
| -14 | (-)-terpinen-4-ol |
| 15 | trans-dihydrocarvone |
| 16 | cis-diydrocarvone |
| 17 | (-)-menthol |
| 18 | neodyhydrocarveol |
| 19 | dihydrocarveol III |
| 20 | carvone |
| 21 | dihydrocarvyl acetate |

performed to determine retention time repeatability of using the fluidic modulation GC×GC approach, and to determine enantiomeric ratio of the resolved pairs. Retention time precision was outstanding; in fact % RSD for second-dimension retention time was not greater than 0.45% for any of the target peaks in either separation dimension. Mean second dimension times (n=3), and 95% confidence interval for (+)-β-pinene, (-)-limonene, and (+)-terpinen-4-ol were: 0.815 ± 0.000 s, 0.849 ± 0.001 s, 1.250 ± 0.003 s respectively. Mean second dimension times (n=3), and 95% confidence interval for (-)-β-pinene, (+)-limonene, and (-)-terpinen-4-ol were: 0.810 ± 0.001 s, 0.825 ± 0.000 s, 1.277 ± 0.007 s respectively. Mean first dimension times (n=3), determined from the retention time of the tallest modulation slice for (+)-β-pinene, (-)-limonene, and (+)-terpinen-4-ol were: 5.75 min, 8.10 min, and 14.30 min respectively. For (-)-β-pinene, (+)-limonene, and (-)-terpinen-4-ol, the recorded first dimension retention times were: 5.90 min, 8.50 min, and 14.55 min respectively. These results demonstrate the outstanding run-to-run repeatability using fluidic modulation, with the peak maxima being almost perfectly overlaid. Repeatability of quantitative analysis was also highly satisfactory. The mean results (n=3) of enantiomeric ratio determination for these three pairs of enantiomers are summarised in Table 4.2.

Excellent repeatability of the quantitative determination of enantiomeric ratio for these three pairs of optical isomers highlights the modulation performance; without proper modulation these results would be compromised. In particular, unpredictable modulator breakthrough has been avoided by appropriate first dimension column selection. It would be impossible to realise this level of repeatability if sub-optimal modulation were employed. Carveol, (peak 23, Figure 4.4) is characterised by an obvious streaky appearance in the second dimension,

**Table 4.2. Results from determination of enantiomeric ratio. Mean values (n=3) and 95% confidence interval are reported.**

| | (+) | (–) |
|---|---|---|
| **β-pinene** | 50.79 ± 0.46 | 49.21 ± 0.046 |
| **limonene** | 1.05 ± 0.01 | 98.95 ± 0.01 |
| **terpinen-4-ol** | 86.34 ± 2.12 | 13.66 ± 2.12 |

however this behaviour is also apparent in the separation using the cryogenic modulator (Figure 4.5) so it is postulated that this observation is not caused by pneumatic modulation. In fact, the extended tail of the corresponding peak is only observed in the cryogenic system. Marriott and co-workers [223], along with Beens *et al.* [224] have previously highlighted similar behaviour with GC×GC systems, putting this observed behaviour down to injector effects. Haglund *et al.* [225] ascribed the peak tailing to a modulation-induced effect. This theory fits well with the results observed in the present investigation.

### 4.1.4 Concluding remarks

Appropriate pneumatic conditions are readily achieved using long, narrow-bore columns in the first dimension of a comprehensive multidimensional GC column ensemble for fluidic modulation. By operating these columns at low volumetric flow rates, favourable modulation period (without breakthrough) for complex multicomponent samples is readily achievable. Since narrow-bore columns provide high resistance to flow, their use also leads to effective stop-flow modulation and streaks in the two-dimensional separation space caused by ineffective modulation are easily avoided. Long columns (i.e. >10 m) are best suited because these maintain optimal modulation ratio without having to resort to very short modulation period. Although narrow-bore columns have lower mass loadability than their wider-bore counterparts, the simplification of determining rugged pneumatic conditions and modulator timing parameters leading to the general benefits of GC×GC was thought to outweigh this negative characteristic.

## 4.2. Preparation of a pneumatic-modulated GC×GC–qMS approach

### 4.2.1 Introduction

Beens and co-workers presented a paper in 2005 regarding the development of an appropriate flow regime for thermally modulated GC×GC systems operated at ambient outlet [78]. It was noted that the majority of GC×GC separation methods were developed from existing 1D-GC approaches. However, the high resistance to flow provided by the second-dimension column results in higher pressure, and hence slower diffusion observed in the first-dimension column, suggesting this may not be an appropriate choice. This effect is particularly noticeable when a narrow bore column is chosen for the second dimension, meaning that the most common column dimensions are not necessarily the best choice for GC×GC separations.

The present study supplements the discussion presented in Chapter 3 regarding the selection of column length based on desired efficiency at a given head pressure. In this chapter, a pneumatically-modulated GC×GC–qMS system was prepared using three alternative first-dimension columns and a commercially-available Deans switch microfluidic wafer. A short, narrow-bore column was chosen based on the results presented in Chapter 3 to present the option of a faster separation, sacrificing potential efficiency in favour of achieving EOV at a reduced head pressure. A longer, narrow-bore column was installed to present the effect of operating the first dimension significantly below EOV due to the higher resistance to flow. A third column, possessing a wider internal diameter, was also utilised to represent a trade-off between the first two options.

The overarching aim of this research was to develop an inexpensive GC×GC system (in terms of both setup and operational costs) incorporating quadrupole MS

detection and pneumatic modulation which would be suitable for analysis of samples such as petrochemicals, moderately-complex and complex essential oils.

Prior to development, the flow parameters permitting good sensitivity for the mass spectrometer were experimentally determined and used as a starting point to determine the second-dimension flow rate, from which other parameters hinged. The increased peak capacity generated by the longer column was clearly witnessed, and sensitivity remained acceptable despite the low duty cycle of the modulator. Satisfactory separations of diesel and two essential oil samples (hop and vetiver oil) were obtained.

### 4.2.2 Experimental parameters

A 5-port Deans switch microfluidic wafer was obtained from SGE (SGE Analytical Science, Ringwood, Australia) and used throughout this investigation. The Shimadzu QP2010 Plus GC×GC–MS system was configured with the first-dimension column located in the satellite oven and passed through a transfer line held at a constant 250°C to the main oven. The modulator and second-dimension columns were located in the main oven. Auxiliary flow to the modulator was provided by the Shimadzu APC via 30 cm × 0.38 mm i.d. Sulfinert deactivated stainless steel tubing (Restek Corporation, Bellefonte, USA). A 3-way switching valve (part number 091-0094-900; Parker Hannifin Australia, Castle Hill, Australia) was utilised for flow switching and was located outside the GC oven and controlled by an Omron H5BR timer (Lawrence and Hanson, Hobart, Tasmania). Helium carrier gas was used for all separations. The first-dimension columns investigated were coated with a 5% diphenyl equivalent stationary phase (Rtx-5; Restek Corporation, Bellefonte, USA or SGE BPX-5; SGE Analytical Science, Ringwood, Australia). The two second-dimension columns were coated with an ionic liquid

stationary phase (SLB IL-111) and were obtained from Supelco (Sigma-Aldrich, Castle Hill, Australia). The dimensions of the second-dimension columns were 2 m × 0.25 mm i.d. for all separations. The column running to the MS was fitted with an 18 cm × 0.15 mm deactivated fused silica restrictor at the terminus. This restrictor was housed in the MS transfer line and kept at a constant 250 °C. A schematic of the instrument setup is shown in Figure 4.6.

The MS detector was operated at a mass range of 35-350 *m/z* and an acquisition rate of 25 Hz. The FID was operated at 250 Hz for all separations. The modulation time of FID separations was 2.8 s with a duty cycle of 0.14 while for all MS separations the modulation time was 2.5 s with a duty cycle of 0.08. This means that for an FID separation, a 0.4 s wide pulse of first-dimension effluent is directed to the second-dimension column every 2.8 s. For a MS separation, a 0.2 s wide pulse is directed to the second-dimension column every 2.5 s.

A commercial vetiver essential oil (*Vetiveria zizanioides*) sample was obtained from Australian Botanical Products (Hallam, Australia), from which a 20% v/v solution (unless stated) was prepared by diluting the neat essential oil with dichloromethane (Sigma-Aldrich, Castle Hill, Australia). Hop essential oil was obtained and used in the manner described in Section 3.3.2.

Modulation was commenced at the time of injection for all separations. The dimensions of the columns investigated and their operating parameters are listed in Table 4.3.

### 4.2.3. MS sensitivity testing

To determine the suitable flow regime range of the GC×GC–MS system, the determination of the sensitivity of the mass spectrometer at varying carrier gas flow

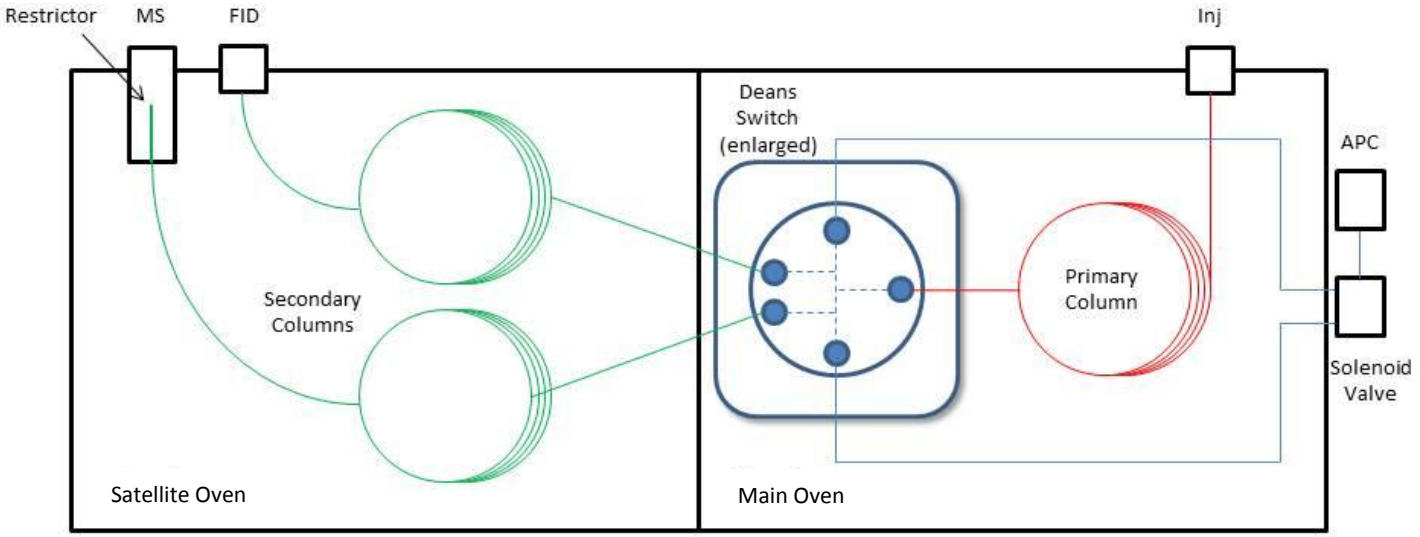


**Figure 4.6. Schematic of the Deans switch GC×GC system**

**Table 4.3. Operating parameters**

| $^{1}$D Column | $^{2}$D Column | Split ratio | $^{1}$D pressure program | $^{1}$D equivalent flow rate | $^{2}$D pressure program | $^{2}$D equivalent flow rate | Flow ratio | Temperature program | Total run time |
|---|---|---|---|---|---|---|---|---|---|
| 20 m × 0.1 mm Rtx-5 | 2 m × 0.25 mm SLB IL-111 (×2) | 100:1 | 277.3-467.6 kPa @ 3.8 kPa/min.<br><br>Hold 1 min at start and 9.91 min at end | 0.2 mL/min | 42.8-76.2 kPa @ 0.4 kPa/min.<br><br>Hold 1 min at start and 21.5 min at end | 5mL/min | 1:25 | 40-250 °C @ 4.2 °C/min.<br><br>Hold 1 min at start. | 61 min |
| 40 m × 0.1 mm Rtx-5 | 2 m × 0.25 mm SLB IL-111 (×2) | 100:1 | 417.1-685.3 kPa @ 2.6 kPa/min.<br><br>Hold 1 min at start and 1.85 min at end | 0.2 mL/min | 42.8-76.2 kPa @ 0.4 kPa/min.<br><br>Hold 1 min at start and 21.5 min at end | 5mL/min | 1:25 | 40-250 °C @ 2 °C/min.<br><br>Hold 1 min at start. | 106 min |
| 25 m × 0.22 mm BPX-5 | 2 m × 0.25 mm SLB IL-111 (×2) | 20:1 | 63.5-114.7 kPa @ 0.5 kPa/min.<br><br>Hold 1 min at start and 12.6 min at end | 0.2 mL/min | 42.8-76.2 kPa @ 0.4 kPa/min.<br><br>Hold 1 min at start and 21.5 min at end | 5mL/min | 1:25 | 40-250 °C @ 2 °C/min.<br><br>Hold 1 min at start and 10 min at end. | 116 min |

rates is paramount. The Shimadzu QP2010 Plus instrument used in this investigation is equipped with a differential dual inlet turbomolecular pumping system to provide a higher vacuum level at the ion source and mass analyser. The manufacturer claims column flow rates of up to 15 mL/min may be used.

MS sensitivity is commonly reported in terms of the amplitude of signal response of a common analyte, usually octafluoronaphthalene (OFN) or hexachlorobenzene (HCB). The signal response is directly linked to the limit of detection or quantification for an analyte and hence provides a suitable metric for this investigation. A 0.1 mg/L sample of OFN was prepared and injected on a 25 m × 0.22 mm i.d. BPX-5 column (SGE Analytical Science, Ringwood, Australia). A 60 s splitless injection was used for all injections and a temperature ramp of 10 °C/$t_0$ selected for all separations. Flow rates between 1-8 mL/min using helium carrier gas were investigated. The detector was used in scan mode at a range of 200-300 *m/z* and an acquisition rate of 20 Hz was employed.

The signal response for this sample was evaluated by determining the peak area for the OFN injection as a function of the flow rate employed. These data are displayed in Figure 4.7. To establish the optimum operating conditions, a Student's t-test was performed to determine the flow rate at which there is a statistically significant drop in peak area using a P value of 0.05. This is shown in Table 4.4. For optimum sensitivity of the mass spectral detector to be realised, the flow rate into the detector should be below 4 mL/min. However, while the detector response dropped off as flow rate increased, the sensitivity at even the highest flow setting examined was still acceptable, with a signal-to-noise ratio of approximately 2000:1 calculated (based on average baseline noise ± 30 s from the sample peak cf. the OFN peak height).

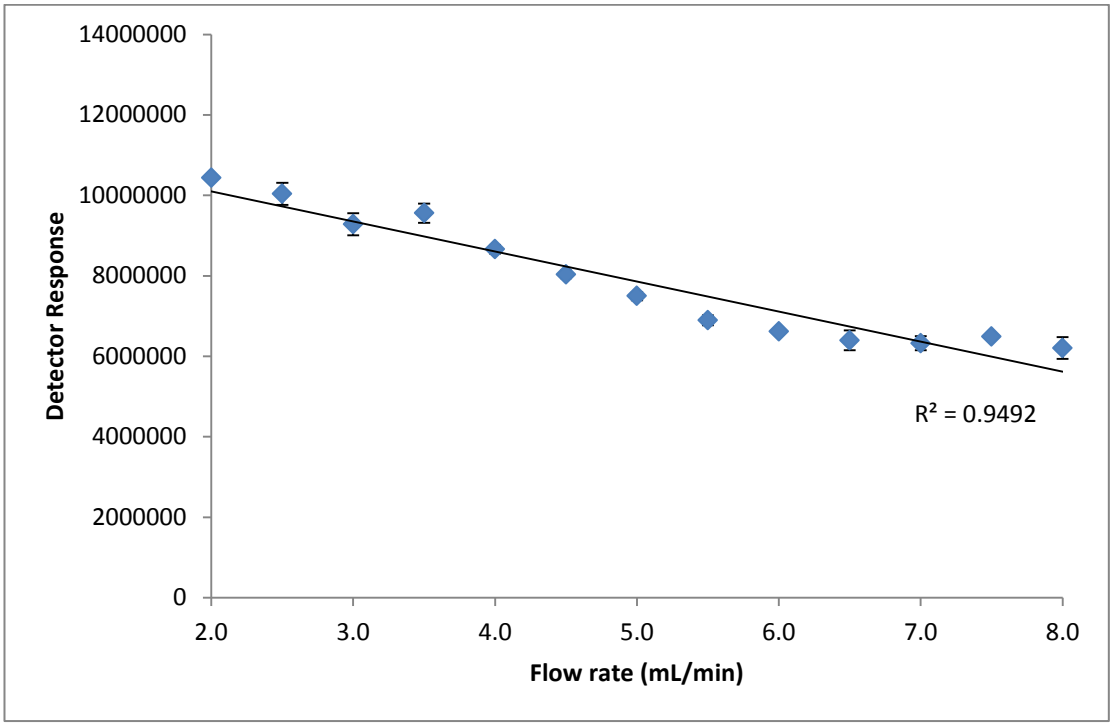


**Figure 4.7. Average peak area of octafluoronaphthalene (0.1 mg/L) as a function of He carrier gas flow rate. Data acquired on a 25 m × 0.22 mm i.d. BPX-5 column at a 10 °C/$t_0$ temperature program.**

| Flow Rate (mL/min) | Average peak area (n=3) | % CV (n=3) | t test result |
|---|---|---|---|
| 1.0 | 10840000 | 5.88 | |
| 1.5 | 10220000 | 0.98 | 0.297 |
| 2.0 | 10440000 | 0.08 | 0.460 |
| 2.5 | 10040000 | 2.73 | 0.207 |
| 3.0 | 9282000 | 2.97 | 0.057 |
| 3.5 | 9557000 | 2.51 | 0.089 |
| 4.0 | 8659000 | 1.26 | 0.037 |
| 4.5 | 8036000 | 1.15 | 0.023 |
| 5.0 | 7498000 | 1.37 | 0.016 |
| 5.5 | 6896000 | 1.82 | 0.011 |
| 6.0 | 6545000 | 0.31 | 0.009 |
| 6.5 | 6373000 | 3.86 | 0.007 |
| 7.0 | 6331000 | 2.78 | 0.004 |
| 7.5 | 6268000 | 0.20 | 0.009 |
| 8.0 | 5587000 | 4.31 | 0.004 |

**Table 4.4. Student's t-test values. Two tailed test of two sample unequal variance, critical value 0.05. Mean values of the three measured peak areas were calculated and compared using this test.**

It is plausible that injector variability played a role in determining the peak intensities in these injections. Three repeat injections were performed at each flow rate and it was thought that this was a sufficient sample size to ensure an accurate response. Based on these data, it was determined that whilst a flow rate of less than 4 mL/min allowed the mass spectrometer to operate at highest sensitivity, a highly satisfactory separation may be obtained at flow rates up to 8 mL/min.

### 4.2.4. Theoretical considerations and GC×GC system development

It has been established that for correct operation of the modulation interface, high carrier gas flow rates (usually 10-20 mL/min) must be employed in pneumatically modulated systems [56, 221]. This is not conducive to the vacuum outlet conditions that exist when a mass spectrometer is used for detection. By using a method that decouples the first and second-dimension flows, this problem can be circumvented. A Deans switch modulator fulfils this requirement. This modulator operates as a flow diversion modulator, meaning it directs the first-dimension flow to one of two secondary capillary columns by application of an auxiliary flow. Typically one of these is the analytical column and the other is a flow restrictor of similar dimensions to the analytical column. In the 'vent' position, the primary column flow is directed to the flow restrictor and to waste. Upon switching to the 'inject' position, the auxiliary flow channels a slice of primary column effluent to the second-dimension column for further analysis and detection. Naturally, this technique has a duty cycle of less than 1, meaning that the primary column effluent is sampled for only a small fraction of the modulation time. Seeley and co-workers investigated the use of a microfluidic Deans switch for GC×GC in 2007 and reported successful results [226]. In contrast to their work, the atmospheric vent was replaced with dual second-dimension columns connected to both FID and MS detectors in the

research presented here. This represents a novel application for the technique and an emerging possibility for low-cost GC×GC–MS modulation.

Arguably the most crucial parameter for pneumatic modulation is the flow ratio observed between the first and second-dimension columns [56, 62]. Unlike thermal modulation, focussing of analytes is not observed during the modulation phase with a flow differential modulation method. To achieve the desired flow ratio, the column dimensions must be selected carefully. In this study, the dimensions of the two second-dimension columns were selected first, and a complementary first-dimension column was chosen subsequently to maintain the flow ratio.

Based on the results presented in Section 3.3, where an approach for determining an optimised column length based on available pressure, the use of a constant pressure mode was desired for the present investigation. This would allow the method translation theory of Klee and Blumberg [33, 35] to be applied such that the elution pattern observed in the separation could be conserved for evaluation of alternative modulation options. Unfortunately, due to the necessity to maintain a constant flow ratio for effective pneumatic modulation using the Deans switch device, this could not be realised. Instead, a pressure program was employed to maintain the desired flow ratio whilst aiming to conclude the temperature program close to the optimum flow of the column. The Shimadzu instrument used for this study does not possess a constant flow mode option; instead a constant linear velocity mode is offered. While a similar result could have been obtained using this setting, the use of a pressure program proved acceptable and simple for the present approach.

In his recent investigation, Harvey and co-workers prepared a dynamic flow model for mapping flow and pressure throughout a pulsed flow GC×GC system [67].

The choice of column dimensions and pressures has often been assigned arbitrarily or determined iteratively; hence the development of this model has provided insight into system design considerations and simplified the development process [67]. Introduction of a restrictor at the terminus of the primary column improved the robustness of the system and allowed more flexibility in the modulation period. Appropriate selection of the restrictor allowed a variety of linear velocities to be used whilst maintaining the functionality of the pneumatic modulator used in the study [67]. This research substantially streamlined the optimisation process for the Deans switch modulator developed in the current study. Previous applications of differential flow modulation [56, 62, 227] prompted the selection of a ratio of 1:25 for this system which proved more than adequate. While a higher flow ratio would have given narrower peaks in the second dimension, this would have pushed the second-dimension flow rate far above optimum. The peak response values shown in Figure 4.7 highlight that this would have an adverse impact on the available sensitivity from the mass spectrometer and may be inappropriate for this application. A secondary effect may involve incompatibility between the relatively slow-scanning mass spectrometer and the fast chromatographic separation, although the acquisition rate of 25 Hz used here may have been adequate to avoid this. As it stands, to generate the desired flow ratio, the flow rate selected for the second-dimension column was slightly above the optimum value for MS influx established in the first section of this chapter.

The determination of the optimum diameter and length for the first-dimension column posed an interesting conundrum. The benefits of a high-efficiency narrow-bore column for the separation of a complex mixture in a one-dimensional environment are self-evident. As a longer column provides greater efficiency and

therefore greater resolution, it would seem prudent to choose the longest column available. However, while a narrow-bore column in the first dimension would be desirable, the constraints imposed by the required flow ratio suggest that the use of a long, narrow-bore column (60 m × 0.10 mm i.d., for example) would not be appropriate. Based on the equations of Fuller *et al.* [216] and Beens et al. [78, 216], which formed the basis of the discussion in Section 3.3 of this thesis, a better choice would be to use a shorter column and try to operate close to the optimum efficiency.

Using a 20 m × 0.10 mm i.d. column as a starting point for selection, a Golay curve was plotted (Figure 4.8). This column was selected as the dimensions are commonly available and would represent an acceptable option for a first-dimension GC×GC column.

The purpose of this investigation was to determine the optimal linear velocity range and investigate the magnitude of the mass transfer and longitudinal diffusion effects on the efficiency of the column when operated outside this range. This reveals the minimum acceptable flow rate for the first-dimension column, and provides a minimum value for the second-dimension flow based on the desired flow ratio. The column was operated at a temperature of 130 °C isothermal and calculations based upon repeat injections of *n*-dodecane. The Golay - van Deemter equation is shown below:

$$H = \frac{B}{u} + C_s u + C_m u$$

H is the height of a theoretical plate, B is the longitudinal diffusion term, u is the flow rate, $C_s u$ is the mass transfer term for the analyte in the stationary phase and $C_m u$ is the mass transfer term for the analyte in the mobile phase. As the flow rate

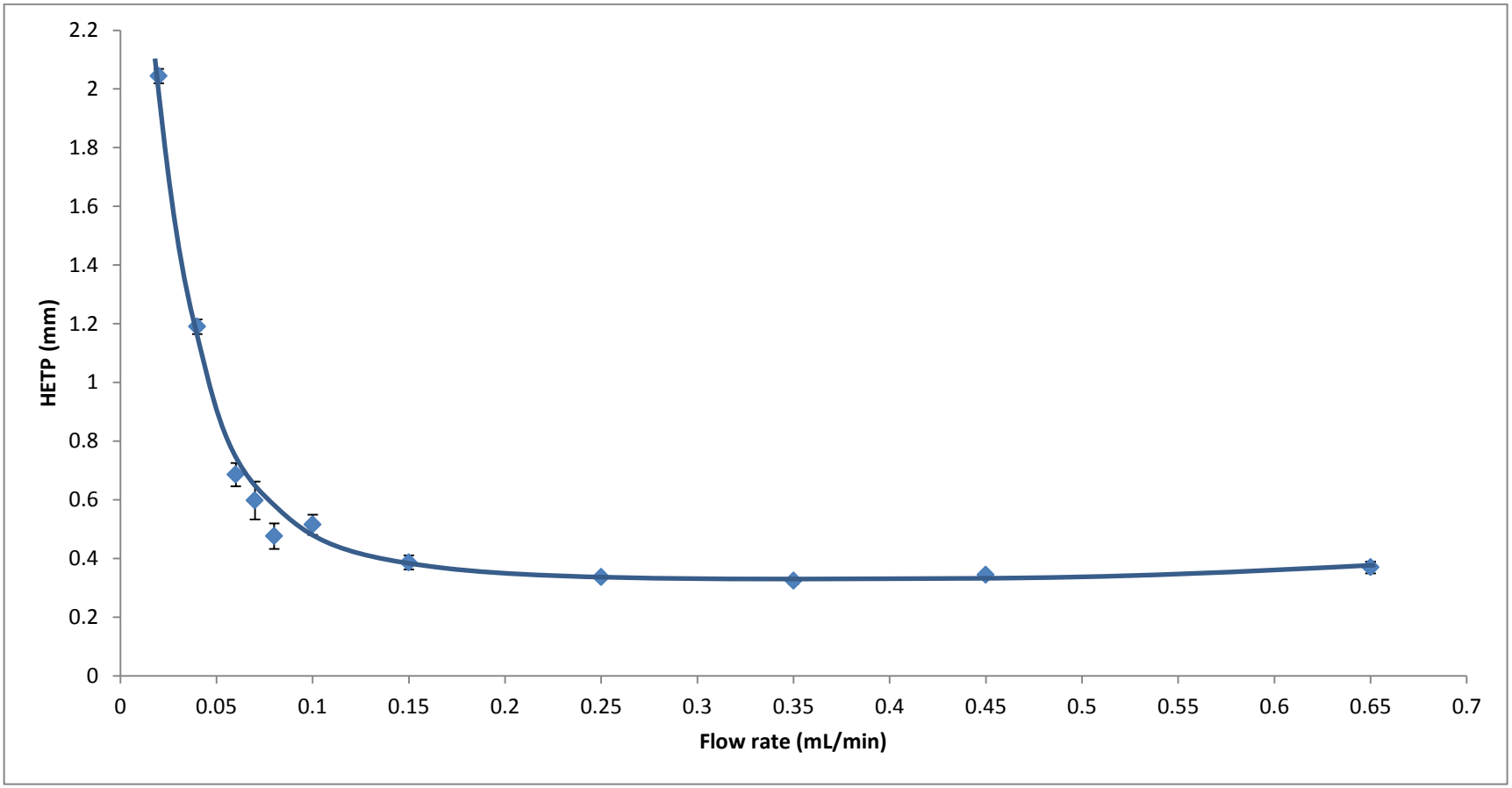


**Figure 4.8. Golay curve collected on 20 m × 0.10 mm i.d. column with *n*-dodecane.**

increases, the dominance of the B term in the equation is diminished as it becomes a smaller and smaller fraction and hence makes less contribution to the theoretical plate height. For this reason, it was sought to operate the primary column at a flow rate sufficiently high to make the contribution of the B term insignificant. 0.2 mL/min was sufficient to fulfil this requirement.

The use of a 0.10 mm i.d. second-dimension column in the Deans switch GC×GC–MS system would require an excessive head pressure to generate the desired flow ratio. This was mooted as a possibility in Section 3.2, where although the high-temperature wax column investigated provided suitable selectivity, it was not investigated further as it was only available in a 0.10 mm internal diameter. It was proposed that a short length of 0.25 mm i.d. column in the second-dimension would provide the best trade-off between speed, resolution and usability. A Supelco ionic liquid stationary phase (SLB IL-111; Supelco, Castle Hill, Australia) was selected for use as it had been provided free-of-charge by the manufacturer for evaluation purposes.

Using a first-dimension flow rate of 0.2 mL/min and the flow ratio of 1:25, second-dimension flow rate is 5 mL/min. Unfortunately, this value is above the EOF. Although it was desired to operate both columns at, or close to EOF, the limitations imposed by the modulator prevented this. As the efficiency offered by the first dimension column is significantly greater than that of the second dimension column, it is more desirable to sacrifice efficiency in the second dimension than the first. For this reason, the flow rates of 0.2 mL/min and 5 mL/min were selected for use in the first and second dimensions respectively.

To obtain a suitably fast separation, a 2 m length of 0.25 mm i.d. capillary was selected for the second-dimension column, as this gives a void time of 0.7 s with vacuum outlet and 1.6 s with ambient outlet. These values were confirmed experimentally to validate the accuracy of the method translation software used [190]. These columns were used throughout this study.

### 4.2.5 Results and Discussion

Using the (20 m × 0.1 mm) × (2 m × 0.25 mm) column set, 6 replicate injections of a diesel sample, plus vetiver and hop essential oils were performed. Figures A1-A12 in *Appendix* show the two-dimensional separation space obtained on this column set for the three samples. Good repeatability was observed between runs.

As the Deans switch modulator used for this study only sampled a portion of the first-dimension effluent, careful tuning of the modulation time was necessary. This was performed iteratively, and it was found that transfer of a 0.2 s wide pulse every 2.5 s was the best setting for a separation using the MS channel. The hardware configuration used for this study allowed the collection of data using either the MS or FID channel without reconfiguration. By adjusting the timing of the auxiliary flow, selection between the channels was easily performed. Although simultaneous collection of data on both channels was not possible, it is possible to change between detectors during the separation. This may be useful for quantitation of components eluting in a particular region of the separation space using the FID channel, whilst collecting data on the MS channel for other regions of the separation space.

Similarly, by installing second-dimension columns with differing selectivity, complementary separations may be performed. As no hardware reconfiguration would be necessary, this would be useful for situations where high sample

throughput is desirable yet only one instrument is available for analysis. This represents an innovative consequence, as these capabilities have not been previously reported for a comprehensive two-dimensional separation system utilising pneumatic modulation and both MS and FID detection.

To investigate the column combinations available, the method used for the 20 m × 0.10 mm i.d. column was translated using a commonly available software program [33] to allow the use of the 40 m × 0.10 mm coupled column and 25 m × 0.22 mm column whilst conserving the flow ratio. The required carrier gas pressure program was theoretically determined using the software and these pressure values are reported in Table 4.3. Confirmation of these flow rates and pressures was performed by checking the void time for each column in a one-dimensional arrangement after the study was performed.

It is no surprise that the use of a 40 m × 0.10 mm coupled column in the first dimension yielded greater peak capacity than the other columns. Such a result is to be expected considering the greater efficiency afforded by the longer column. However, this result came at the expense of the run time, which was almost double that of the 20 m column (61 min vs. 106 min).

### 4.2.6. Concluding remarks

Three alternative columns were investigated for their suitability for use as the first dimension of a Deans switch modulated GC×GC system. For a GC×GC system using this modulation interface to perform adequately, the combination of a high-efficiency, narrow-bore column in the first dimension and a 0.25 mm i.d. column in the second dimension is suggested. The use of a pressure program in both dimensions was satisfactory.

The Deans switch modulator reduced carrier gas flux to the MS, providing a delicate balance between sensitivity loss through either operating the MS above its optimum flow rate, or splitting excessive primary column effluent. The increase in resolution obtained through using a long first dimension column (40 m × 0.10 mm i.d.) did not outweigh the negative aspect of increased analysis time for this application. Based on the results presented in Section 3.3, a 13 m × 0.10 mm column would be appropriate for use in the first dimension considering the available carrier gas head pressure.

## 4.3 Analysis of essential oil samples with valve modulated GC×GC–MS/FID

### 4.3.1 Introduction

While the use of a partial sampling Deans switch modulator for the system development yielded good resolution and satisfactory qualitative analysis of essential oil samples, it is clear that this approach compromises the available sensitivity afforded by the instrumentation by employing a low modulator duty cycle. The use of a valve based approach covers an area which was not previously explored in the current study and would therefore allow a subjective comparison for the partial sampling Deans switch device.

Mohler and co-workers examined the use of a valve-based two-dimensional system which allowed total transfer of first-dimension effluent to the second-dimension separation [228]. While other methods had been examined previously [55, 58, 229], this was the first report of a valve-based modulator that did not split the majority of the primary column effluent to waste. Veriotti and Sacks had previously investigated a similar method for high-speed GC and MDGC separations in 2001 [230]. To achieve total transfer, a six-port modulation valve was employed and the appropriate port was plugged. During the fill period, the primary column effluent is compressed within the sample loop. Actuating the valve stops the flow in the primary column for a short period while the sample loop contents are compressed and flushed by an auxiliary carrier gas pressure. For the method to be successful, the head pressure of the first column must be greater than the auxiliary pressure feeding the second-dimension column. This stop flow concept was previously explored by Sacks' group [230, 231], who generated a successful separation using a coupled column approach. Excessive band broadening was a concern, which may arise from

increased diffusion on the column, but a 10 s stop time did not cause a major increase in peak dimensions.

A commonly perceived drawback of the use of valve based modulators is the necessity to mount the valve outside the oven to prevent thermal damage to the diaphragm. In the current study, a Valco diaphragm valve was used with the portion in the sample path mounted inside the oven, allowing the temperature ramp to reach 220 °C. Considering the maximum recommended temperature for the SLB-IL 111 columns used in the second-dimension were 240 °C this was an acceptable solution. Use at higher temperatures may be possible but this was not investigated to ensure valve functionality throughout the experimental regime.

In the current study, the methods described by Mohler *et al.* [228] for a total transfer diaphragm valve based modulator were followed and supplemented by the addition of a tee piece after the modulator to allow the simultaneous collection of data using MS and FID. A solenoid valve was employed to replace the port stopper, allowing the first-dimension column to flow to waste for a 30 s period following sample injection. The restrictor which was installed previously within the MS transfer line was removed. Furthermore, an alternative second-dimension stationary phase coating, 35% diphenyl polysilphenylene-siloxane (BPX-35) was examined in addition to the ionic liquid stationary phases previously implemented. It was thought that the selectivity of this coating may better complement the samples chosen for analysis. The FID column was 2 m × 0.22 mm (0.25 mm $d_f$) and the MS column 2.6 m × 0.22 mm (0.25 mm $d_f$).

A 13 m × 0.1 mm column was used in the first dimension based on the conditions established in the studies presented in Section 3.3. A schematic of the system setup is shown in Figure 4.9.

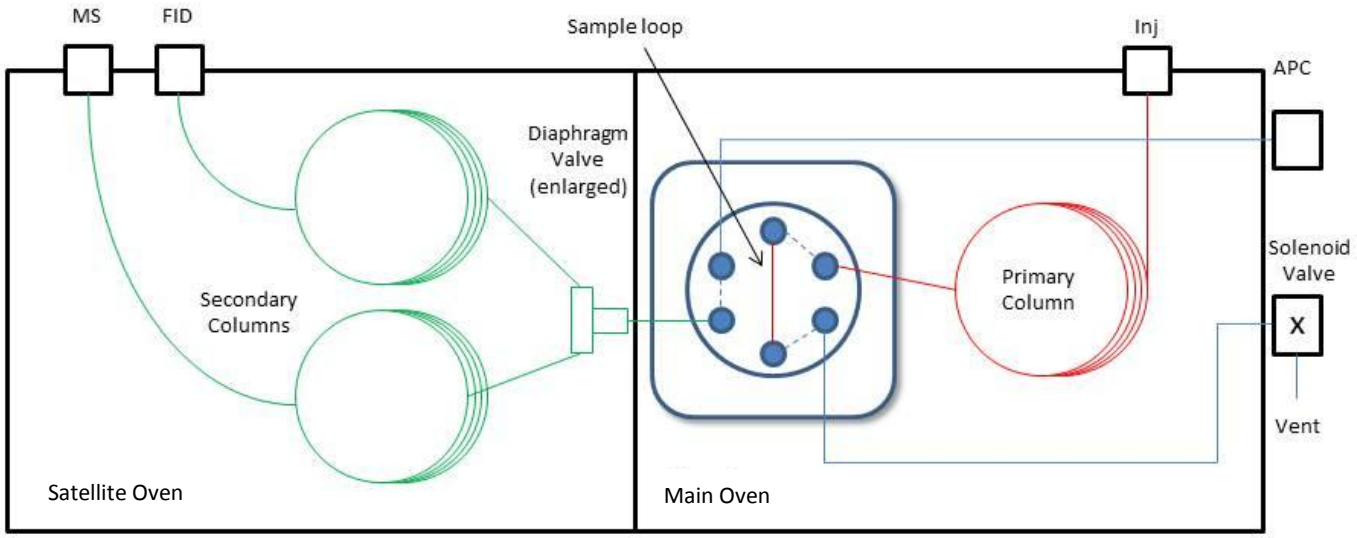


**Figure 4.9. Schematic of the valve modulated GC×GC system in the 'fill' position. Solenoid valve is closed, stopping first-dimension flow.**

### 4.3.2 Experimental

A 13 m × 0.25 mm i.d. Rxi-5 primary column was used in conjunction with a 2m × 0.25 mm i.d. SLB IL-111 secondary column running to the FID and a 2.6 m × 0.25 mm i.d. SLB IL-111 supplying the MS. Helium carrier gas was used at a constant head pressure of 400 kPa (58 psi) and a split ratio of 100:1. Auxiliary helium pressure was a constant 88 kPa (12.8 psi) and was delivered via the APC.

The instrument was temperature programmed from 50-220 °C at 4.5 °C/min for the first-dimension column and 60-230 °C at 4.5 °C/min for the second-dimension column.

A commercial vetiver essential oil (*Vetiveria zizanioides*) sample was obtained from Australian Botanical Products (Hallam, Australia), from which a 20% v/v solution was prepared by diluting the neat essential oil with dichloromethane (Sigma-Aldrich, Castle Hill, Australia).

### 4.3.3 Results and discussion

Samples of hop and vetiver essential oils and kerosene were examined using the diaphragm valve modulated system. Figures 4.10 to 4.12 show chromatograms of these separations. Relevant peak data for hop essential oil separations is displayed in Tables A1 to A3 in *Appendix*.

It is noteworthy that these chromatograms required baseline subtraction to remove a large unmodulated peak occurring approximately 30 min into the separation. Comparison of the spectrum of this peak at the apex with the Shimadzu and NIST spectral libraries did not yield a tentative identity for the peak, but it was suspected that the compound was a breakdown product released from the polyimide

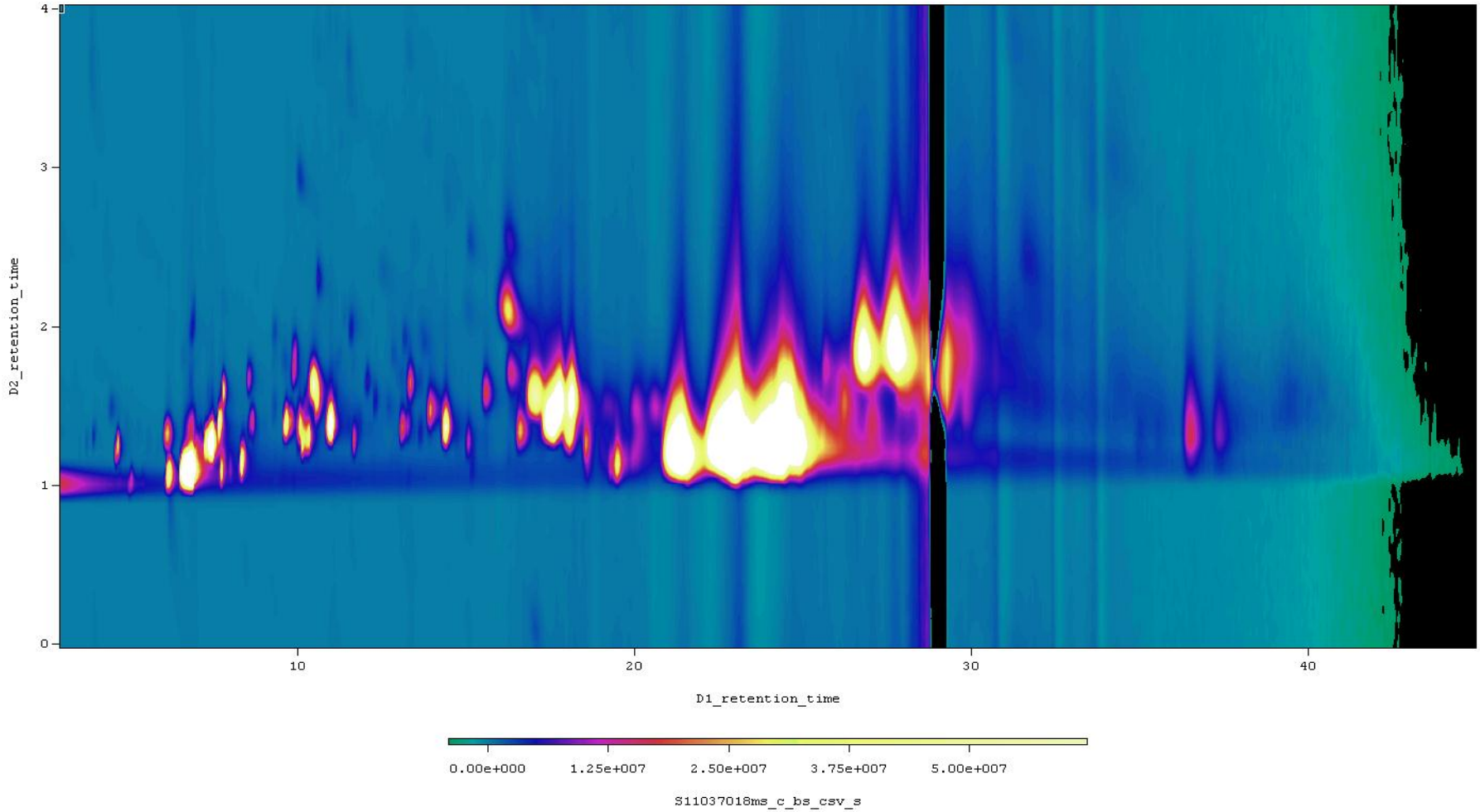


**Figure 4.10. GC×GC–MS chromatogram of hop essential oil obtained using the diaphragm valve modulator. Column set (13 m × 0.22 mm) × (2.6 m × 0.22 mm). He carrier gas at 400 kPa (58 psi) with auxiliary pressure of 88 kPa (12.8 psi). Temperature program 50-220 °C at 4.5 °C/min for the first-dimension column and 60-230 °C at 3.5 °C/min for the second-dimension column.**

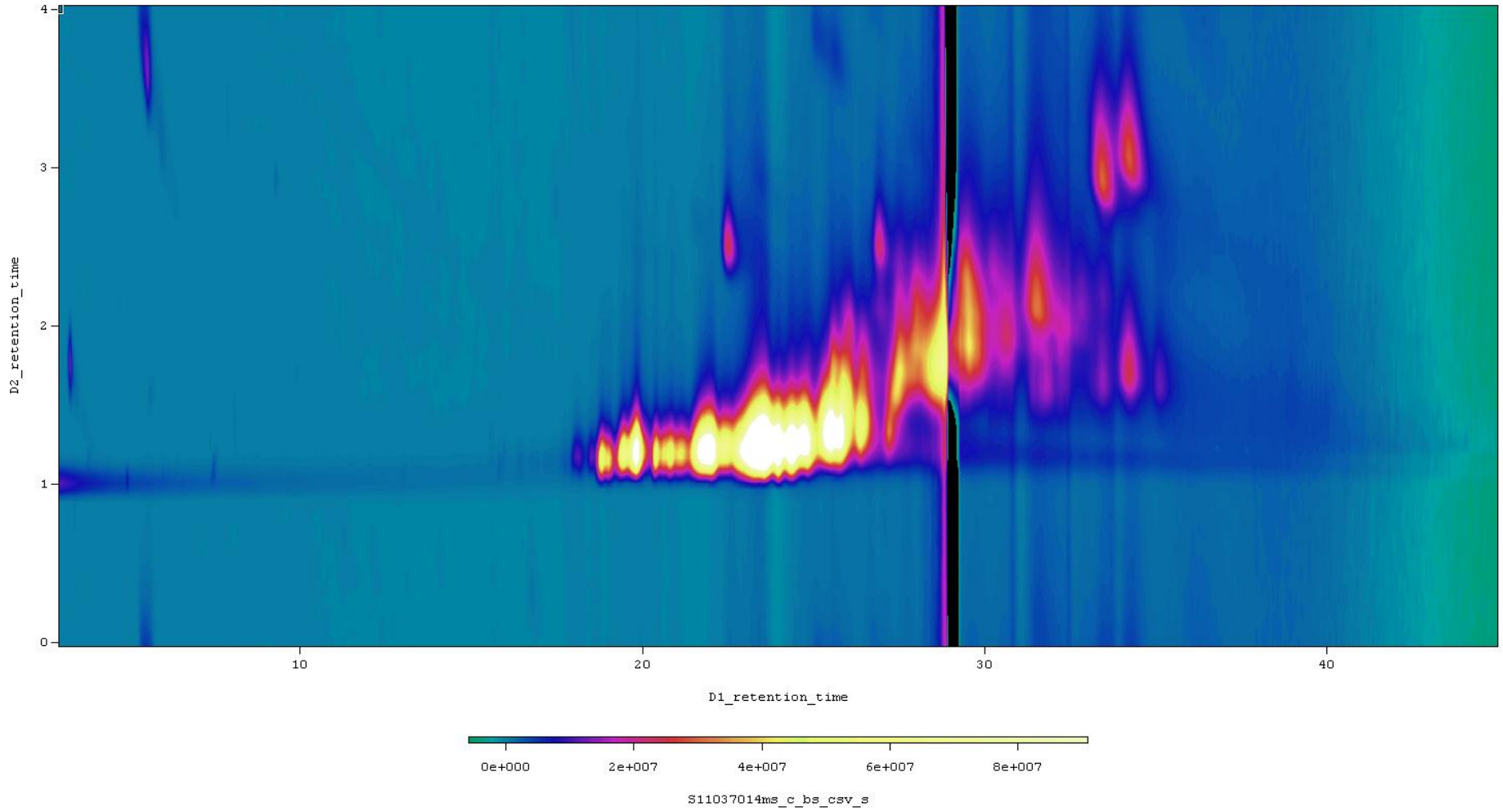


**Figure 4.11. GC×GC–MS chromatogram of vetiver essential oil obtained using the diaphragm valve modulator. Column set (13 m × 0.22 mm) × (2.6 m × 0.22 mm). He carrier gas at 400 kPa (58 psi) with auxiliary pressure of 88 kPa (12.8 psi). Temperature program 50-220 °C at 4.5 °C/min for the first-dimension column and 60-230 °C at 3.5 °C/min for the second-dimension column.**

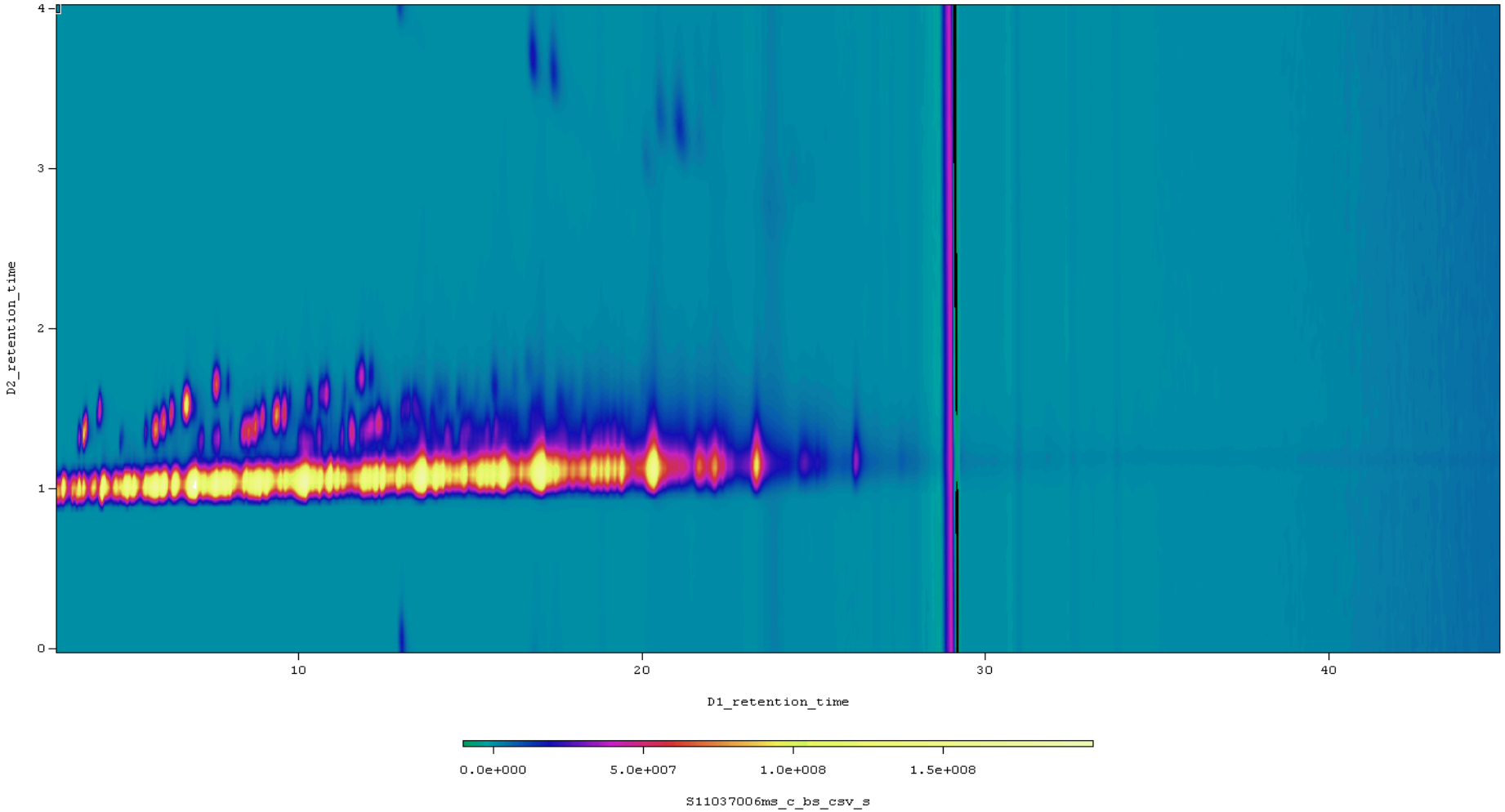


**Figure 4.12. GC×GC–MS chromatogram of kerosene obtained using the diaphragm valve modulator. Column set (13 m × 0.22 mm) × (2.6 m × 0.22 mm). He carrier gas at 400 kPa (58 psi) with auxiliary pressure of 88 kPa (12.8 psi). Temperature program 50-220 °C at 4.5 °C/min for the first-dimension column and 60-230 °C at 3.5 °C/min for the second-dimension column.**

membrane used in the valve diaphragm. This was suspected as the peak was unmodulated, indicating that the contaminant was introduced to the system after the modulator. Additionally, the location of the peak in the two-dimensional chromatogram suggested that it did not match a bleed profile from the second dimension ionic liquid column. While the appearance of this peak was initially concerning as it was suspected the valve was failing from operation at higher than recommended temperatures, the results were repeatable over a period of several weeks. The peak was effectively removed by subtracting the average value of five sample blank separations from each extracted chromatogram prior to conversion to a two-dimensional plot.

The next interesting observation is that band broadening has occurred which has most likely resulted from the stop flow mechanism used in this system, considering the effect becomes more pronounced towards the end of the run. This effect is particularly pronounced in Figure 4.13, which shows a separation of a $C_9$-$C_{20}$ *n*-alkane mixture, in which each component is at a concentration of 5% v/v. The switching of the diaphragm valve to the 'inject' position directs the auxiliary carrier gas flow to the sample loop, which flushes its contents onto the two second-dimension columns via a short transfer line (30 cm × 0.25 mm deactivated capillary) and a three port (tee) flow wafer (SGE Analytical Science, Ringwood, Australia). This actuation causes the flow from the first-dimension column to be directed to the blocked port on the diaphragm valve, preventing efflux from the column and providing an environment conducive to longitudinal diffusion of analytes within the column. This is the trade-off required to achieve total transfer of the primary column sample. At low temperatures, acceptable resolution is obtained, but as the temperature program proceeds, peak broadening severely affects available resolution.

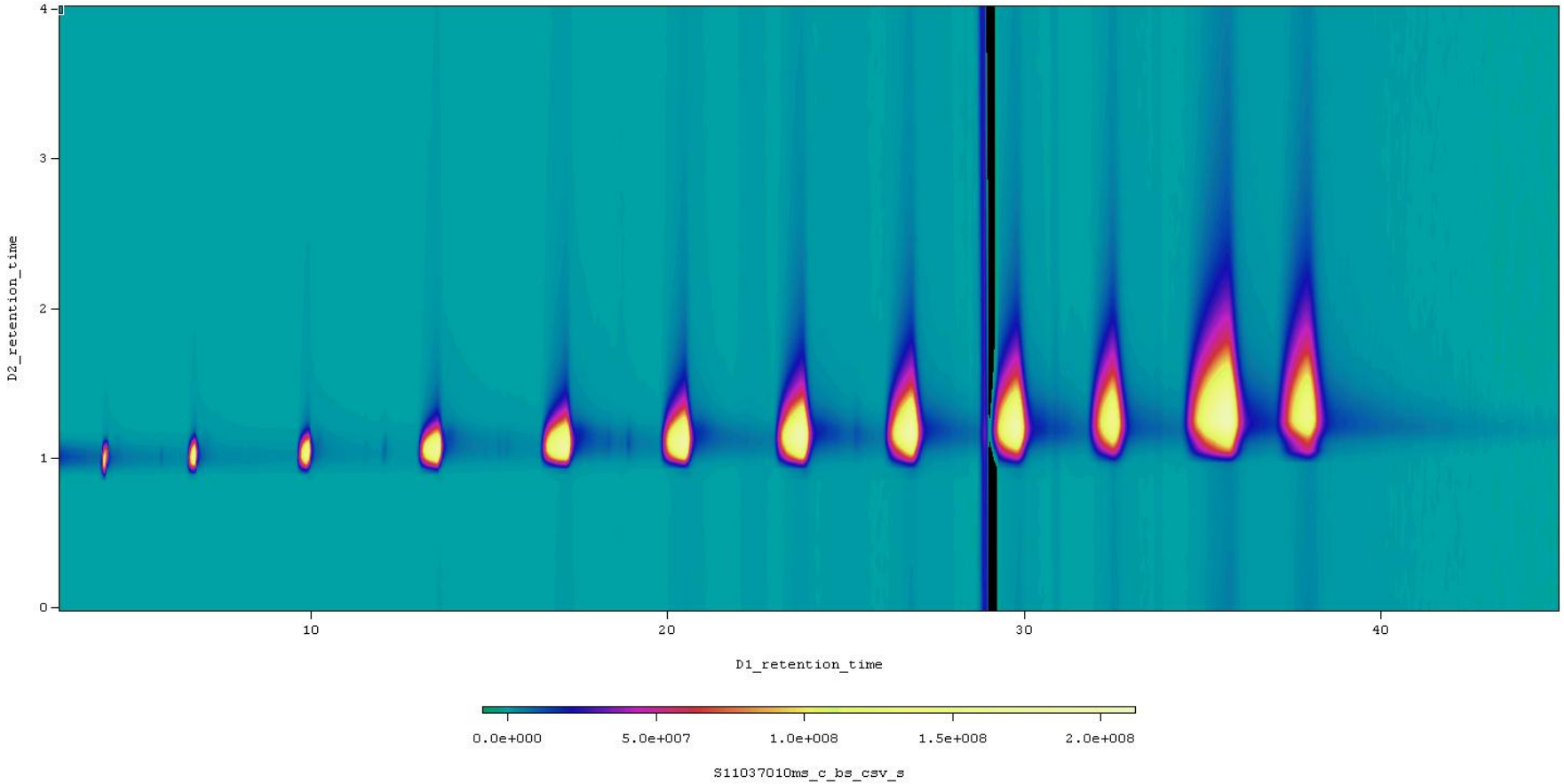


**Figure 4.13. GC×GC–MS chromatogram of $C_9$-$C_{20}$ *n*-alkanes obtained using the diaphragm valve modulator. Column set (13 m × 0.22 mm) × (2.6 m × 0.22 mm). He carrier gas at 400 kPa (58 psi) with auxiliary pressure of 88 kPa (12.8 psi). Temperature program 50-220 °C at 4.5 °C/min for the first-dimension column and 60-230 °C at 3.5 °C/min for the second-dimension column.**

This can also be witnessed when comparing the chromatograms of kerosene and diesel shown in Figure 4.14. The lighter kerosene sample is separated in approximately 26 min, equating to the retention of hexadecane. Resolution of the entire sample is acceptable and suitable for qualitative analysis. However, diesel contains components extending beyond eicosane. At this point, band broadening is excessive and qualitative analysis of the heavy components is not possible. A similar comparison can be made between hop and vetiver essential oils; the former containing a greater proportion of low boiling point components in contrast to the latter.

It is interesting to compare the differences between the separations obtained using the Deans switch modulator with the current system. Preliminary investigations using the diaphragm valve modulator utilised the ionic liquid SLB IL-111 stationary phase in the second-dimension columns. Separations collected on this column set displayed the effect of band broadening more prominently than the BPX-35 stationary phase, suggesting it may not be a suitable coating for this application. A comparison of peak widths and sensitivity between the Deans switch modulator system and the diaphragm valve modulator system are shown in unconverted form in Figure 4.15. This shows the modulated separation of hexadecane on the MS channel of each system. It is evident that the sample is overloaded in both circumstances, although the difference in peak intensity is clearly apparent. The band broadening effect is also clearly observed in the lower figure. A further point of interest in this separation is the use of unequal length second-dimension columns without the use of a restrictor. This option was pursued to allow the alignment of the second-dimension retention times for both detection channels. Should this be achieved, it would conceivably allow the simultaneous qualitative analysis of the sample on MS and

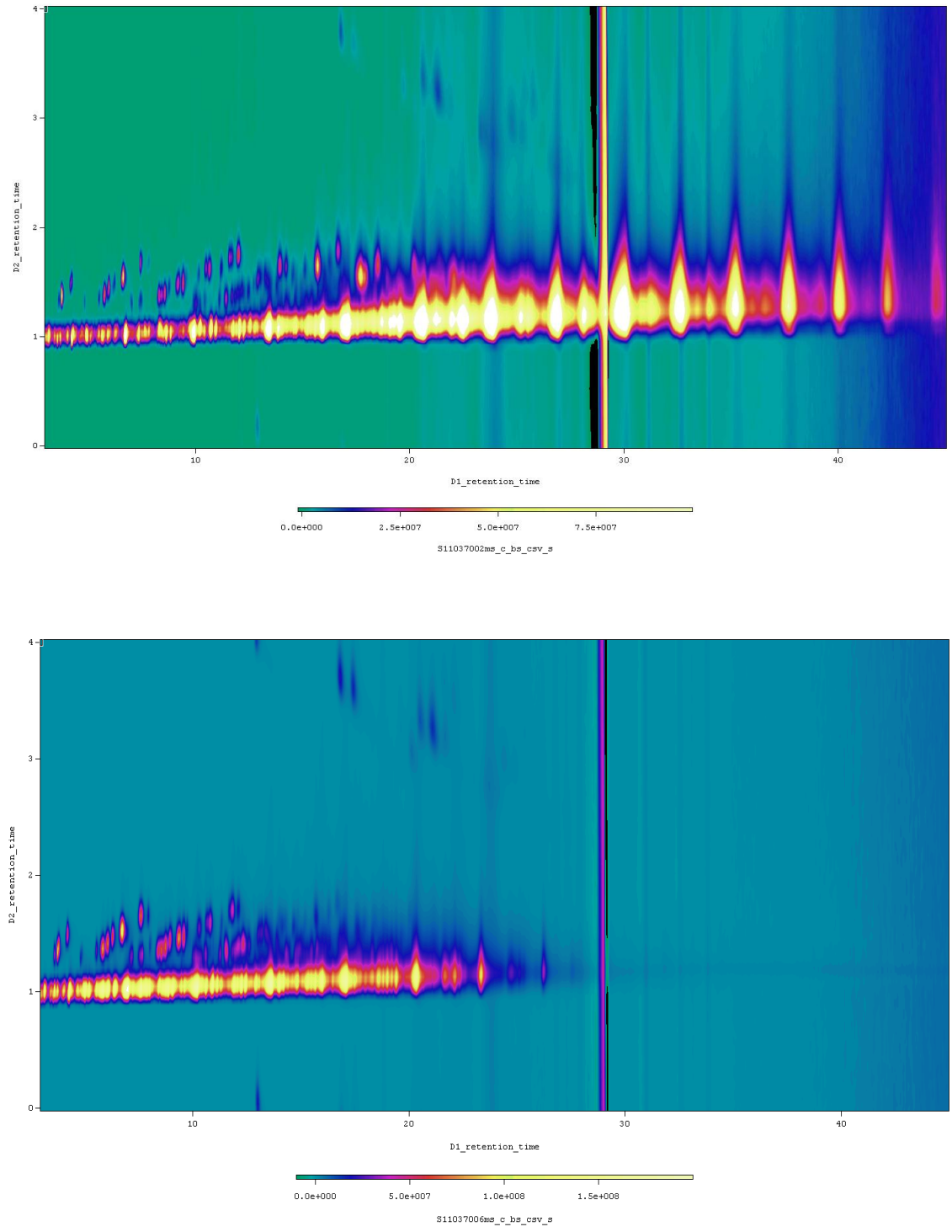


**Figure 4.14. Comparison of diesel (top) and kerosene (below) GC×GC–MS chromatograms. Column set (13 m × 0.22 mm) × (2.6 m × 0.22 mm). He carrier gas at 400 kPa (58 psi) with auxiliary pressure of 88 kPa (12.8 psi). Temperature program 50-220 °C at 4.5 °C/min for the first-dimension column and 60-230 °C at 3.5 °C/min for the second-dimension column.**

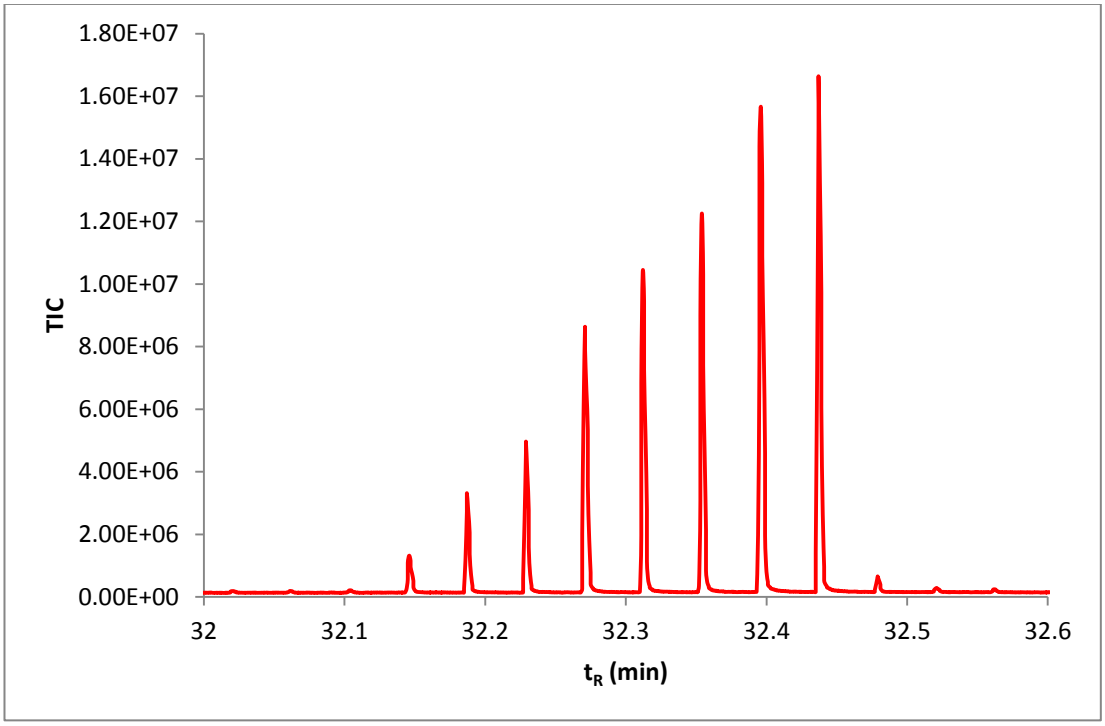


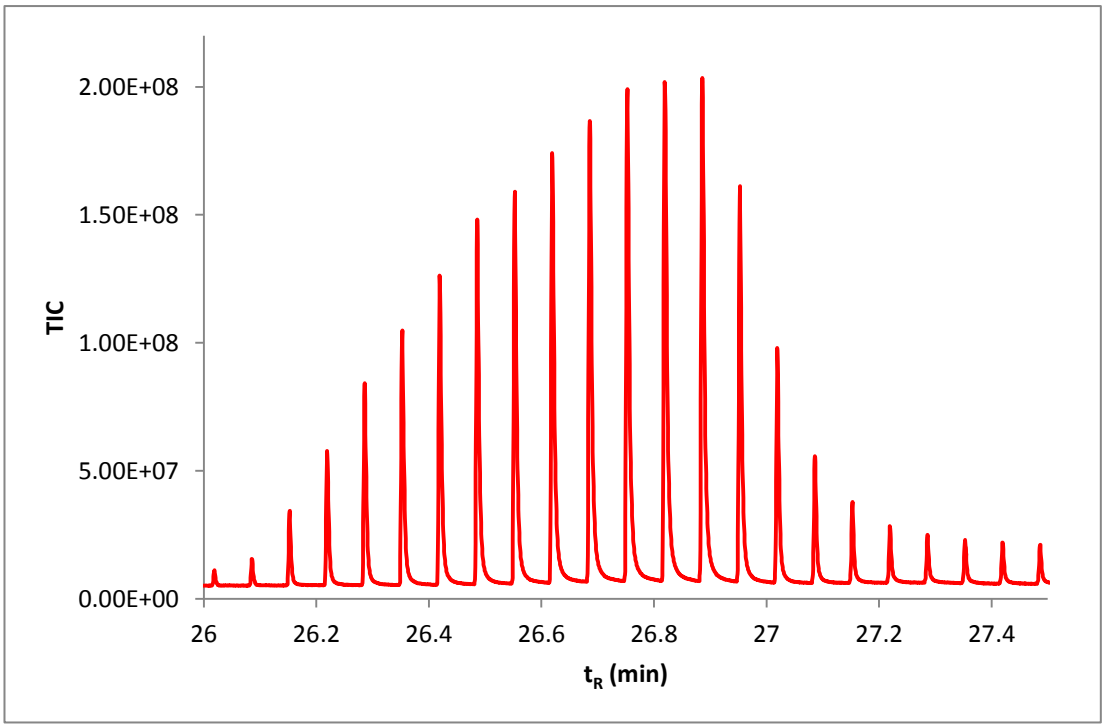


**Figure 4.15. Unconverted chromatograms of hexadecane acquired using Deans switch (top) and diaphragm valve (below) modulators. Experimental conditions listed in text.**

quantitative analysis with FID, utilising the strengths of both detection mechanisms in a single separation. For this reason, the ability to reliably identify peaks in the FID chromatogram from the respective spectrum of their MS counterparts is highly desirable. Figure 4.16 shows extracts of two hop oil chromatograms collected from the same injection. While a slightly greater resolution is afforded by the MS channel which most likely results from the longer column dimension, it is evident that peak identities are conserved from the two separations.

From reviewing the figures presented in this section, it would appear unlikely that the sensitivity benefits of utilising the total transfer diaphragm valve based modulator investigated in this chapter outweigh the loss of resolution arising from the stop flow methodology. It may be argued however, that the use of a more conventional polar column in the second dimension may provide an alternative selectivity that is more suited to the analysis of the fuel and essential oil samples examined here. To address this argument, two BPX-35 columns of similar dimensions were installed in place of the SLB IL-111 secondary columns and the separation of a kerosene sample performed. A chromatogram of this separation acquired on the FID channel is shown in Figure 4.17. It is evident that there was a discrepancy between the selected column flow rate and temperature program from the pronounced ‘hump’ visible in the converted chromatogram. Unfortunately, although the results look promising, it was not possible to resolve this conflict and repeat the separation due to instrumental problems which could not be resolved in a reasonable time. Even so, the resolution appears to have improved over the chromatogram shown in Figure 4.12 which was acquired using the SLB IL-111 column. Furthermore, the longitudinal band broadening effect is far less pronounced, with second-dimension peak widths consistently remaining in the order of 0.3 sec.

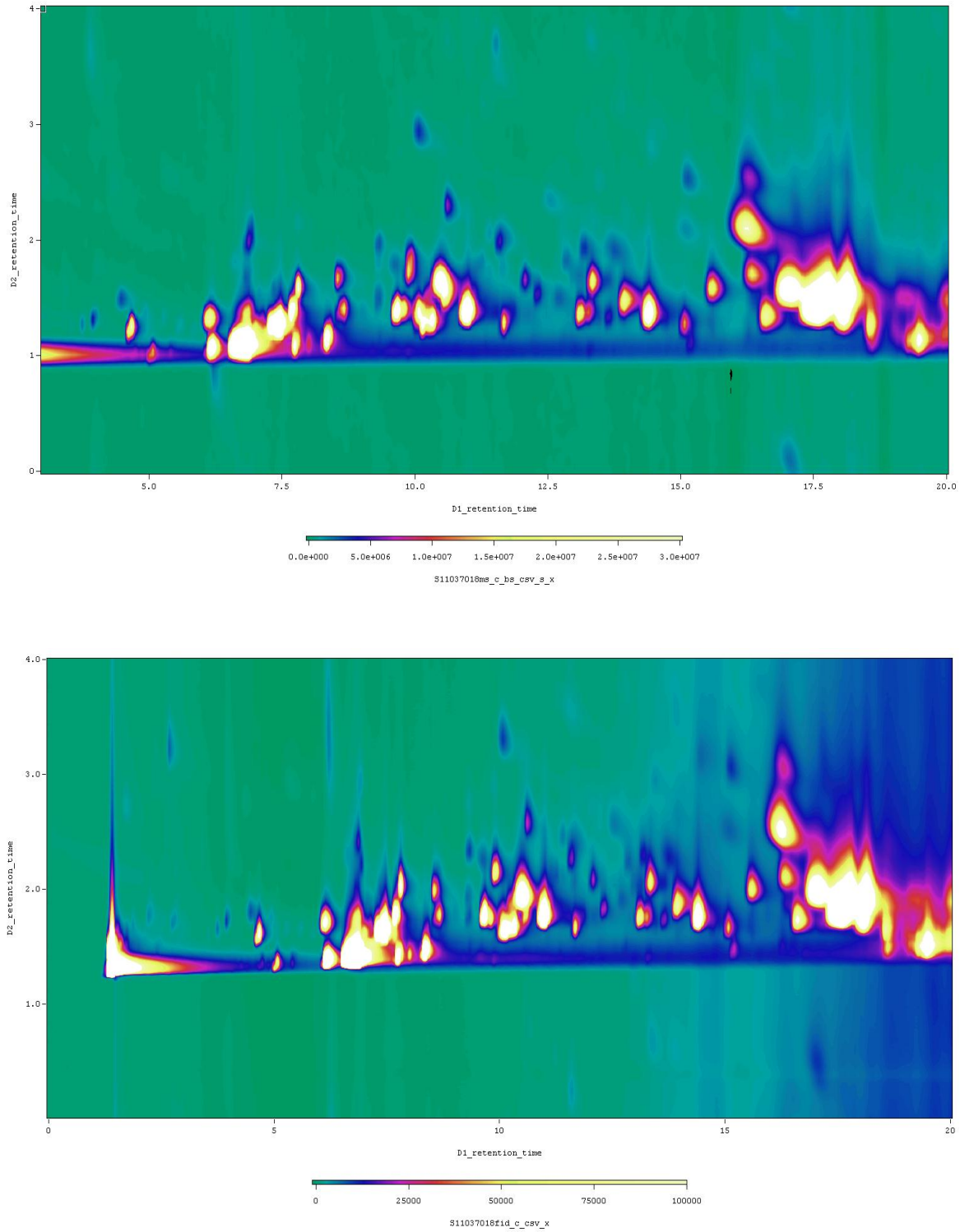


**Figure 4.16. Extract of GC×GC–MS (top) and GC×GC–FID (below) chromatograms showing a concurrent separation of hop essential oil. Column set (13 m × 0.22 mm) × (2.6 m × 0.22 mm) for MS and (13 m × 0.22 mm) × (2 m × 0.22 mm) for FID. He carrier gas at 400 kPa (58 psi) with auxiliary pressure of 88 kPa (12.8 psi). Temperature program 50-220 °C at 4.5 °C/min for the first-dimension column and 60-230 °C at 3.5 °C/min for the second-dimension column.**

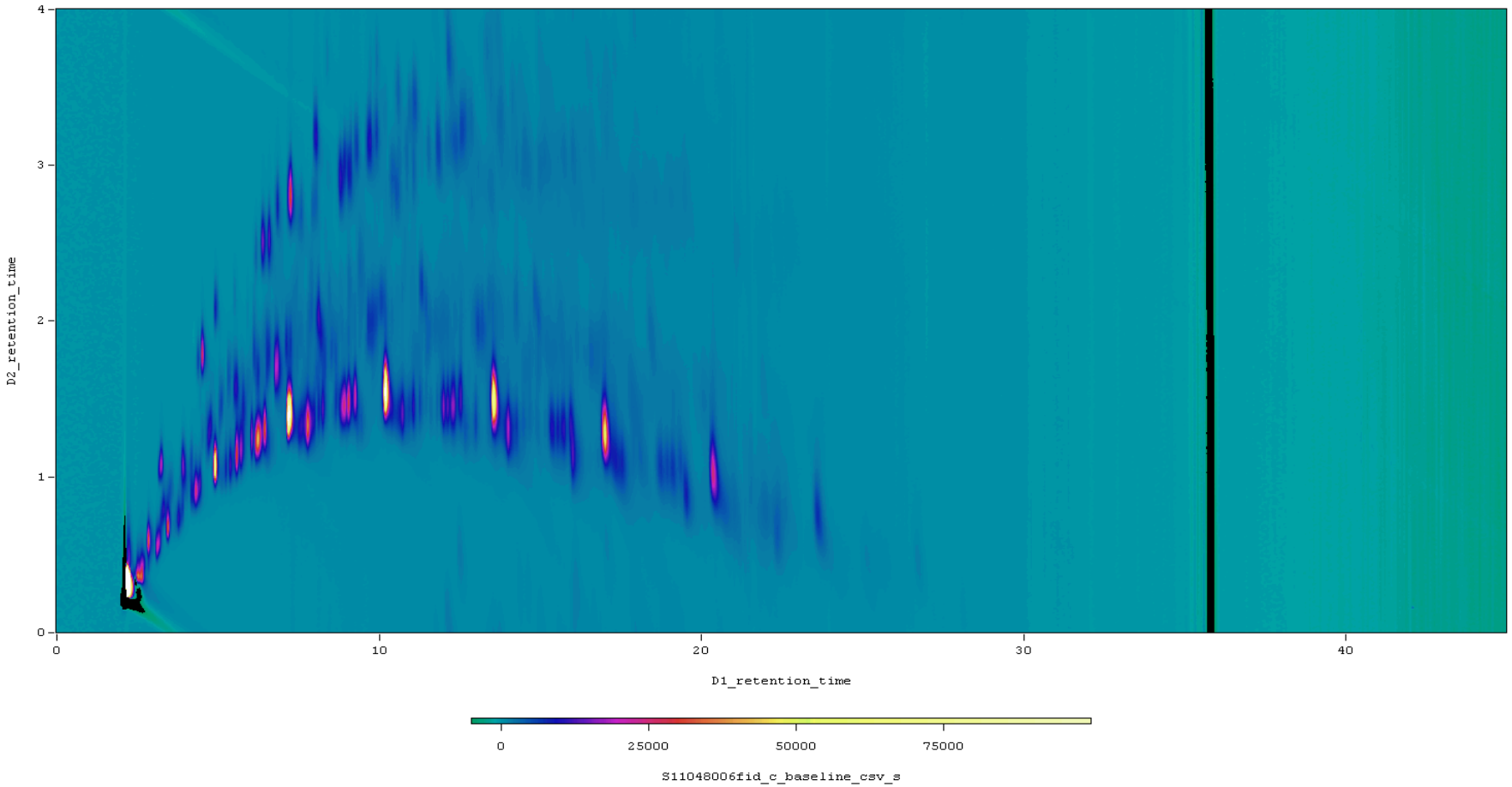


**Figure 4.17. GC×GC–FID chromatogram of a kerosene separation obtained using BPX-35 second-dimension column. Column set (13 m × 0.22 mm) × (2 m × 0.22 mm) for FID. He carrier gas at 400 kPa (58 psi) with auxiliary pressure of 88 kPa (12.8 psi). Temperature program 50-220 °C at 4.5 °C/min for the first-dimension column and 60-230 °C at 3.5 °C/min for the second-dimension column.**

### 4.3.4 Concluding remarks

Valve-based modulation for comprehensive two-dimensional gas chromatography has become an option worthy of consideration for GC×GC applications. The technique has been explored intensively over the last several years, throughout which a common thread has been revealed in the desire to move away from low duty cycle modulators. At the current time, it seems the most effective way to generate a high duty cycle with a valve-based modulator is to utilise a stop-flow technique, whereby the passage of analytes through the primary column is temporarily halted during the flush cycle of the modulator. Research has shown this introduces the benefit of decoupling the flow between the two dimensions, allowing each to be operated at optimum linear velocity in addition to increasing the available sensitivity [228]. However in the current study, which included the innovative application of simultaneous acquisition on both FID and MS channels, the band broadening introduced as a result of stopping the primary column flow yielded poor resolution in the final chromatogram. The use of an ionic liquid second-dimension column, which strongly retained the samples selected for analysis, may not have been the most appropriate choice, as the excessive retention also increased band broadening in this dimension. Preliminary investigations using a less polar BPX-35 column in the second dimension showed promising results. The band broadening issue has been resolved and further research is being conducted in this area by the author's co-workers.

## 4.4. Summary

To commence investigations into pneumatic modulation for a GC×GC–MS approach, a commercial modulator was used for enantioselective separation of a spearmint essential oil sample. The results obtained were compared to a similar

separation obtained using a thermally-modulated GC×GC system. A 20 m × 0.10 mm i.d. first-dimension column was employed, which was coated with an enantioselective stationary phase. This column was operated at 4 mL/min in constant flow mode. To facilitate pneumatic modulation, the flow rate in the second-dimension column (5 m × 0.25 mm i.d. polyethylene glycol) was set to a constant 20 mL/min and a 3 s modulation period was adopted. These values generated effective conditions for stop-flow modulation to occur, without breakthrough. While the available peak capacity was not on par with the thermally-modulated comparison study, highly satisfactory resolution of the terpenoid compounds present in the spearmint oil sample was achieved, with minimal wrap-around. By analysing authentic reference standards of a range of optical isomers present in the sample, quantitative analysis was possible. Outstanding retention time repeatability and quantitation was witnessed, suggesting that this pneumatic modulation approach was a true alternative to cryogenic modulation for quantitative separation of essential oil constituents.

Following this investigation, a GC×GC–MS system was constructed, which incorporated a microfluidic Deans switch acting as a partial sampling modulator. Prior to construction of the system, two preliminary studies were performed. Firstly, a series of injections of OFN were performed in a GC–MS configuration to determine the relationship between carrier gas flow rate and detector sensitivity. The manufacturer of the instrument claims that the MS can operate at flow rates up to 15 mL/min. A steady decline in sensitivity was observed over the range of flow rates examined. It was determined that the decline in sensitivity observed at flows between 1-4 mL/min was not statistically significant. Above 4 mL/min, a significant difference was observed, although acceptable sensitivity was still witnessed at 8

mL/min. This result suggested that from a sensitivity viewpoint, it would be desirable to keep the second-dimension at or below 4 mL/min, but deviation from this flow would not be substantially detrimental. The second preliminary investigation involved the preparation of a Golay – van Deemter plot for one of the first-dimension columns used in the two-dimensional system. It was determined that the EOF was realised at approximately 0.2 mL/min. Using this flow rate in the first dimension, with a 5 mL/min flow rate in the second dimension yields a 1:25 ratio which is suitable for effective pneumatic modulation. It was unfortunate that the second-dimension flow rate was above the EOF for the 2 m × 0.25 mm i.d. columns used, but reduction of the first dimension flow rate would likely have resulted in a greater loss of efficiency than operating above EOF in the second dimension.

Two second-dimension columns were employed, allowing detection on both MS and FID channels. As the first dimension effluent is only partially sampled by each second-dimension column, manipulation of the auxiliary pressure allows the data to be collected on either channel without changing the hardware configuration. Analysis of essential oil and diesel samples suggested that despite the low duty cycle, sensitivity was acceptable. While this technique may not be the best choice for sample characterisation, it should be sufficient for quantitative or qualitative analysis of selected components.

Following this investigation, construction and application of a total-transfer diaphragm valve modulator for the separation of hop essential oil was examined and compared to the results obtained using the Deans switch modulator. In contrast to the Deans switch method, the diaphragm valve modulator could be employed in a true GC×2GC configuration, with two second-dimension columns separated using both FID and MS detection simultaneously. Quantitative transfer of the first-dimension

effluent was achieved. Despite the presence of band broadening issues arising from the stop-flow nature of the modulator, satisfactory separations were obtained. This represented the first description of a GC×2GC–qMS approach using a valve-based pneumatic modulator.

# Chapter 5: Conclusions and Further Research

## 5.1 Summary

This thesis discusses development of pneumatic modulators for use in a GC×GC system with quadrupole mass spectrometric detection. Prior to the implementation of a comprehensive two-dimensional approach, in-depth investigations of three GC–MS techniques were performed. The purpose of this was to determine which aspects of these techniques were suited to inclusion in the subsequent two-dimensional GC research.

The first of these studies involved the operation of a wide-bore column operated under sub-ambient outlet pressure. The reason for selecting this column was the desire to move away from a narrow bore second-dimension column, as this necessitates a high average linear velocity for optimal use of the available efficiency. Concomitantly, the high pressure drop offered by such a column results in a high midpoint pressure, which reduces the optimum average linear carrier gas velocity in the first-dimension column [78] and increases the total analysis time. Using a similar method to the seminal research of de Zeeuw and co-workers [138], a series of essential oils of low to moderate complexity were examined using one-dimensional GC. The results of these separations were compared to those obtained using a 0.10 mm i.d. column. It was revealed that the wide bore column offered greater sample capacity than the narrow bore example, which proved useful for the identification of the more abundant components of the samples. The signal intensity was greater and better matches between the sample and library spectra could be made, due in part to the low peak asymmetry available whilst introducing a larger amount of sample to the column. It was duly noted that the lower efficiency afforded by a wide bore

column impacted negatively on the available resolution and peak capacity in the separation. Multiple critical analyte pairs were not resolved adequately, which may not be a problem with a sample of low complexity but it is anticipated that such samples will not require the use of a GC×GC separation in any case. While this technique was found to be a suitable option for the analysis of samples similar to those used for this study, it would not be an appropriate choice for the second dimension of a GC×GC–MS system of the type to be examined in the current body of research.

The second GC–MS investigation involved the evaluation of a 5 m × 0.10 mm i.d. wax column with high temperature stability. Wax stationary phase coatings are almost universally selected for the second dimension in a GC×GC–MS column set for their highly suitable selectivity for essential oil analysis [166]. However, their low temperature stability is often seen as a disadvantage. The MEGA-WAX HT column selected is stable up to 300 °C (as claimed by the manufacturer), and a low stationary phase bleed was witnessed as expected. Both one-dimensional and comprehensive two-dimensional separations were performed using this stationary phase, the latter incorporating cryogenic modulation. An excellent use of the available peak capacity in the two-dimensional separation was witnessed and it was concluded that this column presented an excellent choice for applications where a 0.10 mm i.d. second-dimension column are suitable. While this may be the case for typical cryogenic modulated GC×GC–MS systems, the use of a 0.10 mm i.d. column in the second dimension of a pneumatically modulated system reliant on a high pressure differential between the first and second dimensions creates a problem. Should a flow rate close to optimum be selected in the second dimension, the necessary midpoint pressure would almost certainly push the required head pressure

for the first-dimension column outside the limits of many gas delivery systems. As this stationary phase coating is unavailable in other dimensions at the present time, it was concluded that it remained an inappropriate choice for the second dimension of a GC×GC–MS system with pneumatic modulation. Based on this observation, a compromise was necessary; utilising a wax column with the highest available temperature stability in a 0.22 or 0.25 mm i.d. fulfilled this. This decision was affirmed by the collection of highly satisfactory separations of essential oil samples using a Deans switch modulated GC×GC–MS system using 2 m × 0.25 mm i.d. SLB IL-111 columns.

The role of high efficiency, high resolution columns as a primary column in a pneumatically modulated GC×GC–MS column set was also investigated. A desire to continually increase the available efficiency and resolution from capillary columns has become apparent in recent years, predominantly driven by the development and uptake of comprehensive two-dimensional systems. The use of a 0.25 mm i.d. column as the primary column in a GC×GC–MS column set is approaching ubiquity, but it is widely known that decreasing the internal diameter of the column increases the number of theoretical plates per unit length of the column. For this reason, it was thought that moving to a 0.10 mm i.d. column in the first dimension of the current system would be a logical area of research. Naturally, increasing the length of the column affords more efficiency and peak capacity, although this is achieved at the cost of required head pressure to approach optimum carrier gas linear velocity, in addition to a decrease in the speed of the separation. It is clear that an intelligent selection of column length and applied pressure would be necessary to achieve a successful result for this research. A 60 m thin film Rtx-WAX couple column was investigated using a translatable method for the analysis of hop essential oil samples.

The column was constructed in-house by serially connecting 20 m columns with zero dead volume connectors. It was established that by operating the system in constant pressure mode, the optimum linear velocity (EOV [34]) would not be sustained throughout the temperature program; rather the two values would intersect at some point during the run. Through the calculations of Golay and van Deemter, the deviation from optimum efficiency shows a greater rate of change at linear velocities below optimum than at those above optimum. For this reason, it was suggested that the most suitable column length be selected so that optimum linear velocity be reached at the end of the temperature program. Such a value was realised with a 0.10 mm i.d. column approximately 39 m in length when operated in constant pressure mode with a head pressure ($H_2$) of 100 psi (689 kPa). Exemplary peak capacity was afforded by a similar (40 m) column during this investigation and it was concluded that this length should not be exceeded for further investigation as part of a GC×GC–MS column set.

To conclude the preliminary GC–MS investigations, separation of hop (*Humulus lupulus* L.) metabolite extracts was performed, which were subsequently used to construct a data matrix for simple statistical analysis. Using a long (60 m) column and speed optimised flow (SOF) conditions [35], over 150 components were detected in the extracts of which 57 were selected for further analysis using chemometric techniques. Two alternative feature selection processes were used to select relevant metabolites for further analysis. Principal component analysis and discriminant analysis techniques were performed, displaying the suitability of this approach for differentiating between α-acid and aroma subgroups, and basic varietal characterisation.

It was anticipated that investigation of hop metabolite extracts could be performed with a pneumatically modulated GC×GC–MS system, although samples were not available at the time of investigation and could only have been acquired by waiting for the next hop breeding season. It is envisaged that the increased peak capacity and resolution afforded by the comprehensive two-dimensional approach would have increased the accuracy and precision of identification procedures. Furthermore, it may enhance the applicability of the technique for even more complex metabolite samples, such as human or animal extracts. This would unlock a key separation attribute, by developing a separation system which does not rely on a cryogen supply yet still delivers sufficient information from complex samples. A novel system such as this has proven difficult to implement.

Following on from the GC–MS investigations, development and application of pneumatic modulators for GC×GC–MS is described. The first application discusses the use of a commercially-available CFT pneumatic modulator for enantioselective essential oil analysis in a GC×GC–FID approach. As a qualitative comparison, a dual-stage loop-type modulator was used in a GC×GC–MS instrument. Excellent repeatability in the quantitative determination of enantiomeric ratio between three pairs of optical isomers was reported, suggesting that performance of the CFT modulator was highly satisfactory. This was due, in part, to appropriate choice of the dimensions of the first-dimension column, reiterating the importance of this aspect of hardware setup for pneumatically modulated GC×GC approaches. Based on this result, the use of a pneumatic modulator for a GC×GC–qMS approach looked promising.

The introduction of microfluidic-type wafer devices to the commercial market posed an opportunity for developing an alternative interface using a partial

sampling technique. Evaluation of a pulsed-flow modulator with these devices has recently been published [232] so a Deans switch type device was investigated with the incorporation of dual second-dimension columns allowing detection with both MS and FID. This system was chosen as it permits the decoupling of the primary and secondary carrier gas flows, which may be more suited to the incorporation of a quadrupole MS in the GC×GC system than other pneumatic modulation techniques [226]. Two 2 m × 0.25 mm i.d. columns were selected for use in the second dimension and the MS channel was fitted with a restrictor at its terminus to balance the split between the two channels. Prior to selection of column lengths and flow parameters, a preliminary study to determine the effect of increasing flow on the sensitivity of the mass spectrometer was performed. The manufacturer of the mass spectrometer used for this study claims that the instrument can operate at flow rates up to 15 mL/min. By performing serial injections of OFN at a variety of flow rates between 1-8 mL/min, it was found that there was no significant difference between the detector response at flows between 1-4 mL/min. While a steady decrease in response was noted as the flow rate increased, acceptable results could still be obtained up to the maximum tested value of 8 mL/min.

Three primary columns were selected for evaluation, namely a 20 m × 0.10 mm i.d., 40 m × 0.10 mm i.d. and a 25 m × 0.22 mm i.d., each with a 5% phenyl equivalent stationary phase coating. A flow ratio of 1:25 was selected based on previous research [56, 226] and appropriate pressure programs selected to maintain this ratio throughout the temperature program. Hop and vetiver essential oil were selected for analysis; utilising the 40 m coupled column, 190 peaks were reported in the hop essential oil and 212 in the vetiver essential oil samples. Of these, 82 and 72 components could be tentatively identified respectively. In their 2004 study, Roberts

*et al.* [178] reported the identification of 119 components in a hop essential oil sample using GC×GC–TOFMS with cryogenic modulation. The column set used was (10 m × 0.18 mm) × (1.9 m × 0.1 mm) in a traditional non-polar/polar configuration. Second-dimension peak widths at base height were around 0.1-0.2 s using this system, while those obtained using the Deans switch modulator in the current study were generally around 0.3 s or greater.

Although the second-dimension peak width obtained using the pneumatic modulation technique was greater than that reported using the cryogenic technique, this suited the concomitantly lower acquisition rate of the quadrupole detector. In addition, it has been reported previously [178, 233] that some 440 components may be contained in hop essential oil, a figure that could not be obtained using either separation technique. All in all, it seems plausible to suggest that the work performed in this study demonstrates the applicability of a pneumatic modulated GC×GC–MS system utilising a quadrupole mass spectrometer for the separation and characterisation of a complex essential oil sample.

To conclude the research presented in this thesis, an alternative pneumatic modulation technique using a total transfer approach was investigated. Although highly satisfactory results were obtained using the Deans switch modulator, it was thought that the potential sensitivity of the system could be improved upon by conserving the entire primary column effluent. The system developed relied upon a 6-port diaphragm valve and achieved total transfer by blocking the port connected to the primary column during the loop flush phase of the modulation cycle. This was achieved with a solenoid valve, which was opened during sample injection to enhance column loading. Previous research with similar devices [228] suggested that this stop-flow approach did not adversely affect the available resolution by

enhancing the effects of longitudinal diffusion within the primary column. To build upon previous research, a new approach was undertaken whereby a three port (tee) flow wafer was incorporated after the modulator, allowing simultaneous separation on two second-dimension columns and both FID and MS detection. Instead of incorporating a flow restrictor to the MS channel to ensure an even flow ratio to each detector, the length of the second-dimension columns was chosen carefully in an attempt to align the two chromatograms. This would better facilitate quali-quantitative analysis should the system be used for such a purpose.

Hop and vetiver essential oil samples, in addition to a kerosene sample were examined using this system. The results obtained were somewhat disappointing as the peak widths increased substantially during the temperature program to a point where the available resolution was severely reduced. Although the detector response was greater than the Deans switch modulated system as was expected, the resolution was unacceptable. An attempt was made to rectify this by installing a BPX-35 stationary phase column which has a less polar coating than the SLB IL-111 columns used previously. Unfortunately the temperature and flow programs could not be satisfactorily aligned, although a substantial improvement in resolution was witnessed for the separation of a kerosene sample.

Based on these results, it was concluded that the Deans switch modulator provided a better technique for the separation of complex essential oil samples, despite the shortcomings surrounding the available sensitivity arising from partial sampling of the primary column effluent. Should a sample have been available, it was anticipated that a successful characterisation of a plant, or even animal, metabolite extract could have been achieved. This would represent the first instance

of a pneumatically modulated GC×GC system incorporating both FID and qMS detection for the separation and characterisation of such a sample.

## 5.2 Further Research

The research presented herein has detailed the selection, development and optimisation of a GC×GC–qMS system which relies upon a pneumatic modulation technique to couple the two dimensions. The separation of essential oil and metabolite extract samples were reported and the results were highly satisfactory. Whilst a superior result may have been obtained using a cryogenic modulation technique, the setup and running costs of such a system are anticipated to be far greater than those of the pneumatic modulator. For this reason, it allows a degree of field deployment or use in areas where resupply of cryogen consumables may be difficult or impossible. This is further assisted by the use of on-line carrier gas generation which is easily achieved. This capability has, to date, proved difficult to implement. While it would have been desirable to introduce a total-transfer based system, acceptable results were not obtained. Further research in this area may prove beneficial, as a promising but un-optimised separation of a kerosene sample was obtained using this method. In addition, it seems prudent that additional data could be collected using the Deans switch modulator to establish other samples that may be successfully separated using this technique. Considering many application papers appear in the literature, this may be a good place to commence further research.

As mentioned in Chapter 3, positive results were obtained in the pilot study into varietal characterisation of hop plants based on metabolite extracts from the cones. Research into this application is continuing within our research group. It is an interesting point of conjecture whether the classification functions derived from the

DA process would have been more successful for separating the conflicting pairs should a comprehensive two-dimensional approach have been used. Additionally, it could be argued that a stronger model could have been constructed by selecting alternative, more powerful chemometrics techniques, such as those discussed by Pierce and co-workers in their review of chemometric processing of comprehensive two-dimensional separation data [234] and the numerous publications by Synovec and co-workers [55, 125, 204, 205, 235, 236].

To further investigate these possibilities, a follow-up study is planned to coincide with the next hop flowering season. A comprehensive two-dimensional separation approach will be adopted, utilising MS detection. Deconvolution and quantitation algorithms such as PARAFAC [236] and GRAM [237] may be applied to generate a larger matrix of relevant, separated metabolites for further processing and generate more accurate quantitation. It is important that additional metabolite data is representative of the variance observed between the hop varieties, so the use of the Fisher Ratio method [123, 204, 205, 238] to identify compounds of interest is suggested once again. This well-reported method depicts the between class ratio to the within class ratio through statistical differentiation of regions of the chromatogram and displays robustness against natural diversity between biological samples within a population [204, 234], and proved useful in the current investigation. PCA remains an appropriate method for varietal classification, but may be extended to incorporate a multi-way data a k-means dendrogram in conjunction with ANOVA feature selection. This would follow the previous research of Johnson and co-workers who applied the same techniques for GC×GC separations of components within jet fuel samples [238, 239].

The adoption of a more sophisticated regression analysis, such as Partial Least Squares regression analysis (PLS) would eliminate the shortfalls inherent in the DA approach, most notably by increasing the number of available prediction functions above the of the number of X and Y variables in the cross-product matrix available. PLS approaches for use in chemometrics applications have been described previously by de Jong [240] and may make better use of the increased gamut of metabolome information available from the GC×GC method proposed. Alternatively, the technique of mean field independent component analysis, as discussed in the recent work by Jalali-Heravi and co-workers [122], may be suitable. The group reported acceptable results for the analysis of GC–MS separated essential oil samples in comparison to other powerful techniques.

The emergence of consumable-free GC×GC systems has opened avenues for alternative low running cost techniques. Several manufacturers have promoted commercially-available systems utilising either closed-cycle refrigerant systems [241] or immersion cooling [242]. It is anticipated that the application of these hardware advances would prove an interesting field of research. The curious researcher may even be prompted to develop a system in-house should the initial outlay for commercial equipment prove out of reach, or the minimum temperature available with commercial closed-loop systems be insufficient (typically in the order of -85 °C cf. approximately -190 °C with a typical run-to-waste $LN_2$ system [241, 242]). Considering the variety of traditional cryogenic modulator techniques, the researcher would be faced with plenty of options regarding the direction of investigation.

Additionally, recent developments in consumable-free resistively heated thermal modulation have proved fruitful [53]. The utilisation of such a system may

couple the unrivalled peak capacity available with current cryogenic technology whilst retaining the benefit of low running costs and field deployment. Should a satisfactory result be obtained, it is anticipated that the accessibility of GC×GC–MS technology will be increased greatly and a significant step made in the body of research already performed with this technique.

# References


1. J.B. Phillips, J. Beens, **1999** *J. Chromatogr. A.* **856**: p. 331-347.
2. Technology, National Institute of Standards and. *NIST Scientific and Technical Databases*. 2002 [cited 2010]; Available from: http://www.nist.gov/data/nist1a.htm.
3. P.J. Schoenmakers, P.J. Marriott, J. Beens, **2003** *LC-GC Eur.* **16**: p. 1-4.
4. G.S. Frysinger, R.B. Gaines, **1999** *HRC J. High Resolut. Chromatogr.* **22**(5): p. 251-255.
5. C. Debonneville, A. Chaintreau, **2004** *J. Chromatogr. A.* **1027**: p. 109-115.
6. R.A. Shellie, P.J. Marriott, P. Morrison, **2004** *J. Chromatogr. Sci.* **42**.
7. S. Zhu, X. Lu, L. Dong, J. Xing, X. Su, H. Kong, G. Xu, C. Wu, **2005** *J. Chromatogr. A.* **1086**: p. 107-114.
8. C. Cordero, C. Bicchi, D. Joulain, P. Rubiolo, **2007** *J. Chromatogr. A.* **1150**: p. 37-49.
9. O. Amador-Muñoz, R. Villalobos-Pietrini, A. Aragón-Piña, T.C. Tran, P. Morrison, P.J Marriott, **2008** *J. Chromatogr. A.* **1201**: p. 161-168.
10. M.K. van der Le, G. van der Weg, W.A. Traag, H.G.J. Mol, **2008** *J. Chromatogr. A.* **1186**: p. 325-339.
11. E. Hoh, S.J. Lehotay, K. Mastovska, H.L. Ngo, W. Vetter, K.C. Pangallo, C.M. Reddy, **2009** *Environ. Sci. Technol.* **43**: p. 3240-3247.
12. R.E. Murphy, M.R. Schure, J.P. Foley., **1998** *Anal. Chem.* **70**(8): p. 1585-1594.
13. M. van Deursen, H.-G. Janssen, J. Beens, P. Lipman, R. Reinierkens, G. Rutten, C. Cramers, **2000** *J. Microcolumn Sep.* **12**(12 613-622).
14. J.F. Holland, C.G. Enke, J. Allison, J.T. Stults, J.D. Pinkston, B. Newcome, J.T. Watson, **1983** *Anal. Chem.* **55**(9): p. 997A-1012A.
15. R.A. Shellie, P.J. Marriott, **2002** *Anal. Chem.* **74**: p. 5426-5430.
16. C.A. Cramers, P.A. Leclercq, **1988** *CRC Crit. Rev. Anal. Chem.* **20**: p. 117-147.
17. R.A. Shellie, P.J. Marriott, **2003** *Analyst*. **128**: p. 879-883.
18. Adams, R.P., *Identification of Essential Oil Components by Gas Chromatography/Mass spectroscopy*, ed. C. Stream. 1995, Illinois, USA: Allured Publishing Corp.
19. R.A. Shellie, P.J. Marriott, C.W. Huie, **2003** *J. Sep. Sci.* **26**: p. 1185-1192.
20. M. Kallio, T. Hyotylainen, M. Lehtonen, M. Jussila, K. Hartonen, M. Shimmo, M.-L. Reikkola, **2003** *J. Chromatogr. A.* **1019**: p. 251-260.
21. D. Ryan, R. Shellie, P. Tranchida, A. Casilli, L. Mondello, P.J. Marriott, **2004** *J. Chromatogr. A.* **1054**: p. 57-65.

22. M. Adahchour, M. Brandt, H.-U. Daier, R.J.J. Vreuls, A.M. Batenburg, U.A.Th. Brinkman, **2005** *J. Chromatogr. A.* **1067**: p. 245-254.

23. N. Ochiai, T. Ieda, K. Sasamoto, A. Fushimi, S. Hasegawa, K. Tanabe, S. Kobayashi, **2007** *J. Chromatogr. A.* **1150**: p. 13-20.

24. M. van Deursen, J. Beens, J. Reijenga, P. Lipman, C. Cramers, **2000** *HRC J. High Resolut. Chromatogr.* **23**: p. 507-510.

25. A.V. Es, J. Janssen, C. Cramers., **1985** *HRC J. High Resolut. Chromatogr.* **11**: p. 852.

26. R.A. Shellie, P.J. Marriott, P. Morrison, **2001** *Anal. Chem.* **73**(6): p. 1336-1344.

27. J. Dalluge, R.J.J. Vreuls, J. Beens, U.A.Th. Brinkman, **2002** *J. Sep. Sci.* **25**: p. 201-214.

28. C. Vendeuvre, F. Bertoncini, D. Thiebaut, M. Martin, M.-C. Hennion, **2005** *J. Sep. Sci.* **28**: p. 1129-1136.

29. J. Beens, R. Tijssen, J. Blomberg, **1998** *J. Chromatogr. A.* **822**: p. 233-251.

30. N.J. Micyus, S.K. Seeley, J.V. Seeley, **2005** *J. Chromatogr. A.* **1086**: p. 171-174.

31. Hovanesian, S.A., **1976** *IEEE Trans. Aerosp. Electron. Syst.* **AES-12**: p. 287.

32. J.C. Hoggard, W.C. Siegler, R.E. Synovec, **2008** *J. Chemometrics*. **23**: p. 421-431.

33. L.M. Blumberg, M.S. Klee, **1998** *Anal. Chem.* **70**: p. 3828-3839.

34. L.M. Blumberg, M.S. Klee., **2000** *J. Microcolumn Sep.* **12**(9): p. 508-514.

35. M.S. Klee, L.M. Blumberg, **2002** *J. Chromatogr. Sci.* **40**: p. 234-247.

36. L.M. Blumberg, M.S. Klee, **2001** *J. Chromatogr. A.* **933**: p. 1-11.

37. R.A. Shellie, P.J. Marriott, P. Morrison, L. Mondello, **2004** *J. Sep. Sci.* **27**: p. 504-512.

38. C.J. Venkatramani, J. Xu, J.B. Phillips, **1996** *Anal. Chem.* **68**: p. 1486-1492.

39. R. Zimmermann, W. Welthagen, T. Groger, **2008** *J. Chromatogr. A.* **1184**: p. 296-308.

40. F.C.-Y. Wang, K. Qian, L.A. Green, **2005** *Anal. Chem.* **77**: p. 2777-2785.

41. K. Qian, G.J. Dechert, **2002** *Anal. Chem.* **74**: p. 3977-3983.

42. W. Welthagen, S. Mitschke, F. Muhlberger, R. Zimmermann, **2007** *J. Chromatogr. A.* **1150**: p. 54-61.

43. L. Hejazi, D. Ebrahimi, M. Guilhaus, D.B. Hibbert, **2009** *Anal. Chem.* **81**: p. 1450-1458.

44. M.M. Bushey, J.W. Jorgenson, **1990** *Anal. Chem.* **62**: p. 161-167.

45. Z.Y. Liu, J.B. Phillips, **1991** *J. Chromatogr. Sci.* **29**: p. 227.

46. H.-J. de Geus, J. de Boer, U.A.Th. Brinkman, **1997** *J. Chromatogr. A.* **767**: p. 137-151.

47. J.B. Phillips, J. Xu, **1995** *J. Chromatogr. A.* **703**: p. 327-334.

48. C.J. Venkatramani, J.B. Phillips, **1993** *J. Microcolumn Sep.* **5**: p. 511-516.

49. J.B. Phillips, E.B. Ledford, **1996** *Field Anal. Chem. Technol.* **1**: p. 23-29.

50. J.B. Phillips, R.B. Gaines, J. Blomberg, F.W.M. van der Wielen, J.-M. Dimandja, V. Green, J. Granger, D. Patterson, L. Racovalis, H.-J. de Geus, J. de Boer, P. Haglund, J. Lipsky, V. Sinah, E.B. Ledford Jr., **1999** *HRC J. High Resolut. Chromatogr.* **22**: p. 3-10.

51. P.J. Marriott, R.M. Kinghorn, R. Ong, P. Morrison, **2000** *HRC J. High Resolut. Chromatogr.* **23**(3): p. 253-258.

52. A. Mostafa, T. Gorecki, P.Q. Tranchida, L. Mondello, *History, evolution, and optimisation aspects of comprehensive two-dimensional gas chromatography*, in *Comprehensive Chromatography in Combination with Mass Spectrometry*, L. Mondello, Editor. 2011, John Wiley and Sons, Inc.: Hoboken. p. 93-144.

53. O. Panic, T. Gorecki, C. McNeish, A.H. Goldstein, B.J. Williams, D.R. Worton, S.V. Hering, N.M. Kreisberg, **2011** *J. Chromatogr. A.* **1218**: p. 3070-3079.

54. A.L. Lee, A.C Lewis, K.D. Bartle, J.B. McQuaid, P.J. Marriott, **2000** *J. Microcolumn Sep.* **12**: p. 187.

55. C.A. Bruckner, B.J. Prazen, R.E. Synovec, **1998** *Anal. Chem.* **70**: p. 2796-2804.

56. J.V. Seeley, F. Kramp, C.J. Hicks, **2000** *Anal. Chem.* **72**: p. 4346-4352.

57. Wells, G., **1985** *J. Chromatogr.* **319**: p. 263.

58. A.E. Sinha, B.J. Prazen, C.G. Fraga, R.E. Synovec, **2003** *J. Chromatogr. A.* **1019**: p. 79-87.

59. J.W. Diehl, F.P. Di Sanzo, **2005** *J. Chromatogr. A.* **1080**: p. 157-165.

60. P.A. Bueno Jr., J.V. Seeley, **2004** *J. Chromatogr. A.* **1027**: p. 3-10.

61. R.W. LaClair, P.A. Bueno, J.V. Seeley, **2004** *J. Sep. Sci.* **27**: p. 389-396.

62. J.V. Seeley, N.J. Micyus, J.D. McCurry, S.K. Seeley, **2006** *Am. Lab.* **38**(9): p. 24-26.

63. M. Kochman, A. Gordin, T. Alon, A. Amirav, **2006** *J. Chromatogr. A.* **1129**: p. 95-104.

64. A. Amirav, A. Gordin, M. Poliak, A.B. Fialkov, **2008** *J. Mass Spectrom.* **43**: p. 141-163.

65. M. Poliak, A.B. Fialkov, A. Amirav, **2008** *J. Chromatogr. A.* **1210**: p. 108-114.

66. Shellie, R.A., **2008** *LC-GC Eur.* **21**(11): p. 572-578.

67. P. McA. Harvey, R.A. Shellie, P.R. Haddad, **2010** *J. Chromatogr. Sci.* **48**: p. 245-250.

68. L. Mondello, P.Q. Tranchida, P. Dugo, G.Dugo, **2008** *Mass Spectrom. Rev.* **27**: p. 101-124.

69. J. Dalluge, L.L.P. van Stee, X. Xu, J. Williams, J. Beens, R.J.J. Vreuls, U.A. Th. Brinkman, **2002** *J. Chromatogr. A.* **974**: p. 169-184.

70. N. Wu, Z. Chen, J.C. Medina, J.S. Bradshaw, **2000** *J. Microcolumn Sep.* **12**: p. 454-461.

71. Dimandja, J.-M.D., **2003** *Am. Lab.* **35**: p. 42-53.

72. T. Górecki, J. Harynuk, O. Panić, *Comprehensive two-dimensional gas chromatography*, in *New Horizons and Challenges in Environmental Analysis and Monitoring*, W.C.a.P.Z. J. Namiesnik, Editor. 2003, Centre of Excellence in Environmental Analysis and Monitoring, Gdansk University of Technology: Gdansk, Poland. p. 61-83.

73. J.H. Wahl, D.M. Riechers, M.E. Vucelick. B.W. Wright, **2003** *J. Sep. Sci.* **26**: p. 1083-1090.

74. R.A. Shellie, P.J. Marriott, **2003** *Flavour Fragr. J.* **18**: p. 179-191.

75. L. Mondello, R. Shellie, A. Casilli, P.Q. Tranchida, P. Marriott, G.Dugo, **2004** *J. Sep. Sci.* **27**: p. 699.

76. L. Mondello, A. Casilli, P.Q. Tranchida, P. Dugo, G.Dugo, **2005** *J. Chromatogr. A.* **1067**: p. 235-243.

77. Kovats, E., **1958** *Helv. Chim. Acta*. **41**: p. 1915-1932.

78. J. Beens, H.-G. Janssen, M. Adahchour, U.A. Th. Brinkman, **2005** *J. Chromatogr. A.* **1086**: p. 141-150.

79. A.E. Sinha, J.L. Hope, B.J. Prazen, E.J. Nilsson, R.M. Jack, R.E. Synovec, **2004** *J. Chromatogr. A.* **1058**: p. 209-215.

80. A.E. Sinha, J.L. Hope, B.J. Prazen, C.G. Fraga, E.J. Nilsson, R.E. Synovec, **2004** *J. Chromatogr. A.* **1056**: p. 145-154.

81. W. Welthagen, R.A. Shellie, J. Spranger, M. Ristow, R. Zimmermann, O. Fiehn., **2005** *Metabolomics*. **1**(1): p. 65-73.

82. J.L. Hope, B.J. Prazen, E.J. Nilsson, M.E. Lidstrom, R.E. Synovec, **2005** *Talanta*. **65**: p. 380-388.

83. R.A. Shellie, W. Welthagen, J. Zrostliková, J. Spranger, M. Ristow, O. Fiehn, R. Zimmermann, **2005** *J. Chromatogr. A.* **1086**: p. 83-90.

84. H. Shunji, T. Yoshikatsy, F. Akihiro, I. Hiroyasu, T. Kiyoshi, S. Yasuyuki, U. Masa-aki, K. Hkihiko, T. Kazuo, O. Hideyuki, A. Katsunori, **2008** *J. Chromatogr. A.* **1178**: p. 187-198.

85. R. van der Westhuizen, H. Potgieter, N. Prinsloo, A. de Villiers, P. Sandra, **2011** *J. Chromatogr. A.* **1218**: p. 3173-3179.

86. M.E. Machado, E.B. Caramao, C.A. Zini, **2011** *J. Chromatogr. A.* **1218**: p. 3200-3207.

87. B.M.F. Avila, R. Pereira, A.O. Gomes, D.A. Azevedo, **2011** *J. Chromatogr. A.* **1218**: p. 3208-3216.

88. L.A. McGregor, C. Gauchotte-Lindsay, N.N. Daeid, R. Thomas, P. Daly, R.M. Kalin **2011** *J. Chromatogr. A.* **1218**: p. 4755-4763.

89. R. van der Westhuizen, M. Ajam, P. De Coning, J. Beens, A. de Villiers, P. Sandra, **2011** *J. Chromatogr. A.* **1218**: p. 4478-4486.

90. B. Omais, M. Courtiade, N. Charon, D. Thiebaut, A. Quignard, M.-C. Hennion, **2011** *J. Chromatogr. A.* **1218**: p. 3233-3240.

91. M. Pena-Abaurrea, A. Covaci, L. Ramos, **2011** *J. Chromatogr. A.* **1218**: p. 6995-7002.

92. T. Ieda, N. Ochiai, T. Miyawaki, T. Ohura, Y. Horii, **2011** *J. Chromatogr. A.* **1218**: p. 3224-3232.

93. S. Hashimoto, Y. Takazawa, A. Fushimi, K. Tanabe, Y. Shibata, T. Ieda, N. Ochiai, H. Kanda, T. Ohura, Q. Tao, S.E. Reichenbach, **2011** *J. Chromatogr. A.* **1218**: p. 3799-3810.

94. D.G. Patterson Jr., S.M. Welch, W.E. Turner, A. Sjodin, J.-F. Focant, **2011** *J. Chromatogr. A.* **1218**: p. 3274-3281.

95. J. de Vos, P. Gorst-Allman, E. Rohwer, **2011** *J. Chromatogr. A.* **1218**: p. 3282-3290.

96. V. Matamoros, E. Jover, J.M. Bayona, **2010** *Anal. Chem.* **82**: p. 699-706.

97. M.J. Gomez, S. Herrera, D. Sole, E. Garcia-Calvo, A.R. Fernandez-Alba, **2011** *Anal. Chem.* **83**: p. 2638-2647.

98. B.S. Mitrevski, P. Wilairat, P.J. Marriott, **2010** *J. Chromatogr. A.* **1217**: p. 127-135.

99. K.A. Kouremenos, J. Pitt, P.J. Marriott, **2010** *J. Chromatogr. A.* **1217**: p. 104-111.

100. P. Wojtowicz, J. Zrostlikova, T. Kovalczuk, J. Scurek, T. Adam, **2010** *J. Chromatogr. A.* **1217**: p. 8054-8061.

101. C. Cordero, E. Liberto, C. Bicchi, P. Rubiolo, P. Schieberle, S.E. Reicenbach, Q. Tao, **2010** *J. Chromatogr. A.* **1217**: p. 5848-5858.

102. L.R. Snyder, J.C. Hoggard, T.J. Montine, R.E. Synovec, **2010** *J. Chromatogr. A.* **1217**: p. 4639-4647.

103. B. Guthery, T. Bassingdale, A. Bassingdale, C.T. Pillinger, G.H. Morgan, **2010** *J. Chromatogr. A.* **1217**: p. 4402-4410.

104. M. Mieth, J.K. Schubert, T. Groger, B. Sabel, S. Kishckel, P. Fuchs, D. Hein, R. Zimmermann, W. Miekisch, **2010** *Anal. Chem.* **82**: p. 2541-2551.

105. M.F. Almstetter, I.J. Appel, K. Dettmer, M.A. Gruber, P.J. Oefner, **2011** *J. Chromatogr. A.* **1218**: p. 7031-7038.

106. M.C. Waldhier, M.F. Almstetter, N. Nurnberger, M.A. Gruber, K. Dettmer, P.J. Oefner, **2011** *J. Chromatogr. A.* **1218**: p. 4537-4544.

107. P.Q. Tranchida, G. Purcaro, C. Fanali, P. Dugo, G. Dugo, L. Mondello, **2010** *J. Chromatogr. A.* **1217**: p. 4160-4166.

108. P.Q. Tranchida, A. Casilli, P. Dugo, G. Dugo, L. Mondello, **2007** *Anal. Chem.* **79**: p. 2266-2275.

109. G. Purcaro, P.Q. Tranchida, C. Ragonese, L. Conte, P. Dugo, G. Dugo, L. Mondello, **2010** *Anal. Chem.* **82**: p. 8583-8590.

110. A. Vallejo, M. Olivares, L.A. Fernandez, N. Etxebarria, S. Arrasate, E. Anakabe, **2011** *J. Chromatogr. A.* **1218**: p. 3064-3069.

111. P.Q. Tranchida, G. Purcaro, D. Sciarrone, P. Dugo, G. Dugo, L. Mondello, **2010** *J. Sep. Sci.* **33**: p. 2791-2795.

112. M. Adachour, M. Brandt, H.-U. Baier, R.J.J. Vreuls, A.M. Batenburg, U.A.Th. Brinkman., **2005** *J. Chromatogr. A.* **1067**: p. 245-254.

113. G. Semard, V. Peulon-Agasse, A. Bruchet, J.-P. Bouillon, P. Cardinael, **2010** *J. Chromatogr. A.* **1217**: p. 5449-5454.

114. F.L. Dorman, P.D. Schettler, L.A. Vogt, J.W. Cochran, **2008** *J. Chromatogr. A.* **1186**: p. 196-201.

115. R.B. Wilson, W.C. Seigler, J.C. Hoggard, B.D. Fitz, J.S. Nadeau, R.E. Synovec, **2011** *J. Chromatogr. A.* **1218**: p. 3130-3139.

116. K.M. Van Geem, S.P. Pyl, M.-F. Reyniers, J. Vercammen, J. Beens, G.B. Martin, **2010** *J. Chromatogr. A.* **1217**: p. 6623-6633.

117. J. Mydlova-Memersheimerova, B. Tienpont, F. David, J. Krupcik, P. Sandra, **2009** *J. Chromatogr. A.* **1216**: p. 6043-6062.

118. M. Zapadlo, J. Krupcik, T. Kovalczuk, P. Majek, I. Spanik, D. Armstrong, P. Sandra, **2011** *J. Chromatogr. A.* **1218**: p. 746-751.

119. Q. Gu, F. David, F. Lynen, P. Vanormelingen, W. Vyerman, K. Rumpel, G. Xu, P. Sandra, **2011** *J. Chromatogr. A.* **1218**: p. 3056-3063.

120. W.C. Seigler, J.A. Crank, D.W. Armstrong. R.E. Synovec, **2010** *J. Chromatogr. A.* **1217**: p. 3144-3149.

121. N.E. Watson, W.C. Siegler, J.C. Hoggard, R.E. Synovec, **2007** *Anal. Chem.* **79**: p. 8270-8280.

122. M. Jalai-Heravi, H. Parastar, H. Sereshti, **2010** *J. Chromatogr. A.* **1217**: p. 4850-4861.

123. A.C. Beckstrom, E.M. Humston, L.R. Snyder, R.E. Synovec, S.E. Juul, **2011** *J. Chromatogr. A.* **1218**: p. 1899-1906.

124. J.C. Hoggard, J.H. Wahl, R.E. Synovec, G.M. Mong, C.G. Fraga, **2010** *Anal. Chem.* **82**: p. 689-698.

125. E.M. Humston, J.D. Knowles, A. McShea, R.E. Synovec, **2010** *J. Chromatogr. A.* **1217**: p. 1963-1970.

126. W.C. Seigler, B.D. Fitz, J.C. Hoggard, R.E. Synovec, **2011** *Anal. Chem.* **83**: p. 5190-5196.

127. J. Beens, M.Adahchour, R.J.J. Vreuls, K. van Altena, U.A. Th. Brinkman, **2001** *J. Chromatogr. A.* **919**: p. 127-132.

128. P. Korytar, H.-G. Janssen, E. Matisova, U.A.Th. Brinkman., **2002** *TrAC, Trends Anal. Chem.* **21**: p. 558.

129. P. Donato, P.Q. Tranchida, P. Dugo, G. Dugo, L. Mondello, **2007** *J. Sep. Sci.* **30**: p. 508.

130. F. David, D.R. Gere, F. Scanlan, P. Sandra, **1999** *J. Chromatogr. A.* **842**: p. 309.

131. C. Bicchi, C. Brunelli, C. Cordero, P. Rubiolo, M. Galli, A. Sironi, **2004** *J. Chromatogr. A.* **1024**: p. 195-207.

132. P. Magni, R. Facchetti, A. Cadoppi, F. Pigozzo, C. Brunelli, **2004** *LC-GC Eur.* **59**: p. 2.

133. C. Bicchi, C. Brunelli, M. Galli, A. Sironi, **2001** *J. Chromatogr. A.* **931**: p. 129-140.

134. P.J. Marriott, R.A. Shellie, **2002** *TrAC, Trends Anal. Chem.* **21**(9-10): p. 573-583.

135. R. Ong, R. Shellie, P. Marriott, **2001** *J. Sep. Sci.* **24**: p. 367-377.

136. J. Harynuk, T. Gorecki, J. de Zeeuw, **2005** *J. Chromatogr. A.* **1071**: p. 21-27.

137. C.A. Cramers, G.Z. Scherpenzeel, P.A. Leclercq, **1981** *J. Chromatogr. A.* **203**: p. 207.

138. J.D. Zeeuw, H.-G. Jansen, X. Lou, **2000** *HRC J. High Resolut. Chromatogr.* **23**(12): p. 677-680.

139. M.M. van Deursen, J. Beens, H.-G. Janssen, P.A. Leclercq, C.A. Cramers, **2000** *J. Chromatogr. A.* **878**: p. 205-213.

140. E. Jover, Z. Moldovan, J.M. Bayona., **2002** *J. Chromatogr. A.* **970**: p. 249.

141. K. Mastovska, S.J. Lehotay, J. Hajslova., **2001** *J. Chromatogr. A.* **926**: p. 291.

142. F.J. Arrebola, J.L. Martınez Vidal, M.J. Gonzalez-Rodrıguez, A. Garrido-Frenich, N. Sanchez Morito, **2003** *J. Chromatogr. A.* **1005**: p. 131-141.

143. A. Garrido-Frenich, F.J. Arrebola, M.J. Gonzalez-Rodrıguez, J.L. Martınez Vidal, N. Mora Dıez., **2003** *Anal. Bioanal. Chem.* **377**: p. 1038.

144. K. Mastovska, J. Hajslova, S.J. Lehotay., **2004** *J. Chromatogr. A.* **1054**: p. 291.

145. K. Ravindra, A.F.L. Godoi, L. Bencs, R. van Grieken., **2006** *J. Chromatogr. A.* **1114**: p. 278.

146. Cochran, J.W., **2002** *J. Chromatogr. Sci.* **40**: p. 254.

147. P.E. Joos, A.F.L. Godoi, R. de Jong, J. de Zeeuw, R. van Grieken., **2003** *J. Chromatogr. A.* **985**: p. 191-196.

148. A.F.L. Godoi, K. Ravindra, R.H.M. Godoi, S.J. Andrade, M. Santiago-Silva, L. van Vaeck, R. van Grieken., **2004** *J. Chromatogr. A.* **1027**: p. 49-53.

149. A.F.L. Godoi, W. Vilegas, R.H.M. Godoi, L. van Vaeck, R. van Grieken., **2004** *J. Chromatogr. A.* **1027**: p. 127-130.

150. G.L. Long, J.D. Winefordner, **1983** *Anal. Chem.* **55**(7): p. 712A-724A.

151. Smith, R.M., *Understanding Mass Spectra: A basic approach*. 2004, Hoboken, NJ.: John Wiley and Sons Inc.

152. L. Mondello, A. Casilli, P. Q. Tranchida, M.L. Pewari P. Dugo, G. Dugo, **2007** *Anal. Bioanal. Chem.* **389**: p. 1755-1763.

153. P. Wynne (Shimadzu Regional Manager, Mass Spectrometry Business Manager), *Pers. Comm.* 8 November 2011.

154. F.W. McLafferty, R.H. Hertel, R.D. Villwock, **1974** *Org. Mass Spectrom.* **9**: p. 690-702.

155. G.M. Pesyna, R. Venkataraghavan, H.E. Dayringer, F.W. McLafferty, **1976** *Anal. Chem.* **48**: p. 1362-1368.

156. Watson, J. Throck, *Introduction to Mass Spectrometry*. 1985, Raven Press: New York. p. 254-276.

157. B.L. Atwater, D.B. Stauffer, F.W. McLafferty, **1985** *Anal. Chem.* **57**: p. 899-903.

158. S.E. Stein, D.R. Scott, **1994** *J. Am. Soc. Mass Spectrom.* **5**: p. 859-866.

159. F.W. McLafferty, M.-Y. Zhang, D.B. Stauffer, S.Y. Loh, **1998** *J. Am. Soc. Mass Spectrom.* **9**: p. 92-95.

160. S. Sokolow, J. Karnofsky, P. Gustafson, *The Finnegan Library Search Program*. Finnegan Application Report 2. 1978, San Jose, CA: Finnigan Corp.

161. Shellie, R.A., **2009** *Compr. Anal. Chem.* **55**: p. 189-213.

162. L. Mondello, A. Casilli, P. Q. Tranchida, P. Dugo, G. Dugo, **2002** *Flavour Fragr. J.* **20**(2): p. 136-140.

163. R.A. Shellie, P.J. Marriott, C. Cornwell, **2001** *J. Sep. Sci.* **24**: p. 823-830.

164. M. Wang, P.J. Marriott, W.-H. Chan, A.W.M. Lee, Carmen W. Huie, **2006** *J. Chromatogr. A*. **1112**: p. 361-368.

165. M. Junge, S. Bieri, H. Hugel, P.J. Marriott, **2007** *Anal. Chem.* **79**: p. 4448-4454.

166. P.Marriott, R. Shellie, J. Fergeus, R. Ong, P. Morrison, **2001** *Flavour Fragr. J.* **15**(4): p. 225-239.

167. J. Thomas, C. Narkowicz, G.M. Peterson, G.A. Jacobson, A. Narayana, **2009** *Vet. Rec.* **164**(20): p. 619-623.

168. D.H. Desty, A. Goldup, W.T. Swanton, in *Gas chromatography*, J.E.C. N. Brenner, M.D. Weiss, Editor. 1962, Academic press: New York. p. 105.

169. W.N. Sanders, J.B. Maynard, **1968** *Anal. Chem.* **40**: p. 527.

170. Whitmore, I.M., in *Chromatography in petroleum analysis*, T.H.G. K.H. Altgelt, Editor. 1979, Marcel Dekker: New York.

171. Berger, T.A., **1996** *Chromatographia*. **42**: p. 63-71.

172. Larsen, B.R., **1995** *HRC J. High Resolut. Chromatogr.* **18**: p. 141.

173. J.W. Cochran, G.M. Frame., **1999** *J. Chromatogr. A*. **843**: p. 323.

174. R.A. Shellie, S.D.H. Poynter, J. Li, J.L. Gathercole, S.P. Whittock, A. Koutoulis, **2009** *J. Sep. Sci.* **32**(21): p. 3720-3725.

175. R.A. Malizia, J.S. Molli, D.A. Cardell, R.J.A. Gran, **1999** *J. Essent. Oil. Res.* **11**(1): p. 13-15.

176. M.T. Roberts, A.C. Lewis, **2002** *Journ. Am. Soc. Brewing Chemists*. **60**(3): p. 116-121.

177. G. Eyres, J.-P. Dufour, **2009** *Beer in Health and Disease Prevention*. **239**(254): p. 239-254.

178. M.T. Roberts, J.P. Dufor, A.C. Lewis, **2004** *J. Sep. Sci.* **27**: p. 473-478.

179. Blumberg, L.M., **1997** *HRC J. High Resolut. Chromatogr.* **20**: p. 597-604.

180. Blumberg, L.M., **1997** *HRC J. High Resolut. Chromatogr.* **20**: p. 679-687.

181. Blumberg, L., **1999** *HRC J. High Resolut. Chromatogr.* **22**: p. 403-413.

182. J.J. van Deemter, F.J. Zuiderweg, A. Klinkenberg., **1956** *Chem. Eng. Sci.* **5**: p. 271.

183. J.C. Giddings, S.L. Seager, L.R. Stucki, G.H. Stewart, **1960** *Anal. Chem.* **32**: p. 867.

184. Thomson, M.Q., in *Electronic Pressure Control in GC*, S.S. Stafford, Editor. 1994, Hewlett-Packard Company: Wilmington, USA.

185. L.M. Blumberg, T.A. Berger, M.S. Klee, **1995** *HRC J. High Resolut. Chromatogr.* **18**: p. 378-380.

186. L.M. Blumberg, W.H. Wilson, M.S. Klee, **1999** *J. Chromatogr. A.* **842**: p. 15-28.

187. Ettre, L.S., **2005** *J. Chromatogr. A.* **1076**: p. 220-221.

188. R.E. Kaiser, R. Rieder, **1975** *Chromatographia*. **8**(9): p. 491-498.

189. L. Mondello, P.Q. Tranchida, A. Casilli, O. Favoino, P. Dugo, G.Dugo, **2004** *J. Sep. Sci.* **27**: p. 1149-1156.

190. Agilent, L.M. Blumberg et al. [cited 2011]; Available from: www.chem.agilent.com.

191. M. Verzele, D. De Keukeleire, *Chemistry and analysis of hop and beer bitter acids*. 1991, Amsterdam: Elsevier.

192. L. de Cooman, E. Everaert, D. de Keukeleire, **1998** *Phytochem. Anal.* **9**: p. 145-150.

193. R.G Buttery, L.C. Ling, **1967** *J. Agric. Food Chem.* **15**: p. 531-535.

194. R.A. Malizia, J.S. Molli, D.A. Cardell, R.J.A. Grau, **1999** *J. Essent. Oil Res.* **11**: p. 13-15.

195. C.P. Cornwell, D.N. Lech, T.G. Hartman, **1995** *J. Essent. Oil Res.* **7**: p. 613-620.

196. S. Eri, B.K. Khoo, J. Lech, **2000** *J. Agric. Food Chem.* **48**: p. 1140-1149.

197. M. Kovacevic, M. Kac, **2001** *J. Chromatogr. A.* **918**: p. 159-167.

198. U. Roessner, A. Luedemann, D. Brust, O. Fiehn, T. Linke, L. Willmitzer, A.R. Fernie, **2001** *Plant Cell*. **13**: p. 11-29.

199. J. Gullberg, P. Jonsson, A. Nordstrom, M. Sjostrom, T. Moritz, **2004** *Anal. Biochem.* **331**: p. 283-295.

200. O. Fiehn, J. Kopka, R.N. Trethewey, L. Willmitzer, **2000** *Anal. Chem.* **72**: p. 3573-3580.

201. A.R. Fernie, N. Schauer, **2008** *Trends Genet.* **25**: p. 39-48.

202. T. Kind, V. Tolstikov, O. Fiehn, R.H. Weiss, **2007** *Anal. Biochem.* **363**: p. 185-195.

203. Tilley, Andrew, *An introduction to research methodology and report writing in psychology*. 1999, Brisbane Pineapple Press.

204. K.M. Pierce, J.C. Hoggard, J.L. Hope, P.M. Rainey, A.N. Hoofnagel, R.M Jack, B.W. Wright, R.E. Synovec, **2006** *Anal. Chem.* **78**: p. 5068-5075.

205. S. Prasad, K.M. Pierce, H. Schmidt, J.V. Rao, R. Guth, R.E. Synovec, G.B Smith, G.A. Eiceman, **2008** *Analyst*. **133**: p. 760-767.

206. L. Pillonel, S. Ampuero, R. Tabacchi, J.O. Bosset, **2003** *Eur. Food Res. Technol.* **216**: p. 179-183.

207. L. Chen, N.C. Carpita, W.-D. Reiter, R.H. Wilson, C. Jeffries, M.C. McCann, **1998** *Plant J.* **16**(3): p. 385-392.

208. G.S. Catchpole, M. Beckmann, D.P. Enot, M. Mondhe, B. Zywicki, J. Taylor, N. Hardy, A. Smith, R.D. Kell, O. Fiehn, J. Draper., **2005** *PNAS*. **102**(40): p. 14458-14462.

209. O. Fiehn, J. Kopka, P. Dormann, T. Altmann, R.N. Trethewey, L. Willmitzer, **2000** *Nat. Biotechnol.* **18**: p. 1157-1161.

210. M. Scholz, S. Gatzek, A. Sterling, O. Fiehn, J. Selbig, **2004** *BMC Bioinf.* **20**: p. 2447-2454.

211. Fiehn, O., **2001** *Comp. Funct. Genom.* **2**: p. 155-168.

212. Cattell, R.B., **1966** *Multivariate Behavioral Research* **1**: p. 245-276.

213. Kaiser, H.F., **1960** *Educational and Psychological Measurement*. **20**: p. 141-151.

214. R.R. Picard, R.D. Cook, **1984** *J. Am. Stat. Assoc.* **79**(387): p. 575-583.

215. F. Mosteller, J.W. Tukey, *Data analysis and regression*. 1977, Reading, MA.: Addison-Wesley.

216. E.N. Fuller, P.D. Schettler, J.C. Giddings, **1966** *Ind. Eng. Chem.* **58**(5): p. 19-27.

217. Agilent. *Products*. 2011; Available from: http://www.chem.agilent.com/en-US/Products/Instruments/gc/techniques/capillaryflowtechnologygcxgcflowmodulator/pages/default.aspx.

218. W. Khummueng, J. Harynuk, P. Marriott., **2006** *Anal. Chem.* **78**(13): p. 4578-4597.

219. P. Schoenmakers, P. Marriott, J. Beens., **2003** *LC-GC Eur.* **16**(6): p. 335-339.

220. P. Manzanoa, E. Arnáiza, J.C. Diegoa, L. Toribioa, C. García-Viguerab, J.L. Bernala, J. Bernal, **2011** *J. Chromatogr. A.* **1218**(30): p. 4952-4959.

221. P. McA. Harvey, R.A. Shellie., **2011** *J. Chromatogr. A.* **1218**(21): p. 3153-3158.

222. Shellie, R.A., *Volatile components of plants, essential oils, and fragrances*, in *Compr. Anal. Chem.*, L. Ramos, Editor. 2009, Elsevier. p. 189-213.

223. R. Shellie, L. Mondello, P. Marriott, G. Dugo, **2002** *J. Chromatogr. A.* **970**(1-2): p. 225-234.

224. J. Beens, H. Boelens, R. Tijssen, J. Blomberg, **1998** *HRC J. High Resolut. Chromatogr.* **962**(1-2): p. 63.

225. P. Haglund, M. Harju, C. Danielsson, P. Marriott, **2002** *J. Chromatogr. A.* **962**(1-2): p. 127-134.

226. J.V. Seeley, N.J. Micyus, S.V. Bandurski, S.K. Seeley, J.D. McCurry, **2007** *Anal. Chem.* **79**: p. 1840-1847.

227. N.J. Micyus, J.D. McCurry, J.V. Seeley, **2005** *J. Chromatogr. A.* **1086**: p. 115-121.

228. R.E. Mohler, B.J. Prazen, R.E. Synovec, **2006** *Anal. Chim. Acta*. **555**: p. 68-74.

229. A.E. Sinha, K.J. Johnson, B.J. Prazen, S.V. Lucas, C.G. Fraga, R.E. Synovec, **2003** *J. Chromatogr. A.* **983**: p. 195-204.

230. T. Veriotti, R. Sacks, **2001** *Anal. Chem.* **73**: p. 3045-3050.

231. R.E. Wittrig, F.L. Dorman, C.M. English, R.D. Sacks, **2004** *J. Chromatogr. A.* **1027**: p. 75-82.

232. P.Q. Tranchida, G. Purcaro, A. Visco, L. Conte, P. Dugo, P. Dawes, L. Mondello, **2011** *J. Chromatogr. A.* **21**: p. 3140-3145.

233. M.T. Roberts, A.C. Lewis, **2002** *J. Am. Soc. Brew. Chem.* **60**: p. 116-121.

234. K.M. Pierce, J.C. Hoggard, R.E Mohler, R.E. Synovec, **2008** *J. Chromatogr. A.* **1184**: p. 341-352.

235. C.G. Fraga, B.J. Prazen, R.E. Synovec, **2000** *Anal. Chem.* **72**: p. 4154-4162.

236. J.C. Hoggard, R.E. Synovec, **2007** *Anal. Chem.* **79**: p. 1611-1619.

237. E. Sánchez, B.R. Kowalski, **1986** *Anal. Chem.* **58**: p. 496-499.

238. K.J. Johnson, R.E. Synovec, **2002** *Chemom. Intell. Lab. Sys.* **60**: p. 225.

239. K.J. Johnson, B.J. Prazen, D.C. Young, R.E. Synovec, **2004** *J. Sep. Sci.* **27**: p. 410-416.

240. Jong, S. de, **1993** *Chemom. Intell. Lab. Sys.* **18**: p. 251-263.

241. Zoex. *ZX-2 Thermal Modulator Specifications*. 2011 [cited 12/11/2011]; Available from: http://www.zoex.com/docs/pdf/ZX2-Product-Specs.pdf.

242. LECO. *Consumable Free GCxGC Modulator Specifications*. 2011 [cited 12/11/2011]; Available from: http://www.leco.com/resources/application_notes/pdf/technical_briefs/sepSci_technical_briefs/209-066-014%20CF%20Modulator.pdf.

# Appendix

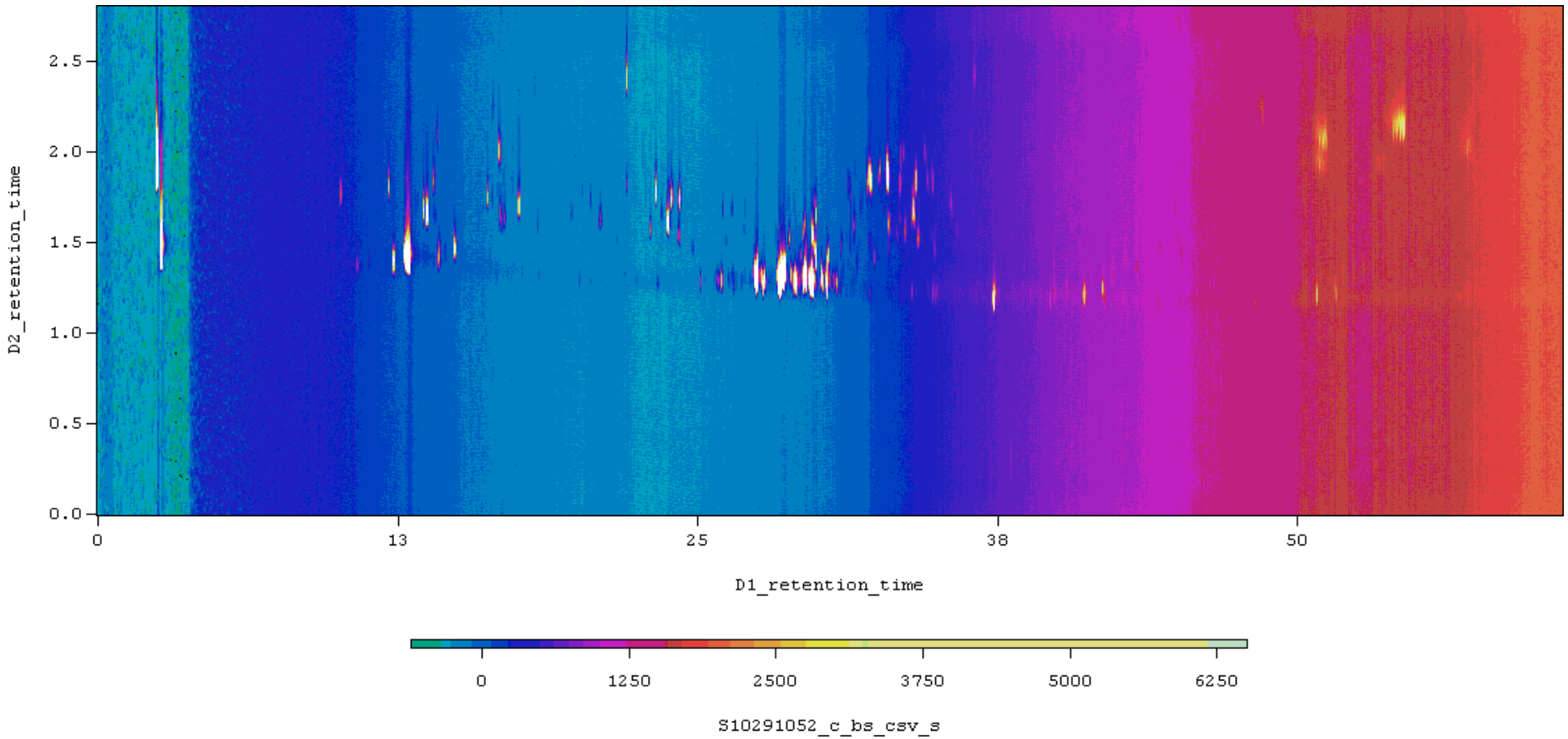


**Figure A1. GC×GC–FID chromatogram of hop essential oil obtained using the (20 m × 0.1 mm) × (2 m × 0.25 mm) column set (blank subtracted). Experimental conditions shown in Table 4.3.**

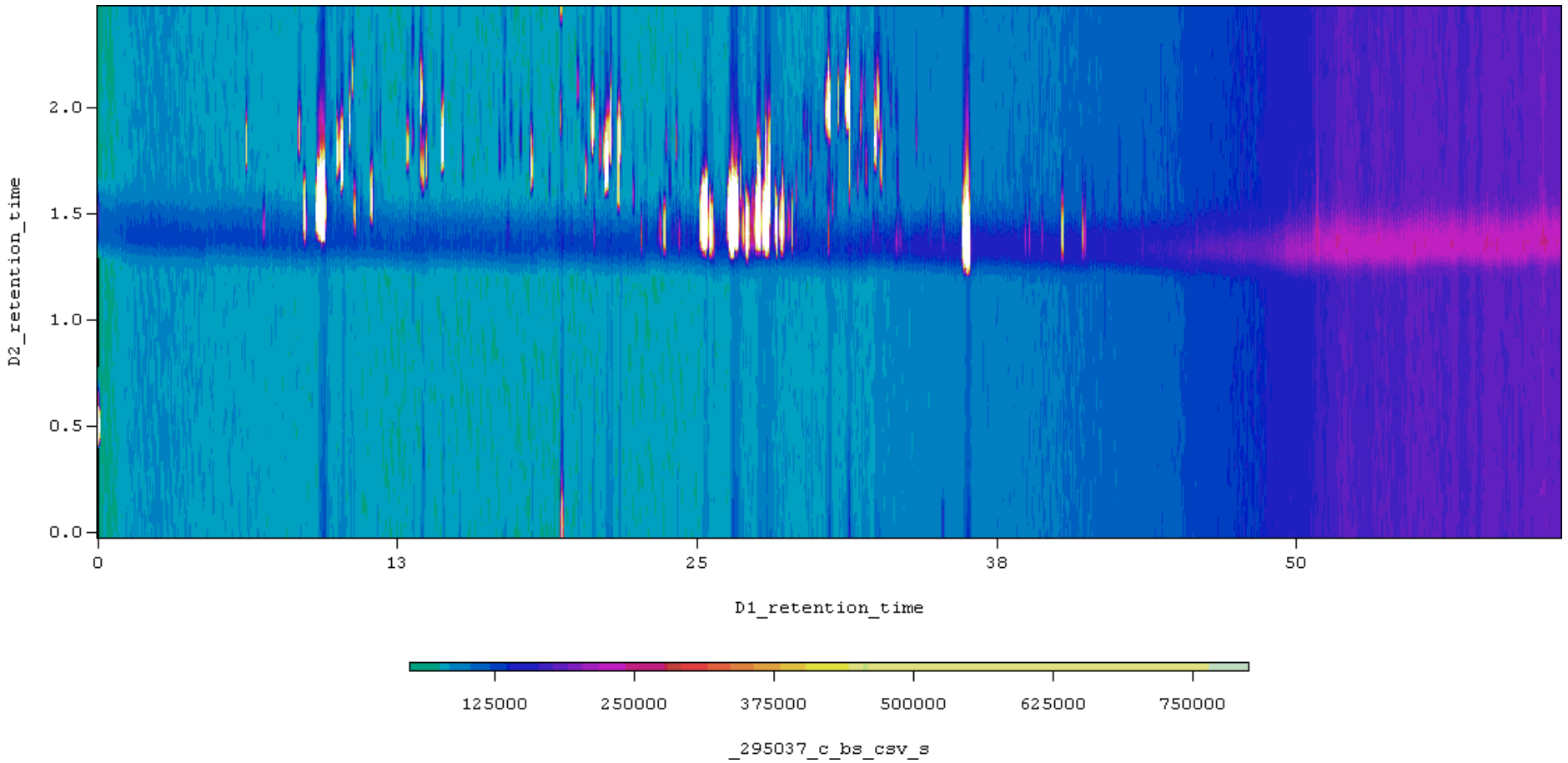


**Figure A2. GC×GC–MS TIC chromatogram of hop essential oil obtained using the (20 m × 0.1 mm) × (2 m × 0.25 mm) column set (blank subtracted). Experimental conditions shown in Table 4.3.**

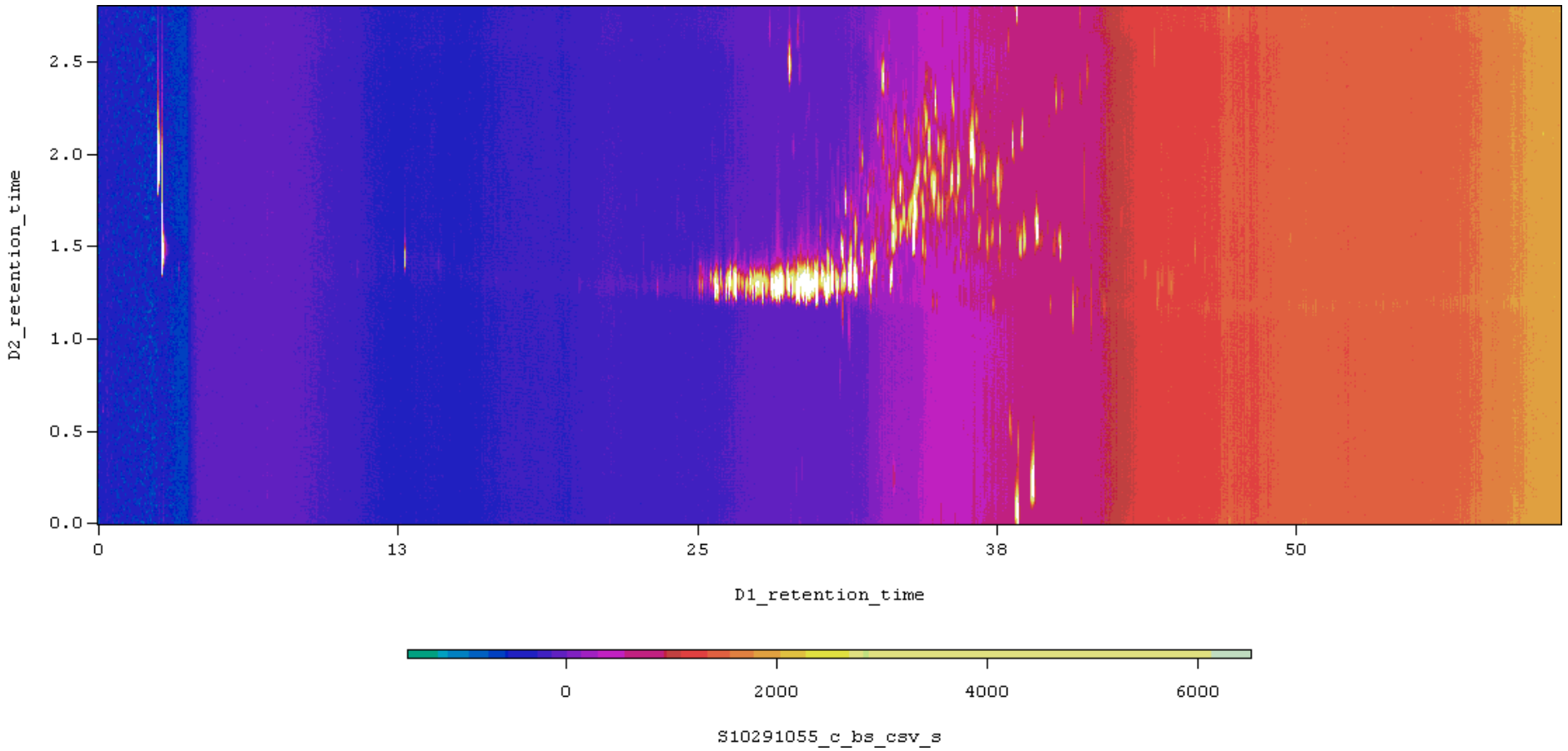


**Figure A3. GC×GC–FID chromatogram of vetiver essential oil obtained using the (20 m × 0.1 mm) × (2 m × 0.25 mm) column set (blank subtracted). Experimental conditions shown in Table 4.3.**

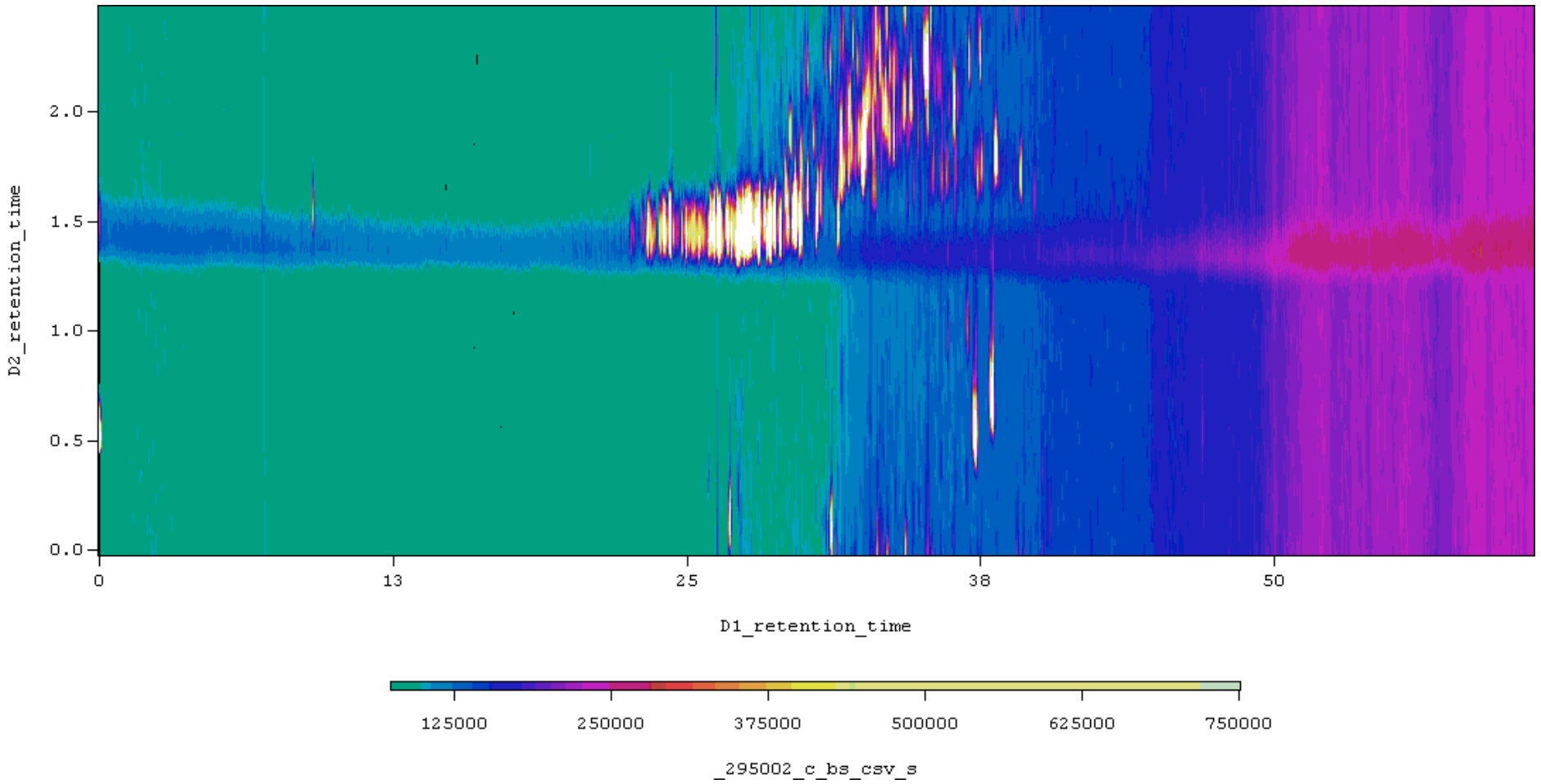


**Figure A4. GC×GC–MS TIC chromatogram of vetiver essential oil obtained using the (20 m × 0.1 mm) × (2 m × 0.25 mm) column set (blank subtracted). Experimental conditions shown in Table 4.3.**

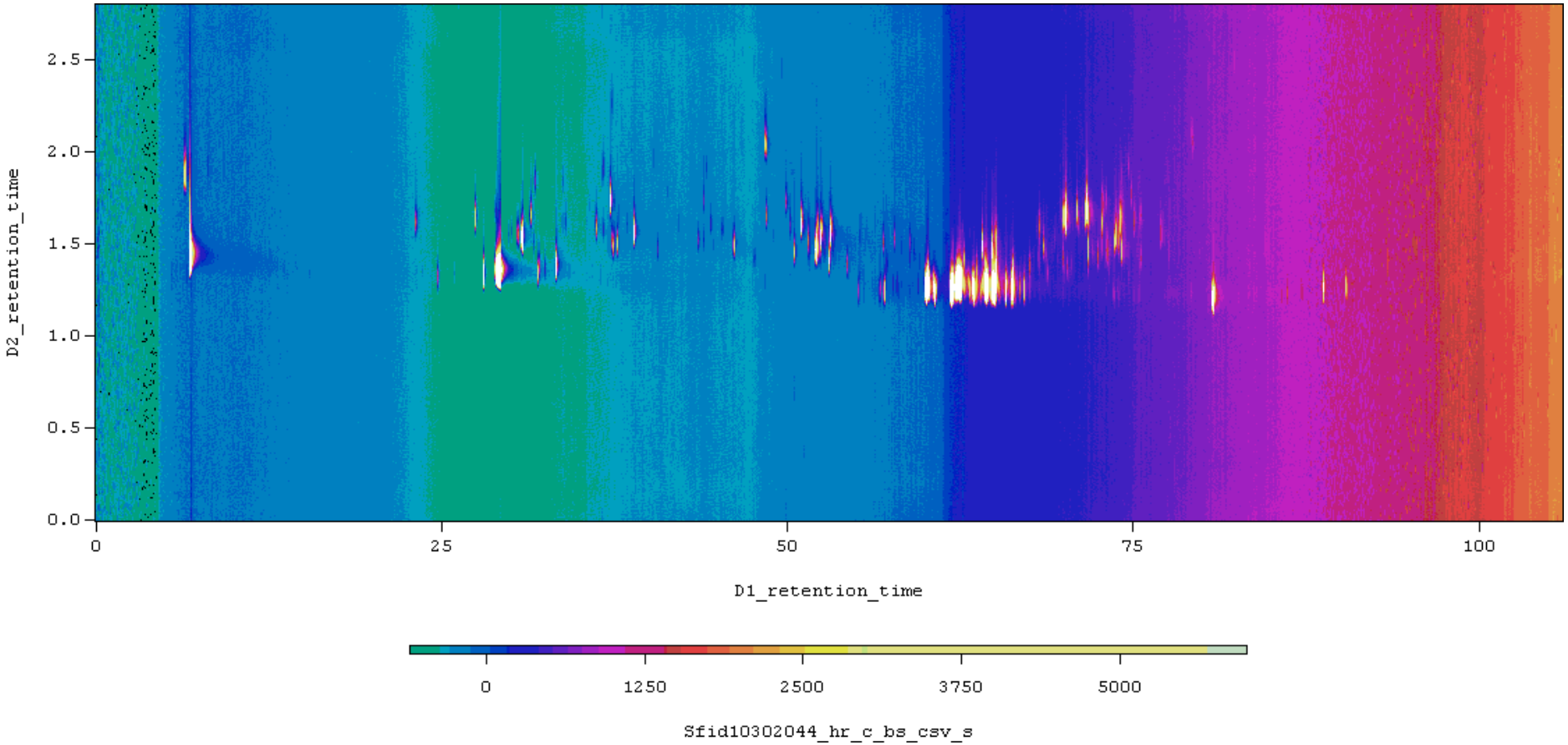


**Figure A5. GC×GC–FID chromatogram of hop essential oil obtained using the (40 m × 0.1 mm) × (2 m × 0.25 mm) column set (blank subtracted). Experimental conditions shown in Table 4.3.**

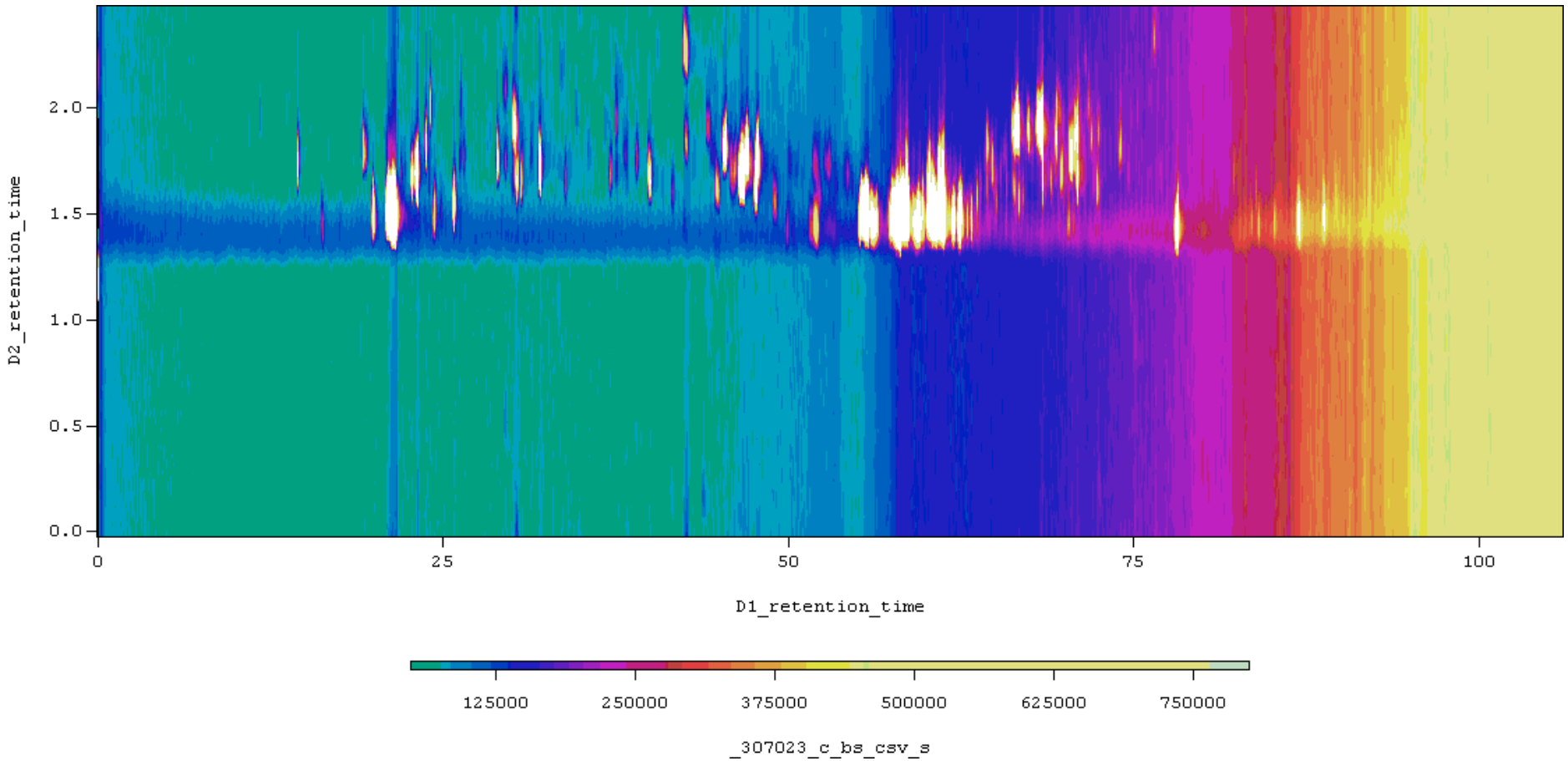


**Figure A6. GC×GC–MS TIC chromatogram of hop essential oil obtained using the (40 m × 0.1 mm) × (2 m × 0.25 mm) column set (blank subtracted). Experimental conditions shown in Table 4.3.**

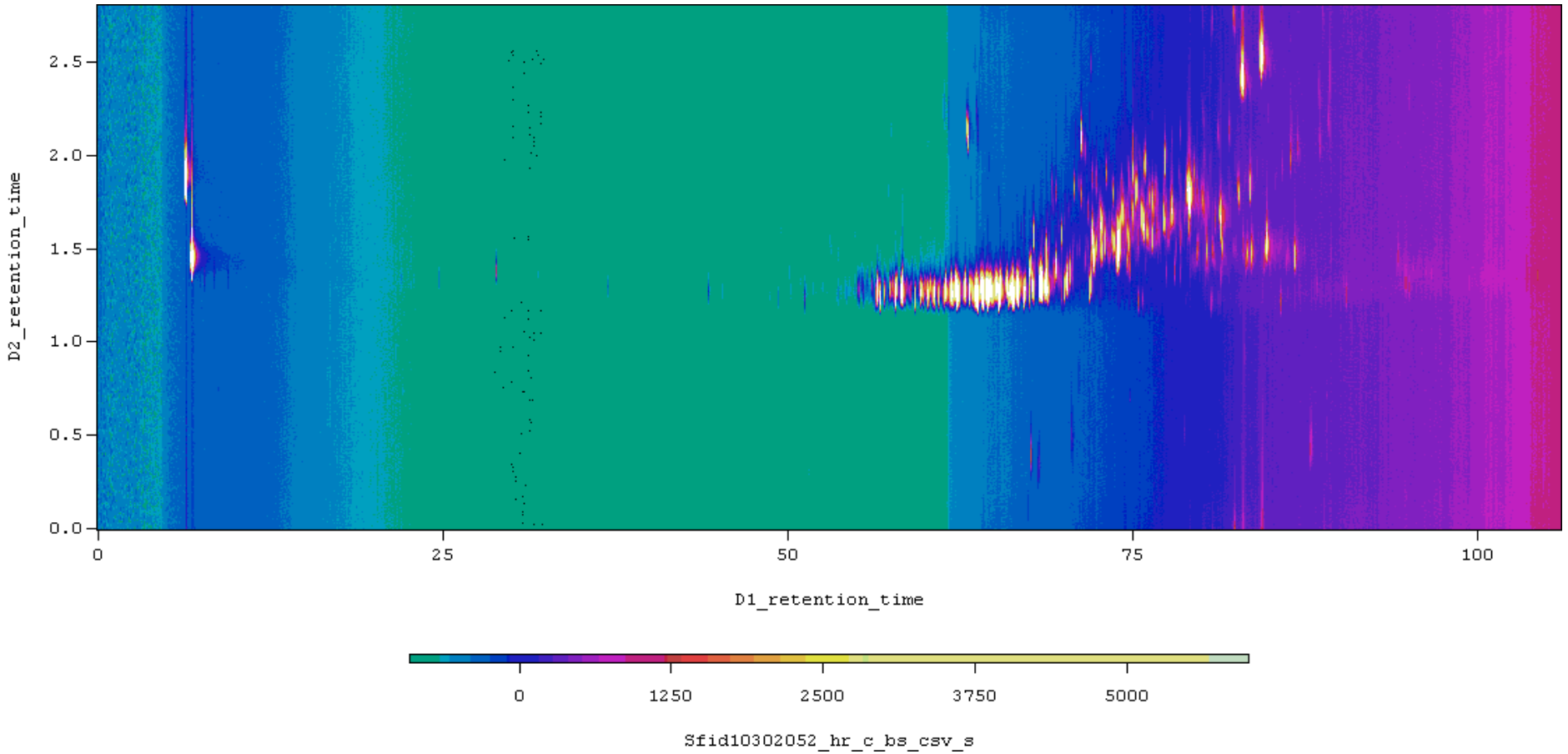


**Figure A7. GC×GC–FID chromatogram of vetiver essential oil obtained using the (40 m × 0.1 mm) × (2 m × 0.25 mm) column set (blank subtracted). Experimental conditions shown in Table 4.3.**

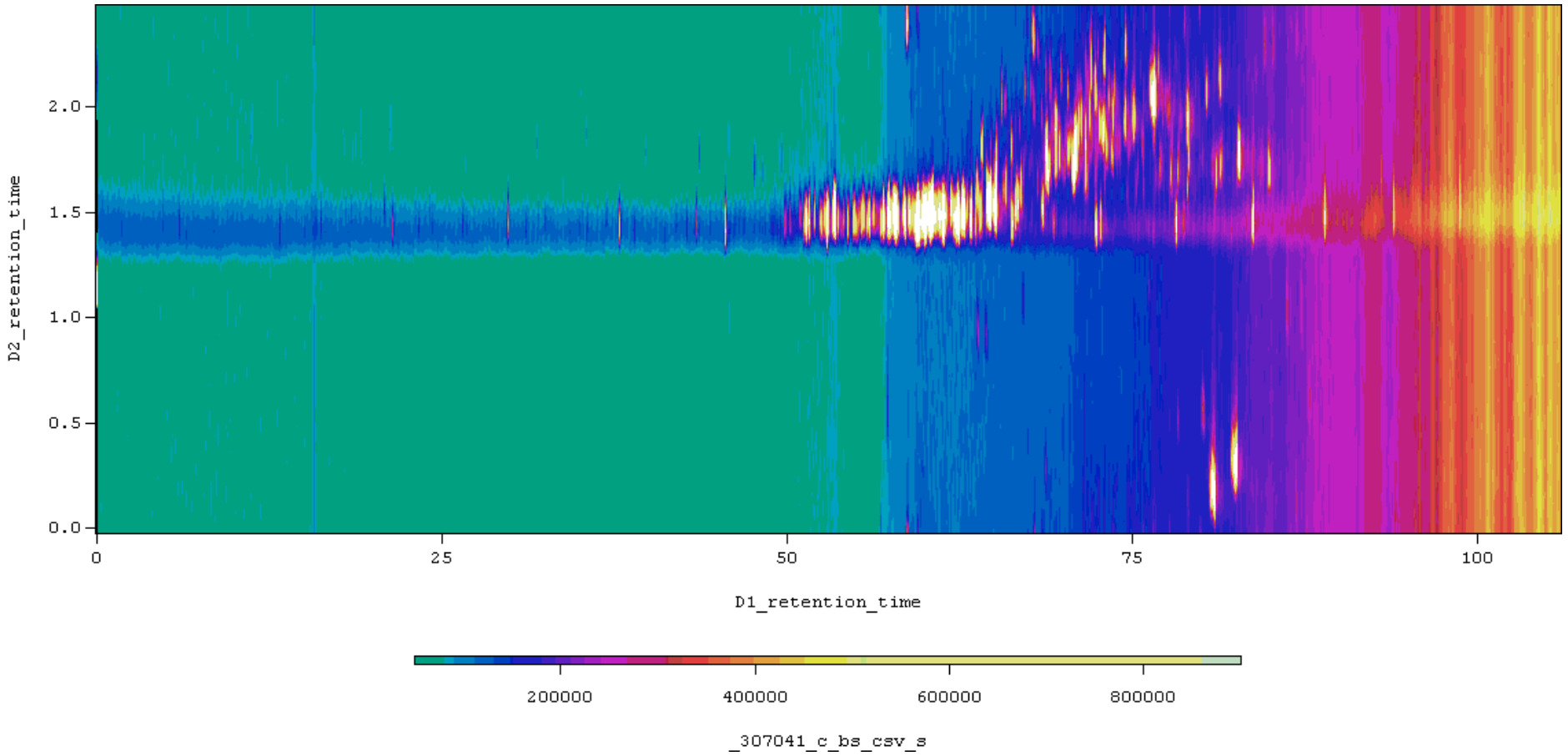


**Figure A8. GC×GC–MS TIC chromatogram of vetiver essential oil obtained using the (40 m × 0.1 mm) × (2 m × 0.25 mm) column set (blank subtracted). Experimental conditions shown in Table 4.3.**

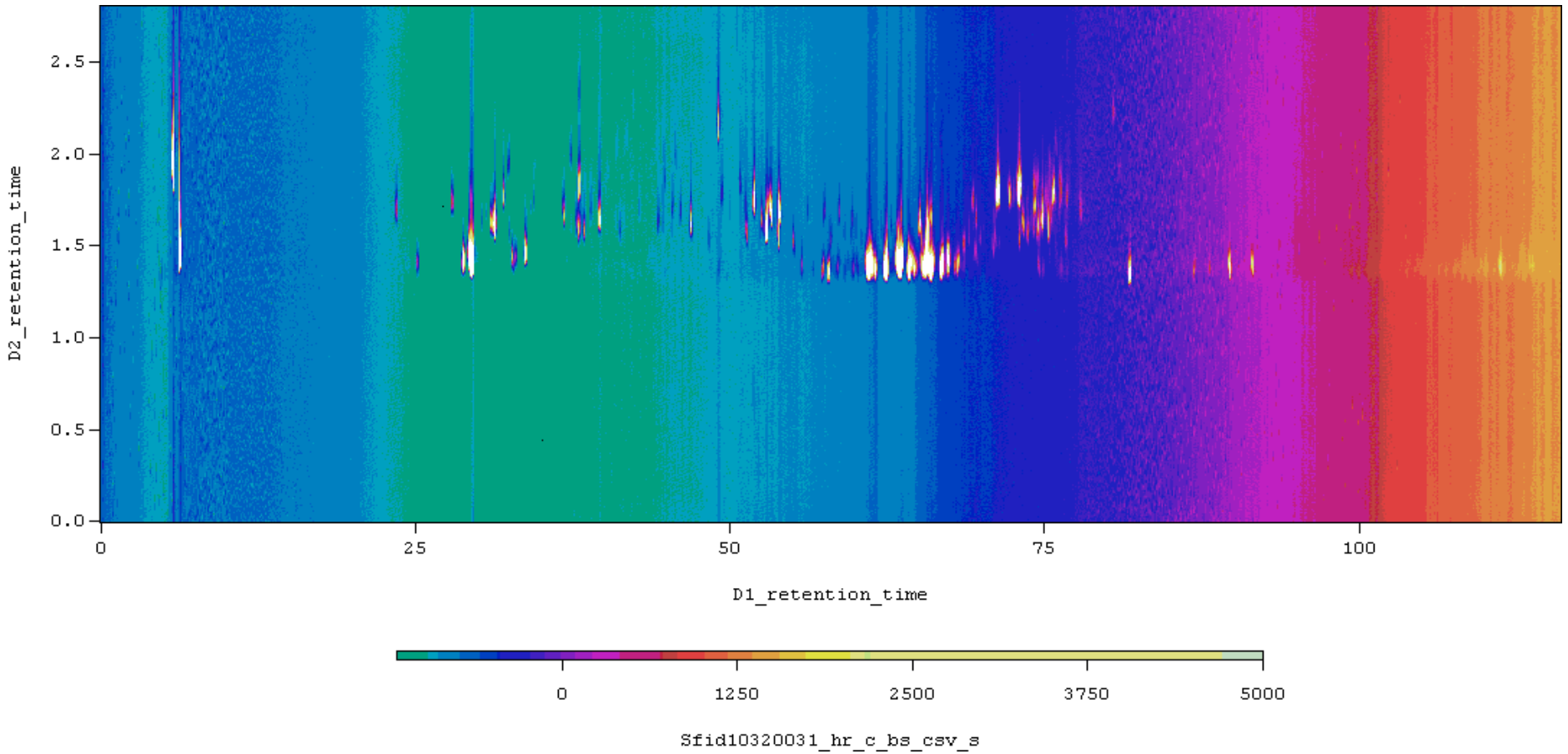


**Figure A9. GC×GC–FID chromatogram of hop essential oil obtained using the (25 m × 0.22 mm) × (2 m × 0.25 mm) column set (blank subtracted). Experimental conditions shown in Table 4.3.**

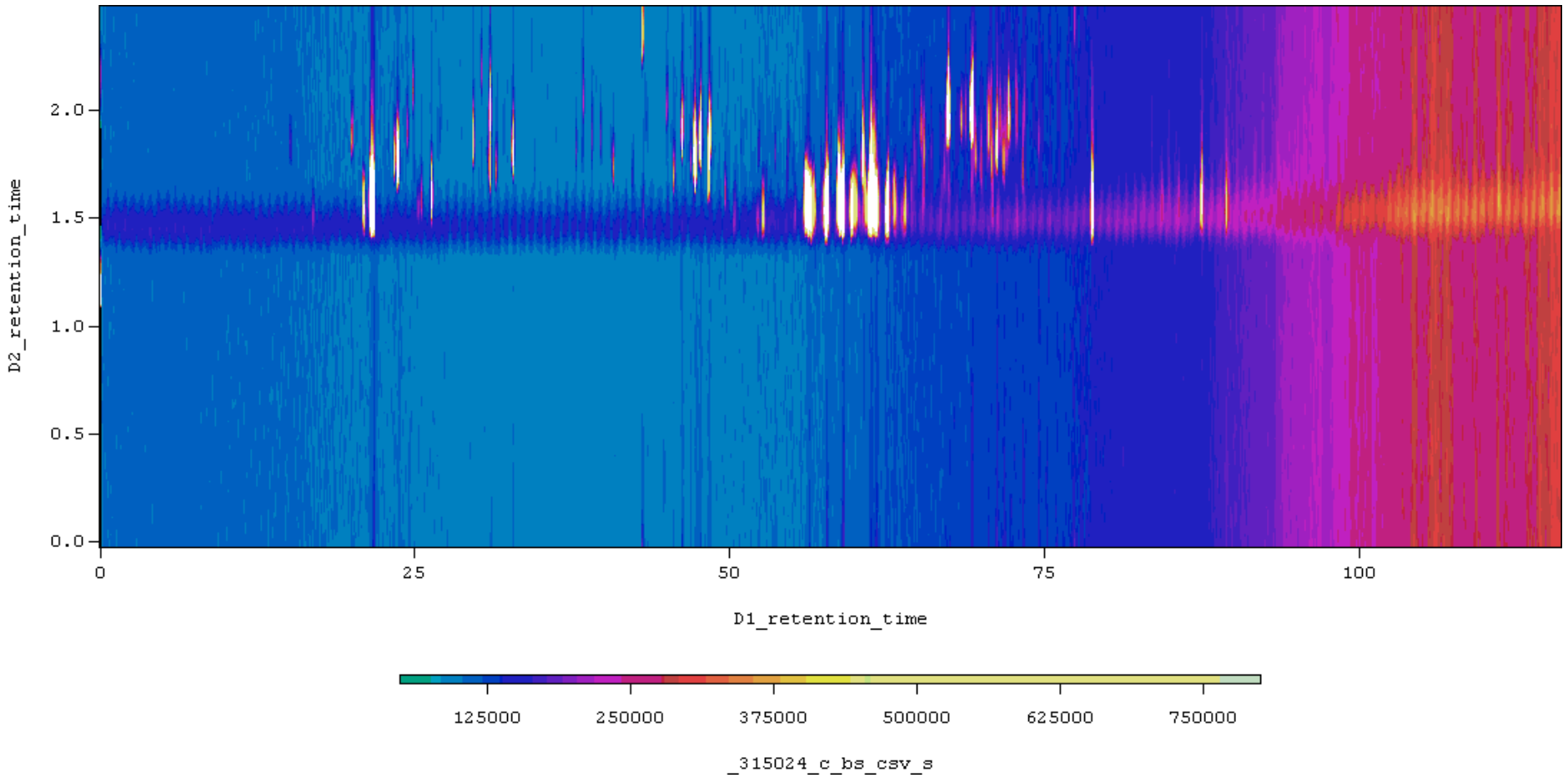


**Figure A10. GC×GC–MS TIC chromatogram of hop essential oil obtained using the (25 m × 0.22 mm) × (2 m × 0.25 mm) column set (blank subtracted). Experimental conditions shown in Table 4.3.**

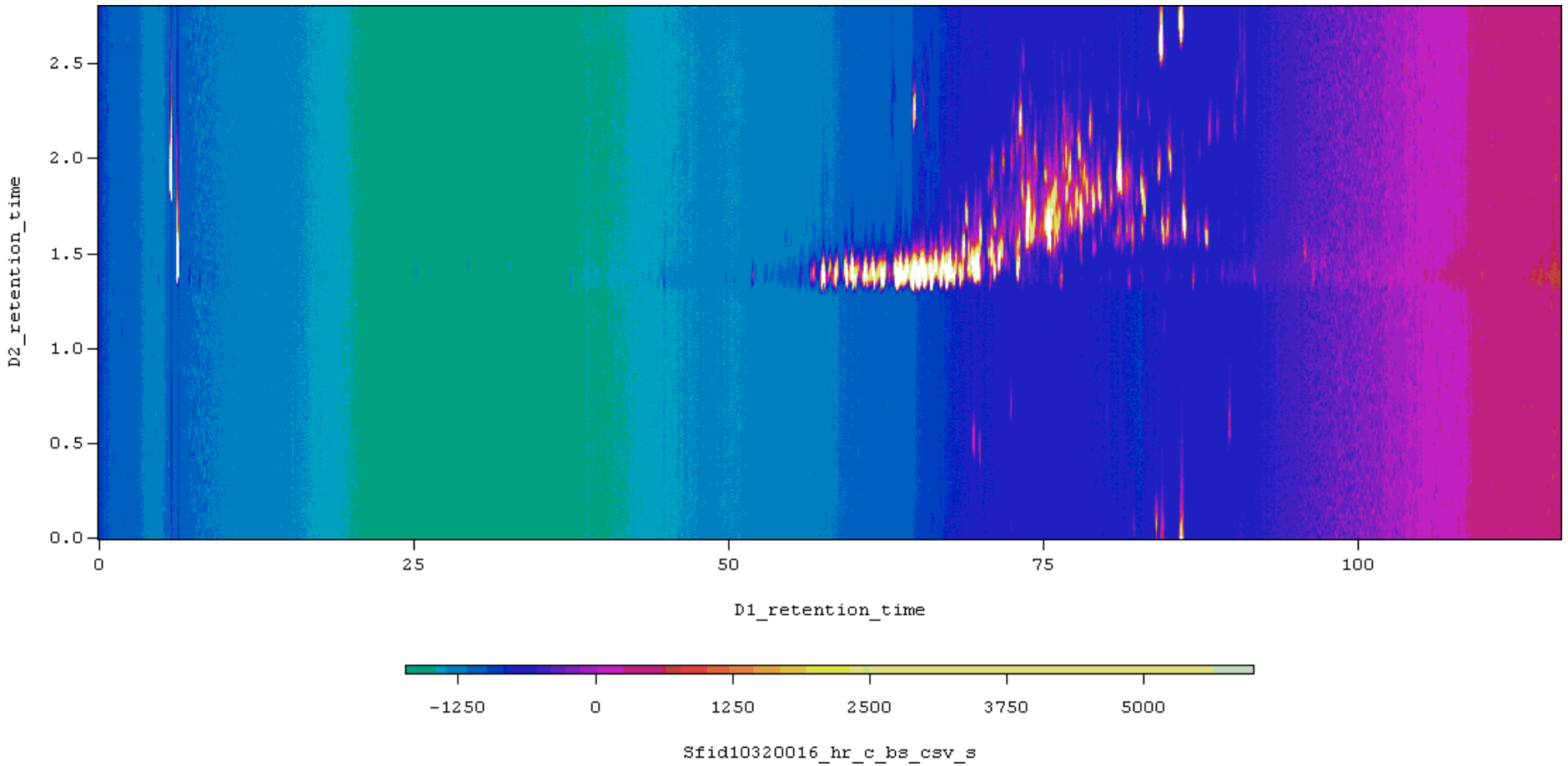


**Figure A11. GC×GC–FID chromatogram of vetiver oil obtained using the (25 m × 0.22 mm) × (2 m × 0.25 mm) column set (blank subtracted). Experimental conditions shown in Table 4.3.**

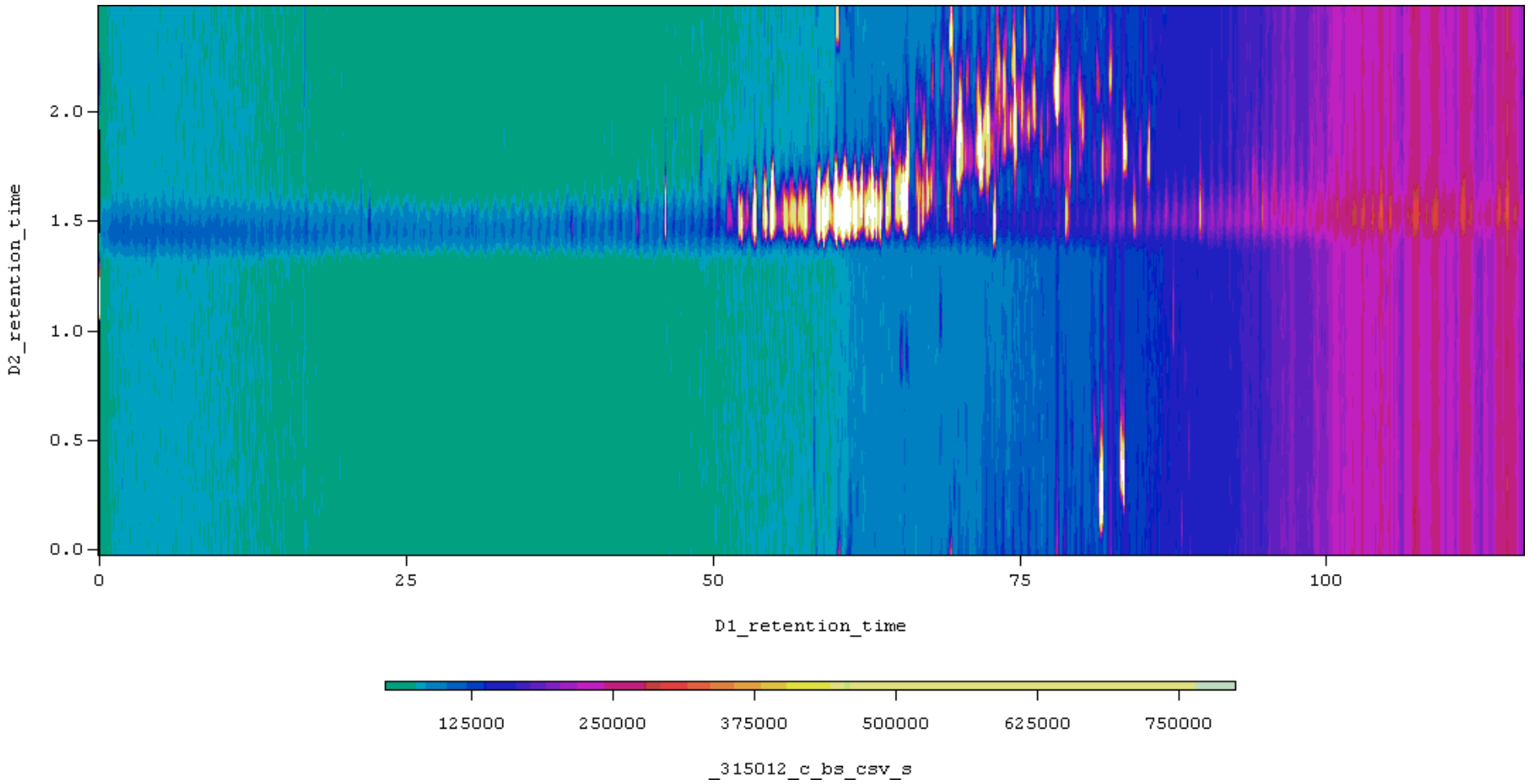


**Figure A12. GC×GC–MS TIC chromatogram of vetiver oil obtained using the (25 m × 0.22 mm) × (2 m × 0.25 mm) column set (blank subtracted). Experimental conditions shown in Table 4.3.**

Data presented in Appendix has been generated using the FFNSC spectral library with a ± 10 retention index unit filter and minimum library match of 85%. Retention times listed in minutes.

**Table A1. Tentative peak identification of hop essential oil using the (20 m × 0.1 mm) × (2 m × 0.25 mm) column set.**

| Name | RI Analyte | RI Library | Percentage agreement | Average $^{1}t_R$ | Average $^{2}t_R$ |
|---|---|---|---|---|---|
| isobutyrate | 914 | 913 | 91 | 10.11 | 0.64 |
| isopentyl propanoate | 971 | 967 | 86 | 12.12 | 0.68 |
| β-pinene | 976 | 978 | 94 | 12.33 | 0.28 |
| myrcene | 998 | 991 | 96 | 13.09 | 0.30 |
| isopentyl isobutyrate | 1017 | 1014 | 94 | 13.74 | 0.54 |
| methyl heptanoate | 1025 | 1025 | 92 | 14.03 | 0.73 |
| limonene | 1031 | 1030 | 86 | 14.23 | 0.28 |
| E-β-ocimene | 1048 | 1046 | 93 | 14.87 | 0.36 |
| linalool | 1101 | 1101 | 90 | 16.75 | 0.87 |
| 2-methyl butyrate | 1104 | 1104 | 92 | 16.82 | 0.49 |
| 2-methylbutyl isovalerate | 1107 | 1109 | 91 | 16.95 | 0.51 |
| methyl octanoate | 1125 | 1125 | 95 | 17.56 | 0.63 |
| methyl nonanoate | 1221 | 1224 | 95 | 20.94 | 0.52 |
| geraniol | 1256 | 1255 | 93 | 22.06 | 1.35 |
| undecan-2-one | 1292 | 1294 | 96 | 23.25 | 0.71 |
| methyl decanoate | 1322 | 1327 | 95 | 24.23 | 0.40 |
| α-copaene | 1378 | 1375 | 93 | 25.98 | 0.21 |
| decyl methyl ketone | 1393 | 1393 | 92 | 26.47 | 0.48 |
| isocaryophyllene | 1428 | 1424 | 90 | 27.53 | 0.25 |
| γ-elemene | 1435 | 1432 | 89 | 27.69 | 0.22 |
| E-β-farnesene | 1455 | 1452 | 93 | 28.61 | 0.25 |
| geranyl propanoate | 1475 | 1471 | 93 | 28.83 | 0.51 |
| neryl isobutyrate | 1483 | 1485 | 93 | 29.32 | 0.36 |
| tridecan-2-one | 1497 | 1495 | 94 | 29.55 | 0.52 |
| α-selinene | 1509 | 1501 | 92 | 29.88 | 0.26 |
| geranyl isobutyrate | 1514 | 1507 | 95 | 29.93 | 0.39 |
| cadinene | 1522 | 1518 | 88 | 30.21 | 0.23 |
| caryophyllene oxide | 1594 | 1597 | 90 | 32.24 | 0.61 |
| tridec-4Z-enyl acetate | 1682 | 1680 | 86 | 34.17 | 0.54 |
| farnesol | 1720 | 1716 | 86 | 35.53 | 0.66 |
| octadecane | 1798 | 1800 | 95 | 37.40 | 0.19 |

**Table A2. Tentative peak identification of hop essential oil using the (40 m × 0.1 mm) × (2 m × 0.25 mm) column set.**

| Name | RI Analyte | RI Library | Percentage agreement | Average $^{1}t_R$ | Average $^{2}t_R$ |
|---|---|---|---|---|---|
| isobutyrate | 913 | 913 | 93 | 23.09 | 0.66 |
| α-pinene | 935 | 933 | 87 | 24.70 | 0.35 |
| isopentyl propanoate | 971 | 967 | 86 | 27.40 | 0.69 |
| β-pinene | 979 | 978 | 94 | 28.02 | 0.40 |
| myrcene | 996 | 991 | 96 | 29.23 | 0.42 |
| isopentyl isobutyrate | 1016 | 1014 | 95 | 30.53 | 0.61 |
| methyl heptanoate | 1025 | 1025 | 94 | 31.40 | 0.75 |
| limonene | 1033 | 1030 | 92 | 32.02 | 0.40 |
| E-β-ocimene | 1050 | 1046 | 94 | 33.26 | 0.46 |
| linalool | 1102 | 1101 | 88 | 37.22 | 0.86 |
| 2-methyl butyrate | 1105 | 1104 | 89 | 37.42 | 0.59 |
| 2-methylbutyl isovalerate | 1108 | 1109 | 92 | 37.67 | 0.60 |
| methyl octanoate | 1124 | 1125 | 94 | 38.92 | 0.66 |
| methyl nonanoate | 1223 | 1224 | 92 | 46.10 | 0.63 |
| geraniol | 1257 | 1255 | 93 | 48.42 | 1.22 |
| undecan-2-one | 1294 | 1294 | 96 | 51.15 | 0.77 |
| methyl decanoate | 1324 | 1327 | 92 | 53.15 | 0.61 |
| geranic acid ester | 1326 | 1320 | 95 | 53.28 | 0.73 |
| α-copaene | 1380 | 1375 | 88 | 57.02 | 0.44 |
| decyl methyl ketone | 1394 | 1393 | 87 | 57.69 | 0.73 |
| isocaryophyllene | 1430 | 1424 | 92 | 60.16 | 0.48 |
| γ-elemene | 1435 | 1432 | 90 | 60.27 | 0.48 |
| β-chamigrene | 1488 | 1479 | 91 | 63.70 | 0.46 |
| tridecan-2-one | 1500 | 1495 | 94 | 64.52 | 0.65 |
| α-selinene | 1506 | 1501 | 89 | 64.67 | 0.59 |
| caryophyllene oxide | 1602 | 1597 | 91 | 70.28 | 0.93 |
| geranyl isovalerate | 1603 | 1604 | 89 | 70.35 | 0.56 |
| epicubenol | 1641 | 1641 | 87 | 27.53 | 0.73 |
| tridec-(4Z)-enyl acetate | 1684 | 1680 | 86 | 30.07 | 0.65 |
| tridecyl methyl ketone | 1695 | 1697 | 93 | 31.76 | 0.95 |
| farnesol | 1723 | 1716 | 90 | 32.44 | 0.44 |
| octadecane | 1796 | 1800 | 95 | 33.95 | 0.73 |

**Table A3. Tentative peak identification of hop essential oil using the (25 m × 0.22 mm) × (2 m × 0.25 mm) column set.**

| Name | RI Analyte | RI Library | Percentage agreement | Average $^{1}t_R$ | Average $^{2}t_R$ |
|---|---|---|---|---|---|
| isobutyrate | 916 | 913 | 93 | 26.67 | 0.61 |
| isopentyl propanoate | 972 | 967 | 85 | 28.76 | 0.71 |
| β-pinene | 977 | 978 | 91 | 29.38 | 0.38 |
| myrcene | 996 | 991 | 97 | 30.90 | 0.42 |
| isopentyl isobutyrate | 1019 | 1014 | 94 | 31.99 | 0.59 |
| methyl heptanoate | 1026 | 1025 | 89 | 32.28 | 0.75 |
| limonene | 1034 | 1030 | 88 | 33.59 | 0.44 |
| E-β-ocimene | 1052 | 1046 | 92 | 36.44 | 0.45 |
| linalool | 1103 | 1101 | 93 | 38.24 | 0.78 |
| methyl octanoate | 1123 | 1125 | 95 | 43.49 | 0.67 |
| methyl nonanoate | 1226 | 1224 | 94 | 47.12 | 0.55 |
| geraniol | 1259 | 1255 | 95 | 50.77 | 1.17 |
| undecan-2-one | 1298 | 1294 | 94 | 52.12 | 0.70 |
| geranic acid ester | 1328 | 1320 | 95 | 56.49 | 0.67 |
| α-copaene | 1381 | 1375 | 86 | 58.05 | 0.35 |
| isocaryophyllene | 1430 | 1424 | 94 | 61.23 | 0.39 |
| (E)-β- farnesene | 1459 | 1452 | 95 | 62.62 | 0.36 |
| geranyl propanoate | 1475 | 1471 | 87 | 63.62 | 0.40 |
| neryl isobutyrate | 1488 | 1485 | 85 | 64.35 | 0.34 |
| β-chamigrene | 1489 | 1479 | 92 | 64.50 | 0.40 |
| tridecan-2-one | 1502 | 1495 | 93 | 65.24 | 0.55 |
| α-selinene | 1510 | 1501 | 93 | 65.73 | 0.37 |
| cadinene | 1521 | 1518 | 93 | 66.36 | 0.40 |
| tridec-(4Z)-enyl acetate | 1682 | 1680 | 87 | 75.73 | 0.63 |
| octadecane | 1799 | 1800 | 94 | 87.17 | 0.35 |